TECHNISCHE UNIVERSITÄT MÜNCHEN

Lehrstuhl für Molekulare Ernährungsmedizin

Novel C-type lectin-mediated signalling mechanisms that activate the NLRP3 inflammasome and IL-1β production: consequences for T_H2 polarized immune responses

Manuel Ritter

Vollständiger Abdruck der von der Fakultät Wissenschaftszentrum Weihenstephan für Ernährung, Landnutzung und Umwelt der Technischen Universität München zur Erlangung des akademischen Grades eines

Doktors der Naturwissenschaften

genehmigten Dissertation.

Vorsitzender:	Univ.-Prof. Dr. D. Haller
Prüfer der Dissertation:	1. Univ.-Prof. Dr. M. Klingenspor
	2. Univ.-Prof. Dr. D. Busch
	3. Priv.-Doz. Dr. C. U. J. Prazeres da Costa
	4. apl. Prof. Dr. Th. Fuchs (nur schriftliche Beurteilung)

Die Dissertation wurde am 06.06.2012 bei der Technischen Universität München eingereicht und durch die Fakultät Wissenschaftszentrum Weihenstephan für Ernährung, Landnutzung und Umwelt am 20.11.2012 angenommen.

Contents

List of Figures

List of Tables

Abbreviations

A

ACT	ammoniumchloride-tris
AHR	airway hyperresponsiveness
AIM2	absent in melanoma 2
$Al(OH)_3$	aluminium hydroxide (alum)
APC	antigen presenting cells
APC (FACS)	allophycocyanin
APDC	(2R,4R)-4-aminopyrrolidine-2,4-dicarboxylic acid
APS	ammonium persulfate
ASC	apoptosis-associated speck-like protein containing a CARD
ATP	adenosine-5`-triphosphate

B

BAL	bronchoalveloar lavage
Bcl10	B cell lymphoma 10
BMDCs	bone-marrow derived dendritic cells
bp	base pair(s)
BSA	bovine serum albumin

C

CARD	caspase recruitment domain
Casp	caspase
Ca^{2+}	calcium ion
CCL17	C-C motif ligand 17
CD	clusters of differentiation
CDC	Center for Disease Control and Prevention
CIITA	MHC class II transcription activator
CLRs	C-type lectin receptors
CpG	cytosine-phosphatidyl-guanine
CytD	cytochalasin D

D

DAMPs	damage associated molecular pattern molecules
DAP12	diaminopimelic acid receptor 12
DC	dendritic cell

DC-SIGN	DC-specific intercellular adhesion molecule-3-grabbing non-integrin
DMEM	Dulbecco's modified eagle medium
DMSO	dimethyl sulfoxide
DNA	deoxyribonucleic acid
DNP	2,4-dinitrophenole
dNTPs	deoxynucleoside triphosphate
DOI	degree of infection
dsRNA	double-stranded RNA
DTT	dithiothreitol

E

EAE	experimental autoimmune encephalomyelitis
ECL	enhanced chemiluminescence technique
ECP	eosinophil cationic protein
EDTA	ethylenediaminetetraacetic acid
EGTA	ethylene glycol tetraacetic acid
ELISA	enzyme linked immunosorbent assay
EPO	eosinophil peroxidase

F

FACS	fluorescence-activated cell sorting
Fc	fragment crystallizable
FCCP	carbonyl cyanide p-(tri-fluromethoxy)phenyl-hydrazone
FcRγ	Fc receptor gamma chain
FCS	fetal calf serum
FITC	fluorescein isothiocyanate
Foxp3	forkhead box P3

G

g	gravitational force
GM-CSF	granulocyte-macrophage colony-stimulating factor

H

HCl	hydrogen chloride
HEPES	4-(2-hydroxyethyl)-1-piperazineethanesulfonic acid
HET-E	incompatibility locus protein from *Podospora anserine*
HIN-200	hemopoietic IFN-inducible nuclear protein 200
HIV	human immunodeficiency virus

HRP	horseradish peroxidase
H_2O	water
H_2SO_4	sulfuric acid

I

ICE	IL-1β-converting enzyme (Casp1)
IFN	interferon
Ig	immunoglobulin
IKKi	inhibitor of nuclear factor kappa-B kinase subunit epsilon isoform 1
IL	interleukin
IL-1R	IL-1 receptor
IL-1Ra	IL-1R antagonist
IPAF	ICE-protease activating factor
IPSE/alpha1	interleukin 4 inducing principle from *S. mansoni* eggs/alpha-1
IRAK	IL-1 receptor-associated kinase
IRF	IFN-regulatory factor
ITAM	immunoreceptor tyrosine-based activation motif

J

JNK	Jun N-terminal kinase

K

kb	kilobase
KCl	potassium chloride
kDa	kilo Dalton
KO	knockout
KOH	potassium hydroxide

L

LABAs	long-acting beta agonists
LDH	lactate dehydrogenase
LLN	lung lymph node
LPS	lipopolysaccharide
LRR	leucine rich repeat

M

mA	milliampere
Mal	MyD88 adapter-like

Malt1	mucosa-associated lymphoid tissue lymphoma translocation protein 1
MAP	mitogen-activated protein
MAPK	MAP kinase
MDP	muramyl dipeptide
MGL	macrophage galactose lectin
Mg^{2+}	magnesium ion
MHC	major histocompatibility complex
MIH	Institute of medical Mircrobiology, Immunology and Hygiene
Mincle	macrophage-inducible C-type lectin
MLN	mesenteric lymph node
MOI	multiplicity of infection
MPO	myeloperoxidase
MRI	Munich Rechts der Isar
MyD88	myeloid differentiation primary response gene 88

N

Nac	N-acetyl-L-cysteine
NaCl	sodium chloride
NAD	nicotinamide adenine dinucleotide
NADH	nicotinamide adenine hydrogen dinucleotide
NADPH	nicotinamide adenine dinucleotide hydrogen phosphate
$NaHCO_3$	sodium hydrogen carbonate
NACHT	NAIP-CIITA-HET-E and TP1 containing protein
NAIP	neuronal apoptosis inhibitory protein
NALP	NACHT-LRR-PYD containing protein
Na_2CO_3	di-sodium carbonate
Na_3VO_4	sodium orthovanadate
NBD	nucleotide binding domain
NF-κB	nuclear factor-κB
NH_4Cl	ammonium chloride
NLRC	NOD-like receptor family, CARD domain-containing protein
NLRP	NOD-like receptor family, pryin domain
NOD	nucleotide oligomerization domain
NOD mice	non-obese diabetic mice

O

OVA	ovalbumin

P

PAGE	polyacrylamide gel electrophoresis
PAMPs	pathogen-associated molecular pattern molecules
PBS	phosphate buffered saline
PCR	polymerase chain reaction
PE	phycoerythrin
PFA	paraformaldehyde
PMSF	phenylmethanesulfonyl fluoride
poly I:C	polyinosinic:polycytidylic acid
PRR	pattern recognition receptors
PVDF	polyvinylidene fluoride
PYD	pyrin domain
P2X7	purinergic receptor P2X, ligand-gated ion channel 7
P_3Cys	palmitoyl-cysteine ((*RS*)-2,3-di(palmitoyloxy)-propyl

R

RLU	relative light unit
RNA	ribonucleic acid
ROS	reactive oxygen species
rpm	revolutions per minute
RPMI	Roswell Park Memorial Institute medium
R406	Syk kinase inhibitor

S

SABAs	short acting beta agonists
SCID	severe combined immunodeficiency
SD	standard deviation
SDS	sodium dodecyl sulfate
SEA	soluble egg antigen
SH2	sarcoma homology 2
SIGNR1	specific intercellular adhesion molecule-3-grabbing non-integrin homolog-related 1
SIP	SH2 domain-containing leukocyte protein
S. mansoni	*Schistosoma mansoni*
spf	specific pathogen-free
S.typh.	*Salmonella typhimurium*
Syk	spleen tyrosine kinase

T

TAE	tris acetat EDTA
TANK	TRAF family member-associated NF-kappa-B activator
TBK	TANK-binding kinase
TBST	tris-buffered saline and Tween 20
TCA	trichloroacetic acid
TCR	T cell receptor
TEMED	tetramethylethylenediamine
TGF	transforming growth factor
T_H cells	T helper cells
TIR	Toll/IL-1 receptor
TIRAP	TIR-containing adapters
TLC	thin layer chromatography
TLR	Toll-like receptor
TMB	3,3',5,5'-tetramethylbenzidine
TM	trademark
TNF	tumor necrosis factor
TP1	telomerase-associated protein 1
TRAF	tumour-necrosis factor-receptor-associated factor
TRAM	TRIF-related adaptor molecule
T_{reg} cells	regulatory T cells
TRIF	TIR-domain containing adaptor protein inducing IFN-β
Tris	tris(hydroxymethyl)aminomethane
TRX	Thioredoxin
TXNIP	TRX-interacting protein
T3/4SS	type 3/4 secretion system

V

v/v	volume per volume

W

WHO	World Health Organization
wt	wildtype
w/v	weight per volume

Z

ZAP70	ζ-chain-associated protein kinase 70 kDa

Abstract

Schistosomiasis is a chronic infection caused by parasitic blood flukes (helminthes), such as *Schistosoma mansoni.* According to the World Health Organization it is the second most socioeconomically devastating parasitic disease with over 207 million infected people worldwide. The propensity of helminths to immunomodulate the host's immune system is an essential aspect of their survival. Previous research has demonstrated how *S. mansoni*-derived soluble egg antigen (SEA), which is a complex mixture of highly glycosylated proteins and lipids, can dampen innate responses after triggering Toll-like receptor (TLR) stimuli.

Expanding on those data, the results presented within this thesis demonstrate that a variety of TLRs are influenced by this dampening effect and moreover appears to be mediated by (glyco-)lipid components within the SEA. Whilst studying TLR-triggered events a further modulatory facet within SEA became apparent, namely the ability of (glyco-)protein-based components to activate the NLRP3 inflammasome and thus IL-1β production. Using an array of biochemical and immunological studies *in vitro* it was elucidated that SEA mediates NLRP3 inflammasome activation by triggering the Dectin-2/Fc receptor γ chain (FcRγ) complex. This elicits a cascade of intracellular events including the activation of spleen tyrosine kinase (Syk) to induce mitochondrial reactive oxygen species (ROS), potassium efflux and the Card9 complex. Furthermore, *in vivo* infections of *S. mansoni* in mice lacking the inflammasome adapters ASC and NLRP3 and the receptors Dectin-2 and IL-1 showed decreased immunopathology and altered antigen-specific adaptive responses (T_H1, T_H2 and T_H17). Overall, these data substantiate the hypothesis that innate responses direct adaptive immunity and highlight the ability of this helminth to modulate various innate pathways. Further work described in this thesis display the critical role for NLRP3 inflammasome activation during a T_H2 polarized model of allergic asthma. In brief, $NLRP3^{-/-}$ and $ASC^{-/-}$ mice showed less eosinophil infiltration and inflammation within the lung and reduced ovalbumin-specific T_H2 responses (IL-5 and IL-13). Moreover, blocking IL-1 signalling with Anakinra, an IL-1 receptor antagonist (IL-1Ra), leads to impaired infiltration of eosinophils within the lung of asthmatic mice. In summary, this study implies a crucial role of the NLRP3 inflammasome signalling platform within T_H2 polarized immune responses, such as Schistosomiasis or asthma. Understanding the NLRP3 inflammasome signalling mechanisms could contribute to the development of novel vaccination strategies against helminth infections and autoimmune diseases.

Zusammenfassung

Schistosomiasis ist eine chronische Infektion, ausgelöst durch parasitisch lebende Pärchenegel (Helminthen), wie zum Beispiel *Schistosoma mansoni*. Nach Angaben der Weltgesundheitsorganisation (WHO) sind weltweit über 207 Millionen Menschen infiziert. Die Eigenschaft das Immunsystem des Wirts zu modulieren bzw. sich seiner Erkennung zu entziehen ist ein essentieller Aspekt für das Überleben von Helminthen. Verschiedene Untersuchungen haben gezeigt, dass schistosomales Eierantigen (SEA), das aus verschiedenen glykosilierten Proteinen und Lipiden besteht, *Toll-like receptor* (TLR) Signalwege der angeborenen Immunantwort unterdrückt.

Die in dieser Arbeit dargelegten Ergebnisse zeigen, dass neben der (Glyko-)Lipid-vermittelten Suppression von TLR Signalwegen auch das NLRP3 Inflammasom aktiviert und IL-1β ausgeschüttet wird. Im SEA enthaltende (Glyko-)Proteine aktivieren den Dectin-2/Fc Rezeptor γ Kette (FcRγ) Komplex und induzieren dadurch die Milz-Tyrosin-Kinase (Syk). Dies führt zur Ausschüttung von radikalen Sauerstoffspezies (ROS) aus den Mitochondrien, Kaliumsekretion und Aktivierung des Card9 Komplexes. Außerdem zeigten *S. mansoni* infizierte Mäuse, denen die zentralen Inflammasomkomponenten ASC und NLRP3, sowie die Rezeptoren Dectin-2 und IL-1 fehlten, reduzierte Immunpathologie und veränderte antigen-spezifische T_H1, T_H2 und T_H17 Immunantworten. Diese Daten zeigen, wie Helminthen das NLRP3 Inflammasom aktivieren und dadurch verschiedene Immunantworten modulieren. Darüber hinaus konnte eine entscheidende Rolle des NLRP3 Inflammasoms im T_H2 polarisierten allergischen Asthmamodel aufgezeigt werden. Demnach zeigten $NLRP3^{-/-}$ und $ASC^{-/-}$ Mäusen verringerte Infiltration von Eosinophilen und Entzündung in der Lunge, sowie reduzierte Ovalbumin-spezifische T_H2 Immunantworten (IL-5 und IL-13). Außerdem führte die Blockierung des IL-1 Signalwegs durch den IL-1 Rezeptorantagonist (IL-1Ra) Anakinra in asthmatischen Mäusen ebenfalls zu einer reduzierten Infiltration von Eosinophilen in der Lunge. Zusammenfassend zeigen die Daten dieser Arbeit, dass das NLRP3 Inflammasom eine entscheidende Rolle in T_H2 polarisierten Immunantworten, wie zum Beispiel während einer *S. mansoni* Infektion und allergischen Asthma, spielt. Die Aufklärung von Signalmechanismen des NLRP3 Inflammasoms könnte zur Entwicklung von neuen Therapien gegen Helmintheninfektionen und Autoimmunkrankheiten beitragen.

1 Introduction

1.1 Immunology

Immunology is a branch of biomedical sciences that covers a wide range of aspects of the immune system in all organisms [1]. The term "immunology" is closely connected to Edward Jenner who is often referred to as the "Father of Immunology". In the year 1796, he discovered that inoculating healthy individuals with cow pox leads to protection (immunity) against human smallpox [2]. Due to this success he coined the term vaccination, which refers to the practice of administrating antigenic material (a vaccine), such as attenuated viruses or virus proteins to stimulate the immune system of an individual so that immunity is developed towards the disease. However, he was not able to decipher the actual disease-causing agents, which are microbes or other pathogens. In the latter half of the 19th century, Robert Koch isolated *Bacillus anthracis* (1877), *Tuberculosis bacillus* (1882) and *Vibrio cholerae* (1883) and postulated a causal relationship between a certain microbe and a disease ("germ theory of disease") [3], which was also supported by Louis Pasteur. He created the first vaccines for rabies and anthrax and invented pasteurization, a method to stop milk and wine from causing sickness due to microbial growth [4]. Today, pathogens which elicit disease are divided into four groups: viruses, microbes (bacteria), pathogenic fungi, and the more complex eukaryotic organisms called parasites.

Another key discovery into the mechanisms of immune reactions was provided by Paul Ehrlich, who coined the term antibody. He described antibodies as "magic bullets" that were secreted into the extracellular fluid to neutralize antigens [5]. Following that conjecture, Emil von Behring and Kitasato Shibasaburō further described antibody activity against diphtheria and tetanus toxins and put forward the theory of humoral immunity, which proposed that a mediator within the serum could specifically bind to an antigen. Today, the antibody-mediated immune response is a critical part of the adaptive immune system. In addition to such adaptive immune responses, Ilya Ilyich Mechnikov (Élie Metchnikoff) discovered immune responses which were independent of antibody secretion. He showed that cells (phagocytes), originating from the host, induced an immune response by attacking and ingesting foreign antigens [6]. These findings lead to the theory of phagocytosis, an example of innate immune responses. Innate and adaptive immunity are the main components of the mammalian immune system and both are crucial for the protection against foreign pathogens.

The mammalian immune system is an example of evolutionary-evolved adaption against various antigens and pathogens and highlights the complexity of immunological mechanisms, which lead to specific immune responses and immunity. The following sections will mainly focus on the triggering and function of innate immune responses and its essential role for the initiation of adaptive immunity.

1.2 Concepts of the immune system

As mentioned above, the immune system protects against a wide variety of agents using a collection of cellular mechanisms to identify and kill pathogens and tumor cells. During infection, the immune system needs to be able to distinguish between its own healthy cells and tissues (self molecules) and foreign substances (non-self molecules). The detection of these foreign components is very complicated since pathogens consistently adapt and evolve new ways to successfully invade the host. To survive this challenge, many organisms have developed multiple mechanisms that recognize and neutralize pathogens. Basic mechanisms can be seen in uni-cellular organisms such as bacteria, which possess enzymatic systems (defensins, phagocytosis and the complement system) that protect against viral infections. More sophisticated mechanisms have only recently developed with the evolution of vertebrates [7]. These more complex immune systems, found in mammals for example, consist of many types of proteins, cells, organs and tissues, which interact in an elaborate and dynamic network. The latter adaptation process also creates so called “immunological memory”, which allows a rapid effective protection against future encounters with the same pathogens. These sophisticated immune responses are classified into the aforementioned innate and adaptive immune system [1].

1.2.1 Innate immunity

The evolutionary ancient innate immune system is an universal non-specific form of host defense and has been identified in all multi-cellular organisms. This form of immunity is a product of multiple and diverse defense mechanisms that incorporates a wide variety of proteins, different tissues and innate immune cells (leukocytes), such as natural killer cells, mast cells, eosinophils, basophils and phagocytic cells (macrophages, neutrophils and dendritic cells). Although this system does not confer long-lasting or protective immunity to the host, it is vital for the immediate recruitment of different immune cells to the sites of infection and inflammation, which is achieved through cytokine release and chemokine

gradients [8]. Moreover, it activates the complement cascade (biochemical cascade) which identifies bacteria, promotes clearance of dead cells or antibody complexes and initiates leukocytes to remove foreign substances in organs, tissues, blood and lymph. In addition, innate cells direct appropriate adaptive immune responses through antigen presentation and the release of distinctive cytokine patterns [1]. Furthermore, innate immune cells (such as dendritic cells and macrophages) express pattern recognition receptors (PRR), which recognize highly conserved products from the metabolic pathways of microorganisms (microbial products), termed pathogen-associated molecular pattern (PAMPs) [9]. Very important members of these PRR are the membrane-bound or intracellular Toll-like receptors (TLR) [10], which are crucial in recognizing pathogens and shaping the ensuing adaptive immune responses [11]. Currently, most mammalian species have between ten and fifteen different TLRs, and classical examples in the literature include the recognition of peptidoglycans and lipopeptides (P_3Cys) from gram-positive bacteria through TLR2 [12], lipopolysaccharide (LPS) from gram-negative bacteria through TLR4 [13] or bacterial DNA with a high frequency of unmethylated pairs of cytosine and guanosine dinucleotides (CpG) through TLR9 [14] (Figure 1.1).

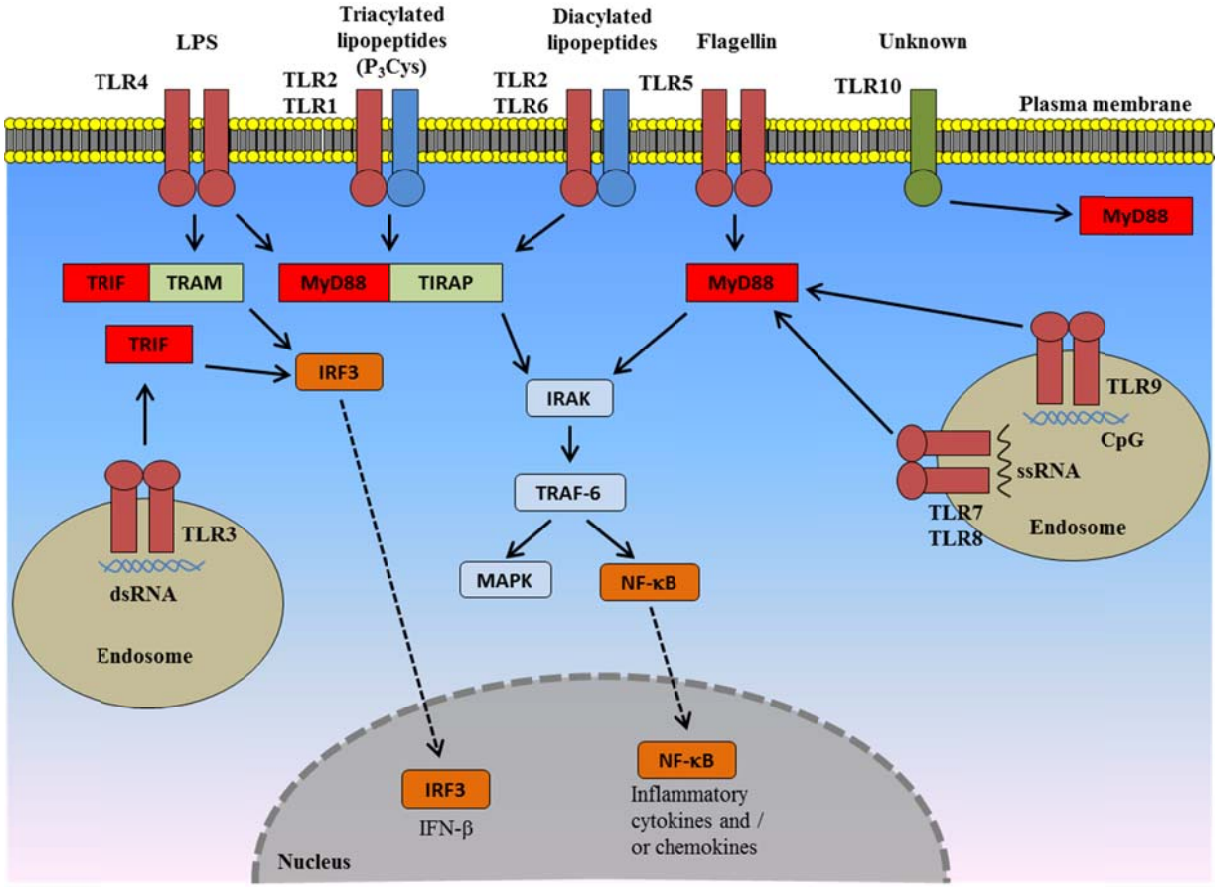

Figure 1.1: TLR signalling pathways of recognized PAMPs
In brief, the central signalling adaptor protein MyD88 (myeloid differentiation primary response gene 88) is used by all TLRs (except TLR3). It interacts with the IRAK (interleukin-1 (IL-1) receptor-associated kinase) family, leading to interaction with TRAF6 (tumour-necrosis factor-receptor-associated factor 6), which ultimately leads to activation of nuclear factor-κB (NF-κB) and mitogen-activated protein (MAP) kinases. This leads to the production of cytokines (such as tumor necrosis factor (TNF)) and other pro-inflammatory proteins. The MyD88 independent pathway is characterized by triggering TLR3 and TLR4, which activate TRIF (Toll/IL-1 receptor-domain containing adaptor protein inducing IFN-β) and TRAM (TRIF-related adaptor molecule), leading to IRF3 (interferon-regulatory factor 3) activation and IFN-β (interferon β) production. Adapted from Harrison`s Practice (http://www.harrisonspractice.com).

As depicted in Figure 1.1, TLR signalling pathways are complex and include a wide range of different adaptor molecules that culminate in the induction of numerous genes that function to promote inflammatory immune responses. Important pro-inflammatory cytokines include tumor necrosis factor alpha (TNF-α), interleukin 1 (IL-1), IL-6, IL-12, chemokines, anti-microbial effector molecules (inducible nitric oxide synthase and anti-microbial peptides) and co-stimulatory molecules [10, 11, 15, 16]. Upon activation, TLRs recruit adapter molecules within the cytoplasm of cells in order to propagate a signal, such as: TIRAP (Toll/interleukin-1 receptor (TIR)-containing adapters; also called Mal (MyD88 adapter-like)) [17, 18], which is required for TLR2 and TLR4 activation; TRIF (Toll/IL-1 receptor-domain containing

adaptor protein inducing IFN-β), which is necessary for interferon β (IFN-β) induction and anti-viral immunity [19, 20]; TRAM (TRIF-related adaptor molecule) [21] and the most important of all, MyD88 (myeloid differentiation primary response gene 88) [22, 23]. With the exception of TLR3, all other TLRs signal through MyD88, leading to the recruitment of TRAF6 (tumour-necrosis factor-receptor-associated factor 6) and activation of certain protein kinases (IRAK 1, IRAK 4, TBK 1, IKKi). The activation of these different protein kinases leads to nuclear factor-κB (NF-κB) translocation to the nucleus, which mediates the induction or suppression of genes and pro-inflammatory responses [10, 11, 15, 23]. Moreover, there are also other pathways downstream of TRAF6 that contribute to TLR function, such as those involving Jun N-terminal kinase (JNK) and mitogen-activated protein kinases (MAPKs) [24, 25]. MyD88 independent signalling pathways have been described for TLR3 and TLR4, which signal through TRIF and TRAM to induce interferon-regulatory factor 3 (IRF3), leading to IFN-β production [10, 11, 15, 23]. All in all, these signalling pathways represents one of the most powerful and important gateways of gene modulation and regulation of different immune responses.

1.2.2 The bridge between innate and adaptive immune responses

As mentioned before, the innate immune system is the first line of defense and can induce and activate adaptive immune responses. A crucial connection between innate and adaptive immune responses is antigen presentation via MHC (major histocompatibility complex) molecules on dendritic cells (DCs), B cells or macrophages. DCs were first identified in the epidermal layers of skin in 1868 by Paul Langerhans, who termed them Langerhans cells and at that time considered them to be part of the nervous system [26]. Almost 100 years later, Steinman and Cohn showed that DCs are actually a class of white blood cells that are important for innate immune responses [27]. Immature DCs are located in peripheral tissues so that they are ready for encounters with invading pathogens [28]. Captured pathogens are recognized by TLRs on the surface of the DCs (section 1.2.1), which induces their maturation [10, 11]. TLR activation can lead to phagocytosis of the pathogen, presentation of the foreign material on MHC molecules [28], and consequential proliferation of specific T cells. Moreover, DCs express high levels of co-stimulatory molecules, such as cluster of differentiation 80 (CD80) and CD86 and secrete chemokines and cytokines, such as CCL17 (C-C motif ligand 17), IL-6 and IL-12, which are important for T cell differentiation [28-31] (Figure 1.2).

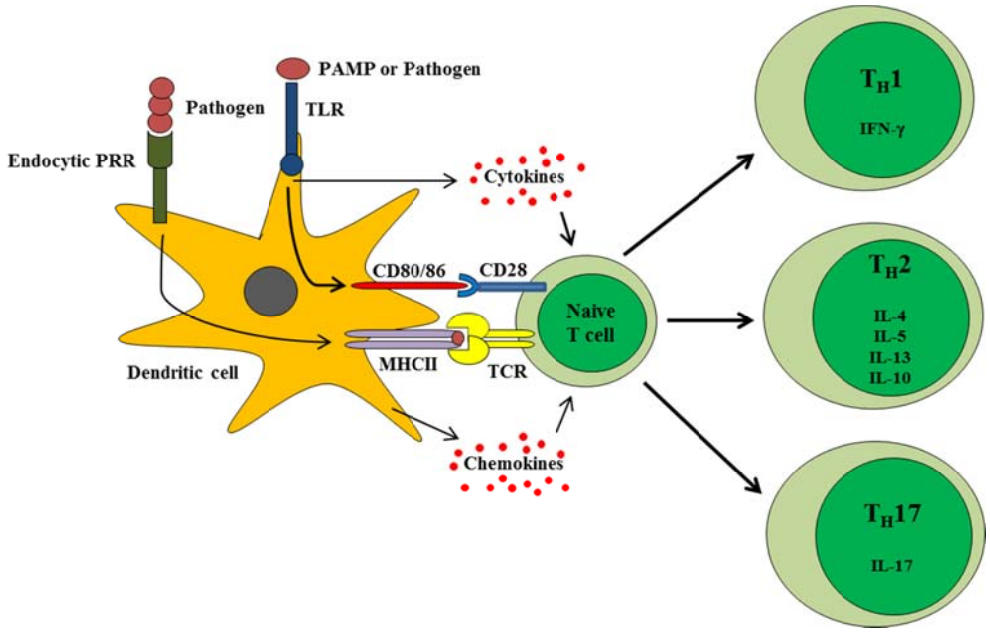

Figure 1.2: DCs induce T cell differentiation and initiate adaptive immunity
In brief, through TLRs DCs sense the presence of PAMPs and upregulates cell-surface expression of co-stimulatory (CD80 and CD86) and MHC glass II (MHCII) molecules, loaded with pathogen-derived antigens. Induction of CD80/86 and MHCII on DCs are recognized by naive T cells via CD28 and T cell receptor (TCR) leading to the activation and differentiation of T helper cells (T_H1, T_H2 and T_H17). Moreover, DCs also secrete cytokines and chemokines that also can induce T_H cell differentiation. Adapted from [10].

Besides induction of T cell differentiation, DCs are also able to directly stimulate B cell proliferation and antibody production [28, 32, 33]. Mature DCs can migrate to the draining lymph nodes and present the pathogen-derived antigens to the adaptive immune cells (naive T and B cells), which initiate the adaptive immune response [10, 11, 28].

1.2.3 Adaptive immunity

As described in section 1.2.2, adaptive immunity is triggered when a pathogen evades destructive mechanisms of the innate immune system. These secondary defenses are initiated through the maturation and presentation of pathogen-derived antigens by antigen-presenting cells (APC) and the consequential release of specific cytokines/chemokines leading to clonal selection of specific T lymphocytes (Figure 1.2) and B lymphocytes. This clonal selection leads to a long-lasting protection against the specific pathogen because of the development of immunological memory (antigen-specific memory T and B cells) [34, 35]. One of the most critical aspects of adaptive immune responses is the ability of cells to distinguish between "self" and "non-self" antigens during the process of antigen presentation. After pathogen-triggering the adaptive immune system uses two different strategies for the clearance of

pathogens. The humoral immune response is based on the release of secreted antibodies (immunoglobulin (Ig)) produced by B lymphocytes (B cells), which are called plasma cells [36]. In mammals there are five known classes of antibodies (IgA, IgD, IgE, IgG and IgM), which differ in their biological properties and have evolved to handle different kinds of antigens within different tissues. Secreted antibodies bind to extracellular pathogens (such as virus or bacteria), leading to their neutralization and destruction by promoting cytotoxicity (natural killer cells) [37], degranulation of granulocytes (mast cells, basophils and eosinophils) [38] and phagocytosis (macrophages) [39].

The cell-mediated immune response involves antigen-specific T lymphocytes. T cells can be divided into two major groups: Cytotoxic T cells and T helper cells (T_H cells). Cytotoxic T cells are characterized by the expression of CD8 on their cell surface and are able to destroy bacterially and virally infected cells and also tumor cells. Infected host cells present foreign antigens on MHC class I (MHCI) molecules which results in the binding to a specific T cell receptor (TCR) and consequential release of cytotoxins to induce apoptosis (programmed cell death) of the target cells [40-42]. T_H cells are characterized by the expression of CD4 on their cell surface and when activated these cells release various cytokines against non-self antigens and attract other immune cells, which help to regulate ongoing immune responses. They are activated through the recognition of specific peptides expressed on MHC class II (MHCII) molecules (section 1.2.2) and based on their production of cytokines differentiate into functional subsets called T helper type 1 (T_H1) and T helper type 2 (T_H2) cells. T_H1 cells are essential for protection against a variety of intracellular infections and mediate those responses through the release of IFN-γ and TNF-β. T_H2 responses on the other hand are effective against certain extracellular infections due to the secretion of various interleukins (IL-4, IL-5, IL-6, IL-10 and IL-13) and by the initiation of humoral immune responses [43-47]. Another important subpopulation of T cells within the adaptive immune system are the regulatory T cells (T_{reg}). These cells express CD4, CD25 and Foxp3 (forkhead box P3) [48], which prevent excessive immune reactions by suppressing the responses of other immune cells. Different studies have shown that T_{reg} cells prevent autoimmunity, control immune homoeostasis and limit chronic inflammatory disorders mediated by the immunosuppressive cytokines transforming growth factor β (TGF-β) and IL-10 [49-51]. Recently, two additional T_H cell subpopulations (T_H17 and T_H9) with effector functions distinct from those of T_H1 and T_H2 have been identified. T_H17 cells, secrete high amounts of IL-17A, IL-17F and IL-22 and are known to mediate the clearance of extracellular pathogens, tissue inflammation and autoimmunity, such as experimental autoimmune encephalomyelitis (EAE), rheumatoid

arthritis, multiple sclerosis, inflammatory bowel disease and psoriasis [52, 53]. On the other hand, T_H9 cells secrete IL-9 and play a crucial role in allergic diseases, such as allergic asthma development [54, 55]. This finely balanced network of cells, tissues and organs has evolved to ensure the survival. Failures in this network can lead to immunodeficiencies, autoimmunity and hypersensitivities.

1.3 Biology of Schistosomiasis

Parasitology is the study of parasitic organisms and their relationship to hosts. Parasites are subdivided into protozoa, arthropods or helminths (worms). The eukaryotic helminths can be categorized into three major groups: Cestodes (tapeworms), Nematodes (roundworms) and Trematodes (flukes). Within the latter, the *Schistosoma* species can elicit a chronic disease in humans called Schistosomiasis. According to the World Health Organization (WHO), Schistosomiasis is the second most socioeconomically devastating parasitic disease (next only to malaria). There are two different clinical manifestations of Schistosomiasis caused by five main *Schistosoma* species. Intestinal diseases are caused by *S. mansoni*, *S. japonica*, *S. mekongi*, *S. intercalatum* and *S. guineansis* whereas the urogenital disease is elicited by *S. haematobium*. Currently, over 207 million people are infected worldwide with an estimated risk of 700 million people in over 74 endemic countries, especially in tropical and sub-tropical areas [56-58] (Figure 1.3).

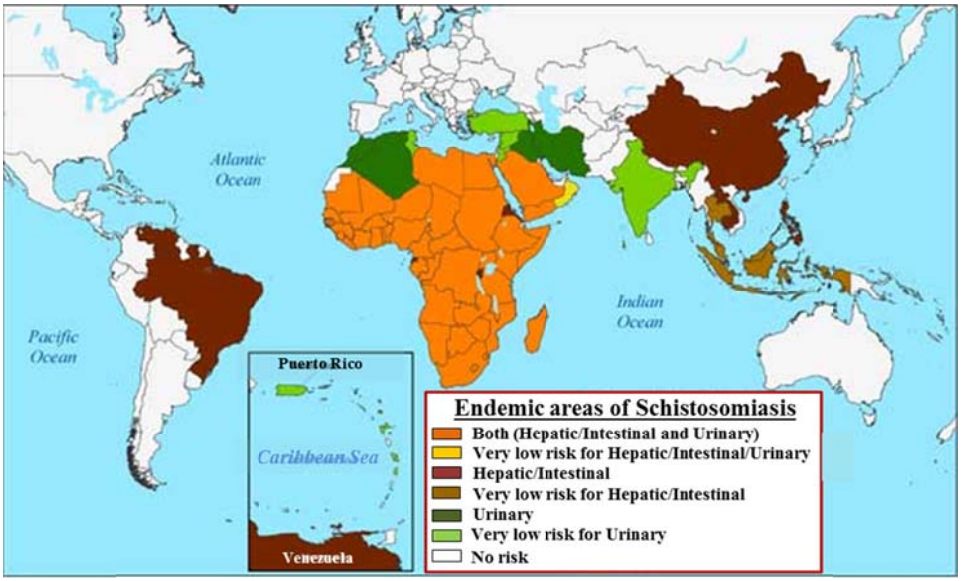

Figure 1.3: Geographic distribution of schistosomiasis
Modified from Relief Central, CDC Yellow Books, 2010.

Through the close relationship of *Schistosoma* species to their hosts (human) and the coevolutionary development with the human immune system, these parasites have evolved mechanisms to modulate the host immune system and exploit/induce different immunoregulatory pathways. Since mice are susceptible to *S. mansoni* infection and develop pathology and immune responses in almost the same manner as humans, a murine infection model can be used to decipher different immune responses against *Schistosoma* infection. The studies described in the later chapters of this thesis were performed using a murine *Schistosoma mansoni* infectious cycle, established in the laboratory of Dr. Layland and Dr. Prazeres da Costa.

1.3.1 Life cycle of *Schistosoma* species

The life cycle of *Schistosoma* species is complex and includes six developmental stages with two hosts. Humans and other mammals function as definitive hosts whereas fresh water snails such as *Biomphalaria glabrata* serve as intermediate host (Figure 1.4).

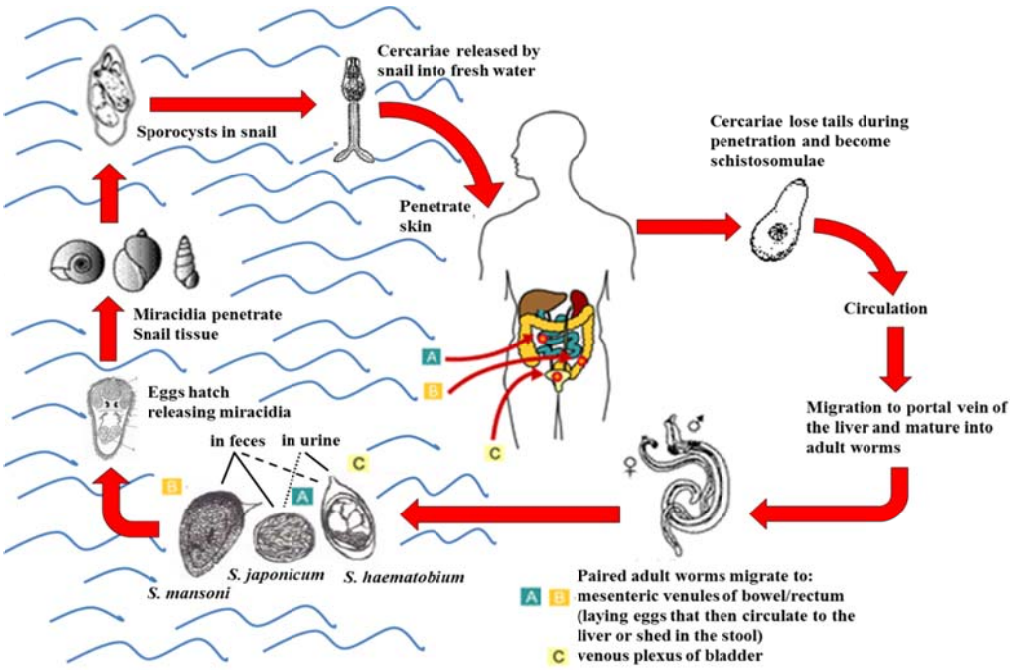

Figure 1.4: Life cycle of *Schistosoma* species
In brief, within fresh water, *Schistosoma* eggs hatch and release miracidia which penetrate into the snail. Within the snail, miracidia metamorphose into sporocysts and produce thousands of cercariae, which are released back into fresh water. Cercariae actively penetrate human skin, lose their tails and become schistosomulae. They then circulate and migrate through the portal venous system and mature into adult worms (female and male). Adult worms pair up and migrate to mesenteric venules of the bowel/rectum (*S. japonicum* and *S. mansoni*) or venous plexus of the bladder (*S. haematobium*). Thereby the female worm releases numerous of eggs per day which are excreted with feces or urine. Adapted from [59].

Figure 1.4 shows diagrammatic representation of the life cycle of Schistosoma species. Infections occur when free-swimming cercariae penetrate into the skin of the human host. Whilst penetrating the skin, cercariae lose their tails and develop into another larval form, the schistosomulae, which migrate via the blood stream into the lung. During a further migration through the portal and urogenital venous system, the larvae mature into adult female or male worms (also known as blood flukes). Adult worms reside and attach to the mesenteric venules in various locations, depending on the species. For example, *S. mansoni* is more likely found in the superior mesenteric veins draining the large intestine, whereas *S. japonicum* resides more frequently in the superior mesenteric veins draining the small intestine. In contrast, *S. haematobium* frequently occurs in the venous plexus of bladder, genital and rectal venules. The adult worms live as a couple, mate by pairing and survive within the human body for long periods of time by feeding on red blood cells. The female worms produce approximately 300-1000 eggs per day, which are deposited into bloodstream and progressively move towards the vein walls and into the lumen of the intestine (*S. mansoni* and *S. japonicum*) or bladder and ureters (*S. haematobium*). These eggs are then excreted with feces or urine, respectively. When eggs are released into fresh water, miracidia hatch from them and steadily swim until they find their intermediate snail host, which mostly belongs to three genera, Biomphalaria glabrata, *Bulinus glabrata* and *Oncomelania glabrata*. Within the snail the miracidia undergo complicated metamorphoses involving asexual reproduction (sporocysts stage) and the production of thousands of the cercariae, which are the infectious form to definite human host [56, 59-61]. However, up to half the eggs do not enter the intestinal lumen and become trapped in the intestinal tract, the liver [56, 62] and sometimes the lung [63]. The continuous deposition of eggs is the underlying instigator of chronic inflammatory host responses and is responsible for the pathology of the disease, called Schistosomiasis or bilharzia (named after Theodor Bilharz, who first identified the parasite in Egypt in 1851).

1.3.2 Pathology of Schistosomiasis

The different forms of pathology that arise during Schistosomiasis correspond to the developmental stages of the worm within the human (section 1.3.1). For example, during penetration and migration through the skin, cercariae secrete proteolytic enzymes that are capable of digesting epidermal keratin [64, 65]; this results in temporary mild itching and a papular dermatitis [66] (Figure 1.5 A). After exposure to heavy numbers of cercariae, patients may present symptoms of pulmonary eosinophilia, also called Loeffler`s syndrome due to the

migration of schistosomulae to the lung. Symptoms include a hypersensitive response associated with elevated IgG and IgE levels and mast cell degranulation, shortness of breath, wheezing and nonproductive cough [69, 70]. Furthermore, acute Schistosomiasis may occur at the beginning of egg laying from adult female worms. The clinical symptoms of this Katayama syndrome include fever, malaise, hepatosplenomegaly development (Figure 1.5 B), eosinophilia, diarrhea, and, in some cases, edema, urticarial, lymphadenopathy, and arthralgia [56, 67, 68].

Chronic Schistosomiasis is characterized by constant local inflammatory responses to trapped schistosome eggs in different host tissues (especially liver and intestine), which form granulomas due to release of soluble egg antigen (SEA) and immune cell infiltration (Figure 1.5 C). The constant inflammation leads to symptoms that include obstruction of the urinary system (*S. haematobium*) or intestinal disease manifested as hepatosplenic inflammation (Figure 1.5 B) and liver fibrosis (*S. mansoni, S. intercalatum, S. japonicum and S. mekongi*). Moreover, renal failure, portal hypertension, diarrhea, anemia, undernutrition and bladder cancer have also associated with the infection [56, 68, 71, 72].

Figure 1.5: Aspects of pathology that arise during Schistosomiasis
(A) Cercarial dermatitis. Adapted from [73]. (B) A woman with hepatosplenomegaly from the Phillipines. (C) An example of an acute liver granuloma developing around *S. mansoni* egg in mouse liver tissue. Infiltrating immune cells include eosinophils, lymphocytes, and some macrophages. Strong levels of fibrotic tissue can been observed through staining histology sections with Masson's blue since the aniline component within the staining procedure stains collagen fibers blue.

1.3.3 Immune responses during Schistosomiasis

The various stages of the parasite (penetrating cercaria, schistosomulae, adult worms and eggs) are all potential sources of antigenic material. Possible antigens include secretory products, especially the histolytic secretions of the penetrating cercariae; excretory products (such as glycosylated proteins and/or lipids), especially those from adult worms and eggs and breakdown products of all stages that may occur from dying or degraded lifestages within the host [60].

As mentioned above, the *Schistosoma* species employ a wide range of strategies to evade and exploit the host immune system in order to ensure their survival. Indeed, adult worms have been shown to live up to 37 years within the humans, fully exposed to the immune system [74]. Strategies employed by the worm to evade host reactions include the ability of worms to coat themselves with host proteins, to enzymatically cleave antibodies and to replace their surface structures with membrane vesicles from the host [61, 75-77]. Moreover, the parasite also uses molecular mimicry, using immunomodulating neuropeptides, such as Proopiomelanocortin-derived peptides, to evade the immune defenses in both hosts (snail and human) [61, 78]. Besides these immune evasion tactics, the parasite also exploits the host immune system to facilitate its own development and transmission. Different studies have shown that the translocation of eggs from the portal capillaries to the gut lumen depends on a competent immune response, as it is diminished in immunosuppressed (such as human immunodeficiency virus (HIV)-infected patients) [79] or *S. mansoni* egg-tolerized mice [80]. Furthermore, adult worms use host cytokine responses for their own growth and development. For example, TNF-α seems to be a necessary signal for female worms to begin egg production [81] and host TGF-β has been shown to regulate worm growth and development, especially during embryogenesis [82, 83]. Despite these intricate immunomodulatory mechanisms, some reactions do occur against the parasite and are summarised in Figure 1.6.

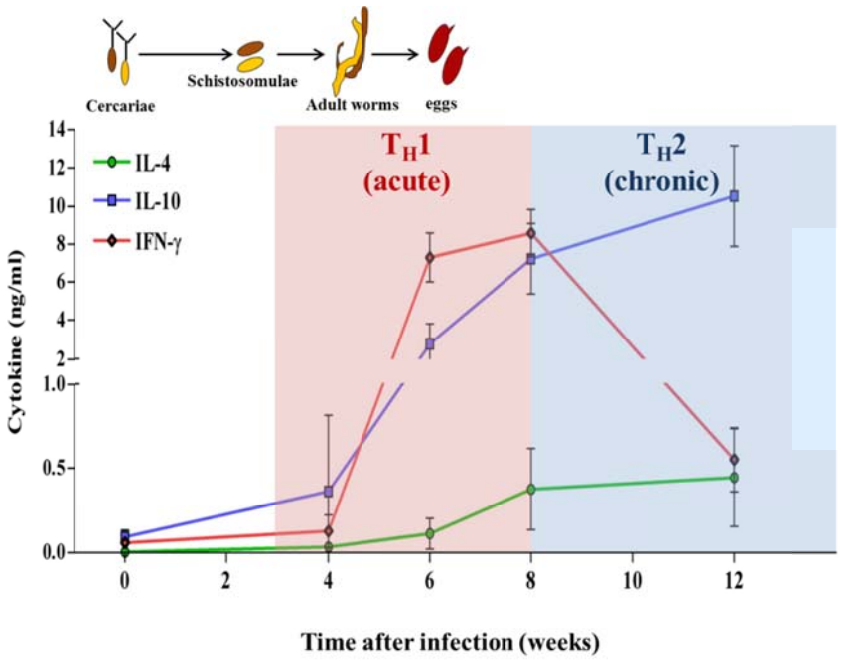

Figure 1.6: Induction and development of T_H1 and T_H2 responses during *S. mansoni* infection
In brief, following cercariae penetration, a T_H1-cell response (such as IFN-γ production) develops (acute phase). As the worms mature and eggs are deposited, a stronger T_H2-cell response (such as IL-4 and IL-10 production) develops (chronic phase).

Since it is problematic to pinpoint the actual timepoint of infection, individual immune responses of humans infected with *Schistosoma* species are difficult to define. Due to the fact that parasite development and pathological outcomes are similar in man and mouse, numerous murine studies have been performed with *S. mansoni* in order to decipher cellular interactions and mechanisms. As depicted in Figure 1.6, T_H1 responses are initiated during the first 5-6 weeks of infection and are characterized by high levels of proinflammatory cytokines, such as IL-1, IL-6, TNF-α and especially IFN-γ [61]. This early T_H1 response is considered to be important for the parasite since it has been shown that during cercarial penetration there is a release of the specific mediator prostaglandin, which usually inhibits the migration of Langerhans cells (DC type) and thereby delays any immune responses [84]. Furthermore, mice which are deficient for this specific prostaglandin receptor (D prostanoid receptor 1) showed normal DC migration and less IFN-γ production, leading to a T_H2-cytokine based response to the parasite [85]. This latter phenotype is usually associated with a reduced number of adult worms [61]. More pronounced T_H2 immune responses are apparent when worms start to mate and produce eggs [86]. Classical T_H2 cytokines include IL-5, one of the hallmarks of helminth infections, but also other circulating cytokines such as IL-4, IL-13 and IL-10 [87-90]. This switch is also accompanied by increased number of specific immune cells (eosinophils, neutrophils, basophils and mast cells) and heightened circulation of immunoglobulins, such as IgE [61]. The strong T_H2 immune response is mostly driven by trapped schistosome eggs, which secrete soluble egg antigen (SEA) within the liver and intestine, leading to granuloma formation (Figure 1.5 C). Components within SEA are such powerful T_H2-cell-response-promoting adjuvants that it encourages immune cell infiltration and supports other T_H2 immune responses to unrelated antigens [86, 87, 91]. Besides the T_H1 and T_H2 immune responses, T_H17 and T_H9 immune responses also play a crucial role during Schistosomiasis. It is known that innate proinflammatory responses against *S. mansoni* induce T_H17 cells which control immunopathology [92]. In addition, T_H9 cells promote T_H2 immune responses leading to pleiotropic effects during *S. mansoni* infection, such as enlargement of the ileum, muscular hypertrophy, mastocytosis, eosinophilia, goblet cell hyperplasia, and increased mucin expression [93].

1.3.4 Granuloma formation

Granulomas that develop around trapped schistosome eggs in the intestine and liver are mainly mediated by T helper cell populations [94-96]. Indeed in the absence of $CD4^+$ T cells or without the possibility to present antigens on MHCII molecules granulomas are absent. Interestingly, the development of hepatic and intestinal granulomas differs. Whilst the granulomas in the liver shrink and become fibrinogenic in the chronic phase of infection, intestinal granulomas do not change in size and appearance [97]. Layland *et al.* further described three developmental stages of granuloma development. They observed that as granulomas became progressively older the makeup of cellular infiltrate altered from high numbers of $CD4^+$ T cells, macrophages and eosinophils to increased levels of $Foxp3^+$ T_{reg} cells. Moreover, these latter cells accumulated in the circumference of older granulomas, in which the eggs had been destroyed and the mass of granuloma contained fibrotic tissue [98, 99]. It was suggested that the migration of these cells into the granulomas controlled the infiltration of other immune cells and their responses, especially eosinophils. As mentioned above, older granulomas contain many collagen fibres indicating high levels of fibrotic tissue. IL-13 is the main T_H2 cytokine driving fibrosis development and different studies have shown that *Schistosoma* infected mice, in which IL-13 is absent [100] by either neutralization with anti-IL-13 antibody treatment [101] or impairment of the IL-13 pathway using IL-4 and IL-13 receptor deficient mice [102, 103], fail to develop fibrosis and thus, prolong host survival [100, 103]. In contrast, further studies have also shown that granuloma formation and fibrosis development are reduced in infected mice if the egg-specific response is converted from a T_H2-dominant to a T_H1-dominant reaction [104-107]. The fine balance of T_H1 versus T_H2 immune responses and the arising immunopathology within the host during Schistosomiasis highlights the complexity and necessity of regulatory mechanisms and represents an example of evolutionary evolved host-parasite interaction.

1.3.5 SEA-mediated immune responses

SEA contains a multitude of various highly glycosylated proteins and lipids [108, 109] and the release of SEA within granulomas propagates strong T_H2 immune responses [86, 87, 91]. Further in-depth research has also been able to identify components within SEA, such as lysophosphatidylserine [110], N-glycans [111] and glycans containing the trisaccharide Lewis X [112-114] that interact with different TLRs and promote T cell polarization. For example, T2 ribonuclease (omega-1), the glycoprotein IPSE/alpha-1 (interleukin 4 inducing principle

from *Schistosoma mansoni* eggs/alpha-1) and the antioxidant peroxiredoxin all drive T_H2 responses by conditioning DCs [115, 116], triggering IL-4-producing basophils [117, 118] or inducing the development of alternatively activated macrophages [119], respectively. In addition, lysophosphatidylserine, derived from *S. mansoni* egg lipid fractions, activates DCs in a TLR2-dependent manner to induce T_H2 and T_{reg} development [110]. Also *in vivo* studies with NOD (non-obese diabetic) mice, which develop spontaneous autoimmune insulin dependent diabetes mellitus, showed that SEA induces TGF-β expression on $CD4^+$ T cells and $Foxp3^+$ T_{reg} cells [120]. Moreover, LNFPIII (lacto-N-fucopentaose III), a Lewis X containing glycan within SEA triggers TLR4 [114], whereas schistosome dsRNA activates TLR3 signalling [121] to induce polarization of DCs towards T_H2 immune responses. As mentioned earlier (section 1.2.1 and 1.2.2), DCs pulsed with various TLR stimuli, such as poly-I:C or P_3Cys (TLR2), LPS (TLR4) or CpG (TLR9) secrete high levels of TNF-α, IL-6 and IL-12 and up-regulate surface molecules associated with DC maturation and activation, such as CD80, CD86 and MHCII. Interestingly, SEA inhibits such TLR-mediated immune responses of DCs [122-127] and augments production of IL-10 [125], which is a regulator of various cytokines [128, 129]. Interestingly, stimulation of DCs with SEA alone did not lead to alteration of co-stimulatory molecule expression and cytokines responses [123, 125]. In addition to triggering TLR, recent studies have also identified components which are recognized and internalized by different C-type lectin receptors (CLRs) [122, 123], such as DC-SIGN (dendritic cell-specific intercellular adhesion molecule-3-grabbing non-integrin) [130], MGL (macrophage galactose lectin) [131] and SIGNR1 (specific intercellular adhesion molecule-3-grabbing non-integrin homolog-related 1) [132]. The exact role of C-type lectin receptors in connection with SEA-mediated immunomodulation is still unclear. However, recently C-type lectin receptors were shown to play a crucial role in the activation of inflammasome complexes [133], such as Dectin-1 recognizes the fungus *Candida albicans* to induce NLRP3 inflammasome activation and IL-1β production [134, 135]. Over the last years much research has focused on the activation of the inflammasome and consequently release of IL-1β. This exciting field of immunology and its connection to parasitic infections is described in detail in the following sections.

1.4 IL-1β and the inflammasome

The history of IL-1β and the discoveries of its immunological properties are closely associated with leukocytes, which elicit fever through the production of endogenous proteins [136]. In 1948, Beeson presented pioneering studies which demonstrated that an endotoxin-free protein from rabbit leukocytes caused fever after bolus injection into rabbits [136, 137]. Almost 30 years later, Dinarello *et al.* purified the human leukocytic pyrogen (LP) and showed that it could induce fever [138]. With advances in technology, the IL-1 gene was also fully cloned and it became apparent that it consists of two distinct proteins, which were termed IL-1α (also called IL-1F1) and IL-1β (also called IL-1F2) [139-141]. Research then elucidated that recombinant IL-1β, in contrast to IL-1α, could induce fever in humans [142, 143] and it was realized that this molecule was actually the endogenous pyrogen published by Beeson [137] and the LP published by Dinarello [138]. Furthermore, in 1984 after molecular cloning a third member of the IL-1 family was described and called the IL-1-inhibitor although later renamed as the IL-1 receptor antagonist (IL-1Ra or IL-1F3) [144-146]. IL-1Ra is a naturally occurring antagonist that blocks IL-1 signals by binding to the IL-1 receptor with almost the same affinity as IL-1α and IL-1β. Since the discovery of these players, IL-1 biology has rapidly developed and further IL-1 family members (IL-1F1-F11) have been discovered [147], such as IL-18 (IL-1F4) [148] and IL-33 (IL-1F11) [149]. However, IL-1β, as well as IL-18, secretion depends on a complex pathway which utilizes a cytoplasmic multiprotein complex called the inflammasome, which cleaves the inactive cytokine precursors (pro-IL-1β or pro-IL-18) into their bioactive forms [150, 151]. The discovery of the inflammasome pathway has provided the basis for deeper understanding of various autoimmune and inflammatory diseases associated with IL-1β activity. Among others, research fields include neonatal-onset multiinflammatory disease (NOMID), Muckle-Wells syndrome, familial cold autoinflammatory syndrome (FCAS), hyper IgD syndrome, familial Mediterranean fever, urate crystal arthritis (gout) [152], diabetes [153], rheumatoid arthritis [154] and bronchial asthma development [155-157] (section 1.4.4).

1.4.1 Architecture of the inflammasome

The association of IL-1β with inflammation and pathogenesis has been known for almost 50 years (section 1.4). Nevertheless, the intracellular mechanisms, which are responsible for IL-1β activation and production, have only recently been deciphered by the purification of the multiprotein complex termed the inflammasome [150]. As depicted in Figure 1.7, the inflammasome consists of different proteins: NALP, pyrin domain (PYD), caspase activation and recruitment domain (CARD), central oligomerization domain (NACHT), leucine rich repeat (LRR) domain and caspase-1 (Casp1); occasionally there is also the involvement of caspase-5 (Casp5) [150, 151, 158].

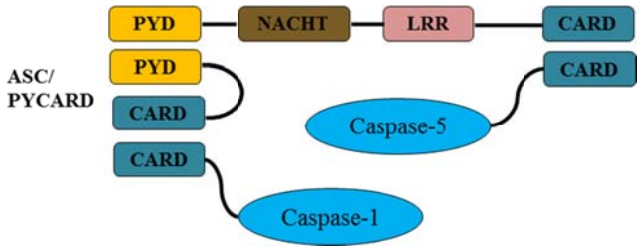

Figure 1.7: The inflammasome, a multiprotein complex
An example of an inflammasome complex is NALP1 (also called NLRP1) which consists of a central oligomerization domain (NACHT), a leucine rich repeat (LRR) domain and a caspase binding region. The latter can also be called CARD (caspase recruitment domain), which is further associated with a pyrin domain (PYD). The PYCARD is more commonly referred to as ASC (apoptosis-associated speck-like protein containing a CARD) and forms the basis for the final recruitment of caspase-1 (Casp1) or sometimes caspase-5 (Casp5). Adapted from [158].

The NALPs [**NA**CHT (NAIP (neuronal apoptosis inhibitory protein); CIITA (MHC class II transcription activators); HET-E (incompatibility locus protein from *Podospora anserina*); TP1 (telomerase-associated protein)), **L**RR (domain-leucine-rich repeat) and **P**YD (pyrin domains)-containing protein] belong to the nucleotide oligomerization domain (NOD)-like receptor (NLR) family of PRR (section 1.2.1) and are involved in aspects of inflammation [158]. Most NLR family members consist of three functional domains: NACHT, which serves as the central oligomerization domain, a C-terminal ligand sensing leucine rich repeats (LRRs) domain and an N-terminal caspase binding region, also called CARD (caspase recruitment domain), which is further associated with a pyrin domain (PYD) [158-161]. This PYCARD, often referred to as ASC (apoptosis-associated speck-like protein containing a CARD), works as an adaptor recruiting Casp1 through PYD-PYD (with NALPs) and CARD-CARD (with Casp1) interaction [162]. Currently, five inflammasome complexes, NALP1 (also called NLRP1) [163], AIM2 [164-167], NALP3 (also called NLRP3) [168], NLRC4

(also called IPAF) [169] and NALP6 (also called NLRP6) [170, 171] have been described. They have been identified through their constellation of inflammasome components and the response to PAMPs and DAMPs (damage associated molecular pattern molecules). An overview of five structures (NLRP3, AIM2, NLRP1/NLRP1b, NLRC4 and NLRP6) and their triggers are depicted in Figure 1.8.

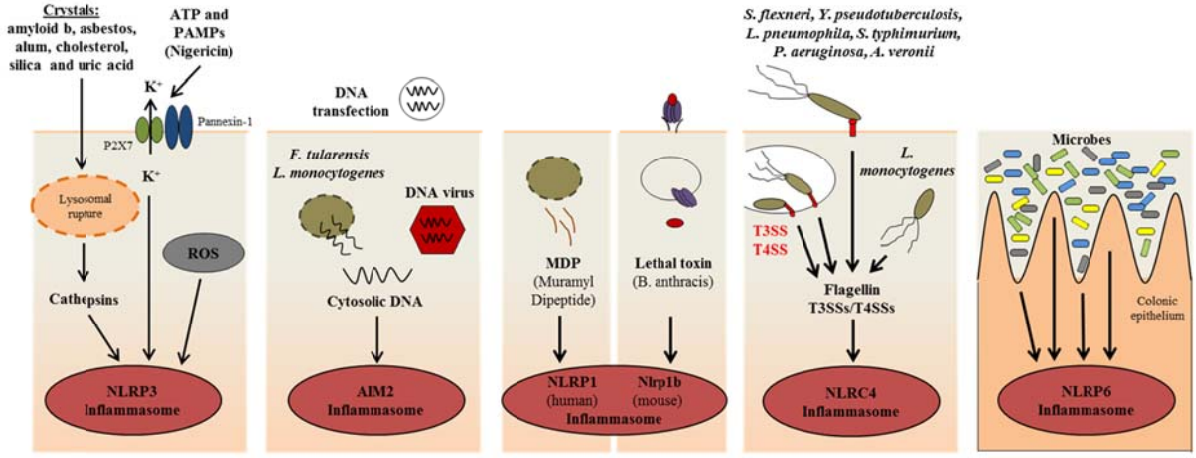

Figure 1.8: Inflammasome complexes are triggered by different stimuli
The NALP3 (also called NLRP3) inflammasome is activated through various stimuli, such as crystals, adenosine triphosphate (ATP) or Nigericin. The activation depends on reactive oxygen species (ROS) production, potassium release (K^+), lysosomal rupture and the release of Cathepsins. The AIM2 inflammasome responds to cytosolic DNA produced from viruses or cytosolic bacterial pathogens, such as *Francisella tularensis* or *Listeria monocytogenes*. The human NLRP1 inflammasome senses muramyl dipeptide (MDP) and the murine Nlrp1b inflammasome has been shown to respond to anthrax lethal toxin. The NLRC4 inflammasome detects flagellin or the type 3/4 secretion systems (T3SS/T4SS) from different bacteria, such as *Shigella flexneri*, *Yersinia pseudotuberculosis*, *Legionella pneumophila*, *Salmonella typhimurium*, *Pseudomonas aeruginosa*, *Aeromonas veronii* and *Listeria monocytogenes*. The NLRP6 inflammasome recognize microbes within the colon. Adapted from [170-172].

Besides the various stimuli and the different activation pathways of the five inflammasome complexes, they all contain the central effector molecule cysteine protease caspase-1 that, upon activation cleaves immature pro-IL-1β and pro-IL-18 into their biological active forms IL-1β and IL-18 respectively [150-152, 158-161, 172].

1.4.2 Mechanisms of inflammasome activation

The majority of studies that have been performed, in order to elucidate the different activation mechanisms of inflammasome complexes, have used NLRP3 since this inflammasome responds to a wide range of structurally unrelated stimuli. Figure 1.9 depicts mainly the different activation mechanisms of the NLRP3 inflammsome.

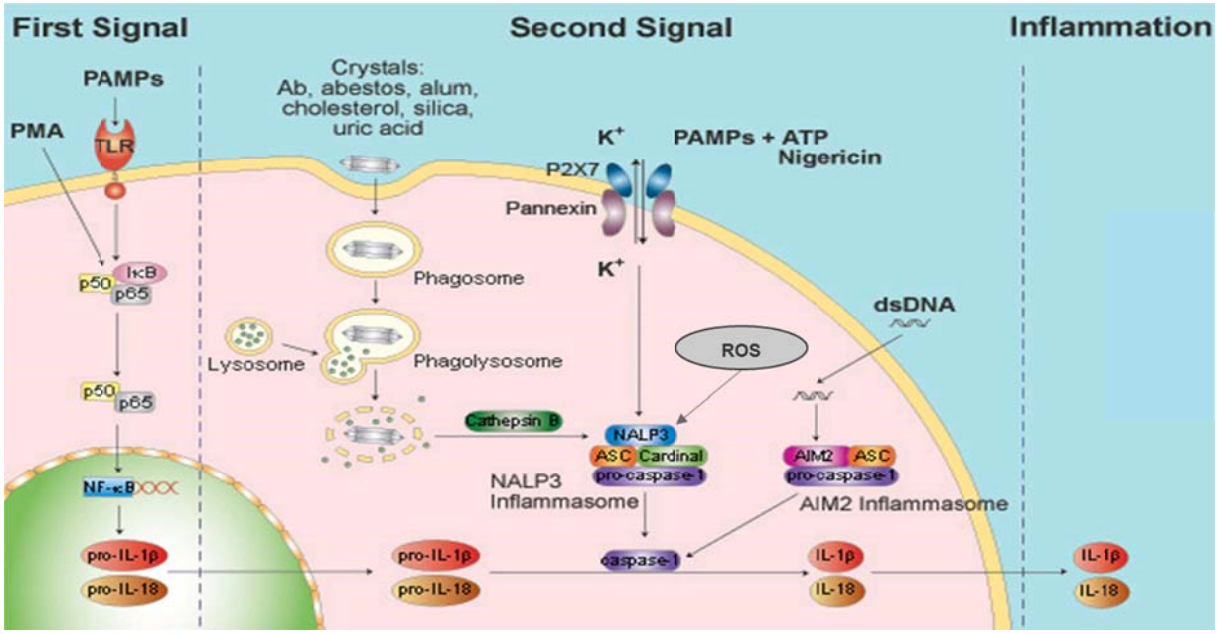

Figure 1.9: Mechanisms of inflammasome activation
To activate the inflammasome two signals are required. The first signal is a TLR-mediated response triggered by PAMPs, leading to activation of NF-κB and accumulation of intracellular inactive pro-IL-1β and pro-IL-18. The second signal leads to the formation of the inflammasome complex (such as NALP3). This is induced by various stimuli such as pore forming toxins like nigericin and ATP, of which the latter is recognized by the P2X7/ pannexin receptor. Alternatively, stimuli are not receptor mediated but promote phagocytosis, such as amyloid-β (Ab), asbestos, alum salt, cholesterol, silica and uric acid crystals. The receptor triggered mediated activation leads to downstream activation of different molecules and signalling pathways, such as potassium efflux and reactive oxygen species (ROS) production, whereas the promotion of phagocytosis leads to lysosomal rupture and the release of cathepsin B into the cytosol. Both mechanisms activate the NALP3 inflammasome leading to the cleavage of pro-caspase-1 into bioactive caspase-1 (Casp1), which then cleaves the accumulated pro-IL-1β and pro-IL-18 into their bioactive forms (IL-1β and IL-18). These cytokines are then secreted and aid inflammatory responses. In addition, AIM2 inflammasome activation is triggered by cytoplasmic double-stranded DNA (dsDNA), leading also to Casp1-mediated cleavage of IL-1β and IL-18. Modified from InvivoGen (http://www.invivogen.com/review-inflammasome).

In general, the activation of the inflammasome can be divided into two signals. The first signal are PAMPs, which activate TLRs, leading to downstream activation of the nuclear factor-κB (NF-κB) and transcription and accumulation of precursor cytokines, such as pro-IL-1β (31 kDa) and pro-IL-18 (22 kDa). Interestingly, pro-IL-1β can also be induced by IL-1β itself [173] via triggering the IL-1 receptor complex, which leads to MyD88 recruitment and downstream NF-kB activation (see section 1.2.1 for details). The second signal recruits the inflammasome components and is mediated through a specific activator. Each of the five inflammasomes is activated through specific danger signals or pathogens, such as the bacterial cell wall component muramyl dipeptide (MDP), which activates the human NLRP1 [174] and anthrax lethal toxin that triggers murine NLRP1b inflammasome [163]. Other well-

described inflammasome triggers include gram-negative bacteria, consisting of type III or type IV secretion systems (*Salmonella, Shigella, Legionella* and *Pseudomonas* species) that activate the NLRC4 inflammasome [175-178] and cytosolic DNA from viruses or bacteria (*Francisella tularensis* or *Listeria monocytogenes*) which mobilize the AIM2 inflammasome [164-167]. Numerous pathogens, such as viruses (Sendai, influenza and adenoviral strains) [179, 180], fungi (*Candida albicans* and *Saccharomyces cerevisiae*) [134, 135] and bacteria (*Staphylococcus aureus*, *Neisseria gonorrhoeae*, *Listeria monocytogenes* and *Salmonella typhimurium*) [181-184] or danger signals, such as elevated ATP [181], ultraviolet B irradiation [185], crystalline forms of monosodium urate (MSU) [186], asbestos, silica [187-189] and amyloid-β aggregates [190] have been shown to activate the NLRP3 inflammasome. To date, there are two main processes that are known to be important for the assembling of the NLRP3 complex. Phagocytosis for example is mainly triggered by crystals and their uptake leads to lysosomal rupture and the release of cathepsin B into the cytosol resulting in NLRP3 inflammasome activation [188]. As an alternative to cathepsin production, the NLRP3 inflammasome can also be activated in a receptor mediated manner and results in the production of reactive oxygen species (ROS) and release of potassium (potassium efflux). For instance, the triggering of the P2X7 receptor through ATP leads to potassium efflux [191-193] and pannexin-1 mediated pore formation [193], which allows the entry of extracellular PAMPs (such as nigericin) leading to NLRP3 inflammasome activation [160]. Another example for receptor mediated NLRP3 inflammasome activation is the fungus *Candida albicans*, which was shown to trigger the Dectin-1 receptor (another CLR; section 1.3.5) [194] and induce downstream signalling by activating the spleen tyrosine kinase Syk via potassium efflux and production of ROS [135]. In addition, it was shown that the source of ROS during NLRP3 inflammasome activation is probably the mitochondria [195], suggesting a close relationship between inflammasome activation and metabolism. Recently, another inflammasome complex termed NLRP6 was discovered. The NLRP6 inflammasome seems to be a crucial regulator for inflammatory responses in the colon and allows recovery from intestinal epithelial damage, but the specific signal that triggers the activation is currently unclear [170, 171].

A result of inflammasome assembling is the activation of the cysteine protease caspase-1 (Casp1) that autocatalytically processes its precursor form (45 kDa) into the active form, which is a heterodimer consisting of 20 kDa and 10 kDa subunits [196]. Active Casp1 then cleaves the precursors of IL-1β (31 kDa) and IL-18 (22 kDa) into bioactive IL-1β (17.5 kDa) and IL-18 (17 kDa) [152, 160]. The mature cytokines are then secreted out of the cell by

different mechanisms, such as exocytosis of secretory lysosomes [197, 198], shedding of plasma membrane microvesicles and/or release via transporters or multivesicular bodies containing exosomes [199].

1.4.3 Biological effects of IL-1β

IL-1β can be secreted by a multitude of immune cells, such as DCs, monocytes, macrophages, mast cells, neutrophils, B and T cells endothelial cells, epithelial cells and even dying cells. It has been described as an important cytokine for the initiation of inflammation and T_H1/T_H2 immune responses and represents a crucial link in translating innate immune responses into the appropriate adaptive immune response [200]. In addition, it is also known that IL-1β can induce gene expression and synthesis of different enzymes, which are essential for metabolisms pathways. These encompass cyclooxygenase type 2, a key enzyme in arachidonic acid metabolism; type 2 phosholipase A, an enzyme responsible for fatty acid metabolism; inducible nitric oxide synthase, an enzyme which is necessary for prostaglandin-E2 platelet activating factor and nitric oxide production. The activation and synthesis of different genes and enzymes can lead to the induction of fever, lowered pain threshold, vasodilation, and hypotension [142, 143, 152]. The ability of IL-1β to increase the expression of adhesion molecules on endothelial cells and to induce different chemokines promotes the infiltration of immune cells into tissues and directs the developing inflammation [152]. Interestingly, it was also shown that IL-1β is an important angiogenesis factor and therefore plays an important role in tumor metastasis and blood vessel formation [201].

Besides its proinflammatory effects, IL-1β can also induce adaptive immune cells and initiate their responses. In correlation, it has been shown that IL-1β contributes to the T_H2 polarized immune responses during murine asthma development by promoting the infiltration of eosinophils and inflammation within the lung [202, 203]. Finally, the role of IL-1β in B cell initiation and antibody production has also been reported [204]. Moreover, different studies observed that IL-1β itself can induce IL-17A production and T_H17 cell differentiation [205-207], a distinct T helper cell type, which induces high amounts of IL-17 and plays a crucial role in different autoimmune diseases, such as multiple sclerosis, juvenile diabetes, rheumatoid arthritis, and Crohn's disease [52, 53] (section 1.2.3).

1.4.4 IL-1β-mediated autoinflammatory diseases

Almost all autoimmune diseases are caused by overreaction or impaired regulation of the immune system. During an infection or tissue injury controlled inflammatory responses are crucial for protection and maintenance of cell and tissue functionality but become destructive if they persist. The critical role of IL-1β during inflammatory responses was highlighted by the importance of the inflammasome during the development of autoinflammatory immune diseases. In general, autoinflammatory diseases are usually induced by dysfunctional activation of Casp1 which corresponds with increased secretion of IL-1β [152]. Elevated levels of IL-1β and autoinflammatory diseases have also been associated with NLRP3 mutations [208, 209], or impaired signalling of the inflammasome [192, 198]. Indeed, investigations into the understanding of inflammasome activation pathways provided the basis for the treatment of several autoinflammatory diseases. Anakinra (Kineret®), an IL-1 receptor antagonist (IL-1Ra), is now the standard therapy for patients with systemic-onset juvenile idiopathic arthritis [210] and refractory adult Still's disease [211], as well as a reagent for the treatment of gout [212], type 2 diabetes [213], rheumatoid arthritis [152] and diverse fever syndromes [200]. Recently, two new reagents called rilonacept (IL-1 trap) and canakinumab (specific anti-IL-1β monoclonal antibody) have been developed and approved for the treatment of diverse autoinflammatory diseases, such as rheumatoid arthritis, gout and type 2 diabetes [200].

1.4.5 IL-1β influences allergic asthma development

Besides the autoinflammatory diseases mentioned in section 1.4.4., several studies have demonstrated the pivotal role of IL-1β during bronchial asthma development since it promotes the infiltration of eosinophils and inflammation within the lung [155-157, 202, 203]. In addition, a recent study also implied that NLRP3 inflammasome activation influences allergic airway inflammation [214]. According to the WHO, over 235 million people currently suffer from allergic asthma disease [215]. Asthmatic development is characterized by T_H2 polarized immune responses, such as IL-4, IL-5 and IL-13, allergen-specific immunoglobulin production and eosinophilic inflammation, as well as goblet cell infiltration and increased mucus production within the lung leading to airway hyperresponsiveness (AHR) [216, 217]. The long-term unresolved airway inflammation leads to structural changes, called airway remodelling that is characterized by constant epithelial alterations, goblet cell and submucosal gland hyperplasia, smooth muscle cell hyperplasia and hypertrophy,

subepithelial fibrosis, microvascular proliferation, cartilage changes, airway wall edema, and inflammatory cell infiltration [218, 219]. However, the mechanisms of asthma development and especially the role of the NLRP3 inflammasome and IL-1β remain unclear and required further investigation. Therefore, to characterize asthma development, murine allergic airway inflammation models are widely used to characterize allergic asthma development. For example, ovalbumin (OVA) is used as a common allergen since it elicits allergic airway inflammation with features similar to those found in asthmatic humans [220].

1.5 Aims of the study

The helminth *S. mansoni* is one of the major pathogens of the disease Schistosomiasis, which, next to malaria, is the second most socioeconomically devastating parasitic disease. As mentioned above a main characteristic of Schistosomiasis is the change in adaptive immune responses since the initial T_H1 polarised response is replaced by T_H2 reactions once fecund females begin to lay eggs. Some trapped schistosoma eggs, within the liver and intestine tissues, induce the development of granulomas, the major cause of morbidity. Viable or degrading eggs release SEA and components thereof promote antigen-specific T_H2 cells. In contrast, the presence of SEA in co-culture with DCs elicits little cellular activity. Indeed, SEA actually suppresses innate responses of TLR-triggered cells although the responsible mechanisms behind this immunomodulating capacity remain unclear. In order to obtain a better understanding into the complex mechanisms of *S. mansoni* infection and SEA-mediated responses, a murine infection model of *S. mansoni* was used to analyse parasitological and immunopathological parameters. Furthermore, an *in vitro* assay was established with DCs to decipher whether SEA could mediate or induce inflammasome activation and the mechanisms thereof. The aims of the present study are as followed:

1. Investigating the innate immunomodulatory mechanisms of SEA *in vitro*.

    a. Does SEA suppress immune responses from TLR-primed DCs?
    b. What components are required for SEA-mediated responses on DCs?
    c. Is the inflammasome complex involved in SEA-mediated immune responses?

2. Investigation of SEA-mediated inflammasome complex activation.

    a. Which inflammasome complex is activated after SEA stimulation?
    b. What are the signalling mechanisms of SEA-mediated inflammasome activation?

3. Deciphering inflammasome activation mechanisms during the T_H2 phase of an ongoing *S. mansoni* infection.

    a. What is the role of the inflammasome during *S. mansoni* infection?
    b. Are immune responses influenced by inflammasome activation during *S. mansoni* infection?

4. Investigating the role of inflammasome activation during a T_H2 polarized murine allergic airway inflammation model.

    a. Is there a role for inflammasome activation during allergic airway inflammation?
    b. Is it possible to treat allergic airway inflammation with anti-autoinflammatory reagents, such as Anakinra?

2 Material and methods

2.1 Materials

2.1.1 Equipment

Agarose gel documentation system	Bio-Rad
Agarose gel electrophoresis system (Sub-Cell® GT)	Bio-Rad
Automatic ice machine (Scotsman MF36)	Gastro
Automatic pipettes (2-1000µl)	Gilson®
ÄKTAprime™ plus	GE Healthcare
Balance (440-33N)	Kern
Balance (XB120A)	Precisa
BD FACSCalibur™ flow cytometer	BD
Biological safety cabinet (Hera safe)	Thermo Scientific®
Centrifuge (Biofuge fresco)	Heraeus
Centrifuge (Eppendorf 5424)	Eppendorf
Centrifuge (Megafuge 3.0R)	Thermo Scientific®
Centrifuge (Shandon Cytospin 3)	Thermo Scientific®
Cooling plate (COP 30)	Medite
CyAn ADP Lx P6	DakoCytomation
CyAn ADP Lx P8	DakoCytomation
Disperser (T10 basic Ultra-Turrax®)	IKA
ELISA microplate reader (Sunrise™)	Tecan
EZ Cytofunnels®	Thermo Scientific®
Freezer (-20°C)	Bosch
Freezer (-80°C)	Thermo Scientific®
Freezing container (Nalgene® Mr. Frosty)	Sigma®
Fridge	Bosch
Glassware's	Schott
Homogeniser (5ml)	B Braun
Incubator (BBD 6220)	Heraeus
LumiNunc™ 96-well plates (white)	Nunc

Microplate luminometer (Orion II)	Berthold Technologies
Microscope (Axioscop)	Zeiss
Microscope (Axiovert)	Zeiss
Microwave (1100W)	Panasonic
Milli-Q Integral System	Millipore™
Mini-PROTEAN electrophoresis system	Bio-Rad
Mini-Pump variable flow	Neolab®
MoFlo™ XDP	Beckman Coulter
Multichanel pipettes (Acura® 855; 5-350µl)	Socorex
Multipette® plus	Eppendorf
Orbital shaker (3005)	GFL
OVA-challenge chamber	MRI
Paraffin embedding system (TB 588)	Medite
Paraffin oven	Memmert
Pari Boy® SX nebulizer	Pari
pH-meter (MultiCal®)	WTW
Pipetboy (acu)	IBS
Power supply (Power Pac 3000)	BioRad
Power supply (EV231)	Peqlab
Radiographic cassettes	Goos-Suprema
Rotary microtome automatic (RM 2245)	Leica
Rotating mixer (RM 5)	Assistant
Semi-dry electroblot system	Bio-Rad
Shandon cytoclips	Thermo Scientific®
Shandon Excelsior ES tissue processor	Thermo Scientific®
Stericup® filter units (500ml)	Millipore™
Superdex™ 75 column	GE Healthcare
Thermocycler (T3000)	Biometra
Thermomagnetic stirrer (IKAMAG® REO)	IKA
Thermomixer (compact)	Eppendorf
Tissue cool plate (COP 20)	Medite
Tissue flotation bath (TFB 35)	Medite
Ultracentrifuge (Optima™ L-100 XP)	Beckman Coulter
Vertical dual gel electrophoresis (Perfect Blue; Twin M)	Peqlab

Vortex mixer (Reax top)	Heidolph
Water bath	Memmert
Western blot processor (Curix 60)	AGFA
Wet electroblotter system (PerfectBlue)	Peqlab

2.1.2 Additional software

FlowJo (Flow cytometry analysis software)	TreeStar
GraphPad Prism 5 (Biostatistics, curve fitting and scientific graphing programme)	GraphPad Software
Magellan™ (Data analysis software for microplate reader)	Tecan
Simplicity 2.1 (Data analysis software for microplate luminometer)	Berthold Technologies

2.1.3 Consumables

Blood agar plates	BD
Cell scraper	TPP®
Cell strainer (40-100µm)	BD
Centripreps®	Amicon
Combitips plus® (0.2-2.5ml)	Eppendorf
Cover slips	Roth®
Cryo vials	Alpha Laboratories
Culture plates (6-, 12-, 24-, 96-well)	BD
Disposable bags	Roth®
ELISA plates (96 well)	Nunc
Eppendorf tubes (0.5-2ml)	Eppendorf
FACS tubes (Microtubes, 1.2ml)	Alpha Laboratories
Fast-Read 102®	Biosigma
Glass slide	Langenbrinck
Gloves	Meditrade®
Hypodermic needles (Sterican®)	B Braun
MacConkey agar plates	BD
Medical x-ray films (100NIF, 18x24)	FUJI
Parafilm M®	Pechiney
Petri dishes	Greiner

Pipet tips (10-1000µl)	Starlab
Protran® nitrocellulose transfer membrane (pore size 0.45µm)	Whatman®
Reaction tubes	Zefa-Laborservice
Scalpels	Feather
Shandon filter cards	Thermo Scientific®
Sterile filters (0.22µm, 0.4µm)	VWR Lab Shop
Serological pipettes (5-50ml)	Greiner
Sub-Q syringes (1ml)	BD
Syringes (1-25ml)	B Braun
Syringe filter (0.2µm, 0.45µm)	Sartorius
Tissue culture flask (50-500ml)	BD
Tubes (15ml, 50ml)	Greiner
Whatman™ papers	Schleicher & Schuell

2.1.4 Reagents

Acetic acid	Roth®
Acetone	Fischer Scientific
Acid fuchsin	Morphisto
Acrylic/Bis-Acrylic-solution 30% (v/v) 29:1	Roth®
Adenosine-5`-triphosphate (ATP) disodium salt	Roth®
Agarose	Sigma®
Aluminium hydroxide ($Al(OH)_3$)	Sigma®
Ammonium chloride (NH_4Cl)	Roth®
Ammonium persulphate (APS)	Roth®
Anakinra (Kineret®)	Sobi
Aniline blue	Morphisto
Bovine serum albumin (BSA)	PAA
Bromophenol blue	Roth®, Sigma®
Chloroform	Roth®
Collagenase (from *Clostridium histolyticum*)	Sigma®
CpG1668 (Cytosine phosphate guanine)	TIB MolBiol
Deoxynucleoside triphosphate (dNTPs)	Promega
Deoxyribonuclease I from bovine pancreas (DNAse)	Sigma®

Di-sodium carbonate (Na_2CO_3)	Sigma®
DirectPCR-tail lysis reagent	Peqlab
Dithiothreitol (DTT)	Roth®
Entellan®	Merck
Eosin 1% (v/v)	Morphisto
Ethanol 70%-99.8% (v/v)	MRI Pharmacy
Ethidium bromide	Roth®
Ethylenediaminetetraacetic acid (EDTA)	Roth®
Ethylene glycol tetraacetic acid (EGTA)	Sigma®
Forene®	Abbott
Formaldehyde solution 37% (v/v)	Sigma®, Merck
Gentamicin (10mg/ml)	PAA
Glycerine	Roth®, Sigma®
β-Glycerophospate	Sigma®
Glycine	Sigma®
Hydrogen chloride (HCl)	Roth®
4-(2-Hydroxyethyl)-1-piperazineethanesulfonic acid (HEPES)	Sigma®
IGEPAL (Nonionic detergent)	Sigma®
Isopropanol	MRI Pharmacy
LPS 0127:B8 (Lipopolysaccharide)	Sigma®
Mayer`s haematoxylin	Morphisto
Methanol	Roth®
β-Mercaptoethanol	Roth®, Sigma®
Narcoren®	Merial
OVA (Albumin, from chicken egg white) grade V and VI	Sigma®
Paraformaldehyde (PFA)	Sigma®
Percoll™	GE Healthcare
Periodic acid	Morphisto
Phenol	Roth®
Phenylmethanesulfonyl fluoride (PMSF)	Sigma®
Phosphate buffered saline (PBS)	MRI
Phosphomolybdic acid	Morphisto
Potassium hydroxide (KOH)	Merck
Powdered PBS (Phosphate buffered saline)	Biochrom

Powdered milk	Roth®
Protease inhibitor cocktail tablets (complete)	Roche
Proteinase K (20mg/ml)	Peqlab
P_3Cys (Palmitoyl-cysteine ((*RS*)-2,3-di(palmitoyloxy)-propyl)	Sigma®
RNAlater®	Ambion®
Roti®-Histofix 4% (v/v)	Roth®
Roti®-Safe GelStain	Roth®
Schiff reagent	Morphisto
Sodium chloride (NaCl)	Roth®, Merck
Sodium dodecyl sulfate (SDS)	Roth®
Sodium hydrogen carbonate ($NaHCO_3$)	Merck
Sodium orthovanadate (Na_3VO_4)	Sigma®
Sucrose	Roth®
Sulphuric acid (H_2SO_4)	Merck
3,3',5,5'-Tetramethylbenzidine (TMB) substrate	BD
Tetramethylethylenediamine (TEMED)	Bio-Rad, Sigma®
Trichloroacetic acid (TCA)	Sigma®
Tris(hydroxymethyl)aminomethane (Tris)	Merck, Roth®
Trisodium citrate dihydrate	Roth®
Triton® X-100	Bio-Rad
Trypan blue solution 0.4% (v/v)	Sigma®
Tween® 20	Sigma®
Vancomycin hydrochloride (VANCO-cell® 500mg)	Cellpharm
Weigert`s haematoxylin	Morphisto
Western blot developer reagent (GV60)	Adefo
Western blot fixer reagent (GV60)	Adefo
Xylene	Engelbrecht

2.1.5 Medium supplements

DMEM High Glucose (4.5g/l; with L-Glutamine)	PAA
Dimethyl sulfoxide (DMSO)	Sigma®
Dulbecco`s PBS (Endotoxin-free)	PAA
Fetal calf serum (FCS)	PAA

GM-CSF (Granulocyte-macrophage colony-stimulating factor)	PeproTech
HEPES (cell culture)	PAA
β-Mercaptoethanol for cell culture	Gibco®
Non-essential amino acids (100x)	PAA
OPTI-Mem®	Gibco®
Penicillin/Streptomycin (100x)	PAA
RPMI 1640 (with L-Glutamine)	PAA
Sodium pyruvate solution (100mM)	PAA

2.1.6 Chemical inhibitors, blocking and uncoupling agents

(2R,4R)-4-Aminopyrrolidine-2,4-dicarboxylic acid (APDC)	Alexis®
Carbonyl cyanide p-(tri-fluromethoxy)phenyl-hydrazone (FCCP)	Sigma®
Cytochalasin D (CytD)	Sigma®
2,4-Dinitrophenole (DNP)	Sigma®
Glibenclamide	Alexis®
N-Acetyl-L-cysteine (Nac)	Sigma®
Potassium chloride (KCl)	Roth®
R406 (Syk kinase inhibitor)	Rigel

2.1.7 Kit systems

BD OptEIA™ (TMB substrate)	BD
CellTiter-Glo® (Luminescent cell viability assay)	Promega
CytoTox 96® (Non-radioactive cytotoxicity assay)	Promega
DC protein assay	Bio-Rad
Diff-Quik staining set	Medion Diagnostics
EZ-Run™ protein gel solution (10-15%)	Fisher BioReagents®
Foxp3 staining buffer set	eBioscience
Glyko® (Enzymatic deglycosylation kit)	ProZyme®
GoTaq® DNA polymerase (including 5x Green GoTaq® reaction buffer)	Promega
Mouse ELISA Kits (Duo Set®; IL-5, IL-10)	R&D
Mouse ELISA Kits (Ready-Set-Go) (TNF-α, IFN-γ, IL-1β, IL-5, IL-6, IL-10, IL-13, IL-17A)	eBioscience
Western Lightning®-ECL (Chemoluminescence substrate)	Perkin Elmer

2.1.8 Size standards

Gene Ruler^{TM} 1kb DNA ladder	Fermentas
Protein marker V (peqGold)	Peqlab

2.1.9 Antibodies

Table 2.1 depicts all antibodies which were used for the data presented in this study. ELISA antibodies from the eBioscience and R&D ELISA-Kits are not included (section 2.1.7).

Name	Antigen	Con-jugate	Species	Dilution	Producer	Method
α-mouse CD3e (Clone 17A2)	CD3	-	Rat	1:1000	eBioscience	*in vitro* stimuli
α-mouse CD4-APC (Clone GK1.5)	CD4	APC	Rat	1:1000	eBioscience	FACS
α-mouse CD4-FITC (Clone GK1.5)	CD4	FITC	Rat	1:1000	eBioscience	FACS
α-mouse CD4-PE (Clone GK1.5)	CD4	FITC	Rat	1:1000	eBioscience	FACS
α-mouse CD11b-PE (Clone M1/70)	CD11b	PE	Rat	1:1000	eBioscience	FACS
α-mouse CD11c-FITC (Clone N418)	CD11c	FITC	Armenian Hamster	1:1000	eBioscience	FACS
α-mouse CD11c-PE (Clone N418)	CD11c	PE	Armenian Hamster	1:1000	eBioscience	FACS
α-mouse CD25-APC (Clone PC61.5)	CD25	APC	Rat	1:1000	eBioscience	FACS
α-mouse CD25-PE (Clone PC61.5)	CD25	PE	Rat	1:1000	eBioscience	FACS
α-mouse CD16/32 Fc receptor block (Clone 93)	CD16/ 32	-	Rat	1:1000	eBioscience	FACS
α-mouse CD28 (Clone 37.51)	CD28	-	Golden Syrian Hamster	1:1000	eBioscience	*in vitro* stimuli
α-mouse CD83-FITC (Clone Michel-17)	CD83	FITC	Rat	1:1000	eBioscience	FACS
α-mouse CD86-APC (Clone GL1)	CD86	APC	Rat	1:1000	eBioscience	FACS
α-mouse F4/80-APC (Clone BM8)	F4/80	APC	Rat	1:1000	eBioscience	FACS
α-mouse F4/80-FITC (Clone PC61.5)	F4/80	FITC	Rat	1:1000	eBioscience	FACS
α-mouse/rat Foxp3-FITC (Clone FJK-16s)	Foxp3	FITC	Rat	1:1000	eBioscience	FACS
α-mouse IgE-Biotin (Clone RME-1)	IgE	Biotin	Rat	1:400	Biozol	ELISA

α-mouse IgG1-Biotin (Clone RMG1-1)	IgG1	Biotin	Rat	1:400	Biozol	ELISA
Mouse α-ovalbumin IgE (Clone 3G2E1D9)	OVA	-	Mouse	1:1000	Biozol	ELISA
Mouse α-ovalbumin IgG1 (Clone 2C6)	OVA	-	Mouse	1:1000	Biozol	ELISA
Goat-α-rabbit-HRP (#7074)	Rabbit IgG	HRP	Goat	1:1000	Cell signaling	WB
Poly-rabbit-αCasp1 p10 (sc-514)	Casp1 (p10)	-	Rabbit	1:200	Santa Cruz®	WB
Poly-rabbit-αCasp1 p20	Casp1 (p20)	-	Rabbit	1:200	Gift from O. Groß	WB
Poly-rabbit-αIL-1β (sc-7884)	IL-1β	-	Rabbit	1:200	Santa Cruz®	WB
Poly-rabbit-α-β-Actin (#4970)	β-Actin	-	Rabbit	1:1000	Cell signaling	WB
Rat-α-mouse-Dectin-2 (Clone D2.11E4)	Dectin-2	-	Rat	-	AbD Serotec	*in vitro* blocking
Rat IgG2a (Isotype control)	Negative control	-	Rat	-	AbD Serotec	*in vitro* blocking

Table 2.1: Antibodies used for ELISA, FACS, Western blot (WB) analysis and *in vitro* stimulation and blocking experiments

2.1.10 Buffers and solutions

All buffers and solutions were prepared with Millipore Q distillated water.

2.1.10.1 Buffers for genotyping PCR

Polymerase buffer	400µl	5x Green GoTaq® reaction buffer (including loading buffer)
	40µl	10mM dNTPs
	40µl	1% BSA (w/v)
	1260µl	H_2O
TAE buffer	40mM	Tris-Acetic acid (pH8.3)
	1mM	EDTA
Tail-digestion solution	250µl	DirectPCR-tail lysis reagent
	3µl	Proteinase K (20mg/ml)

2.1.10.2 Buffers and solutions for SDS-polyacrylamide-gel electrophoresis

5x Sample buffer	250mM	Tris-HCl (pH6.8)
	10% (w/v)	SDS
	10% (v/v)	Glycerine
	500mM	DTT
	0.1% (w/v)	Bromophenol blue
Laemmli buffer	2.9g/l	Tris-HCl (pH 8.3)
	14.4g/l	Glycine
	1g/l	SDS
SDS-separating gel 10%	3.3ml	Acrylic/Bis-Acrylic-solution
	2.5ml	1.5M Tris-HCl (pH 8.8)
	100µl	10% SDS (w/v)
	4ml	H_2O
	50µl	10% APS (w/v)
	5µl	TEMED
SDS-separating gel 15%	5ml	Acrylic/Bis-Acrylic-solution
	2.5ml	1.5M Tris-HCl (pH 8.8)
	100µl	10% SDS (w/v)
	2.3ml	H_2O
	50µl	10% APS (w/v)
	5µl	TEMED
SDS-stacking gel	0.66ml	Acrylic/Bis-Acrylic-solution
	0.3ml	2M Tris-HCl (pH 6.8)
	200µl	10% SDS (w/v)
	3.9ml	H_2O
	25µl	10% APS (w/v)
	5µl	TEMED

SDS-ready to use gel (10-15%)	10ml	EZ-Run™ protein gel solution
	60µl	10% APS (w/v)
	6µl	TEMED

2.1.10.3 Buffers and solutions for Western blot

10xTrisGylcine buffer	0.25M	Tris
	1.92M	Glycine
TBST	20ml	1M Tris
	30ml	5M NaCl
	1ml	Tween® 20
	949ml	H_2O
Transfer buffer	200ml	Methanol
	100ml	10xTrisGlycine buffer
	700ml	H_2O
Blocking buffer	25g	Powdered milk
	25ml	1M Tris (pH 7.5)
	15ml	5M NaCl
	5ml	10% Triton® X-100 (v/v)
	455ml	H_2O
Stripping buffer	100mM	Glycin
	10mM	β-Mercaptoethanol
	pH 2.75	

2.1.10.4 Buffers and solutions for ELISA

Reagent buffer	1x	PBS (pH 7.2-7.4)
	1% (w/v)	BSA
Washing buffer	1x	PBS (pH 7.2-7.4)
	0.05% (v/v)	Tween® 20

Stopping solution	2M	H_2SO_4
OVA-coating buffer	8.4g/l	$NaHCO_3$
	3.56g/l	Na_2CO_3
OVA-washing buffer	50mM	Tris
	0.5% (v/v)	Tween® 20
	pH 7.4	
OVA-blocking buffer	50mM	Tris
	3% (w/v)	BSA

2.1.10.5 Buffers and solutions for FACS

FACS buffer	1x	PBS (pH 7.2-7.4)
	2% (v/v)	FCS
Fc block solution	1x	FACS buffer
	0.1% (v/v)	α-mouse CD16/32 (Fc receptor block)

2.1.10.6 Buffers for cell lysis and bronchoalveloar lavage preparation

Lysis buffer	50mM	HEPES
	150mM	NaCl
	1mM	DTT
	1mM	EDTA
	1% (v/v)	IGEPAL (Nonionic detergent)
	10% (v/v)	Glycerine
	20mM	β-Glycerophospate
	1mM	Na_3VO_4
	0.4mM	PMSF
	1 tablet	Protease inhibitor cocktail tablets
	1mM	EGTA

BAL (Bronchoalveloar lavage) buffer	50ml	Dulbecco`s PBS (1x)
	1 tablet	Protease inhibitor cocktail tablets

2.1.10.7 Solutions used for worm perfusion

Worm rinsing solution	7.5g/l	Trisodium citrate dehydrate
	85g/l	NaCl
Worm perfusion solution	1x	DMEM High Glucose
	5% (v/v)	FCS
	2% (v/v)	HEPES (cell culture)

2.1.10.8 Buffers and solutions for Egg preparation

Vancomycin solution	500mg	Vancomycin hydrochloride
	10ml	0.9% NaCl (w/v)
Collagenase solution	500mg	Collagenase
	5ml	Dulbecco`s PBS (1x)
DNase solution	1g	DNase I
	146ml	Dulbecco`s PBS (1x)
Egg-PBS solution	1x	Dulbecco`s PBS (1x)
	0.1% (v/v)	Vancomycin solution
	0.5% (v/v)	Gentamicin
Liver digestion solution	25ml	Egg-PBS solution
	1ml	Collagenase solution
	3ml	DNase solution
	500µl	Penicillin/Streptomycin
Percoll solution	8ml	Percoll™
	32ml	0.25M Sucrose

2.1.11 Cell culture mediums and buffers

Complete medium	1x	RPMI 1640
	10% (v/v)	FCS
	1% (v/v)	Penicillin/Streptomycin
	1% (v/v)	Non-essential amino acids
	1% (v/v)	Sodium pyruvate solution
	0.1% (v/v)	β-Mercaptoethanol for cell culture
BMDC medium	50ml	Complete medium
	10µg	GM-CSF
Freezing medium	1x	RPMI 1640
	40% (v/v)	FCS
	10% (v/v)	DMSO
ACT buffer	17mM	Tris
	160mM	NH_4Cl
	pH 7.2	

2.1.12 Primers for genotyping PCRs

All genotyping primers were solved with Millipore Q distilled water to a concentration of 100pmol/µl.

ASC genotyping primers (Metabion)

JT 4295	5`-CTAGTTTGCTGGGGAAAGAAC-3`	(mutant)
JT 4296	5`-CTAAGCACAGTCATTGTGAGCTCC-3`	(wt common)
JT 4297	5`-AAGACAATAGCAGGCATGCTGG-3`	(wt)

NLRP3 genotyping primers (Metabion)

JT 6030 Ay	5`-AAGTCGTGCTGCTTCATGT-3`	(mutant)
JT 6031 Ay	5`-TCAAGCTAAGAGAACTTTCTG-3`	(wt common)
JT 6032 Ay	5`-ACACTCGTCATCTTCAGCA-3`	(wt)

Dectin-2 genotyping primers (Metabion)

D2A	5`-CATTATACGAAGTTATCTCGAGTCGC-3`	(mutant)
D2B	5`-AGGACAAGCAGCTAACCATTCAGC-3`	(wt common)
D2C	5´-AGATCCTCATCACAGTACGTATTCC-3`	(wt)

IL-1R genotyping primers (Sigma®)

JT 7088 Ay	5`-ATTCTCCATCATCTCTGCTGGTA-3`	(wt forward)
JT 7089 Ay	5`-ATCTCAGTTGTCAAGTGTGTCCC-3`	(wt reverse)
JT 7090 Ay	5`-TGAATGAACTGCAGGACGAGGCA-3`	(mutant forward)
JT 7091 Ay	5`-TCAGCCCATTCGCCGCCAAGCTC-3`	(mutant reverse)

2.1.13 Mice

C57BL/6 and BALB/c wildtype mice were obtained from Harlan®. NLRP3-, IL-1R-deficient mice on C57BL/6 and BALB/c background, as well as the ASC-deficient mice on BALB/c background were obtained from Prof. Juerg Tschopp (University of Lausanne) and bred under specific pathogen-free (spf) conditions in the animal house of the Institute of Medical Microbiology, Immunology and Hygiene (MIH), TU Munich. Murine Casp1- and P_2X_7-deficient bone-marrow cells (C57BL/6) were a further kind gift from Prof. Juerg Tschopp. ASC-, CD36- and DAP12-deficient mice on C57BL/6 background were obtained from and bred in the MIH under spf conditions. Dectin-1- and Dectin-2-deficient mice on C57BL/6 were obtained from Prof. Gordon Brown (University of Aberdeen) and Prof. Yoichiro Iwakura (University of Tokyo) respectively and bred in the MIH under spf conditions. FcRγ-, CD206- and Card9-deficient mice on C57BL/6 background were a kind gift from Prof. Falk Nimmerjahn (University of Erlangen-Nuernberg), Sigrid E. M. Heinsbroek (University of Oxford) and Prof. Jürgen Ruland (University Munich), respectively. All mouse strains were backcrossed at least nine generations onto either the C57BL/6 or BALB/c strain. Experimental mice were sex- and age-matched and the experiments were performed in accordance with local government regulations (license number for animal testing 2112531 147/08). Finally, NMRI mice were also obtained from Harlan® as mammalian host for *Schistosoma mansoni* cycle and to obtain infected livers for the preparation of eggs or SEA.

2.2 Molecular biological methods

2.2.1 Polymerase chain reaction (PCR)

The polymerase chain reaction (PCR) was developed in 1983 by Kary Mullis and is a technique that amplifies a few specific DNA sequences into thousands of copies. A basic PCR reaction consists of a DNA template, primers that are complementary to the 3` ends of the desired DNA template strand, DNA-polymerase, deoxynucleoside triphosphates (dNTPs) and a buffer solution supplying optimal conditions for DNA-polymerase activity. The essential function of the PCR reaction is the ability of the DNA-polymerase to duplicate DNA sequences. The amplifying reaction is classified into 5 specific steps (initiation, denaturation, annealing, elongation and final elongation) and each step requires discrete temperature changes. The first step is the initialization or activation of the DNA-polymerase, such as Taq polymerases, at 94-98°C. Taq polymerases are frequently used in PCR reactions because of their thermostability and optimal amplification rates at high temperatures. In addition to the initiation of the Taq polymerase, the hydrogen bonds between the complementary bases of the DNA template are also disrupted at temperatures between 94°C and 98°C, leading to single-stranded DNA (denaturation step). After lowering the temperatures to 48-65°C primers anneal specifically to the closely matched single-stranded DNA template sequence (annealing step). After primer annealing, the Taq polymerase can bind to the primer-template hybrid and synthesizes a new DNA strand, complementary to the DNA template strand, using dNTPs (elongation step). The elongation temperature depends on the optimum activity of the Taq polymerase, which ranges between 70°C and 80°C. However, the commonly used temperature for elongation is 72°C. The denaturation, annealing and elongation steps are repeated up to 40 times (cycles) to reach sufficient amounts of amplified DNA. A final elongation step at 72°C is performed to ensure that all single stranded DNA templates are extended. The new synthesized DNA sequences are then stored at 4°C until further use.

For the present study PCR reactions were performed to verify the genotype of specific knockout-strain of mice namely, NLRP3-, ASC-, IL-1R- and Dectin-2-deficient mice. Therefore, approximately 0.5cm of a mouse`s tail was digested with 250µl tail-digestion solution (section 2.1.11.1) overnight using a thermomixer (55°C, 450rpm). The crude lysate was then heat inactivated at 85°C for 45min, centrifuged (10s, 16000g) and the resulting supernatant stored at -20°C or directly used for genotyping PCR reactions.

The following recipes denote the PCR reaction mixes used to verify the genotype on C57BL/6 and BALB/c background of:

NLRP3$^{-/-}$, ASC$^{-/-}$ and Dectin-2$^{-/-}$

1µl	Crude lysate (including mouse DNA)
1µl	Primer (mutant)
1µl	Primer (wt common)
1µl	Primer (wt)
21µl	Polymerase buffer (section 2.1.10.1)
0.1µl	GoTaq® DNA polymerase

IL-1R$^{-/-}$

1µl	Crude lysate (including mouse DNA)
1µl	Primer (wt forward)
1µl	Primer (wt reverse)
1µl	Primer (mutant forward)
1µl	Primer (mutant reverse)
20µl	Polymerase buffer
0.1µl	GoTaq® DNA polymerase

The corresponding primers for the several PCR reactions are depicted in section 2.1.12. The PCR reactions were performed using the Thermocycler T3000 (Biometra) as follows:

NLRP3 genotyping PCR programme

Initiation	95°C	5min	
Denaturation	95°C	45s	39 cycles
Annealing	55°C	30s	
Elongation	72°C	40s	
Final elongation	72°C	5min	
Storage	4°C	∞	

Amplification products: 500bp mutant allele 250bp wildtype allele

ASC genotyping PCR programme

Initiation	94°C	5min	
Denaturation	94°C	15s	3 cycles
Annealing	60°C	40s	
Elongation	72°C	30s	
Denaturation	94°C	15s	36 cylces
Annealing	57°C	25s	
Elongation	72°C	30s	
Final elongation	72°C	5min	
Storage	4°C	∞	

Amplification products: 260bp mutant allele 450bp wildtype allele

Dectin-2 genotyping PCR programme

Initiation	94°C	5min	
Denaturation	94°C	15s	40 cycles
Annealing	64°C	30s	
Elongation	72°C	30s	
Final elongation	72°C	5min	
Storage	4°C	∞	

Amplification products: 440bp mutant allele 550bp wildtype allele

IL-1R genotyping PCR programme

Initiation	95°C	5min	
Denaturation	95°C	45s	40 cycles
Annealing	65°C	20s	
Elongation	72°C	40s	
Final elongation	72°C	5min	
Storage	4°C	∞	

Amplification products: 543bp mutant allele 300bp wildtype allele

2.2.2 Separation of DNA-fragments using agarose-gel electrophoresis

Agarose-gel electrophoresis is the standard technique used to determine the specific size (length) of DNA fragments. Nucleic acid molecules are negatively charged and can be separated by applying an electric field to move the molecules through an agarose matrix. Agarose is a polysaccharide-derived matrix with a relatively large pore size and neutral charging. Thus, short DNA fragments move faster and migrate further through the agarose gel than longer molecules. The migration behavior indicates the size of the new synthesized DNA fragment and can be evaluated by using size standards with defined DNA fragment lengths. The detection of separated DNA is performed using a DNA intercalating agent, which fluoresces after exposure to ultraviolet (UV) light.

For the present study, agarose gels (1%) were produced by boiling up agarose in TAE buffer (section 2.1.10.1). After cooling to approximately 50°C, an intercalating agent, such as ethidium bromide (300µg/l) or Roti®-Safe GelStain (5µl/100ml), was added to the agarose gel solution. The final polymerization was then performed in a horizontal gel chamber at room temperature, in which a comb was placed to form pockets for sample application. Afterwards 15µl of PCR product (including the synthesized DNA fragments) and 5µl of Gene Ruler™ 1kb DNA ladder were loaded into the gel pockets. The addition of loading buffer to the PCR reaction was not necessary due to the 5x Green GoTaq® reaction buffer (section 2.1.10.1). The DNA fragments were separated by applying 130mA for 40-60min within an electrophoresis system filled with TAE buffer. Separated DNA fragments were detected by exciting the intercalating agents with UV light at 254nm. The emission of the DNA fragments were measured and photographed using the agarose gel documentation system. Analysis of DNA sizes was performed by comparing them to the applied standard (Gene Ruler™ 1kb DNA ladder) and results in the correct identification of the mouse.

2.3 Cell biological methods

2.3.1 Preparation of immune cells

2.3.1.1 Preparation of spleen, mesenteric and lung lymph node cells

Mice were sacrificied after inhaling Forene® and spleen, mesenteric lymph node (MLN) and lung lymph node (LLN) were removed using scissors and tweezers under sterile conditions. Thereafter, spleen, MLNs and LLNs were placed in separate petri dishes filled with Dulbecco`s PBS (endotoxin-free) and crushed with a plunger. The resulting cell suspension was transferred to a 50ml tube and centrifuged at 230g for 10min (4°C). The pellet was then resuspended in 5 ml ACT buffer (section 2.1.11) and incubated for approximately 5min at room temperature to lyse erythrocytes. Immediately after 5min incubation, the cell suspensions were filtered through a 100µm cell strainer into a new 50ml tube and washed with Dulbecco`s PBS. After centrifugation at 230g for 10min (4°C), the supernatant was discarded and the cell pellet dissolved in the appropriate buffer or culture medium. Finally, the cells were counted (section 2.3.2.1) and used for cell stimulation assays (section 2.3.3.3) and flow cytometry (section 2.3.6).

2.3.1.2 Preparation of dendritic cells from bone marrow

To obtain bone marrow cells, mice were sacrificed by inhaling Forene® and pinned onto a dissection board. Using sterile scissors and tweezers the pre-ethanol sprayed fur around the hind limbs was opened and the muscles were separated from the bones. The bones were cut at hip joint and ankle and divided into lower and upper leg bones by removing the knee. Bone marrow was then flushed out of the bone into a 50ml tube using Dulbecco`s PBS and Sterican® hypodermic needles connected to 1ml syringe. The resulting bone marrow was briefly disrupted by gently pipetting with a glass pipette and then centrifuged at 230g for 10min (4°C). After centrifugation, the pellet was solved in 5ml of ACT buffer for approximately 3min at room temperature. Immediately after erythrocytes lysis, the bone marrow suspension was filtered through a 100µm cell strainer into a new 50ml tube and washed with Dulbecco`s PBS, before a further centrifugation at 230g for 10min (4°C). Afterwards, the supernatant was discarded and the cell pellet was resuspended, counted and cultured in BMDC medium (section 2.1.11 and 2.3.3.1).

2.3.2 Cell handling

2.3.2.1 Cell counting

For counting cells, Fast-Read 102® counting chambers, which are based on the principle of a Neubauer hemocytometer, were used. To distinguish between dead and viable cells, the cells were coloured with Trypan blue solution, which is a diazo dye that cannot pass through the intact membrane of viable cells. The result is that only dead cells are stained blue. Thus, total living cells were counted in 16 quadrants of the grid. The cell titer (cell/ml) of the original suspension was then calculated using the following formula:

$$\text{cell/ml} = \text{counted cells} \times \text{dilution factor (Trypan blue dilution)} \times 10^4 \times \text{ml}^{-1}$$

2.3.2.2 Freezing of cells

To freeze cells, it is necessary to use a special medium consisting of dimethyl sulfoxide (DMSO) and fetal calf serum (FCS), called freezing medium (section 2.1.11). FCS prevents starvation of the cells, whereas DMSO prevents crystallization of water within the cells that will cause cell lysis during the freezing process. To preserve different cell types, especially progenitor DCs (section 2.3.1.2), $1x10^7$ cells were resuspended after prior centrifugation in 1ml freezing medium and transferred to a cryotube. Immediately, the cell suspension was frozen at -1°C/min to -80°C by using a freezing container.

2.3.2.3 Thawing of cells

The freezing medium contains DMSO, which is toxic for cells after extended amounts of exposure at warm temperatures. Therefore, frozen cells were rapidly thawed by warming the cryotube between the hands and immediately after thawing added to 50ml of warmed complete medium (section 2.1.11). After centrifugation at 230g for 10min (4°C), the supernatant was discarded, the pellet resuspended in 20ml complete medium and centrifuged once again. After centrifugation the pellet was resuspended in the appropriate buffer or culture medium and counted (section 2.3.2.1). Cells were then used for cell stimulation assays (section 2.3.3) and/or flow cytometry (section 2.3.6).

2.3.3 Cultivation and stimulation of immune cells

2.3.3.1 Cultivation of bone-marrow derived dendritic cells

To cultivate bone-marrow derived dendritic cells (BMDCs), $5x10^6$ progenitor DCs (section 2.3.1.2) were seeded in 10ml BMDC medium (section 2.1.11) on a petri dish. A pivotal component within the DC medium is the granulocyte-macrophage colony-stimulating factor (GM-CSF), which induces precursor bone-marrow cells to mature into BMDCs. After 3 days of cultivation within an incubator at 37°C, another 10ml of DC medium were added to the BMDC culture. On cultivation day 6, 10ml of BMDC culture supernatant was removed, centrifuged at 230g for 10min (4°C) and the supernatant consisting of old DC medium was discarded. The BMDC pellet was resuspended in 10ml fresh DC medium and added again to the culture plates. On cultivation day 7, the BMDCs were dislodged from the petri dish with a cell scraper and pipetted into a 50ml tube. Thereafter, each petri dish was rinsed with 10ml Dulbecco`s PBS, which was also added to the 50ml tube. The cells were centrifuged as above described, the supernatant discarded and the pellet resuspended in the appropriate medium for cell stimulation assays (section 2.3.3.2) and/or flow cytometry (section 2.3.6).

2.3.3.2 Stimulation of bone-marrow derived dendritic cells

After cultivation (section 2.3.3.1), $1x10^6$ BMDCs/ml were seeded onto flat-bottom 6-well or flat bottom 96-well plates. For suppression studies, BMDCs were preincubated with 50µg/ml SEA, $SEA_{h.i.}$ or SEA_{PK} (section 2.5.1) for 30min and then further stimulated with TLR stimuli, such as 25ng/ml P_3Cys and CpG or 5ng/ml LPS for 24h or as indicated.

For inflammasome induction studies, BMDCs were preincubated with TLR stimuli, such as 25ng/ml P_3Cys and CpG or 5ng/ml LPS for 4-6h. After TLR-priming, BMDCs were stimulated with 5mM ATP for 1h and with 50µg/ml SEA, $SEA_{h.i.}$ or SEA_{PK} for 24h or as indicated. Control stimulations of TLR-primed BMDCs were performed with *Salmonella typhimurium* (multiplicity of infection (MOI) of 10) and 500µg/ml $Al(OH)_3$ for 6h. Chemical inhibitors, reagents and blocking antibodies (Table 2.2) were added 30min before BMDCs stimulation with SEA, ATP, *S. typhimurium* and $Al(OH)_3$.

Name	Function	Concentration	Producer
APDC ((2R,4R)-4-Aminopyrrolidine-2,4-dicarboxylic acid)	Inhibits the NADPH-oxidase dependent reactive oxygen species (ROS) system	50-250µM	Alexis®
CytD (Cytochalasin D)	Inhibits actin polymerization and particle internalization and the binding stage of phagocytosis	0.5-1.5µM	Sigma®
Dectin-2 Ab (Rat-α-mouse-Dectin-2 antibody)	Blocks mouse DC-associated C-type lectin-2 (Dectin-2)	5-25µg/ml	AbD Serotec
DNP (2,4-Dinitrophenole)	Uncouples the mitochondrial electron transport chain leading to impaired ROS production	100nM-1mM	Sigma®
FCCP (Carbonyl cyanide p-(tri-fluromethoxy)phenyl-hydrazone)	Uncouples the mitochondrial electron transport chain leading to impaired ROS production	10nM-100µM	Sigma®
Glibenclamide	Inhibits ATP-sensitive potassium channels	25-200µM	Alexis®
KCl (Potassium chloride)	Blocks potassium channels	25-150mM	Roth®
Nac (N-acetyl-L-cysteine)	Antioxidant and free radical scavenger	25-150mM	Sigma®
R406 (Syk inhibitor)	Inhibits the spleen tyrosine kinase (Syk)	0.2-1.5µM	Rigel

Table 2.2: Blocking antibodies, uncoupling agents, chemical inhibitors and reagents used for *in vitro* inhibition experiments

To measure cytokine responses, BMDCs were stimulated in 96-well plates with a total volume of 200µl/well complete medium (section 2.1.11). After stimulation, up to 150µl supernatant was removed and frozen at -20°C for ELISA (section 2.3.5).

For Western blot (section 2.4), BMDCs were stimulated in 6-well plates with a total volume of 1ml/well OPTI-Mem®, a medium with a minimum of 50% reduction of FCS. FCS is the main source of background labelling during Western blot technique. Thus, OPTI-Mem® was always used for Western blot stimulations. After stimulation, 1ml supernatant was removed and frozen at -20°C or directly used for protein precipitation (section 2.3.4).

2.3.3.3 Stimulation of spleen, MLN and LLN derived lymphocytes

Isolated and counted spleen, MLN and LLN cells (section 2.3.1.1 and 2.3.2.1) were solved in complete medium and plated onto round-bottom 96-well plates (total volume 200µl) at the concentration of $1x10^6$ cells/ml. Thereafter, different stimuli, such as 20µg/ml SEA or 20µg/ml ovalbumin (OVA) or α-mouse CD3e and CD28 antibodies (Table 2.1) as polyclonal T-cell activator (positive control) were added to the cultures for 72h at 37°C. After this period

of time culture supernatant (100-150µl) was removed and frozen at -20°C until the T_H levels were determined by ELISA.

2.3.4 Protein precipitation and cell lysis

2.3.4.1 Methanol/chloroform precipitation

The methanol/chloroform precipitation method precipitates proteins from diluted solutions. Whilst, at the same time removing salts and detergents. For the present study, supernatants of stimulated BMDCs (section 2.3.3.2) were transferred into 2ml tubes and centrifuged at 230g for 10min (4°C). Afterwards, 500µl of the resulting supernatant was transferred into another 2ml tube and mixed with 500µl methanol and 200µl chloroform. After centrifugation at 16,000g for 10min (4°C), three different phases can be observed (methanol/H_2O phase), the interphase (protein phase) and the lower phase (chloroform phase). Without touching the interphase, the upper phase was discarded and 800µl of methanol was added and thoroughly mixed. After another centrifugation (as above), the supernatant was removed, the protein dried at room temperature and then resuspended in 35µl Laemmli buffer and 15µl 5x sample buffer (section 2.1.11.2). Finally, the protein suspension was frozen at -20°C or directly used for SDS-Page (section 2.4.1).

2.3.4.2 Trichloroacetic acid precipitation

Here, supernatant of stimulated BMDCs (section 2.3.3.2) were transferred in 2ml tubes and centrifuged at 230g for 10min (4°C). Afterwards, 1 volume of supernatant was mixed with 1 volume 20% (v/v) trichloroacetic acid (TCA) and incubated at 4°C overnight. After protein precipitation, the suspension was centrifuged at 16,000g for 10min (4°C), the supernatant removed and the protein pellet solved in 500µl of acetone. After another centrifugation (as above), the supernatant was removed, the protein pellet dried at room temperature and resuspended in 35µl Laemmli buffer and 15µl 5x sample buffer (section 2.1.10.2). Finally, the protein suspension was frozen at -20°C or directly used for SDS-PAGE (section 2.4.1). This method is fast but changes the pH, whereas the methanol/chloroform method takes longer, but is more efficient compared to the TCA method.

2.3.4.3 Cell lysis

Cell pellets that resulted from BMDC stimulations (section 2.3.3.2), were resuspended in 50µl lysis buffer (section 2.1.10.6) for 20min on ice. The lysis buffer consists of various detergents and lyses cells under non-denaturing conditions. After the incubation time, the lysis suspension was centrifuged at 16,000g for 20min (4°C) and the supernatant was frozen at -20°C to be later assessed by ELISA (section 2.3.5). For Western blot analysis, the supernatant was mixed with 15µl 5x sample buffer and frozen at -20°C or directly used for SDS-PAGE (section 2.4.1).

2.3.5 Enzyme-Linked ImmunoSorbent Assay (ELISA)

For the measurement of cytokine or immunoglobulin's an Enzyme-Linked ImmunoSorbent Assay (ELISA) was performed. ELISA is a biochemical technique that detects and quantifies the presence of an antibody or antigen, such as a cytokine. For the present study, a "Sandwich ELISA" was used, which is based on the binding and recognition of two independent specific antibodies towards an antigen (cytokine). The principle of the "Sandwich ELISA" is based on an immobilised antibody (coating antibody), which provides the platform for the binding of specific cytokines. The bounded target molecule is then recognized by a detection antibody which is coupled to a horse radish peroxidase (HRP). The enzyme HRP reacts with its substrate TMB (3,3',5,5'-Tetramethylbenzidine) which leads to a colour change (blue colouring). The reaction can be stopped by the addition of sulphuric acid leading to a colour change from blue to yellow, which can be detected by using a spectrophotometer.

For the detection of the cytokines IL-1β, TNF-α, IL-5, IL-10, IL-13, IL-17A and IFN-γ, from stimulated immune cells (section 2.3.3.2 and 2.3.3.3), cell lysates (section 2.3.4.3), within homogenised liver, intestine and lung tissues (section 2.5.5 and 2.6.3) and bronchoalveolar lavage (BAL) fluids (section 2.6.2), mouse Ready-Set-Go ELISA kits from eBioscience (section 2.1.7 and 2.3.5.1) and Duo Set® ELISA kits from R&D (section 2.1.7 and 2.3.5.2) were used. For the detection of OVA-specific IgE and IgG1 levels within mouse sera (section 2.6.3), ELISAs with antibodies from Biozol (Table 2.1) were performed (section 2.3.5.3).

2.3.5.1 Ready-Set-Go ELISA kits (eBioscience)

The Ready-Set-Go ELISA kits consist of all necessary reagents and antibodies, except washing buffer and stopping solution. The ELISAs were performed according to the manufacturer's instructions. In brief, 96-well ELISA plates were coated with 50µl/well capture antibody, which was diluted for optimal concentration in coating buffer and incubated overnight at 4°C. Plates were then washed thrice with washing buffer (section 2.1.10.4) and unspecific bindings were blocked with 100µl/well blocking buffer for at least 1h at room temperature. The plates were washed again 3 times with washing buffer and samples containing cytokines were diluted in blocking buffer (1:2 to 1:5 dilutions) and 50µl/well were added to the antibody-coated plates. In addition, the specific standard was also applied in a two-fold serial dilution in blocking buffer with the highest concentration of 2000pg/ml. The plates were then incubated for at least 2h at room temperature. During this time cytokines bind to the specific capture antibody coated on the plate. After three additional washing steps with washing buffer, 50µl/well of biotinylated detection antibody was applied and incubated for a further 1h at room temperature. The detection antibody binds specifically to the target cytokine, which is linked to the capture antibody on the plate bottom. Surplus detection antibodies were then washed away (3 times with washing buffer), before adding 50µl/well of streptavidin-horseradish peroxidase (HRP) conjugate. Afterwards, the plates were again incubated for approximately 45min at room temperature in the dark. Following this incubation, plates were washed thrice with washing buffer before adding 50µl/well of substrate solution (TMB substrate). The enzymatic reaction causes the wells to turn blue since the HRP, which is linked to the biotinylated Fc part of the detection antibody, converts the chromogenic substrate (TMB) into the oxidized TMB. Therefore, this last step should be carried out in the absence of light sources. After the first five standard dilutions became visibly blue, the reaction was stopped with 50µl/well of stopping solution (section 2.1.10.4), since the low pH denatures the enzyme. Immediately after stopping the reaction, the plates were measured at 450nm using the Sunrise^{TM} ELISA microplate reader. The resulting optical densities (ODs) of the samples were compared with the prepared standard dilution series (standard curve) to calculate concentrations within each sample.

2.3.5.2 Duo Set® ELISA kits (R&D)

The Duo Set® ELISA kits consist only contain the necessary standards and antibodies. The ELISAs were performed according to the manufacturer's instructions. In brief, 96-well ELISA plates were coated with 50µl/well of capture antibody, which was diluted for optimal concentration in PBS and incubated overnight at room temperature. Plates were then washed 3 times with washing buffer and unspecific bindings were blocked with 100µl/well of reagent buffer (section 2.1.10.4) for at least 1h at room temperature. The plates were washed again 3 times with washing buffer and samples containing cytokines were diluted in reagent buffer (1:2 to 1:5 dilutions) and 50µl/well added to the antibody-coated plates. In addition, the specific standard was also applied in a two-fold serial dilution in reagent buffer with the highest concentration of 2000pg/ml. The plates were then incubated for at least 2h at room temperature. After three additional washing steps with washing buffer, 50µl/well of biotinylated detection antibody was applied and incubated for a further 1h at room temperature. Surplus detection antibodies were then washed away (3 times with washing buffer), before 50µl/well of streptavidin-horseradish peroxidase (HRP) conjugate was applied. Plates were then incubated for approximately 45min at room temperature in the dark. Thereafter, plates were washed thrice with washing buffer and 50µl/well of BD OptEIA™ TMB substrate was added, before further incubating the plates in the dark. After the first five standard dilutions became visibly blue, the reaction was stopped with 50µl/well of stopping solution (section 2.1.10.4). Immediately after stopping the reaction, the plate was measured at 450nm using the Sunrise™ ELISA microplate reader. The concentration of the samples was calculated according to the standard curve as described in the previous section 2.3.5.1.

2.3.5.3 OVA-specific immunoglobulin ELISA

To measure OVA-specific IgE and IgG1 levels, 96-well ELISA plates were coated with 1µg (IgE measurement) or 0.1µg (IgG1 measurement) OVA grade V in 100µl OVA-coating buffer (section 2.1.10.4) per well and incubated at 4°C overnight, respectively. Plates were then washed 5 times with OVA-washing buffer (section 2.1.10.4) and unspecific bindings were blocked with 200µl/well of OVA-blocking buffer (section 2.1.10.4) for at least 2h at room temperature. The plates were again washed 5 times with OVA-washing buffer. Blood serum samples (section 2.6.3) containing immunoglobulins were diluted with OVA-blocking buffer (1:200 to 1:100,000 dilutions) and 50µl/well were added to the OVA-coated plates. In addition, a specific standard with mouse α-OVA IgE or IgG1 antibody (Table 2.1) was

applied in a two-fold serial dilution in OVA-blocking buffer with the highest concentration of 1000ng/ml or 250ng/ml, respectively. The plates were then incubated at 4°C overnight, allowing OVA-specific immunoglobulins to bind to coated OVA. After 5 additional washing steps with OVA-washing buffer, 50µl/well of biotinylated detection antibody, α-mouse IgE-Biotin or α-mouse IgG1-Biotin (Table 2.1), was applied and incubated for at least 2h at room temperature. The detection antibody binds specifically to the target immunoglobulins, which are bound to the OVA molecules on the plate bottom. Surplus detection antibodies were then washed away (5 times with OVA-washing buffer), before 50µl/well streptavidin-horseradish peroxidase (HRP) conjugate from the Duo Set® ELISA kits was applied. Afterwards, the plates were again incubated for approximately 30min at room temperature in the dark. Following the incubation, the plates were washed 5 times with OVA-washing buffer and 50µl/well of BD OptEIA™ TMB substrate was added, before further incubating the plates in the dark. After the first five standard dilutions became visibly blue, the reaction was stopped with 50µl/well of stopping solution. Immediately after stopping the reaction, the plates were measured at 450nm using the Sunrise™ ELISA microplate reader. The Ig concentration within the sample was then calculated according to the standard curve.

2.3.6 Flow cytometry

Flow cytometry is a widely used technique for the counting and characterization of microscopic particles suspended in a stream of fluid. It allows simultaneous multi-parametric analysis of the physical and/or chemical characteristics of single cells flowing through an optical and/or electronic detection apparatus. Basically, all physical and biochemical characteristics of a particle can be described using light reflection, light scatter and the emission of wavelength, which can be detected with a flow cytometric system, so called Fluorescence-activated cell sorting (FACS). There are two types of FACS, the FACS scan and the FACS sorter. The FACS scan reveals characteristics of the particles whereas the FACS sorter can sort desired particles according to specific parameters. The target particles are suspended in a hydro-dynamically focused stream of fluid. A beam of light of a single wavelength is directed into this stream of fluid. Each suspended particle passing through the beam scatters the light in varying direction and the machine employs two primary parameters to indicate granularity or inner complexity of particles (side scatter (SSC)) and the size/volume of the particles (forward scatter (FSC)). Fluorescent chemicals attached to the particles may be excited into emitting light at a lower frequency than the light source. This

combination of scattered and fluorescent light is picked up by the detectors. Thus, by analysing the fluctuations in brightness with each detector, it is possible to derive various types of information about the physical and chemical structure of each individual particle. Various fluorophores conjugated to antibodies specific against cell surface molecules, such as CD molecules expressed on immune cells, are used for immunophenotyping. Thus, activation, differentiation and composition of immune cells within different tissues and *in vitro* cultures can be analysed using the fluorophore-conjugated antibodies.

For the present study, 3 types of fluorophores were used, APC (Allophycocyanin) with an excitation/emission spectrum of 633/660nm, FITC (Fluorescein isothiocyanate) with an excitation/emission spectrum of 488/518nm and PE (Phycoerythrin) with an excitation/emission spectrum of 488/575nm. Thus, combinations of APC, FITC and PE conjugated antibodies (Table 2.1) were used to scan or sort immune cells using the BD FACSCalibur™ flow cytometer, CyAn ADP Lx P6 and CyAn ADP Lx P8.

2.3.6.1 Cell surface staining

To analyse the activation, differentiation and composition of cultivated and stimulated BMDCs (section 2.3.3.1 and 2.3.3.2) or LLN, MLN and spleen cells (section 2.3.1.1), FACS analysis with different flourophore-conjugated FACS antibodies were performed (Table 2.1). Thus, $2x10^5$ target cells were suspended in 100µl FACS buffer (section 2.1.10.5) in a 96-well plate and centrifuged at 230g for 5min (4°C). The supernatant was discarded, the pellet resuspended in 50µl Fc block solution (section 2.1.10.5) and incubated for 15-20min at 4°C. The Fc block solution contains a rat IgG2b α-mouse CD16/CD32 monoclonal antibody and blocks the Fc-mediated adherence of antibodies to mouse as well as unspecific bindings of the derived antibody to cells. After incubation, 100µl FACS buffer was applied and the cells were centrifuged as before. Immediately afterwards, the cells were incubated in the dark for 20min on ice with 50µl FACS buffer containing fluorophore-conjugated α-mouse monoclonal antibodies specific for different cell surface marker combinations of CD4, CD11b, CD11c, CD25, CD83, CD86 and F4/80 (Table 2.1). When the antibodies bind to the different cell types, the cells are marked and can be scanned or sorted according the different fluorophores, which emit different wavelengths. Additionally, unstained samples and compensation samples, which were stained with only one of the fluorophore-conjugated antibody, were prepared. These controls were used to compensate cell background and overlapping emission signals during FACS scan or sort acquisition (section 2.3.6.3). After incubation, 100µl FACS

buffer was added to the stained cells, which were then centrifuged as before and resuspended in 100µl FACS buffer. In some cases, surface stained cells were then used for intracellular Foxp3 staining (section 2.3.6.2) or acquired directly with the previously described FACS scan or FACS sorter devices (section 2.3.6). Finally, stained cells were sometimes further incubated in the dark with 1% paraformaldhyde (PFA) for 20min at 4°C. Afterwards, the cells were centrifuged as before and then resuspended in 100µl FACS buffer. The PFA treatment fixes the cells and allows the storage for a few days at 4°C.

2.3.6.2 Intracellular Foxp3 staining

To stain Foxp3 (Forkhead box P3), which is the transcription factor and master control gene for the development and function of natural Tregs (section 1.2.3), α-mouse/rat Foxp3-FITC or Foxp3-PE antibodies (Table 2.1) were used. For fixation and permeabilization of immune cells the Foxp3 staining buffer set from eBioscience (section 2.1.7) was used. Therefore, CD4 stained cells (section 2.3.6.1) were centrifuged at 230g for 5min (4°C) and resuspended in 50µl fixation/permeabilization working solution. Cells were then incubated at 4°C overnight in the dark and then washed twice with permeabilization buffer. Afterwards, either FITC or PE conjugated Foxp3 antibodies, diluted in permeabilization buffer, were applied and cells were incubated for 30min at 4°C in the dark. After incubation, cells were washed twice with permeabilization buffer and resuspended in 100µl FACS buffer and acquired with the previously described FACS scan.

2.3.6.3 FACS acquisition and analysis

A quantitative and qualitative analysis of flow cytometer data was performed using the FlowJo software from TreeStar. Before measurement, the autofluorescence of unstained cells and compensation between fluorophore colours was tuned using unstained cells and cells stained only with single fluorophore-conjugated antibodies. Furthermore, the voltage of the laser was tuned so that the target cells were visible in the FSC-SSC dot blot diagram.

2.3.7 Cytotoxicity assay

To confirm that stimulated BMDCs were still viable, a non-radioactive cytotoxicity assay from Promega (section 2.1.7) was performed. This assay is based on the activity of lactate dehydrogenase (LDH), a cytosolic enzyme, which is released upon cell lysis. LDH occurrence within the supernatant of stimulated BMDCs can be measured in a coupled enzymatic assay, using tetrazolium salts in conjunction with diaphorase, a flavin-bound enzyme that catalyze the reduction of various hydrogen acceptors, such as NAD^+ (nicotinamide-adenine-dinucleotide). The chemical reactions are as follows:

LDH

NAD^+ + lactate → pyruvate + NADH

Diaphorase

NADH + tetrazolium salts → NAD^+ + formazan (red)

The conversion of tetrazolium salts into a red formazan product is proportional to the number of lysed cells and can be used to measure cell viability via a spectrophotometer. The cytotoxicity assay was performed according to the manufacturer's instructions. In brief, 50µl supernatant from stimulated BMDCs, a LDH positive and a LDH negative control (included within the assay) were mixed with 50µl reconstituted substrate mix and incubated for 30min at room temperature in the dark. After incubation, the chemical reaction was stopped with 50µl stop solution and the absorbance was acquired at 490nm using the Sunrise™ ELISA microplate reader.

2.3.8 ATP measurement

To decipher ATP levels within the supernatants of stimulated BMDCs, a luminescent cell viability assay from Promega (section 2.1.7) was performed. This assay is based on the activity of luciferase, a thermostable oxidative enzyme, which generates a stable luminescent signal mediated by ATP. The Ultra-Glo™ recombinant luciferase within this assay catalyses the following reaction:

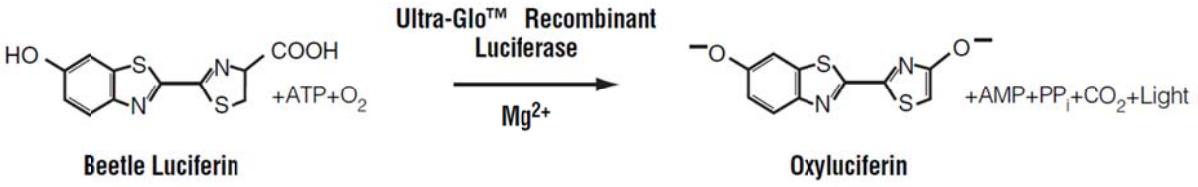

(Adapted from the Promega CellTiter-Glo® luminescent cell viability assay protocol)

The luminescent cell viability assay was performed according to the manufacturer's instructions. In brief, 100µl of stimulated BMDCs suspension was transferred to white/non-transparent LumiNunc™ 96-well plates, before 100µl of the CellTiter-Glo® reagent. The solution was mixed for 2min on an orbital shaker to induce cell lysis and generation of a luminescent signal proportional to the amount of ATP present, which signals the presence of metabolically active cells. In addition, an ATP standard was also applied in a two-fold serial dilution in complete medium (section 2.1.11) with the highest concentration of 1µM. The plate was then incubated for 10min at room temperature to stabilize the luminescent signal, which was recorded with an integration time of 1s/well using the Orion II microplate luminometer. In order to calculate the amount of ATP within the samples, the recorded luminescent was compared to the ATP standard dilution series (standard curve).

2.3.9 Statistics

Resulting data from ELISA (section 2.3.5), FACS (section 2.3.6), cytotoxicity assay (section 2.3.7) and ATP measurements (section 2.3.8) were analyzed using the GraphPad Prism 5 software. Parametrically distributed data was analyzed with unpaired T test (2 groups) or one-way ANOVA (more than 2 groups). Parametric data were represented as mean ± standard deviation (SD).

2.4 Methods of protein purification and analysis

2.4.1 SDS-Polyacrylamide gel electrophoresis (SDS-PAGE)

Sodium dodecyl sulfate polyacrylamide gel electrophoresis (SDS-PAGE) is a technique to separate proteins according to size under denaturizing conditions. The anionic detergent SDS binds to the polypeptide chain in proportion to its relative molecular mass (one SDS molecule binds to two amino acid residues). This results in disruption of non-covalent bonds and destruction of complex protein structures leading to impaired native protein conformation. Moreover, since proteins are surrounded with negatively charged SDS molecules they are all attracted to the positive electrode once an electric field is applied. Thus, smaller proteins migrate faster through the gel, while larger ones are held back by the polyacrylamide net.
For the present study, the Laemmli based discontinuous polyacrylamide gel was used, which consists of two different polyacrylamide gels: a SDS-separating gel and a SDS-stacking gel (section 2.1.10.2). The SDS-stacking gel has a lower acrylamide content and pH compared to

the SDS-separating gel, which is actually responsible separating the protein by size. These conditions lead to a stacking of proteins at the interphase between the two gels, which allows a more accurate separation. Thus, a 15% polyacrylamide gel, for the small bioactive molecules, IL-1β (17kDa) and Casp1 (10 and 20kDa), and a 10% polyacrylamide gel, for the larger precursor molecules, pro-IL-1β (31 kDa) and pro-Casp1 (45kDa), were prepared as described in section 2.1.10.2. The components ammoniumpersulphate (APS) and tetramethylethylenediamine (TEMED) act as catalysts in the polymerisation reaction of acrylamide and were therefore added last to the SDS-separating gel mixture. Immediately after APS and TEMED addition, the SDS-separating gel solution was poured between two plates which were held in place by the vertical dual gel electrophoresis system. To ensure an even interface, a layer of isopropanol was added to the top of the setting. After polymerisation, the isopropanol was discarded and the SDS-stacking gel solution was added and a comb inserted to form pockets for sample application. SDS-ready to use gels from Fisher BioReagents® (section 2.1.7 and 2.1.10.2) were also used. These gels also required the addition of APS and TEMED but provided an optimal resolution without the need of a stacking gel. After polymerisation the vertical dual gel electrophoresis system were filled with Laemmli buffer or running buffer, which is included in the EZ-Run™ protein gel solution kit (section 2.1.7), to connect the cathode with the anode. Samples were prepared as previously described in section 2.3.4 and denaturized at 95°C for 5min. After centrifugation at 16,000g for 20s, 15µl sample and 3µl protein marker V were loaded onto the gel. SDS-PAGE was performed at 80V while the samples were in the SDS-stacking gel and increased to 120V for approximately 2h once they reached the SDS-separating gel. The SDS-ready to use gels were run at 120V from the beginning for approximately 2h.

2.4.2 Western blot

Western blot is a technique to transfer SDS-PAGE-separated proteins (section 2.4.1) onto a nitrocellulose or polyvinylidene fluoride (PVDF) membrane so that a specific target protein can be detected via antibodies. Following a successful SDS-PAGE run, the SDS-stacking gel and the sample pockets were removed and one Protran® nitrocellulose transfer membrane and 6 Whatman filter papers were cut to the size of the SDS-separation gel. Two different methods were used for the transfer of proteins to the nitrocellulose membrane: the wet blot and the semi-dry blot. In short, 6 Whatman filter papers were pre-soaked in transfer buffer (section 2.1.10.3) and 3 of them were stacked onto either a wet electroblotter system or to a

semi-dry electroblotter system, followed by the membrane and the gel. Another 3 Whatman filter papers completed the gel sandwich. The wet electroblotter system was filled with transfer buffer and blotting was performed at 100mA. For the semi-dry blot, air bubbles were removed, the chamber was closed and blotting was performed at amperage of 1.2mA/cm^2 gel area (approximately 64mA/gel). The blotting time varied between 50min and 2h depending on the size of the target protein. After transfer, the membrane was washed with PBS, on an orbital shaker. All washing and blocking steps were performed at 4°C for 5min. To block unspecific bindings, the membrane was incubated with blocking buffer (section 2.1.10.3) at 4°C for at least 1h. After 2 washing steps with PBS, the membrane was transferred to a 50ml tube containing the primary antibody, such as poly-rabbit-αCasp1 (p10), poly-rabbit-αIL-1β or poly-rabbit-αβ-Actin (Table 2.1), which were diluted in 2ml TBST (section 2.1.10.3). The membrane was then incubated overnight at 4°C using a rotating mixer. The next day, the membrane was washed three times with blocking buffer before adding the secondary antibody goat-α-rabbit-HRP (Table 2.1), which was diluted in 5ml TBST and specific against the primary antibody. The membrane was incubated with the secondary antibody at 4°C for at least 2h and afterwards washed at least 5 times with blocking buffer and 2 times with PBS to ensure a clean blot. Finally, the membrane was placed in a radiographic cassette, covered with 1ml Western Lightning®-ECL chemoluminescence substrate and incubated in daylight for 1min. After incubation, the membrane was kept dark and exposed to medical x-ray films for different periods of time (depending on the signal intensity) for the chemoluminescent reaction of the HRP. The principle of the ECL-method is based on the binding of the secondary antibody, which is coupled with a HRP. HRP catalyses the oxidation of luminal (5-amino-2,3-dihydro-1,4-phthalazinedione) to 3-aminophtaalate via H_2O_2. The redundant energy is released in the form of light leading to local exposure of the medical x-ray films, which were developed in the Curix 60 Western blot processor. The size of the detected protein was confirmed by using the loaded protein marker V. To detect another specific protein on the same blot, the membrane was washed 5 times with blocking buffer and 3 times with PBS and then incubated with stripping buffer (section 2.1.10.3) in a water bath at 50°C for 1h. The stripping buffer has a low pH of 2.75 and includes β-mercaptoethanol which destroys antibodies and leads therefore to the total removal of membrane-bound primary and secondary antibodies. After stripping, the membrane was extensively washed with PBS and blocking buffer and then incubated again with a primary antibody and treated as described above.

2.5 Parasitological methods

Murine infection of *S. mansoni* reflects both the immunological and parasitological consequences that arise in man. Indeed, it is one of only a few helminthes that infect both mouse and man. To maintain the *S. mansoni* cycle at the MIH, NMRI mice are regularly (every 3 weeks) infected with 140-200 cercariae intraperitoneal (i.p.) from a Brazilian strain of *S. mansoni* from *Biomphalaria glabrata* snails (also of Brazilian origin). After 8 weeks of infection, mice are sacrificed, miracidia isolated from the intestine and exposed to snails to continue the infectious cycle (section 1.3.1). In addition, the livers are used for the preparation of eggs and SEA (section 2.5.1). All other strains were infected i.p. with a lower dose of 100-120 cercariae from the Brazilian strain. After at least 8 weeks of infection, mice were sacrificed and used for the evaluation of *S. mansoni* infection (section 2.5.2).

2.5.1 SEA preparation

2.5.1.1 Egg preparation from liver tissue

To prepare fresh eggs from liver tissue, NMRI mice were sacrificed after 8 weeks and infected livers were isolated using sterile scissors and tweezers. Livers were then washed in pre-cooled 1.2% (v/v) NaCl solution and bile ducts and gallbladders were removed. 4 livers were then minced using a scalpel and transferred into a 50ml tube containing 25ml liver digestion solution (section 2.1.10.8). The tube was then filled up with Dulbecco`s PBS to 50ml and incubated under continuous agitation at 37°C overnight using an orbital shaker. Thereafter, digested livers were centrifuged at 400g for 5min (4°C), the supernatant removed and the remains resuspended in 50 ml Dulbecco`s PBS. Livers were washed twice in this manner, before the pellet was resuspended in 25ml Dulbecco`s PBS and filtered twice through a 250µm sieve. The filtrate solution was then layered on a Percoll solution (section 2.1.10.8) and centrifuged at 800g for 10min (4°C). Due to the density gradient of the Percoll solution, eggs were separated from liver tissue and formed a pellet at the bottom of the tube. Eggs were then washed three times with 15ml and 30ml of 1mM EDTA solution, respectively and finally with 30ml Dulbecco`s PBS as previously described. After the washing steps, the egg pellet was resuspended in 700µl Dulbecco`s PBS and 5µl were microscopically analysed (x10 magnification) to confirm the purity and to calculate the total egg count using the following formula:

$$\text{total egg count} = (\text{counted eggs} \times 700\mu l) / 5\mu l$$

Finally, isolated eggs were either frozen at -80°C or directly used for SEA preparation (section 2.5.1.2). To confirm the sterility, 1-2µl of the egg suspension was plated out on a blood agar and a MacConkey agar plate and incubated at 37°C for 48h. Possible contaminations were analysed by standard microbiological assessments.

2.5.1.2 SEA preparation from liver-derived eggs

The egg suspension (section 2.5.1.1) was transferred to a glass homogenizer and pestled for at least 20min on ice. During this procedure the eggs release soluble egg antigens (SEA), which are a mixture of different (glyco-)proteins and (glyco-)lipids. To confirm that most of the eggs were disrupted, 2-3µl of the SEA solution was microscopically investigated, before an ultracentrifugation step at 100,000g for 1h (4°C) using the Optima™ L-100 XP ultracentrifuge was performed. Afterwards, the supernatant that contains the derived SEA was transferred to a cryotube, whereas the remaining egg shell pellet was resuspended in 200µl Dulbecco`s PBS. To confirm the sterility, 1-2µl of both suspensions were plated out on a blood agar and MacConkey agar plate and incubated at 37°C for 48h. The protein concentration within the SEA solution and egg shell pellet solution was measured using the DC protein assay kit from Bio-Rad (section 2.5.1.3). Finally, both suspensions were frozen at -80°C until required for further assays or analysis (section 2.3.3.2 and 2.3.3.3).

2.5.1.3 Measurement of protein concentration

To measure the protein concentration of freshly prepared SEA, egg shell pellet suspension (section 2.5.1.2), a DC protein assay kit from Bio-Rad (section 2.1.7) was performed, which included all the necessary solutions and reagents. This assay is based on the Lowry assay, which relies on the reaction of proteins with alkaline copper tartrate solution and Folin reagent. The method combines the reaction between proteins (especially aromatic protein residues) and copper ions under alkaline conditions, which results in the subsequent reduction of Folin reagent by the copper-treated protein. The reduced Folin species have a characteristic blue colour, which is usually measured with an absorbance at 750nm. For the present study, the DC protein assay kit was performed according to the manufacturer's instructions. In brief, to prepare working solution A, 20µl of reagent S was added to 1ml reagent A. In addition, a specific BSA standard was prepared in serial dilutions in PBS with the highest concentration of 1.5mg/ml. Afterwards, 5µl of the samples, for example SEA preparation (diluted 1:2), egg shell pellet suspension (dilution 1:2 to 1:10) or BSA standard were mixed with 25µl working

solution A and transferred into a 96-well plate, 200µl of reagent B was then added. The solution were gently mixed for 5s and incubated for 15min at room temperature in the dark. The absorbance was measured at 650nm using the Sunrise™ ELISA microplate reader. The resulting optical densities (ODs) of the samples were compared to the BSA standard dilution series (standard curve) to calculate the protein concentrations within the samples.

2.5.1.4 Modulation of SEA

To decipher the role of protein components within the SEA, preparations were either heat-inactivated ($SEA_{h.i.}$) or digested with proteinase K (SEA_{PK}). Heat-inactivation was performed at 95°C for 5min, whereas digestion of SEA was carried out with 200µg/ml proteinase K at 56°C for 1h. Both SEA preparations were then used for BMDC stimulation assays (section 2.3.3.2).

2.5.2 Evaluation of *Schistosoma mansoni* infection

Different knockout and wildtype mice were infected with *S. mansoni* cercariae as described in the previous section 2.5 and after at least 8 weeks of infection the mice were sacrificed and investigated with parasitological (section 2.5.2), histological (section 2.5.3) and immunological methods (section 2.5.4).

2.5.2.1 Worm burden analysis

For worm burden analysis, mice were euthanized with an i.p. injection of Narcoren (50µl). This chemical is a muscle-relaxant which affects both worms and mice and causes the schistosomes to detach from the vein wall and shift to the liver. To obtain the worms, pre-ethanol sprayed mice were opened using sterile scissors and tweezers. Exposed organs were then rinsed with worm rinsing solution (section 2.1.10.7) before the portal vein was slightly cut and worm perfusion solution (section 2.1.10.7) was pumped into the left heart ventricle and through the cardiovascular system using the Mini-Pump variable flow. After worm perfusion, the organs were rinsed again with worm rinsing solution and flushed worms from the portal vein and mesenteric veins were collected on a filter and kept in RPMI 1640 at 37°C. In addition, livers and intestines were intensively examined microscopically for additional worms. For counting, the worms were separated into females and males.

2.5.2.2 General infection status

The general infection status was judged by the degree of visual infection and organ damage. Specifically, the liver was examined for signs of fibrosis, changes in colour and visible granulomas. The infection status was graded on a scale from 0 to 3 DOI (degree of infection) with 3 denoting the highest level of infection. In addition, total body weight of each individual mouse and organ weight (liver, intestine and spleen) were obtained and compared with uninfected mice.

2.5.2.3 Egg count analysis

Weighed liver and intestine samples from individual mice were digested in 5ml of 5% (w/v) KOH solution under continuous agitation at 37°C for at least 2h. After incubation, the released eggs were centrifuged at 400g for 10min and 4.5ml of the supernatant was immediately removed. The remaining eggs (within 500µl) were then resuspended and counted with the microscope (x10 magnification) in three samples of 10µl. The number of eggs in the liver was then calculated as follows:

eggs/mg tissue = (average of counted eggs x 50) / weight of tissue sample (mg)

2.5.3 Histological methods

Infection of *S. mansoni*, especially chronic infection, is characterized by chronic local inflammatory responses to trapped schistosome eggs in liver and intestinal tissues. Around the trapped eggs granuloma formation is induced, leading to a unique form of liver and intestine fibrosis, which is the main elicitor of morbidity and mortality (section 1.3.2). For the present study, liver granuloma formation and infiltration of immune cells within granulomas formed in the various knockout mice were analysed and compared to wildtype controls.

2.5.3.1 Tissue preparation for histological staining

Left liver lobe or lung samples (section 2.6.4) from each individual mouse were fixed in Roti®-Histofix (4%), dehydrated using the Shandon Excelsior ES tissue processor and embedded in paraffin using the TB 588 paraffin embedding system. 3µm sections were cut using the RM 2245 automatic rotary microtome and fixed on glass slides for staining techniques (section 2.5.3.2 and 2.6.4).

2.5.3.2 Staining techniques

For analysis of granuloma formation and immune cell infiltration two different staining methods were performed. The trichrome Masson's blue stain was used to differentiate between collagen and smooth muscle in liver and to visualize the increase of collagen in granuloma formation, since the aniline component in the staining buffer turns collagen fibres blue. Liver sections stained with Masson's blue stain were also used for size analysis of the granuloma. The Masson's blue staining procedure is depicted in Table 2.3.

Reagent	Producer	Incubation time	Function
Xylene	Engelbrecht	10min	Dissolving of paraffin
Ethanol (96%)	MRI	1min	Rinsing with mounting water content (watering)
Ethanol (96%)	MRI	1min	
Ethanol (80%)	MRI	1min	
Ethanol (70%)	MRI	1min	
Aqua bidest.	MRI	1min	
Weigert`s haematoxylin	Morphisto	2min	Complexation of positive hematoxylin to the negative nucleic acids phosphate groups (nuclear staining)
Tap water	-	Constant rinsing for 5min	Achievement of deep blue staining by alteration of the pH
Acid fuchsin	Morphisto	2min	Staining of the smooth muscle tissue
Phospho-molybdic acid	Morphisto	5min	Differentiation and increasing of contrast between collagen and smooth muscle tissue
Aniline blue	Morphisto	4min	Staining of collagen
Tap water	-	Rinsing until water is clear	Dissolving of aniline blue
Ethanol (96%)	MRI	1min	Rinsing with mounting alcohol content (dehydration)
Ethanol (96%)	MRI	1min	
Isopropanol	MRI	1min	
Xylene	Engelbrecht	10min	Fixation
Entellan®	Merck	-	Fixation and covering with coverslip

Table 2.3: Masson's blue staining protocol

Alternatively, the standard hematoxylin and eosin stain (HE staining) is a combined staining method and was used to analyse immune cell infiltration within the granuloma. Hemalum, a complex formed from aluminium ions and oxidized haematoxylin, colours the nuclear of cells blue and the eosin solution stains eosinophilic structures in various shades of red. The HE staining procedure is depicted in Table 2.4.

Reagent	Producer	Incubation time	Function
Xylene	Engelbrecht	10min	Dissolving of paraffin
Ethanol (96%)	MRI	2min	Rinsing with mounting water content (watering)
Ethanol (80%)	MRI	2min	
Ethanol (70%)	MRI	2min	
Ethanol (60%)	MRI	2min	
Aqua bidest.	MRI	2min	
Mayer`s haematoxylin	Morphisto	5min	Complexation of positive hematoxylin to the negative nucleic acids phosphate groups (nuclear staining)
Tap water	-	Constant rinsing for 12min	Achievement of deep blue staining by alteration of the pH
1% (v/v) Eosin	Morphisto	5min	Staining of eosinophilic structures
Tap water	-	Rinsing until water is clear	Dissolving of eosin
Ethanol (80%)	MRI	1min	Differentiation and increasing of contrast between eosinophilic structures and smooth muscle tissue
Ethanol (96%)	MRI	2min	Rinsing with mounting alcohol content (dehydration)
Ethanol (96%)	MRI	2min	
Isopropanol	MRI	2min	
Xylene	Engelbrecht	10min	Fixation
Entellan®	Merck	-	Fixation and covering with coverslip

Table 2.4: Hematoxylin and eosin staining protocol

2.5.3.3 Microscopical analysis of stained liver sections

Stained liver sections were analysed microscopically for granuloma formation and size evaluation using the Masson's blue stained sections (Table 2.3) and for immune cell infiltration using HE stained sections (Table 2.4). The size of the granuloma was determined by measuring the diameters with the help of an ocular micrometer along the longitudinal axis of the eggs at x10 magnification using the Axioscop microscope. Up to 40 granulomas of each individual liver section were evaluated and the average size of the granulomas from each liver section was calculated.

2.5.4 Immunological methods

To analyse cytokine responses or composition of immune cells during *S. mansoni* infection, ELISA analysis (section 2.3.5) and FACS techniques (section 2.3.6) were performed, respectively. To decipher *in situ* cytokine levels, weighed liver or intestinal samples were transferred into 2ml tubes containing 500µl of RPMI 1640 and homogenized using the T10 basic Ultra-Turrax® disperser. The homogenised samples were then centrifuged at 16,000g for

10min (4°C) and the resulting supernatant was frozen at -20°C until analysed by ELISA (section 2.3.5.1 and 2.3.5.2). This method was also employed to measure the cytokine levels from cultured supernatants of restimulated MLN and spleen cells. In brief, freshly prepared MLN and spleen cells ($2x10^5$) were restimulated according to the previously described protocol in sections 2.3.1.1 and 2.3.3.3. To investigate the composition of immune cells, MLN and spleen cells were prepared and stained for certain cell populations and analysed by FACS according to the previously described method in sections 2.3.1.1 and 2.3.6, respectively.

2.6 Evaluation methods for allergic airway inflammation

To investigate aspects of allergic asthma in a murine model, mice have to be sensitized to an typical allergens in the air such as pollen, mold and dust mites. To achieve a controlled experimental response, ovalbumin (OVA) is often used as a standard allergen and is commonly combined with an adjuvant such as H_2O_2 or alum. Once sensitized and challenged such allergens leads to airway destruction, elevated levels of IgE causing mast cell activation, chronic airway inflammation and airway hyperresponsiveness (AHR). To decipher the role of inflammasome activity in another T_H2 polarized *in vivo* model besides the *S. mansoni* infection, an alum-free OVA-induced allergic airway inflammation model was developed and the protocol and assessment parameters are described in the following sections.

2.6.1 Induction of allergic airway inflammation

To investigate the role of inflammasome activity during an *in vivo* T_H2 allergic airway inflammation model, ASC-, NLRP3-deficient and wildtype control mice (BALB/c background) were sensitized and challenged with OVA as depicted in Figure 2.1.

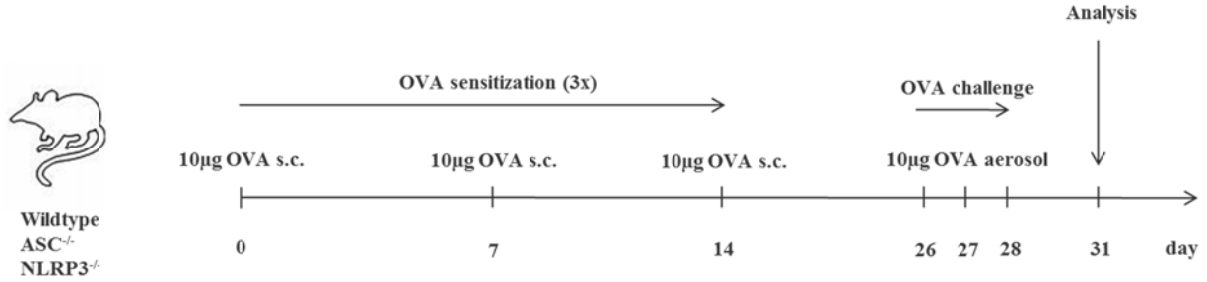

Figure 2.1: Alum-free OVA-induced allergic airway inflammation model
In brief, wildtype, ASC- and NLRP3-deficient mice were thrice sensitized with 10µg OVA s.c. on day 0, 7 and 14. On days 26-28, OVA challenge was performed with 10µg OVA aerosol. Finally on day 31, the mice were sacrificed and immunological parameters were investigated.

The activity of the inflammasome during allergic asthma development was determined using the alum-free OVA-induced allergic airway inflammation model. This was a necessary adjustment to the normal protocol with i.p. injection of alum, since alum is a strong activator of the inflammasome (section 1.4.2). As depicted in Figure 2.1, BALB/c mice were sensitized subcutaneously (s.c.) with 10µg OVA grade VI or PBS (control mice) on 3 days (day 0, 7 and 14). On days 26-28, mice were placed into the OVA-challenge chamber and challenged with 10µg OVA grade V by intranasal route using a Pari Boy® SX nebulizer. The OVA-challenge provokes within the OVA-sensitized mice allergic airway inflammation and leads to airway destruction, elevated levels of IgE causing mast cell activation, chronic airway inflammation, airway hyperresponsiveness (AHR) and airway remodeling. Finally, on day 31 (3 days after the last OVA challenge), mice were sacrificed and bronchoalveolar lavage (BAL) analysis (section 2.6.2), T_H profiling via cytokine analysis (section 2.6.3) and lung inflammation scoring (section 2.6.4) were evaluated.

2.6.2 Analysis of immune parameters in the bronchoalveolar lavage (BAL)

2.6.2.1 Preparation of the BAL

To analyse the composition of the infiltrated immune cells and cytokine responses within the bronchoalveolar lavage (BAL), mice were first euthanized with an i.p. injection of 50µl Narcoren. Afterwards, the mouse body was opened using sterile scissors and tweezers. The exposed trachea was disconnected below the larynges using a haemostatic forcep, before the lung was flushed twice with 1ml BAL buffer (section 2.1.10.6) using Sterican® hypodermic needles connected to 1ml syringes. The obtained material, called BAL, was then transferred to two 1ml tubes, which were weighed and centrifuged at 230g for 5min (4°C). Thereafter, the supernatant from the first BAL (BAL I) was frozen at -20°C and used for ELISA analysis (section 2.3.5.1 and 2.3.5.2), whereas the supernatant from the second BAL (BAL II) was discarded. The cell pellets from BAL I and BAL II were then pooled together in 200µl FACS buffer, counted and used for cytospin preparation (section 2.6.2.2).

2.6.2.2 Cytospin preparation

To microscopically analyse the composition of immune cells within the BAL, a cytospin was performed. In short, glass slides were covered with Shandon filter cards and EZ Cytofunnels® and placed into Shandon cytoclips. Before adding 150µl BAL cell suspension (section

2.6.2.1) the Shandon cytoclips were mounted into the slots of the Shandon Cytospin 3 centrifuge. Centrifugation was then performed at 400rpm for 5min. During the centrifugation the fluid forms a circle of cells which is guided by the filter. Finally, cytospins were dried overnight at room temperature and stained with Diff-Quik staining set (section 2.6.2.3).

2.6.2.3 Staining and analysis of BAL cells

The cytospins (section 2.6.2.2) were stained with the Diff-Quik staining set according to the manufacturer's instructions. The Diff-Quik staining is based on the Romanowski stain and includes aqueous solutions of methylene blue and eosin, dissolved in methanol. This kit allows selective staining of macrophages, eosinophils, neutrophils and lymphocytes. Thus, glass slides were placed consecutively for 10s into Diff-Quik Fix (cell fixation), Diff-Quik I (staining of eosinophils) and Diff-Quik II (staining of basophils) solutions. Afterwards, the glass slides were washed in aqua bidest. and dried for 2h at room temperature. To differentiate the immune cell populations within the BAL, the Diff-Quik stained sections were microscopically analysed. At least 100 cells were differentiated into macrophages, eosinophils, neutrophils and lymphocytes using the Axiovert microscope (x40 magnification) to determine the frequency and percentage of each cell type.

2.6.3 Sample preparation for ELISA

To decipher *in situ* cytokine levels, weighed lung samples were placed in 500µl of RPMI 1640 and homogenized using the T10 basic Ultra-Turrax® disperser. The homogenised samples were then centrifuged at 16,000g for 10min (4°C). After centrifugation, the resulting supernatant was frozen at -20°C and used for ELISA analysis (sections 2.3.5.1 and 2.3.5.2). Cytokine levels from antigen-specifically restimulated lung lymph node (LLN) cells were also analysed. This was done in accordance with the previously described methods (sections 2.3.1.1 and 2.3.3.3). For the measurement of OVA-specific IgE and IgG1 levels, blood samples were taken from each individual mouse and centrifuged at 16,000g for 20min (4°C). Resulting sera was frozen at -20°C and used for OVA-specific immunoglobulin ELISA analysis (section 2.3.5.3).

2.6.4 Evaluation of lung inflammation

To evaluate lung inflammation, sections were prepared as described in the previous section 2.5.3.1 and stained using the Periodic acid-Schiff (PAS) method. This stain helps to detect glycogen and other polysaccharides in tissues, especially in the basilar membranes. PAS staining is based on the reaction of periodic acid which can oxidize the diol groups of sugars, especially glucose. This produces aldehyde groups, which react with the Schiff reagent leading to bright red colouring. The PAS staining is an excellent method to stain goblet cells, which are glandular epithelial cells, filled with mucin (a glycoprotein). These cells are responsible for mucus (mucin dissolved in water) production, which is a characteristic of lung inflammation. Thus, to evaluate inflammation and goblet cell infiltration within the lung, the PAS staining was performed as depicted in Table 2.5.

Reagent	Producer	Incubation time	Function
Xylene	Engelbrecht	10min	Dissolving of paraffin
Ethanol (96%)	MRI	2min	Rinsing with mounting water content (watering)
Ethanol (80%)	MRI	2min	
Ethanol (70%)	MRI	2min	
Ethanol (60%)	MRI	2min	
Aqua bidest.	MRI	2min	
Periodic acid (1%)	Morphisto	15min	Oxidation of diol sugar groups leading to aldehyde group formation
Tap water	-	Constant rinsing for 10min	Dissolving of periodic acid
Aqua bidest.	MRI	2min	Watering
Aqua bidest.	MRI	2min	
Schiff reagent	Morphisto	20min	Staining due to the reaction of aldehyde groups with Schiff reagent
Tap water	-	Constant floating for 5min	Dissolving of Schiff reagent
Aqua bidest.	MRI	10s	Rinsing
Mayer`s haematoxylin	Morphisto	6min	Complexation of positive hematoxylin to the negative nucleic acids phosphate groups (nuclear staining)
Tap water	-	Constant floating for 10min	Achievement of deep blue staining by alteration of the pH
Ethanol (96%)	MRI	3min	Rinsing with mounting alcohol content (dehydration)
Ethanol (96%)	MRI	3min	
Isopropanol	MRI	5min	
Xylene	Engelbrecht	10min	Fixation
Entellan®	Merck	-	Fixation and covering with coverslip

Table 2.5: Periodic acid-Schiff (PAS) staining protocol

Stained lung sections were analysed microscopically for tissue inflammation and goblet cell infiltration. Lung tissue inflammation was determined by the degree of visual thickness of the basal membrane, which was graded on a scale from 0 to 3 (inflammation score) according to previous described standard method [221, 222]. In brief, a value of 0 was assigned when no inflammation was detectable, a value of 1 was assigned for occasional cuffing with inflammatory cells, a value of 2 was assigned for most bronchi or vessels surrounded by a thin layer (one to five cells thick) of inflammatory cells, and a value of 3 was given when most bronchi or vessels were surrounded by more than five inflammatory cells thick.

3 Results

3.1 Deciphering the mechanisms of SEA-mediated immunomodulation

A main characteristic of Schistosomiasis is the polarized T_H2 immune response which is promoted by SEA released from schistosome eggs (section 1.3.3). In addition, several studies have deciphered that TLR-mediated immune responses from DCs and macrophages can be suppressed by SEA (section 1.3.5). The first sections of this chapter highlight research aspects which have strived to investigate SEA-mediated immunomodulating mechanisms leading to either T_H2 polarization, inflammasome activation or the suppression of innate immune responses. Whereas the former was mainly deciphered through *in vivo* infection studies the latter used various *in vitro* experiments with BMDCs. The second half of this chapter revolved around inflammasome studies in another T_H2 model namely allergic airway inflammation. These *in vivo* studies also addressed the outcome of allergy upon blocking IL-1 signalling using already registered drugs.

3.1.1 SEA suppresses TLR-triggered innate immune responses

As mentioned above, previous studies have shown that SEA inhibits TLR-mediated immune responses [122-127]. To confirm and expand upon those data BMDCs were prepared and cultured as described in section 2.3.1.2 and 2.3.3.1, respectively. Before enacting the described suppression assays (section 2.3.3.2), a portion of the generated BMDCs were stained with CD11c, CD11b, F4/80, CD80, CD83 and CD86 FACS antibodies (section 2.3.6.1) to examine them for maturation and activation status. BMDC populations, which consisted of at least 85% $CD11c^+$ cells and showed low expression of the maturation markers CD80, CD83 and CD86, were used for the assays. In short, BMDCs were pre-treated with SEA for 30min and then activated with various TLR stimuli for 24h. The resulting cytokine responses (IL-6 and TNF-α) were then measured using ELISA (section 2.3.5) and the results are depicted in Figure 3.1.

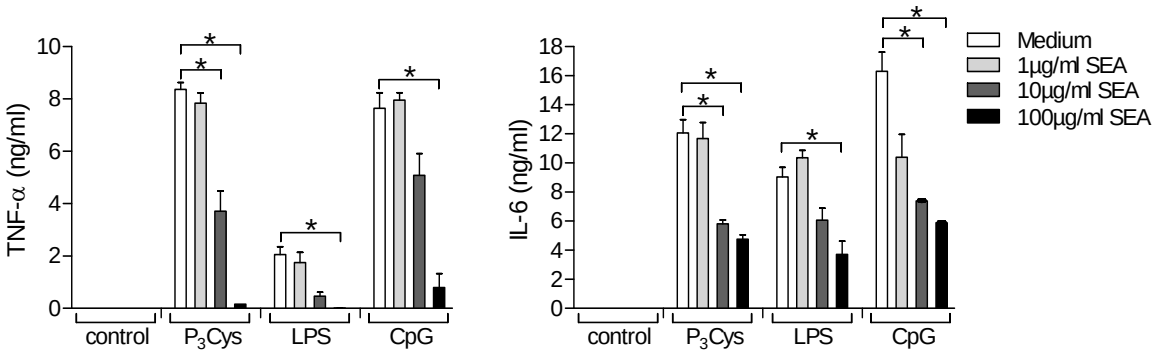

Figure 3.1: SEA suppresses TLR-mediated TNF-α and IL-6 responses in a dose dependent manner
BMDCs ($1x10^6$/ml) were primed with 1µg/ml, 10µg/ml and 100µg/ml SEA or medium (white bars) for 30min and then stimulated with 25ng/ml P_3Cys, LPS and CpG or medium (control) for an additional 24h. Culture supernatants were evaluated for TNF-α and IL-6 release by ELISA. Bars represent an example of the mean ± standard deviation (SD) of three independent experiments. Asterisks show significant differences between brackets * $p<0.05$

BMDCs stimulated with TLR stimuli alone (white bars) released high amounts of TNF-α and IL-6. However, addition of SEA significantly inhibited these TLR-mediated TNF-α and IL-6 responses. The suppressive effect of SEA was dose dependent as stimulation with low dose SEA concentration of 1µg/ml (light grey bars) showed almost no suppressive ability. In addition, cell cultures with SEA without TLR stimuli (control bars) did not elicit TNF-α or IL-6 nor did it up-regulate co-stimulatory markers CD80 and CD86 expression (data not shown). These data confirm results described from previous studies but in addition show that SEA can also suppress TLR2 and TLR9 triggering responses [123, 125].

3.1.2 SEA induces IL-1β production

As shown above and in accordance to current literature, no stimulatory effects of SEA on innate immune cells, such as DCs or macrophages, have been reported. However, other parasites, such as the Plasmodium species, which causes malaria infection due to the release of hemozoin, can activate the NLRP3 inflammasome which facilitates the release of high amounts of the proinflammatory cytokine IL-1β [223-225]. Moreover, recent studies identified components within SEA which are recognized by different C-type lectin receptors (CLRs) [122, 123]. In addition, some CLRs have also been shown to initiate inflammasome activation and IL-1β production upon triggering with fungal products [134, 135]. To examine whether schistosome-derived antigens could induce the release of IL-1β, BMDCs were co-

cultured in the manner described in section 2.3.3.2. In brief, BMDCs were pulsed with TLR stimuli for 4-6h to accumulate pro-IL-1β within the cells. Thereafter, SEA was added to the cultures for 24h to activate the inflammasome complex leading to the cleavage of IL-1β which was then determined within the supernatant by ELISA. The results are illustrated in Figure 3.2.

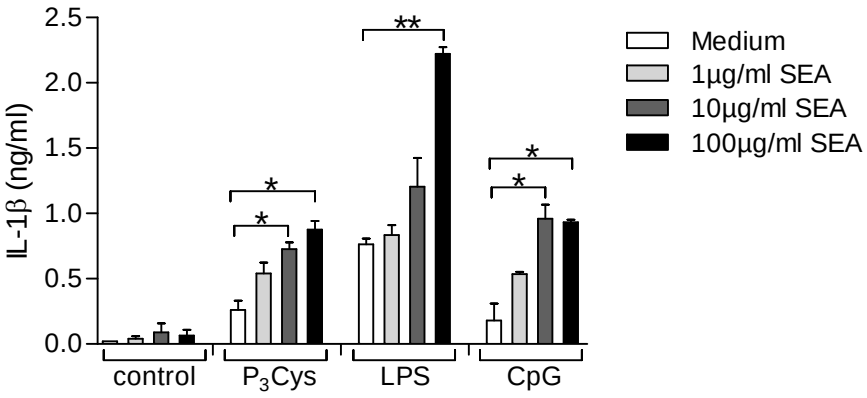

Figure 3.2: SEA induces IL-1β production in a dose dependent manner
BMDCs ($1x10^6$/ml) were primed with 25ng/ml P_3Cys, LPS and CpG or medium (control) for 4-6h and then stimulated with 1µg/ml, 10µg/ml and 100µg/ml SEA or medium (white bars) for an additional 24h. The supernatants were evaluated using a specific IL-1β ELISA. Bars represent an example of the mean ± SD of three independent experiments. Asterisks show significant differences between brackets ** $p<0.01$ and * $p<0.05$.

As shown in Figure 3.2, BMDCs primed with TLR stimuli alone (white bars) released low amounts of IL-1β, whereas additional stimulation with SEA significantly increased the production of this cytokine. This SEA-mediated IL-1β induction was also dose dependent as stimulation with increasing amounts of SEA lead to increased IL-1β release. In addition, SEA alone (control bars) did not elicit IL-1β release, which was also observed for TNF-α and IL-6 responses in the previous section 3.1.1. Moreover, IL-1β production was also not observed within stimulation experiments using worm antigen, frozen whole eggs or egg shells (data not shown), implying that viable eggs secrete SEA component(s) that specifically trigger inflammasome activation. The following induction or suppression stimulation assays were always performed with a concentration of 50µg/ml SEA.

3.1.3 SEA-mediated IL-1β induction depends on viable BMDCs

IL-1β is a strong proinflammatory cytokine, which is secreted from various cell types upon triggering with DAMPs or PAMPs (section 1.4.2). However, dying or necrotic cells are also a source of IL-1β [200, 226] . Dying or lysed cells secrete lactate dehydrogenase (LDH) which

can be measured in a coupled enzymatic assay. Therefore, to exclude that the observed IL-1β production in these SEA co-cultures was not due to cell death or lysis, the viability of stimulated BMDCs were analysed using a LDH cytotoxicity assay according to the description in the section 2.3.7. The results of the LDH cytotoxicity assay are shown in Figure 3.3.

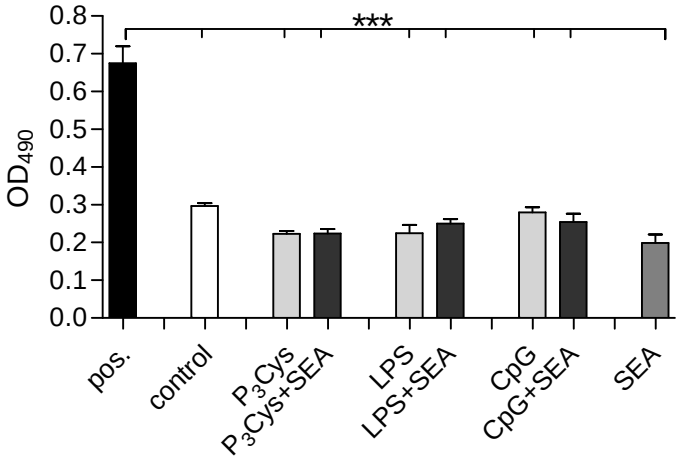

Figure 3.3: Cell viability is maintained after SEA stimulation
BMDCs ($1x10^6$/ml) were primed with 25ng/ml P_3Cys, LPS and CpG or medium (control) for 4-6h and then stimulated with or without SEA (50µg/ml) for an additional 24h. The amounts of the released lactate dehydrogenase (LDH) within the supernatants were then measured at 490nm and compared to a LDH positive control (black bar). Bars represent an example of the mean ± SD of three independent experiments. Asterisks show significant differences between brackets *** $p<0.001$.

As depicted in Figure 3.3, BMDCs stimulated with TLR and/or SEA did not release increased amounts of LDH compared to unstimulated (white bar) BMDCs. Moreover, stimulated BMDCs supernatants contained significantly less LDH compared to the LDH positive control (black bar). These data confirm that the presence of SEA within the cell cultures does not lead to cell death, suggesting that SEA specifically triggers TLR-primed BMDCs to induce IL-1β secretion. Interestingly, regardless of the employed TLR stimuli (P_3Cys, LPS and CpG), SEA was able to elicit the same result. Moreover, BMDCs showed almost the same LDH release and this was also independent of the TLR stimuli. Therefore, the results shown in the following sections are depicted only for those conducted with the TLR2 stimulus P_3Cys. However, all experiments were performed with CpG and some were also confirmed with LPS.

3.1.4 SEA-mediated immunomodulatory effects depend on glycosylated proteins and lipids

SEA is a complex mixture consisting of highly glycosylated proteins and lipids [108, 109]. To narrow down which type of component was responsible for the observed *in vitro* effects (section 3.1.1 and 3.1.2) or moreover, whether the IL-1β induction and suppression of TLR-mediated immune responses was due to the same component, the following assays were performed. In short, both experimental cultures were repeated using SEA in which the protein components were degraded either by heat inactivation ($SEA_{h.i}$) or digestion with proteinase K (SEA_{PK}) as described in section 2.5.1.4. The results demonstrated in Figure 3.4 show the levels of IL-1β and TNF-α responses.

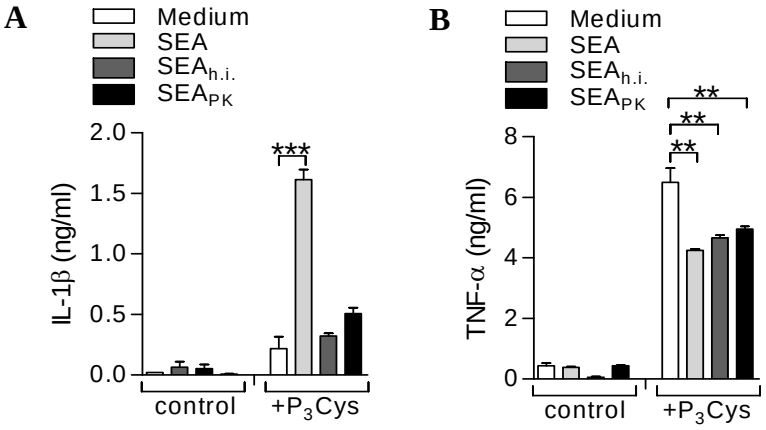

Figure 3.4: SEA-mediated IL-1β induction depends on a (glyco-)protein, whereas a (glyco-)lipid mediates the suppression of TNF-α
(A) BMDCs ($1x10^6$/ml) were primed with 25ng/ml P_3Cys or medium (control) for 4-6h and then stimulated with 50µg/ml SEA, $SEA_{h.i.}$ (heat inactivated) and SEA_{PK} (proteinase K digested) or medium (white bars) for an additional 24h. (B) BMDCs ($1x10^6$) were primed with 50µg/ml SEA, $SEA_{h.i.}$ and SEA_{PK} or medium (white bars) for 30min and then stimulated with 25ng/ml P_3Cys or medium (control) for a further 24h. The supernatants were evaluated using (A) IL-1β and (B) TNF-α ELISAs. Bars represent the mean ± SD of three independent experiments. Asterisks show significant differences between brackets *** $p<0.001$ and ** $p<0.01$.

Indeed, protein-inactivated SEA could no longer induce IL-1β production (Figure 3.4 A) but could still suppress TNF-α responses (Figure 3.4 B), suggesting that the IL-1β-inducing component was a (glyco-)protein. Interestingly, the opposite was observed for the suppression of TLR-triggered responses indicating that this component was a non-protein ((glyco-)lipid).

3.2 Investigating SEA-mediated inflammasome activation

As described in the previous section 3.1, SEA-mediated IL-1β induction depends on a (glyco-)protein (Figure 3.4 A) and was not mediated by induction of cell death (Figure 3.3). However, the secretion of the proinflammatory cytokine IL-1β highly depends upon the activation of the multiprotein complex called the inflammasome [150, 151]. To date, five inflammasome complexes have been reported which sense PAMPs and DAMPs and lead to the cleavage of pro-IL-1β into its bioactive form (section 1.4.1). Therefore, to investigate the inflammasome complex and the upstream activation mechanisms that are responsible for the SEA-mediated IL-1β induction, immune responses from stimulated BMDCs of wildtype and several knockout mice (C57BL/6 background) were analysed and evaluated.

3.2.1 SEA mediates the cleavage of IL-1β through caspase-1 activation

The main regulatory component of the inflammasome is caspase-1 (Casp1), which cleaves pro-IL-1β into its functional bioactive form [150-152, 158-161, 172]. To confirm the necessity of Casp1 in the observed release of IL-1β by SEA stimulation, the appearance of cleaved IL-1β (p17) and Casp1 (p20) products (section 1.4.2) were detected using the Western blot technique (section 2.4). Furthermore, BMDCs from Casp1$^{-/-}$ and wildtype mice were stimulated as described in section 2.3.3.2 and supernatants were analysed using ELISA. Results are depicted in Figure 3.5.

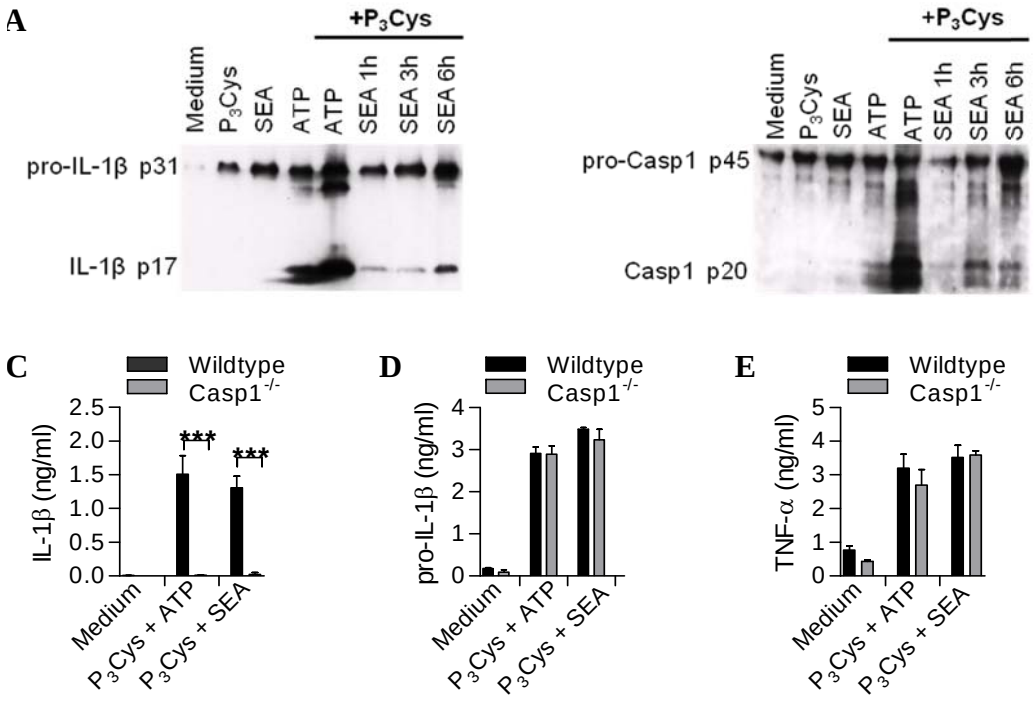

Figure 3.5: SEA-mediated IL-1β induction depends on caspase-1 activation
Wildtype and Caspase-1$^{-/-}$ (Casp1$^{-/-}$) BMDCs (1x10^6/ml) were primed with 25ng/ml P_3Cys or medium for 4-6h and then stimulated with 5mM ATP for 1h or 50µg/ml SEA and medium for (A-B) 1h, 3h and 6h or (C-E) 24h. The supernatants were evaluated by Western blot technique using antibodies against (A) IL-1β p17 and (B) Casp1 p20 cleavage products or by (C) IL-1β and (E) TNF-α ELISA. (D) BMDCs were lysed and intracellular pro-IL-1β was measured by IL-1β ELISA. (A, B) Examples of Western blot membranes from four independent experiments. (C-E) Bars represent the mean ± SD of three independent experiments. Asterisks show significant differences between brackets *** $p<0.001$.

In addition to the previous ELISA measurements (section 3.1), Western blot analysis (Figure 3.5 A) confirmed that TLR-stimulated BMDCs which were additionally cocultured with SEA (lane 6-8) induced cleavage of pro-IL-1β (p31) into the bioactive IL-1β (p17) form. Moreover, pro-IL-1β was also cleaved when TLR-primed BMDCs were stimulated with ATP (lane 5) which is a potent inflammasome activator leading to enhanced IL-1β production within a short time (1h) [181, 191-193]. As shown in Figure 3.5 B, the cleavage of pro-Casp1 (p45) into the functional Casp1 (p20) could also be detected with ATP (lane 5) and SEA (lane 6-8) in the same extent as the IL-1β cleavage, suggesting that SEA mediates IL-1β cleavage through a Casp1-dependent inflammasome pathway. Nevertheless, slight cleavage of IL-1β and Casp1 was also seen when using ATP alone, an extremely strong inflammasome activator (sections 1.4.2 and 4.2.1). However, stimulation with SEA alone (lane 3 in Figure 3.5 A and B) did not lead to inflammasome activation and cleavage of the precursor forms. To substantiate the Western blot results, TLR-primed Casp1-deficient BMDCs were also

stimulated with SEA or ATP. As shown in Figure 3.5 C, Casp1-deficient BMDCs showed impaired IL-1β production but normal intracellular pro-IL-1β accumulation (Figure 3.5 D). Interestingly, BMDC cultures maintained normal TNF-α secretion (Figure 3.5 E), confirming the two independent immunmodulating mechanisms of SEA described in section 3.1.4.

3.2.2 SEA-mediated IL-1β induction depends on NLRP3 inflammasome activation

The finding that Casp1 activation is responsible for the SEA-mediated IL-1β cleavage (section 3.2.1) further suggested that the inflammasome was also involved in this IL-1β release. In addition to Casp1, the inflammasome consists of ASC and a protein of the NLR family, such as NLRP1, NLRP3, NLRP6, NLRC4 and AIM2 (section 1.4.1). However, the majority of tested PAMPs and DAMPs, including the plasmodium studies [223-225] have been shown to trigger the NLRP3 inflammasome (section 1.4.2). Thus, the NLRP3 inflammasome seem to be a prime candidate driving SEA-mediated IL-1β production. To confirm this hypothesis, NLRP3- and ASC-deficient BMDCs were stimulated as previously described and supernatants were analysed using Western blot and ELISA techniques. The results are summarized in Figure 3.6.

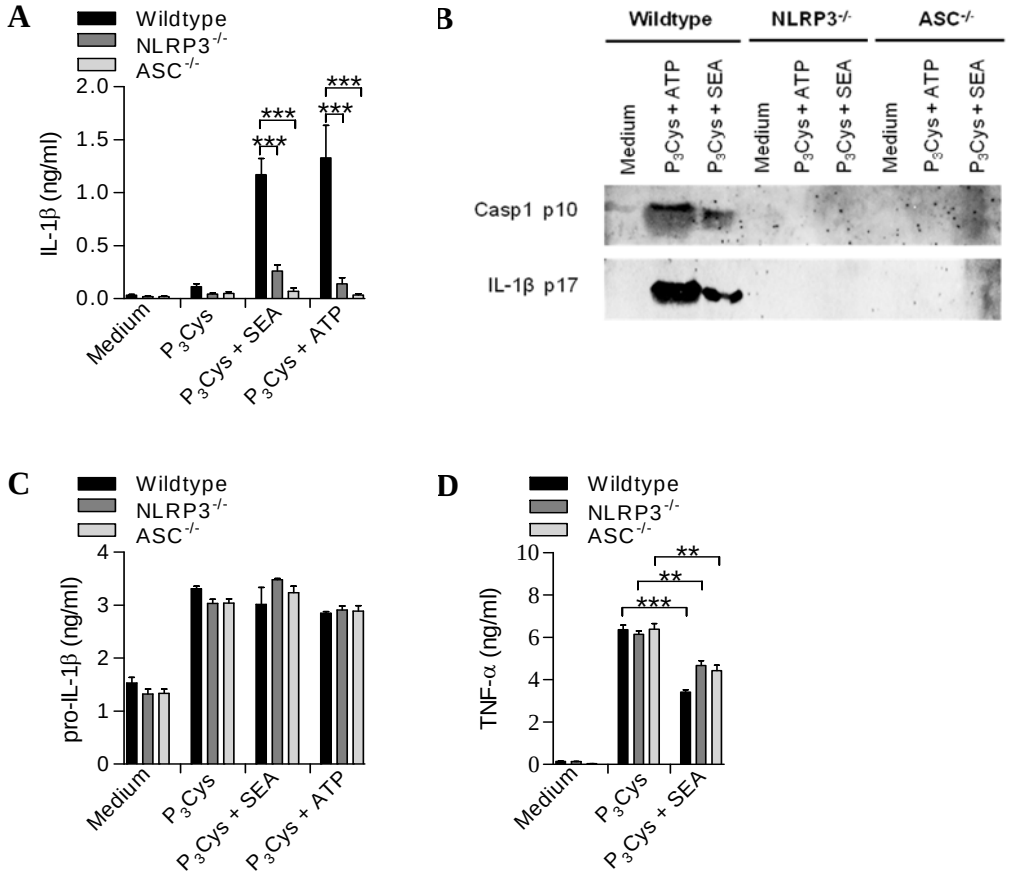

Figure 3.6: SEA mediates IL-1β release in an ASC- and NLRP3-dependent manner
Wildtype, NLRP3$^{-/-}$ and ASC$^{-/-}$ BMDCs (1x10^6/ml) were primed with 25ng/ml P_3Cys or medium for 4-6h and then stimulated with either 5mM ATP for 1h or 50µg/ml SEA and medium for (B) 6h or (A, C) 24h. (D) Wildtype, NLRP3$^{-/-}$and ASC$^{-/-}$ BMDCs were primed with 50µg/ml SEA or medium for 30min and then stimulated with 25ng/ml P_3Cys or medium for an additional 24h. The supernatants were evaluated in (B) by Western blot technique using antibodies against IL-1β p17 or Casp1 p10 cleavage products or in (A) IL-1β and (D) TNF-α by ELISA. (C) BMDCs were lysed and intracellular pro-IL-1β was measured by IL-1β ELISA. (A, C-D) Bars represent the mean ± SD of three independent experiments. Asterisks show significant differences between brackets *** $p<0.001$ and ** $p<0.01$. (B) Example of Western blot membrane from five independent experiments.

As shown in Figure 3.6 A, SEA-mediated IL-1β secretion was impaired in the absence of ASC or NLRP3 and furthermore, these NLRP3 inflammasome-deficient BMDCs failed to process the cleaved products of Casp1 and IL-1β (Figure 3.6 B). Interestingly, pro-IL-1β accumulation was not altered in the absence of ASC and NLRP3 (Figure 3.6 C), confirming that the accumulation of the precursor is independent of inflammasome assembling and based on the NF-κB pathway activation. These findings were also confirmed with ATP (Figure 3.6 A-C). However, SEA-mediated suppression of TNF-α was unaffected by the absence of ASC and NLRP3, confirming the above described results with Casp1-deficient BMDCs (section 3.2.1 and Figure 3.5 E).

3.2.3 SEA-mediated NLRP3 inflammasome activation depends on intracellular potassium efflux and mitochondrial reactive oxygen species

Several studies have indicated that NLRP3 inflammasome activation is triggered by different upstream events such as potassium efflux and reactive oxygen species (ROS) production [135, 187-193]. To decipher the role of these intermediary signals, BMDCs were treated with potassium chloride or glibenclamide to block potassium channels and ROS inhibitors to block the accumulation of ROS (see section 2.3.3.2 for details).

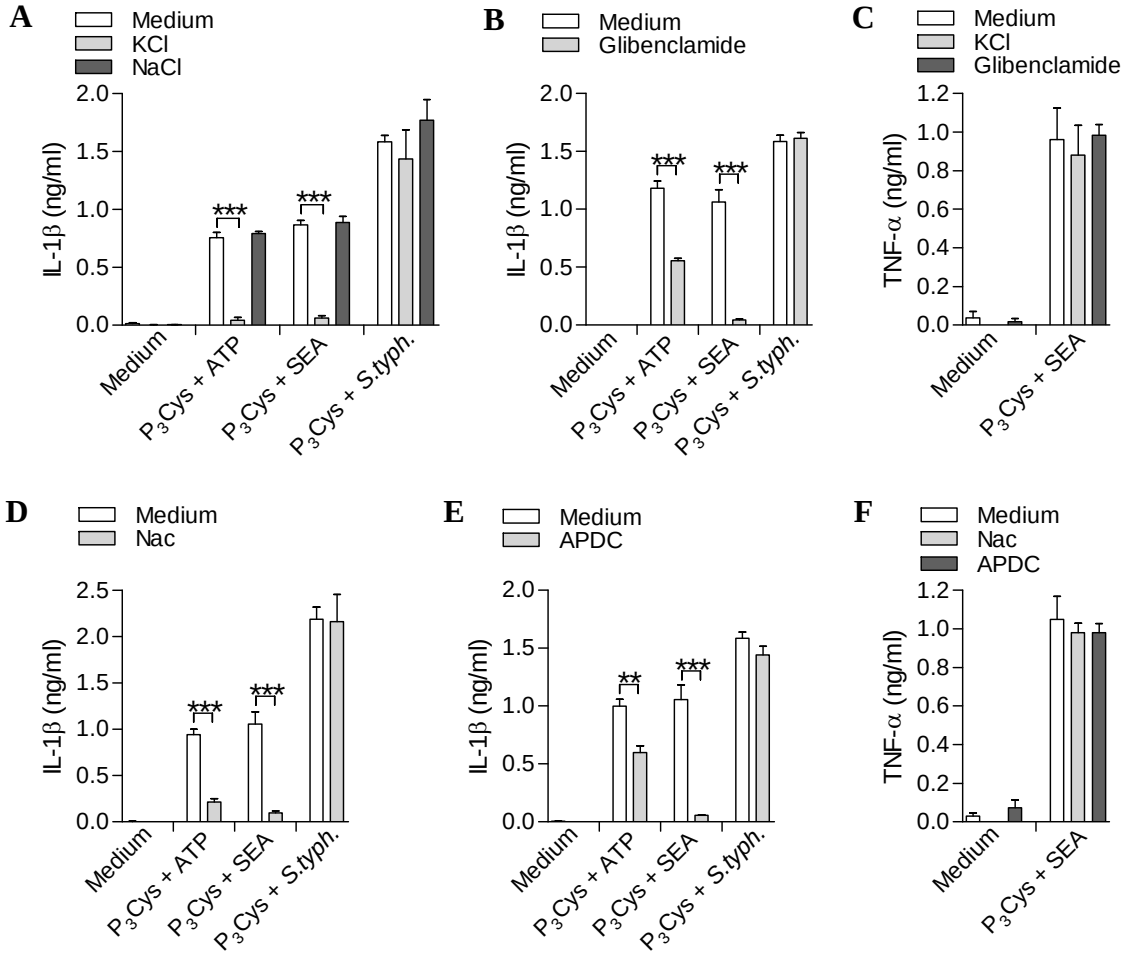

Figure 3.7: SEA-mediated NLRP3 inflammasome activation requires potassium efflux and reactive oxygen species (ROS) production
BMDCs were primed with 25ng/ml P_3Cys or medium for 4-6h and then stimulated with either 5mM ATP for 1h, *Salmonella typhimurium* (*S.typh.*) with a multiplicity of infection (MOI) of 10 for 6h, 50µg/ml SEA or medium for 24h. In some cultures, BMDCs were pretreated for 30min with (A, C) 60mM KCl, (A) 60mM NaCl, (B, C) 150µM glibenclamide to block potassium channels, (D, F) 50mM Nac or (E, F) 200µM APDC to inhibit ROS production. The resulting supernatants were evaluated by ELISA for (A-B, D-E) IL-1β and (C, F) TNF-α production. Bars represent the mean ± SD of three independent experiments. Asterisks show significant differences between brackets *** $p<0.001$ and ** $p<0.01$.

Potassium efflux can be blocked by either increasing the extracellular potassium concentration through additional KCl or by inhibiting the ATP-sensitive potassium channels through glibenclamide. Both of these pretreatment methods lead to impaired IL-1β production in TLR-triggered SEA or ATP stimulated BMDC cultures (Figure 3.7 A and B). However, the SEA- and ATP-mediated IL-1β secretion was not impaired with NaCl (Figure 3.7 A), confirming that activation of potassium channels followed by potassium efflux specifically mediates NLRP3 inflammsome assembling. In addition, treatment with the ROS inhibitors *N*-acetyl-*L*-cysteine (Nac), which is an antioxidant and free radical scavenger, or (2R,4R)-4-aminopyrrolidine-2,4-dicarboxylic acid (APDC), which inhibits the NADPH-oxidase dependent ROS system, also inhibited the SEA- and ATP-mediated IL-1β production (Figure 3.7 D and E). As a control, *Salmonella typhimurium* (*S.typh.*) was used as a secondary stimulus since this bacterium has been shown to specifically acitvate the NLRC4 inflammasome [175]. In the experiment depicted in Figure 3.7, IL-1β production continues to be induced during inhibition of potassium efflux and ROS production, demonstrating that these two intermediary signals are specific for NLRP3 inflammasome activation. Interestingly, blocking potassium efflux and ROS production did not influence the SEA-mediated secretion profile of TNF-α (Figure 3.7 C and F).

Recently, Zhou *et al.* have been shown that *Candida albicans* mediated NLRP3 inflammasome activation depends on mitochondrial ROS production [195]. Therefore, to investigate the role of mitochondrial ROS production during SEA-mediated NLRP3 inflammasome activation, BMDCs were inhibited with 2,4-dinitrophenole (DNP) or carbonyl cyanide p-(tri-fluromethoxy)phenyl-hydrazone) (FCCP). These substances uncouple oxidative phosphorylation within the mitochondrial electron transport chain by carrying protons across the mitochondrial membrane. This leads to impaired ROS production and ATP generation. Since, ATP is a molecule used for energy transfer and is therefore crucial for maintaining cell viability it was essential to control in these experiments that the BMDCs were still viable and could produce efficient amounts of ATP upon DNP and FCCP treatment. This analysis was performed using an ATP-mediated luminescent cell viability assay as described in section 2.3.8. Additionally, IL-1β and TNF-α secretions were evaluated using ELISA and the results of these mitochondrial based assays are illustrated in Figure 3.8.

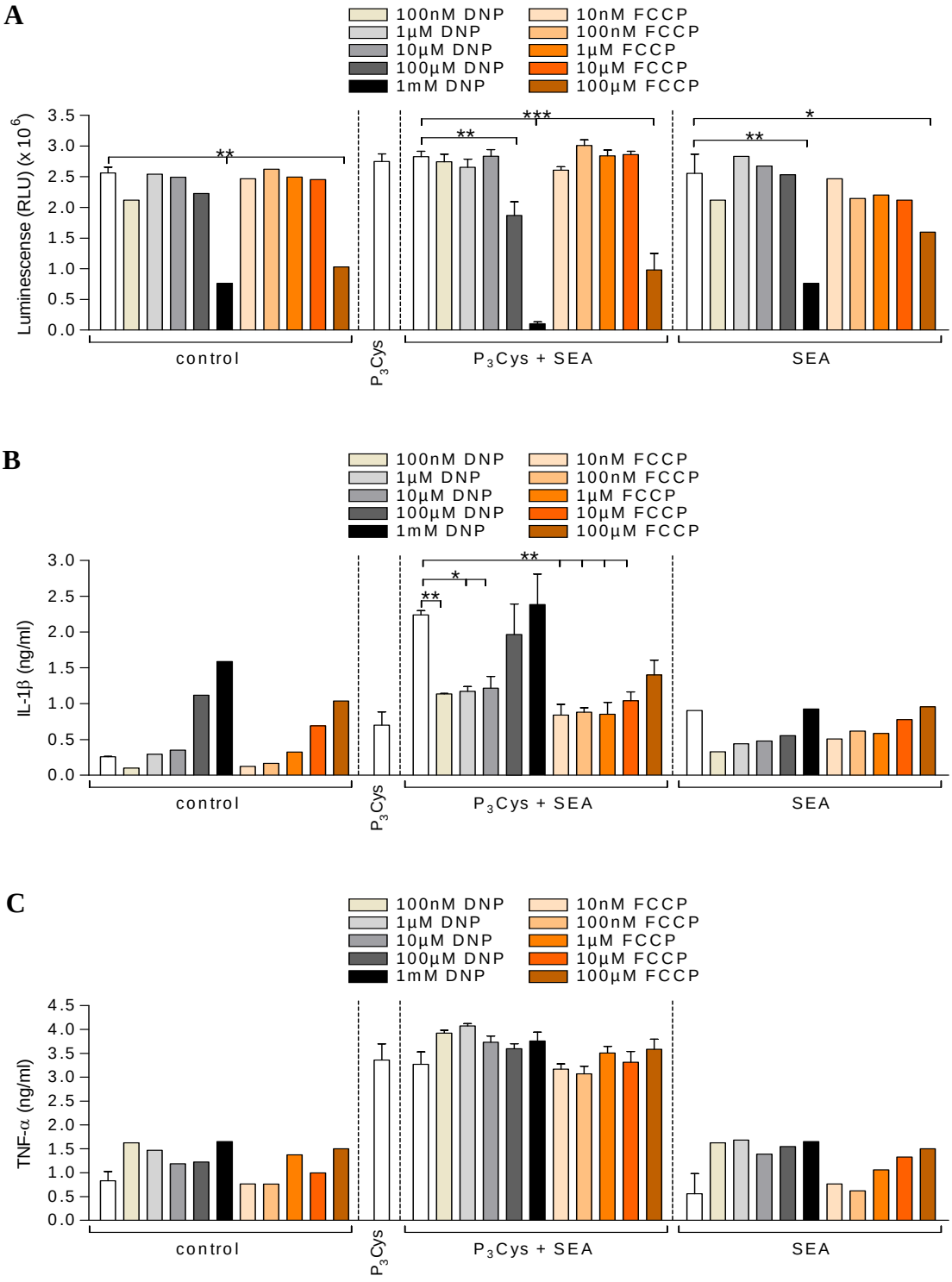

Figure 3.8: Mitochondrial ROS facilitates SEA-mediated NLRP3 inflammasome activation
BMDCs ($1x10^6$/ml) were primed with 25ng/ml P_3Cys or medium for 4-6h and then stimulated with or without SEA (50µg/ml) for a further 24h. To inhibit mitochondrial ROS production, BMDCs were pretreated with 100nM-1mM DNP (2,4-dinitrophenole**)** or 10nM-100µM FCCP (carbonyl cyanide p-(tri-fluromethoxy)phenyl-hydrazone)) for 30min before the addition of SEA. (A) ATP levels within the supernatants were evaluated using a luminescent cell viability assay and (B) IL-1β and (C) TNF-α amounts were measured by ELISA. Bars represent the mean ± SD of two independent experiments. Asterisks show significant differences between brackets *** $p<0.001$, ** $p<0.01$ and * $p<0.05$.

The ATP-derived luminescent signals were detected in relative light units (RLU) and as shown in Figure 3.8 A, ATP levels were significantly decreased when BMDCs were additionally treated with high concentrations of DNP and FCCP. Thus, these high concentrations of DNP and FCCP had to be excluded in the experiments evaluating the effects of mitochondrial ROS during SEA-mediated IL-1β and TNF-α secretion. Indeed, SEA-mediated IL-1β production was significantly impaired when BMDCs were treated with the concentrations of DNP (100nM-10µM) and FCCP (10nM-10µM) (Figure 3.8 B), suggesting that mitochondrial ROS production is crucial for SEA-mediated NLRP3 inflammasome activation. Interestingly, IL-1β levels increased when BMDCs were treated with the high concentrations of DNP (100µM-1mM) and FCCP (100µM), confirming that the ATP production was abolished in these BMDCs (Figure 3.7 A) and leading to cell death, which is a source of IL-1β [200, 226]. TNF-α secretion was not affected by blocking mitochondrial ROS (Figure 3.8 C) clearly showing that this SEA-mediated effect is not dependent on the inflammasome.

3.2.4 NLRP3 inflammasome activation by SEA is independent of phagocytosis

To activate the NLRP3 inflammasome two mechanisms are known to be important, phagocytosis and receptor triggering. Several studies have shown that triggering phagocytosis leads to lysosomal rupture and the release of cathepsin B which in turn results in NLRP3 inflammasome activation [186-190]. To investigate whether the SEA-mediated assembly of the NLRP3 inflammsome was via phagocytosis mechanisms, BMDCs culture assays were performed using cytochalasin D (CytD), which blocks actin polymerization, particle internalization and the binding stage of phagocytosis (Figure 3.9).

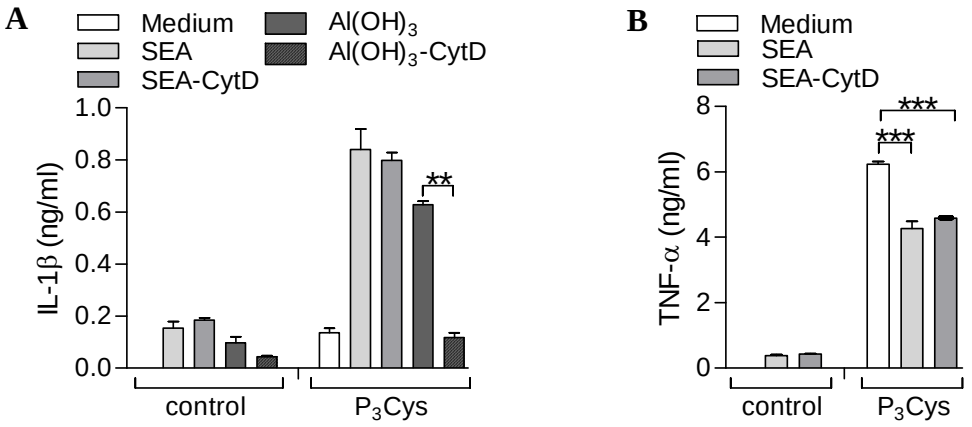

Figure 3.9: SEA-mediated NLRP3 inflammasome activation is independent of phagocytosis
(A) BMDCs ($1x10^6$/ml) were primed with 25ng/ml P_3Cys or medium (control) for 4-6h and then stimulated in the presence or absence of SEA (50µg/ml) for an additional 24h. (B) BMDCs ($1x10^6$/ml) were primed with 50µg/ml SEA or left alone (white bars) for 30min and then stimulated with 25ng/ml P_3Cys or medium (control) for an additional 24h. For the inhibition of phagocytosis, BMDCs were pretreated with 1µM cytochalasin D (CytD) for 30min before the addition of SEA. The supernatants were evaluated using (A) IL-1β and (B) TNF-α ELISAs. Bars represent an example of the mean ± SD of three independent experiments. Asterisks show significant differences between brackets *** $p<0.001$ and ** $p<0.01$.

As shown in Figure 3.9 A, SEA-mediated IL-1β production was maintained after treatment with CytD, whereas BMDCs treated with aluminium hydroxide ($Al(OH)_3$), which activate the NLRP3 inflammasome via phagocytosis [188], could no longer induce IL-1β. In addition, SEA-mediated TNF-α suppression was not impaired by CytD (Figure 3.9 B).

3.2.5 SEA triggers the Dectin-2 receptor to activate the NLRP3 inflammasome

In the previous section 3.2.4, it was demonstrated that SEA-mediated NLRP3 inflammasome activation and IL-1β induction is independent of phagocytosis indicating that the responsible mechanism is elicited through specific triggering of a receptor. Several studies have provided evidence that ATP activates the NLRP3 inflammasome by triggering the P2X7 receptor [191-193]. Thus, to elucidate whether SEA-mediated NLRP3 inflammasome activation also involved this receptor, P2X7-deficient BMDCs were stimulated in the above described manner (section 2.3.3.2) and culture supernatants were evaluated for levels of IL-1β and TNF-α (Figure 3.10).

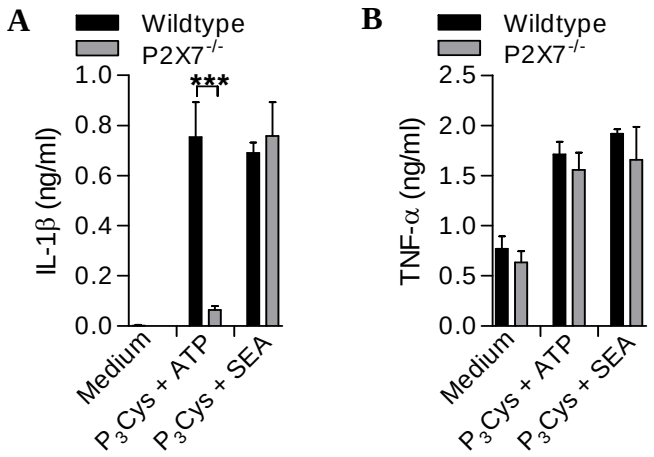

Figure 3.10: SEA-mediated NLRP3 inflammasome activation is independent of the P2X7 receptor
P2X7$^{-/-}$ and wildtype BMDCs (1x10^6/ml) were primed with 25ng/ml P_3Cys or medium for 4-6h and then stimulated with either 5mM ATP for 1h or 50µg/ml SEA for an additional 24h. The resulting supernatants were evaluated for (A) IL-1β and (B) TNF-α release using ELISA. Bars represent the mean ± SD of three independent experiments. Asterisks show significant differences between brackets *** $p<0.001$.

In contrast to ATP, SEA-mediated IL-1β production was still detectable in P2X7 receptor-deficient BMDCs (Figure 3.10 A), excluding the requirement for intracellular ATP in the SEA-mediated NLRP3 inflammasome activation. In addition, no ATP could be detected within SEA preparations (data not shown) and again, TNF-α secretion remained intact (Figure 3.10 B). These data demonstrate that SEA-mediated NLRP3 inflammasome activation is independent of the P2X7 receptor which additionally implied that this process was conducted through a different type of receptor. Since components within the SEA are highly glycosylated [108, 109], C-type lectin receptors obviously play a role in its recognition. Indeed, several studies have shown that different C-type lectin receptors (CLRs) are triggered by SEA [122, 123, 130-132]. Interestingly, studies with the fungus *C.albicans* revealed a critical role of the CLR Dectin-1 for NLRP3 inflammasome activation [134, 135] (see section 1.3.5 for details). Thus, CLRs seem to be critical candidates for SEA-mediated NLRP3 inflammasome activation. To identify the specific receptor that is responsible for SEA-triggering, BMDCs, deficient of different receptors (especially C-type lectin receptors), were stimulated in the above described manner with TLR stimuli and SEA. The resulting levels of IL-1β and TNF-α secretions are depicted in Figure 3.11.

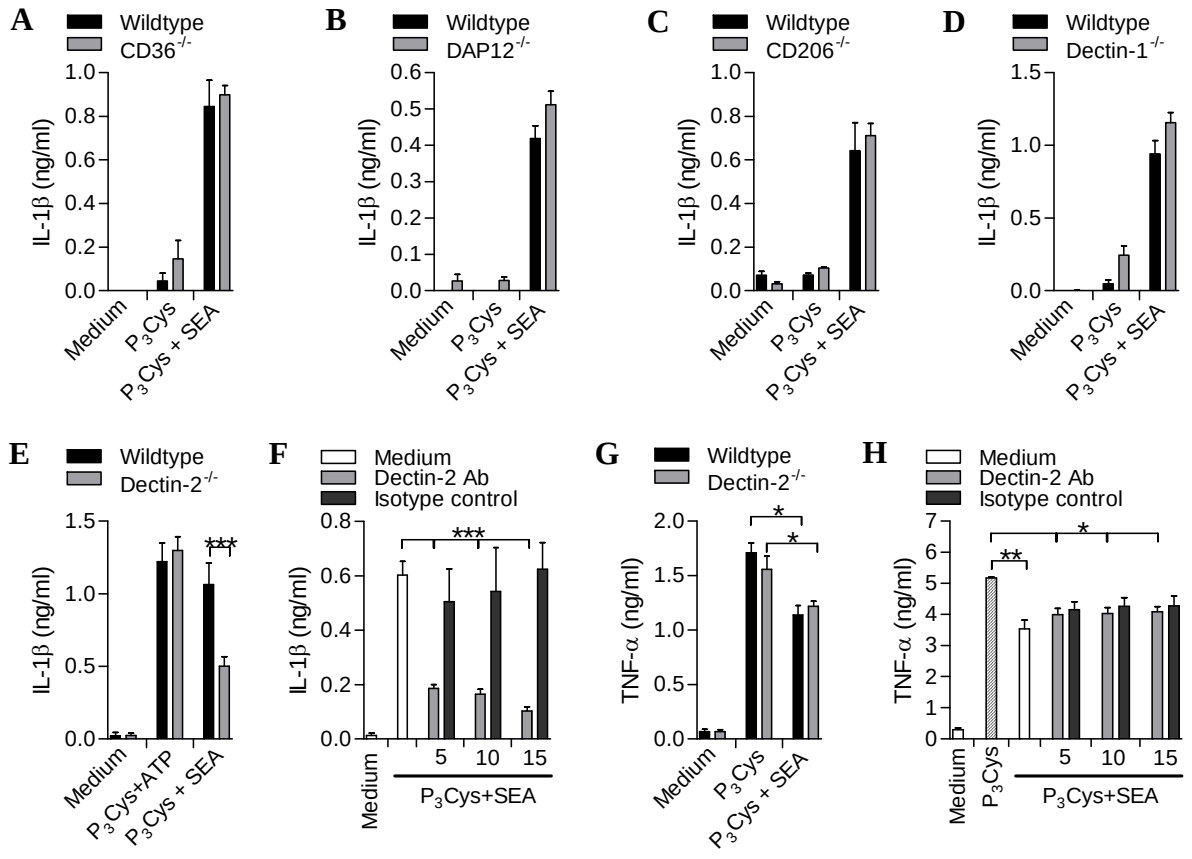

Figure 3.11: SEA triggers the Dectin-2 receptor to induce NLRP3 inflammasome activation
(A-F) Wildtype, (A) CD36$^{-/-}$, (B) DAP12$^{-/-}$, (C) CD206$^{-/-}$, (D) Dectin-1$^{-/-}$ and (E) Dectin-2$^{-/-}$ BMDCs ($1x10^6$/ml) were primed with or without 25ng/ml P_3Cys for 4-6h and then stimulated with either 5mM ATP for 1h or 50µg/ml SEA for an additional 24h. Alternatively, (G-H) Wildtype and (G) Dectin-2$^{-/-}$ BMDCs ($1x10^6$/ml) were primed with 50µg/ml SEA for 30min and then stimulated with 25ng/ml P_3Cys for a further 24h. (F, H) For Dectin-2 blocking experiments, BMDCs ($1x10^6$/ml) were pretreated with 5-15µg/ml Dectin-2 antibody or IgG2a isotype control for 2h before the addition of SEA. Culture supernatants were evaluated for (A-F) IL-1β and (G-H) TNF-α by ELISA. Bars represent the mean ± SD of three independent experiments. Asterisks show significant differences between brackets *** $p<0.001$, ** $p<0.01$ and * $p<0.05$.

As shown in Figures 3.11 A and C, BMDCs lacking the scavenger coreceptor CD36, which senses lipids, especially diacylglycerides [227], or the mannose receptor CD206, which recognizes mannose structures to initiate phagocytosis [228], showed no alteration in IL-1β production. These data confirme that SEA-mediated IL-1β induction is probably due to the triggering of a (glyco-)protein (section 3.1.4 and Figure 3.4 A) and independent of phagoytosis processes (section 3.2.4 and Figure 3.9 A), respectively. Moreover, no impaired SEA-mediated IL-1β secretion was observed using BMDCs lacking the adapter protein DAP12 (Figure 3.11 B). This molecule transmits signals from different receptors into the cytosol via the immunoreceptor tyrosine-based activation motif (ITAM) [229]. IL-1β

production was still present from cells deficient for the Dectin-1 receptor (Figure 3.11 D). The receptor has already been shown to facilitate NLRP3 inflammasome activation and IL-1β production by the fungus *Candida albicans* [134, 135]. However, SEA-mediated IL-1β production was significantly inhibited in Dectin-2-deficient BMDCs, whereas the ATP-mediated IL-1β production remained unaltered (Figure 3.11 E). This finding could be confirmed by the treatment of BMDCs with Dectin-2 blocking antibodies (Figure 3.11 F). Nevertheless, SEA-mediated TNF-α suppression was not affected (Figure 3.11 G and H), emphasizing that different components within the SEA mediate different immune reactions.

3.2.6 Dectin-2 couples to FcRγ chain to activate Syk signalling

The C-type lectin receptor Dectin-2 binds high mannose structures [230, 231]. Moreover, it has been further shown to couple with the Fc receptor γ (FcRγ) chain that contains ITAM signalling molecules which are phosphorylated through spleen tyrosine kinase (Syk), a precursor step to the induction of innate immune responses [135, 232-237]. The coupling and signalling mechanisms of these three molecules have been studied in experiments using the fungus *Candida albicans*. To analyse the role of FcRγ and Syk during SEA-mediated triggering of Dectin-2, BMDCs simulation assays using FcRγ$^{-/-}$ BMDCs and Syk inhibitor (R406) were performed and the results are depicted in Figure 3.12.

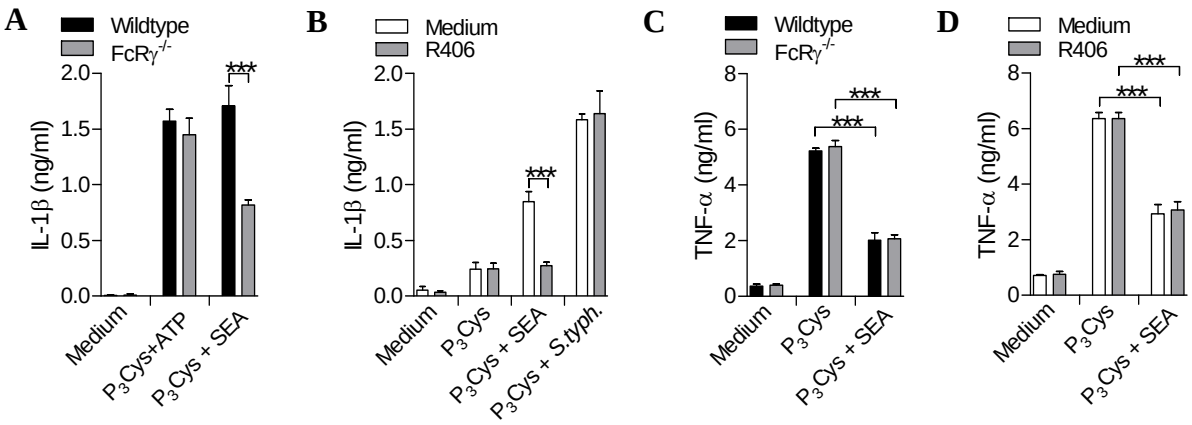

Figure 3.12: SEA triggering of Dectin-2 activates Fc receptor γ chain and spleen tyrosine kinase
(A-B) Wildtype and (A) FcRγ$^{-/-}$ BMDCs (1x10^6/ml) were primed with 25ng/ml P_3Cys for 4-6h and then stimulated with either 5mM ATP for 1h, *Salmonella typhimurium* (*S.typh.*) with a multiplicity of infection (MOI) of 10 for 6h or 50µg/ml SEA for a further 24h. (C-D) Wildtype and (C) FcRγ $^{-/-}$ BMDCs (1x10^6/ml) were primed with or without 50µg/ml SEA for 30min and then stimulated with 25ng/ml P_3Cys for an additional 24h. (B, D) For inhibition of the spleen tyrosine kinase (Syk), BMDCs were pretreated with 1µM R406 for 30min before the addition of SEA. The supernatants were evaluated for (A-B) IL-1β or (C-D) TNF-α by ELISAs. Bars represent the mean ± SD of three independent experiments. Asterisks show significant differences between brackets *** $p<0.001$.

Interestingly, FcRγ-deficient mice showed impaired IL-1β production after stimulation with SEA, whereas ATP-mediated IL-1β induction was not altered (Figure 3.12 A). Moreover, inhibition of Syk signalling with the inhibitor R406, which is already used in clinical trials for the treatment of inflammatory diseases [238], completely blocked SEA-mediated IL-1β production. In contrast, no effect could be observed when BMDCs were stimulated with *Salmonella typhimurium* (*S.typh.*) (Figure 3.12 B), confirming that NLRC4 inflammasome activation is independent of Syk signalling [135]. Contrary, the ability of SEA to suppress TNF-α production upon TLR-triggering was not altered in FcRγ$^{-/-}$ BMDCs (Figure 3.12 C) or after inhibition of Syk signalling (Figure 3.12 D). These results confirm that SEA triggers the Dectin-2 receptor that couples to the FcRγ chain to induce Syk activation.

3.2.7 Card9 is a crucial molecule for SEA-mediated NLRP3 inflammasome activation

Several intermediate molecules are relevant for the transmission of signals downstream from Syk. These molecules can indirectly trigger downstream processes, such as ROS production and potassium efflux which, as shown in previous section 3.2.3, are critical for SEA-mediated inflammasome activation. However, to date, no direct associations have been observed. Nevertheless, several studies have suggested that the Syk-ITAM-based signalling leads to aggregation of caspase recruitment domain 9 (Card9) which links to the adapter protein B cell lymphoma 10 (Bcl10) and mucosa-associated lymphoid tissue lymphoma translocation protein 1 (Malt1) to induce nuclear factor-κB (NF-κB) pathway and proinflammatory cytokine release [233, 234, 239, 240]. These findings are again mainly based on the *C.albicans*-mediated triggering of the Dectin-1 receptor but this fungus is further associated with Dectin-2 triggering and the induction of Card9 signalling aswell [236, 237]. To investigate the role of Card9 during SEA-mediated NLRP3 inflammsome activation, Card9-deficient BMDCs were stimulated with TLR in the presence of SEA and the resulting quantities of IL-1β and pro-IL-1β were evaluated by ELISA (Figure 3.13).

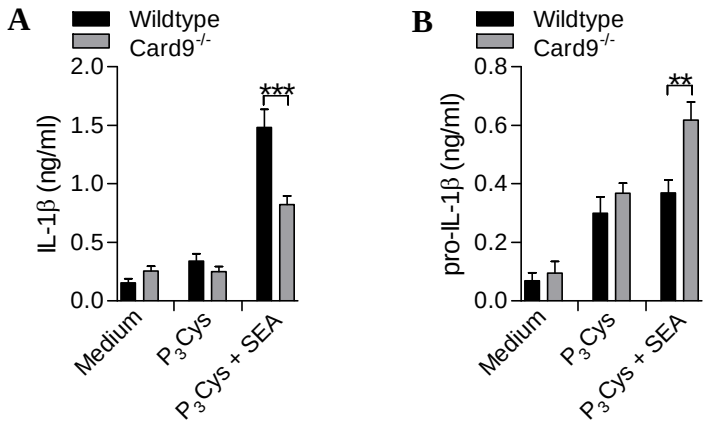

Figure 3.13: SEA-mediated NLRP3 inflammasomme activation depends on the Card9 molecule
Wildtype and Card9$^{-/-}$ BMDCs ($1x10^6$/ml) were primed with 25ng/ml P_3Cys for 4-6h and then stimulated with or without 50µg/ml SEA for an additional 24h. (A) The supernatants were evaluated by IL-1β ELISA. (B) BMDCs were lysed and intracellular pro-IL-1β was measured by IL-1β ELISA. Bars represent the mean ± SD of three independent experiments. Asterisks show significant differences between brackets *** $p<0.001$ and ** $p< 0.01$.

As clearly shown in Figure 3.13, TLR-primed Card9-deficient BMDCs showed impaired IL-1β secretion upon co-culture with SEA (Figure 3.13 A). It is known that Card9 can mediate signals via the induction of the NF-κB lead to the transcription and accumulation of inflammatory and precursor cytokines, such as pro-IL-1β (see section 1.4.2). Therefore the observed reduction in IL-1β secretion of Card9$^{-/-}$ BMDCs seen in Figure 3.13A could have been due to the impaired accumulation of pro-IL-1β. Interestingly, pro-IL-1β was even accelerated in Card9-deficient BMDCs (Figure 3.13 B), suggesting that the Card9 molecule plays a crucial role for the NLRP3 inflammasome activation independent of NF-κB pathway signalling.

3.2.8 Model of SEA-mediated NLRP3 inflammasome activation

The findings of these above described *in vitro* BMDCs stimulation assays (sections 3.2.1-3.2.6), were fused into the manuscript entitled "*Schistosoma mansoni* triggers Dectin-2, which activates the NLRP3 inflammasome and alters adaptive immune responses" by Ritter *et al.* 2010 [241]. With the additional experiments using mitochondrial blocking agents (section 3.2.3 and Figure 3.8) and Card9-deficient cells (section 3.2.7 and Figure 3.13), a model for SEA-mediated NLRP3 inflammasome activation mechanisms begins to emerge (Figure 4.1). In essence, a (glyco-)protein within the SEA triggers the Dectin-2 receptor that is coupled with the FcRγ chain, which contains the ITAM signalling molecule. The repeated tyrosine

sequence of the ITAM motif becomes phosphorylated by Syk leading to signal transmission via indirect and direct processes. Indirect processes are characterized by the activation of the intermediary molecules ROS that are produced by the mitochondria and potassium that is transported out of the cell via potassium channels. Direct processes on the other hand appear to be facilitated by the Syk-mediated association and activation of the Card9-Bcl10-Malt1 complex. Finally, these intermediary molecules activate the NLRP3 inflammasome containing NLRP3, ASC and pro-Casp1 leading to cleavage of the precursor pro-Casp1 into Casp1, which then cleaves the pro-IL1β into the functional bioactive IL-1β that is finally secreted out of the BMDCs (see section 4.2.5 for details).

3.3 Investigation of inflammasome activation during *S. mansoni* infection

As shown in the previous sections, 3.1 and 3.2, SEA induces NLRP3 inflammasome activation of TLR-primed BMDCs *in vitro*. To decipher the role of the NLRP3 inflammasome during an ongoing *S. mansoni* infection, NLRP3$^{-/-}$, ASC$^{-/-}$, Dectin-2$^{-/-}$, IL-1R$^{-/-}$ and Dectin-1$^{-/-}$ mice on C57BL/6 background were infected with *S. mansoni* cercariae as described in section 2.5. After 8 weeks of infection, parasitological, histological and immunological parameters of the infected knockout mice were evaluated and compared with infected wildtype mice.

3.3.1 Parasitological parameters are not altered in the different knockout strains

S. mansoni-infected mice were sacrificed after 8 weeks of infection and the parasitological parameters degree of infection (DOI), organ weight (spleen, liver and intestine), worm count and egg count within the intestine and liver were evaluated as described in section 2.5.3. Data accumulated from these parasitological parameters are summarized in Table 3.1.

Parasitological parameters	Wildtype	ASC$^{-/-}$	NLRP3$^{-/-}$	IL-1R$^{-/-}$	Dectin-2$^{-/-}$	Dectin-1$^{-/-}$
Mouse weight (g)	22.85 (± 0.53)	22.65 (± 0.30)	24.80 (± 0.96)	23.74 (± 0.55)	25.43 (± 0.73)	25.01 (± 0.72)
DOI (degree of infection)	2.45 (± 0.08)	2.25 (± 0.16)	2.16 (± 0.19)	2.21 (± 0.25)	2.45 (± 0.12)	2.50 (± 0.31)
Worms/mouse	12.30 (± 1.26)	15.50 (± 2.77)	9.09 (± 1.68)	9.08 (± 2.26)	9.60 (± 1.58)	12.63 (± 2.83)
Eggs/liver (x10^3)	14.88 (± 2.78)	11.75 (± 3.83)	9.671 (± 2.52)	7.74 (± 2.10)	16.25 (± 3.43)	11.19 (± 2.60)
Eggs/intestine (x10^3)	23.92 (± 3.58)	31.89 (± 8.57)	23.18 (± 4.74)	22.57 (± 8.88)	32.37 (± 6.11)	23.70 (± 9.39)
Liver weight (g)	1.76 (± 0.04)	1.80 (± 0.05)	1.83 (± 0.13)	1.74 (± 0.10)	1.88 (± 0.05)	1.87 (± 0.12)
Intestine weight (g)	3.44 (± 0.07)	3.65 (± 0.07)	3.72 (± 0.22)	3.40 (± 0.16)	3.64 (± 0.10)	3.75 (± 0.15)
Spleen weight (g)	0.24 (± 0.01)	0.24 (± 0.02)	0.20 (± 0.02)	0.21 (± 0.02)	0.26 (± 0.02)	0.27 (± 0.04)

Table 3.1: Parasitological parameters after 8 weeks of *S. mansoni* infection
Wildtype (n=35), ASC$^{-/-}$ (n=16), NLRP3$^{-/-}$ (n=15), IL-1R$^{-/-}$ (n=16), Dectin-2$^{-/-}$ (n=22) and Dectin-1$^{-/-}$ (n=5) mice were infected with 100-120 *S. mansoni* cercariae. After 8 weeks of infection, mice were sacrificed and the parasitological parameters mouse weight, DOI (degree of infection), worm count, egg count within liver and intestine and organ weight (spleen, liver and intestine) were evaluated. Results show the combined data accumulated from three independent *S. mansoni* infections per mouse strain. Values in brackets represent ± SD.

As displayed in Table 3.1, the different knockout mice showed no significant alterations in mouse weight, DOI, worm and egg count or organ weight when compared to the wildtype mice. Parasitologically, no significant differences could be observed either although there were slight changes in some parameters, such as DOI, worm and egg burden. These slight differences occur due to the natural variability of the complex infection within the host. Moreover, the individual comparison of mice from the same strain also showed deviations, especially in DOI and parasite burden (see standard deviations in brackets within Table 3.1), confirming the complexity of the *S. mansoni* infection. In summary, these data suggest that the lack of NLRP3 inflammasome components or CLRs did not influence the development and maturation of the parasite as well as the egg production.

3.3.2 Impaired granuloma formation in infected ASC$^{-/-}$, NLRP3$^{-/-}$, IL-1R$^{-/-}$ and Dectin-2$^{-/-}$ mice

As shown in section 3.3.1, no alterations could be observed in the measured parasitological parameters of infected mice deficient in either NLRP3 inflammasome components, functional IL-1R or the C-type lectin receptors Dectin-1 and Dectin-2. Besides parasite burden, another important parameter of Schistosomiasis is the formation of CD4^{+} T cell-mediated granulomas, which stem from inflammatory responses around schistosome eggs trapped in the liver or intestine (section 1.3.4). To analyse changes in granuloma formation, left liver lobes from infected wildtype, ASC$^{-/-}$, NLRP3$^{-/-}$, IL-1R$^{-/-}$, Dectin-2$^{-/-}$ and Dectin-1$^{-/-}$ mice were cut (3µm), fixed on glass slides and stained with Masson's blue as described in section 2.5.3. Granuloma formation and size was then evaluated microscopically. The results are shown in Figure 3.14.

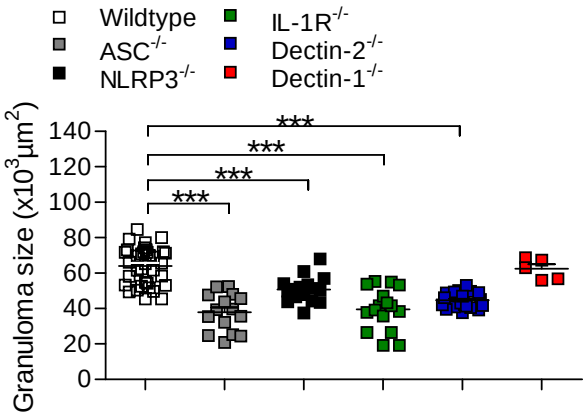

Figure 3.14: *S. mansoni*-mediated Dectin-2 receptor/NLRP3 inflammasome activity and IL-1β signalling influence granuloma formation
Wildtype (n=35), ASC$^{-/-}$ (n=16), NLRP3$^{-/-}$ (n=15), IL-1R$^{-/-}$ (n=16), Dectin-2$^{-/-}$ (n=22) and Dectin-1$^{-/-}$ (n=5) mice were infected with 100-120 *S. mansoni* cercariae. After 8 weeks of infection, mice were sacrificed. Thereafter, left liver lobes from individually infected mice were fixed and embedded in paraffin. 3µm sections were then fixed on glass slides for Masson's blue staining. Finally, liver sections were microscopically assessed (x10 magnification) to calculate the average granuloma size per mouse. 30-40 granulomas per section from each infected mouse were analysed. Results show the combined data accumulated from three independent *S. mansoni* infections per mouse strain. Symbols show mean ± SD and asterisks show significant differences between brackets *** $p<0.001$.

The assessment of liver immunopathology showed that ASC$^{-/-}$, NLRP3$^{-/-}$, IL-1R$^{-/-}$ and Dectin-2$^{-/-}$ mice developed significantly smaller granulomas compared to wildtype and Dectin-1-deficient mice (Figure 3.14). These data reveal a crucial role for the Dectin-2/NLRP3 inflammasome activity and functional IL-1 signalling during an ongoing *S. mansoni* infection and the development of immunopathology: the main cause of morbidity in Schistosomisis.

3.3.3 *S. mansoni* infected NLRP3$^{-/-}$ and ASC$^{-/-}$ mice present decreased *in situ* IL-1β levels within infected organs

Previous studies have shown that the IL-1 receptor antagonist (IL-1Ra), which blocks IL-1 signals by binding to the IL-1 receptor (IL-1R; section 1.4), is up-regulated during *S. mansoni* infection and moreover, treatment with an anti-IL-1Ra protein leads to increased granuloma size [242, 243]. In addition, granuloma formation is induced by trapped *S. mansoni* eggs which secrete SEA (section 1.3.4), suggesting that the granuloma formation could depend on IL-1 signalling. Indeed, previous research from this group identified that mice lacking MyD88, which is a central downstream adaptor molecule of IL-1R, also developed smaller granulomas upon *S. mansoni* infection [96]. Based on the above described model of SEA-mediated NLRP3 inflammasome activation and IL-1β induction (Figure 4.1), it was hypothesized that IL-1β should be detectable within infected organs during *S. mansoni* infection. Therefore, to investigate IL-1β induction *in vivo*, liver and intestine pieces from infected wildtype, NLRP3$^{-/-}$, ASC$^{-/-}$, IL-1R$^{-/-}$, Dectin-2$^{-/-}$ or Dectin-1$^{-/-}$ mice were homogenized in RPMI 1640 (section 2.5.4) and *in situ* IL-1β levels were evaluated by ELISA. Results are shown in Figure 3.15.

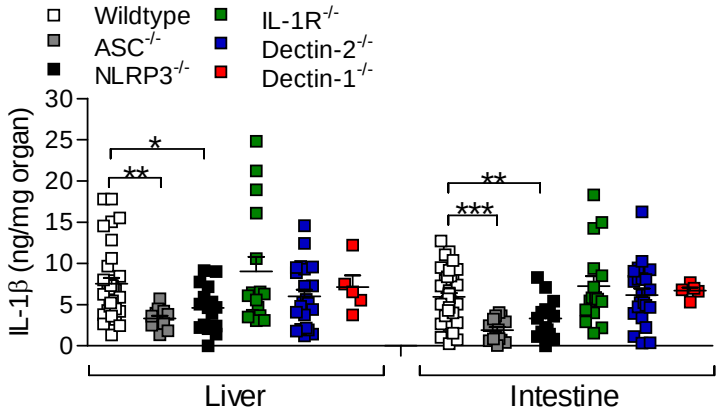

Figure 3.15: ASC$^{-/-}$ and NLRP3$^{-/-}$ mice showed decreased *in situ* IL-1β levels within infected organs
Wildtype (n=35), ASC$^{-/-}$ (n=16), NLRP3$^{-/-}$ (n=15), IL-1R$^{-/-}$ (n=16), Dectin-2$^{-/-}$ (n=22) and Dectin-1$^{-/-}$ (n=5) mice were infected with 100-120 *S. mansoni* cercariae. After 8 weeks of infection, mice were sacrificed and *in situ* IL-1β levels were analysed within infected organs. In short, weighed pieces of liver and intestine from individually infected mice were homogenized, centrifuged and the resulting supernatants evaluated by IL-1β ELISA. Results show the combined data accumulated from three independent *S. mansoni* infections per mouse strain. Symbols show mean ± SD and asterisks show significant differences between brackets *** $p<0.001$, ** $p<0.01$ and * $p<0.05$.

Interestingly, IL-1β levels within infected organs were significantly increased compared to organs from naïve control mice strains (data not shown). As depicted in Figure 3.15, only NLRP3- and ASC-deficient mice showed significantly decreased *in situ* IL-1β levels within the liver and intestine, whereas IL-1R-, Dectin-2- and Dectin-1-deficient mice revealed comparable values to wildtype mice. Again, the results from NLRP3- and ASC-deficient infected mice confirm that SEA-mediated IL-1β induction depends on NLRP3 inflammasome activation, which also seems to be crucial for granuloma formation. Analysis of individually infected IL-1R-deficient mice showed several increased IL-1β values (green symbols), which indicated that there is perhaps impairment of IL-1 recognition and signalling within these mice. In addition, the unaltered *in situ* IL-1β levels in mice lacking the Dectin-2 receptor suggest that an additional receptor could aid SEA-mediated IL-1β induction within infected organs.

3.3.4 ASC$^{-/-}$, NLRP3$^{-/-}$, IL-1R$^{-/-}$ and Dectin-2$^{-/-}$ *S. mansoni* infected mice present altered adaptive immune responses

One of the most interesting aspects of Schistosomiasis is the change from a T_H1 to a dominant T_H2 immune response during the course of infection (Figure 1.6). Previous studies have identified that strong T_H2 immune responses are initiated by trapped schistosome eggs that secrete SEA [86, 87, 91], which was now also shown to induce IL-1β *in vitro* (sections 3.2) and *in vivo* (section 3.3.3). In addition, IL-1β represents a pivotal link in translating innate immune responses into appropriate adaptive pathways [200]. Indeed, both the promotion of T_H2 immune responses [202, 203] and the initiation of distinct T_H cell types, such as T_H17 cells [205-207] have been shown to require IL-1β. Since, granuloma formation also depends on adaptive immune responses mediated by T_H cells, the following experiments were performed in order to decipher the requirement of IL-1β or NLRP3 inflammasome components in directing T_H immune responses. Thus, lymphocyte preparations from the draining mesenteric lymph nodes (MLN) and spleen cells from infected wildtype, NLRP3$^{-/-}$, ASC$^{-/-}$, IL-1R$^{-/-}$ or Dectin-2$^{-/-}$ mice were prepared and stimulated with SEA as described in the section 2.3.1.1 and 2.3.3.3, respectively. Culture supernatants from these stimulated cells were then assessed for their cytokine content using ELISA and the data are demonstrated in Figure 3.16.

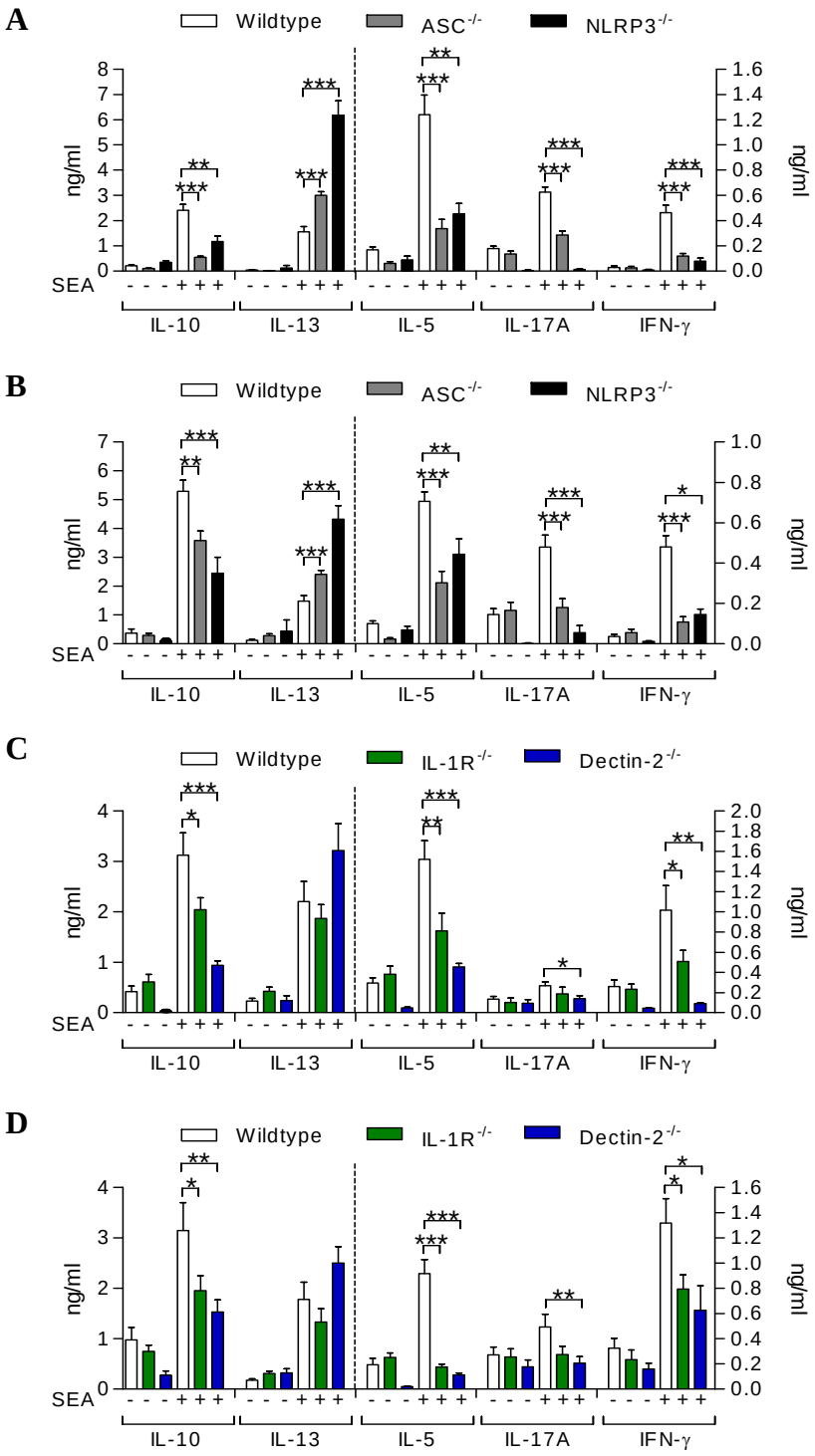

Figure 3.16: *S. mansoni*-mediated Dectin-2 receptor/NLRP3 inflammasome activity and IL-1β signalling influence adaptive immune responses
(A-D) Wildtype (n=35), (A, B) ASC$^{-/-}$ (n=16), NLRP3$^{-/-}$ (n=15), (C, D) IL-1R$^{-/-}$ (n=16) and Dectin-2$^{-/-}$ (n=22) mice were infected with 100-120 *S. mansoni* cercariae. After 8 weeks of infection, mice were sacrificed and lymphocytes were prepared from MLN and spleen. (A, C) 2x10^5 MLN and (B, D) spleen cells were stimulated with or without 20µg/ml SEA for 72h. Culture supernatants were then evaluated for IL-10, IL-13, IL-5, IL-17A and IFN-γ by ELISA. Results show the combined data accumulated from three independent *S. mansoni* infections per mouse strain. Bars show mean ± SD and asterisks show significant differences between brackets *** p<0.001, ** p<0.01 and * p<0.05.

As illustrated in Figure 3.16 A and B, SEA-stimulated MLN and spleen cells from infected ASC- and NLRP3-deficient mice showed significantly suppressed IL-10, IL-5, IL-17A and IFN-γ responses, whereas the IL-13 responses was significantly increased compared to responses from infected wildtype mice. SEA-stimulation of MLN (Figure 3.16 C) and spleen (Figure 3.16 D) cells from infected IL-1R- and Dectin-2-deficient mice also revealed significantly suppressed IL-10, IL-5, IL-17A (not significantly suppressed in IL-1R$^{-/-}$ mice) and IFN-γ responses. However, IL-13 responses were only slightly elevated in MLN and spleen cells from infected Dectin-2$^{-/-}$ mice. In addition, SEA stimulation of MLN and spleen cells from infected Dectin-1$^{-/-}$ mice showed no alterations in T_H immune responses (data not shown), suggesting that the model of the SEA-mediated NLRP3 inflammasome activation, which was analysed *in vitro* (sections 3.2), could also influence antigen specific immune responses during infection since both T_H responses and granuloma formation (section 3.3.2) are skewed. Interestingly, MLN and spleen cells of naive mice did not induce significant amounts of T_H cytokines upon SEA restimulation, confirming that immune responses are specifically primed to SEA *in vivo*. Additionally, FACS analysis of MLN (Figure 3.17) or spleen cells (data not shown) from infected ASC-, NLRP3-, IL-1R-, Dectin-2- and Dectin-1-deficient mice showed no alterations in CD4$^+$ T_H cells and CD4$^+$ CD25$^+$ (Figure 3.17 A) or CD4$^+$ Foxp3$^+$ T_{reg} cell population (Figure 3.17 B) compared to infected wildtype mice.

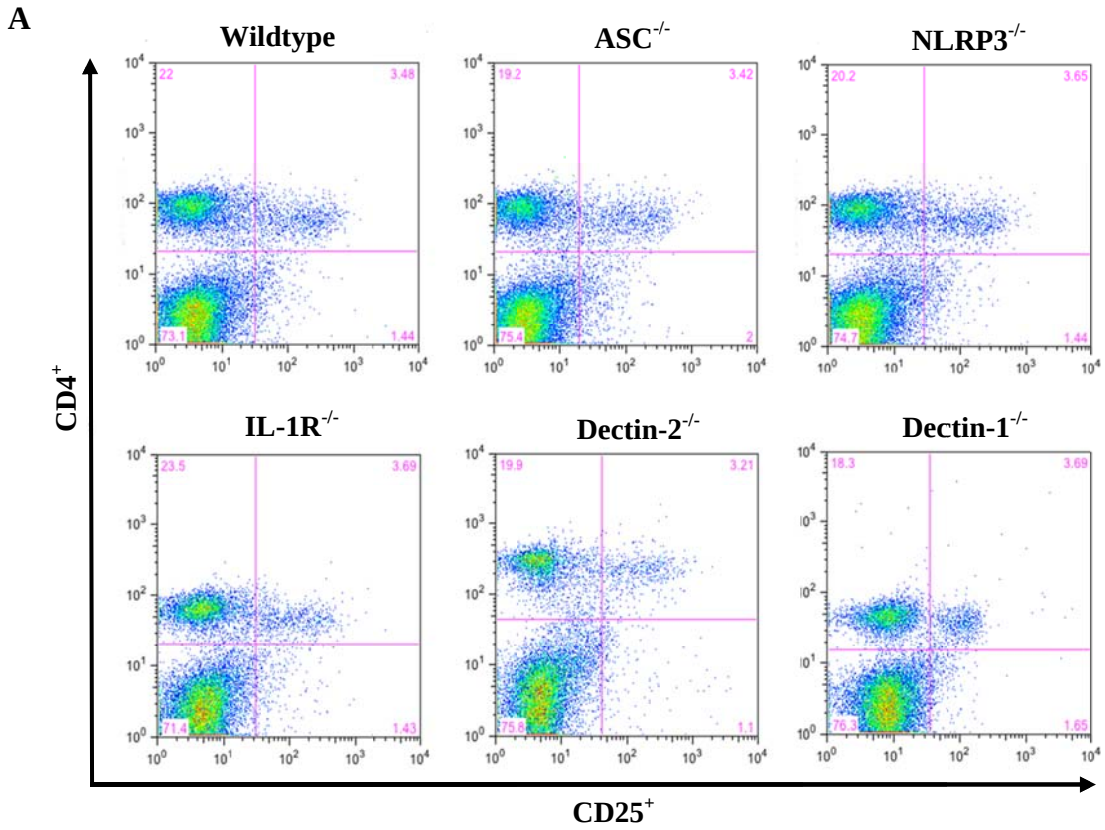

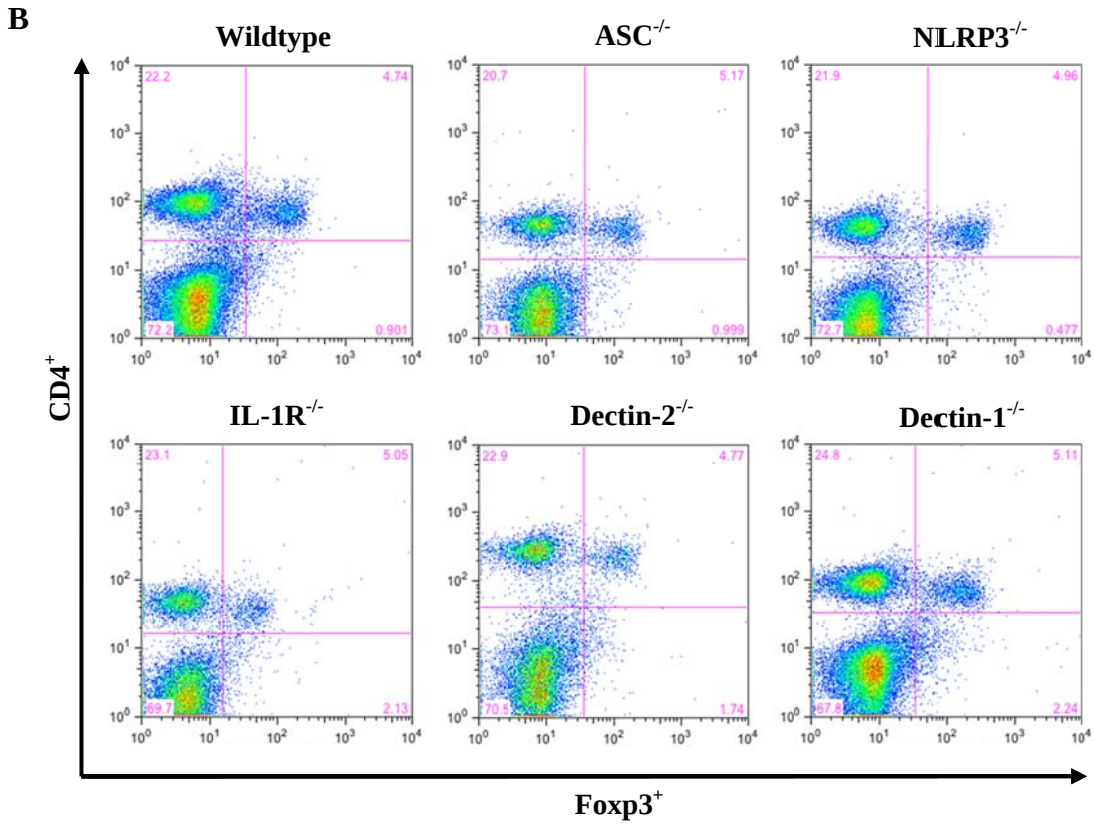

Figure 3.17: FACS analysis of $CD4^+$ T cell populations in the MLN of infected animals
Wildtype, $ASC^{-/-}$, $NLRP3^{-/-}$, $IL\text{-}1R^{-/-}$, $Dectin\text{-}2^{-/-}$ and Dectin-1 mice were infected with 100-120 *S. mansoni* cercariae. After 8 weeks of infection, lymphocytes were prepared from MLNs and stained with CD4, CD25 and Foxp3 FACS antibodies (Table 2.1). Examples of FACS dot blot diagrams from independent *S. mansoni* infection experiments. FACS dot blot diagrams show percentage of (A) $CD4^+CD25^+$ or (B) $CD4^+Foxp3^+$ T_{reg} cell populations.

3.4 Investigation of NLRP3 inflammasome activation during allergic airway inflammation

As shown in the previous sections (3.2 and 3.3), the NLRP3 inflammasome activation and IL-1β production are important for the induction of immune responses against the egg-derived antigens SEA and also play a crucial role during *S. mansoni* infection. In addition, several autoimmune diseases, such as urate crystal arthritis (gout) [152], diabetes [153], rheumatoid arthritis [154] and bronchial asthma development [155-157] have been associated with inflammasome activation and IL-1β production. In fact, the recent understanding of inflammasome activation mechanisms has provided the basis for the treatment of some of these autoinflammatory diseases, such as arthritis [152, 210], gout [212] and diabetes [213]. With regards to allergic asthma development it has been recently suggested that inflammasome activation and IL-1β production play an important role in the development of

this illness aswell [155-157, 214]. Therefore, to investigate the role of the NLRP3 inflammasome in another T_H2 polarized *in vivo* model besides the *S. mansoni* infection, allergic airway inflammation was induced within wildtype, NLRP3$^{-/-}$ and ASC$^{-/-}$ mice on BALB/c background using an alum-free ovalbumin (OVA)-induced allergic airway inflammation model according to the description provided in section 2.6.1.

3.4.1 NLRP3 inflammasome activation influences eosinophil influx within the lung

To decipher the role of the NLRP3 inflammasome during allergic asthma development, wildtype, NLRP3- and ASC-deficient mice were either treated with PBS (control mice) or OVA (asthmatic mice) according to the alum-free OVA-induced allergic airway inflammation model (Figure 2.1). Thereafter, bronchoalveolar lavage (BAL) analysis was performed as described in section 2.6.2. The evaluation of the cell infiltration within the BAL is depicted in Figure 3.18.

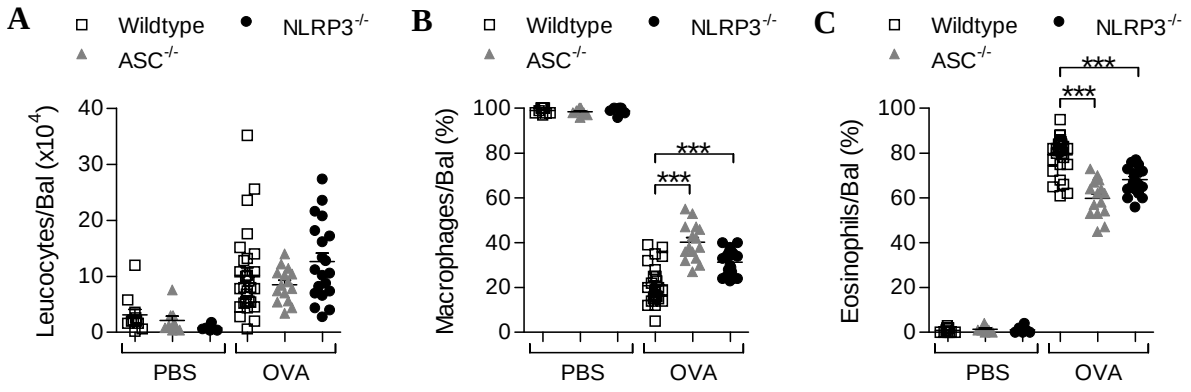

Figure 3.18: NLRP3 inflammasome activation influences immune cell infiltration within the BAL
Wildtype (PBS: n=11; OVA: n=29), ASC$^{-/-}$ (PBS: n=9; OVA: n=15) and NLRP3$^{-/-}$ (PBS: n=6; OVA: n=20) mice were treated with PBS (control group) or OVA to induce allergic airway inflammation according to the alum-free OVA-inducing allergic airway inflammation model (Figure 2.1). After 31 days, mice were sacrificed and isolated BAL cells were used for cytospin preparations. Cytospins were then stained with Diff-Quik to allow differentiation of (A) total leucocytes and percentage of (B) macrophages and (C) eosinophils within the BAL. Results show the combined data accumulated from three independent experimental allergic airway inflammation experiments per mouse strain. Symbols show mean ± SD of individual mice and asterisks show significant differences between brackets *** $p<0.001$.

Allergic airway inflammation induced the promotion of leucocyte infiltration within the lungs (Figure 3.18 A). Analysis of BAL infiltrating cells revealed that in wildtype mice OVA is a potent allergen even in the absence of an adjuvant substance like Alum: most previous studies

have required the use of Alum. The subcutaneous injection in the neck however, facilitates strong sensitization responses, which, as expected, is not the case when using PBS. Upon analysis of mice lacking NLRP3 inflammasome components the total leucocyte infiltration was not impaired (Figure 3.18 A). However, when differentiating the infiltrating cell populations within the BAL it could be shown that OVA-sensitized wildtype mice had significantly more eosinophils when compared to control mice but also OVA-sensitized NLRP3- and ASC-deficient mice (Figure 3.18 C). Since eosinophils are associated with allergic asthma development [216-219], these data suggest a reduced allergic airway inflammation phenotype of mice lacking NLRP3 inflammasome components. In addition, NLRP3- and ASC-deficient mice showed significantly increased infiltration of macrophages (Figure 3.18 B). Macrophages are not associated with asthma development and, in correlation PBS-sensitized mice showed almost 100% of macrophage infiltration within the lungs (Figure 3.18 B), whereas eosinophils were hardly detectable (Figure 3.18 C). These data show that the NLRP3 inflammasome influences the recruitment of immune cells, especially eosinophils, within the lung during allergic airway inflammation development.

3.4.2 NLRP3 inflammasome activation mediates inflammation within the lung

Another feature of asthma development is the inflammatory responses including the infiltration of eosinophils within the lung and goblet cell-mediated mucus production and destruction of lung tissue [216-219]. To evaluate lung inflammation, lung samples from PBS and OVA-sensitized wildtype, ASC- and NLRP3-deficient mice were prepared as described in section 2.5.3.1 and stained with Periodic acid-Schiff (PAS) as described in section 2.6.4. Images of the PAS stained lung sections and the evaluation of tissue thickness (inflammation score) and goblet cell infiltration are presented in Figure 3.19.

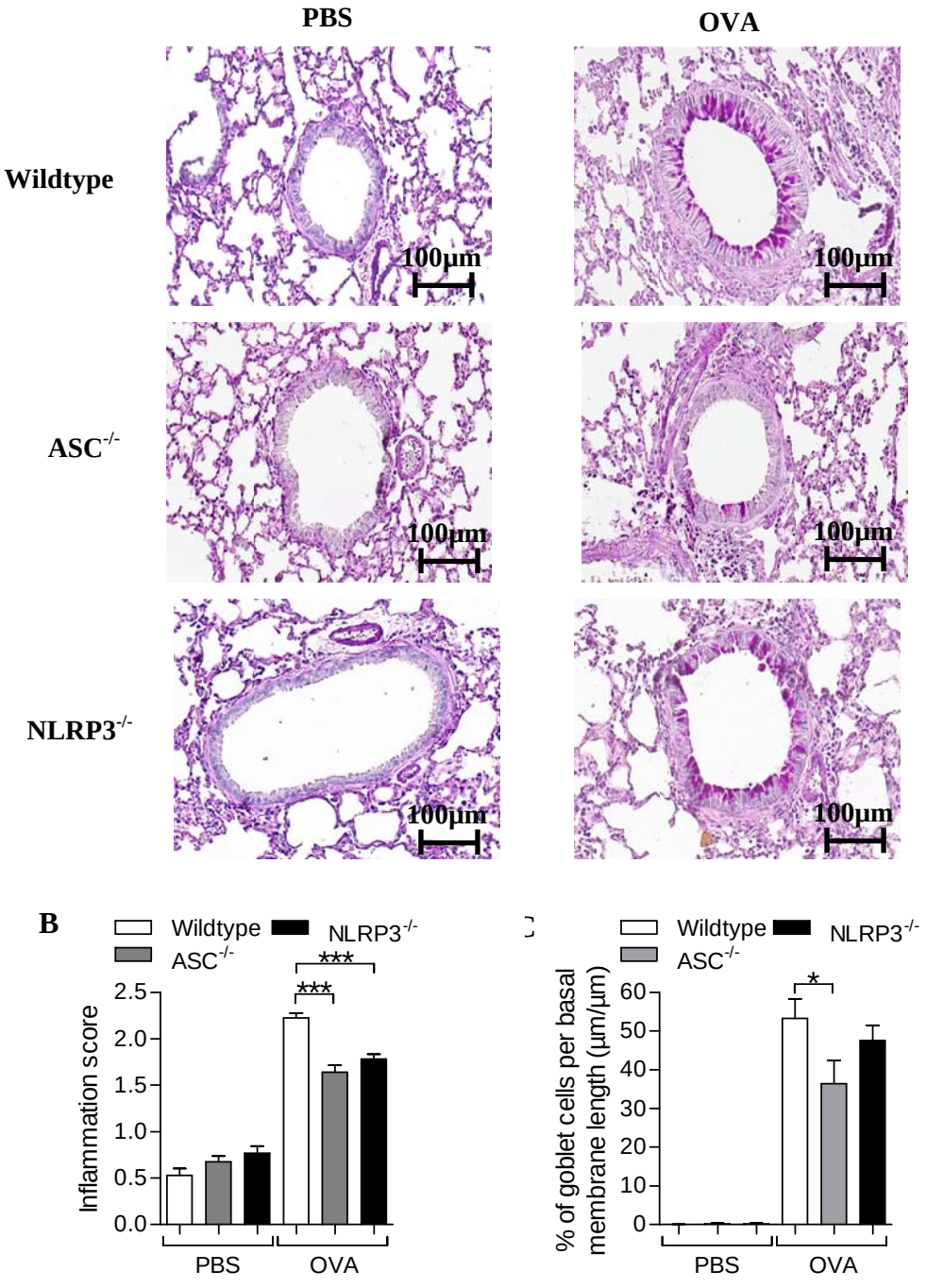

Figure 3.19: Lung inflammation depends on NLRP3 inflammasome activation
Wildtype (PBS: n=11; OVA: n=29), ASC$^{-/-}$ (PBS: n=9; OVA: n=15) and NLRP3$^{-/-}$ (PBS: n=6; OVA: n=20) mice were treated with PBS (control group) or OVA to induce allergic airway inflammation according to the alum-free OVA-inducing allergic airway inflammation model (Figure 2.1). After 31 days, mice were sacrificed and pieces of lungs from individual mice were fixed and embedded in paraffin. 3µm lung sections were fixed on glass slides for goblet cell staining with PAS (bright red colouring). (A) PAS stained lung sections were microscopically assessed (x20 magnification) to calculate (B) the inflammation score in a scale from 0 to 3 and (C) goblet cell count per basal membrane length. (A) PAS stained lung sections are representative samples of PBS and OVA-sensitized wildtype, ASC- and NLRP3-deficient mice. (B, C) Results show combined data accumulated from three independent experimental allergic airway inflammation experiments per mouse strain. Bars show mean ± SD and asterisks show significant differences between brackets *** $p<0.001$ and * $p<0.05$.

As depicted in Figure 3.19 A, PAS stained lung sections of PBS-sensitized wildtype, ASC- and NLRP3-deficient mice showed almost no visual thickness of the basal membrane and goblet cell infiltration (bright red colouring). This impression was then confirmed by the microscopic analysis of the inflammation score (Figure 3.19 B) and percentage of goblet cells per basal membrane length (Figure 3.19 C) according to the description in section 2.6.4. In the allergic airway inflammation groups, the basal membrane thickness of OVA-sensitized ASC- and NLRP3-deficient mice were less thick when compared to wildtype mice which was also reflected in the significantly decreased inflammation score (Figure 3.19 A and B). Goblet cell infiltration however was only significantly decreased in $ASC^{-/-}$ mice, since levels in $NLRP3^{-/-}$ mice were comparable to wildtype mice (Figure 3.19 A and C). These data convey that activating the NLRP3 inflammasome promotes inflammation within the lung during OVA-induced allergic airway inflammation, but several other molecules and mechanisms seem to be also essential for inflammatory responses, such as goblet cell infiltration.

3.4.3 NLRP3 inflammasome activation alters cytokine responses

Besides eosinophil infiltration and inflammation within the lung, cytokine production is another characteristic of OVA-induced allergic airway inflammation [220]. To analyse cytokine responses, BAL and lung lymph node (LLN) cells from OVA-sensitized wildtype, ASC- and NLRP3-deficient mice were prepared as described in section 2.6.2 and 2.3.1.1, respectively. LLN cells were then stimulated with OVA as described in section 2.3.3.3 and cytokines within culture supernatants were measured after 72h by ELISA. This technique was also used to assess the level of T_H cytokines in the BAL. Results are summarized in Figure 3.20.

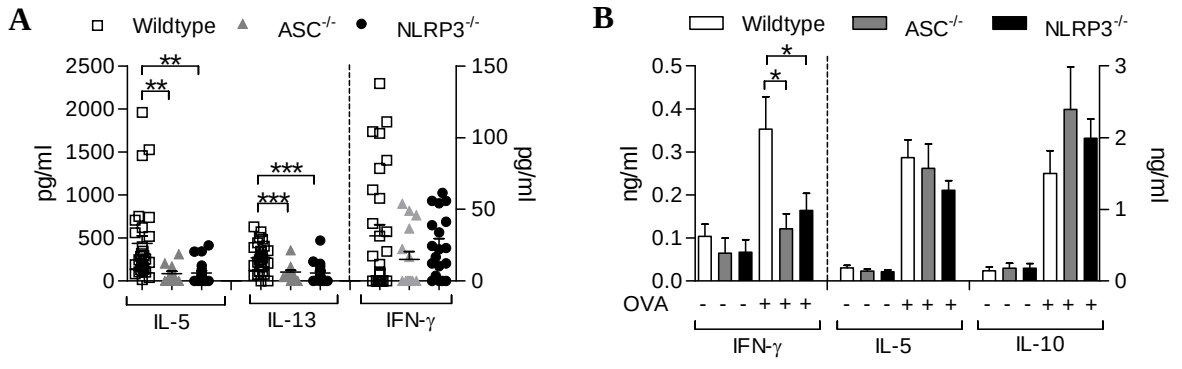

Figure 3.20: NLRP3 inflammasome activation alters cytokine responses during OVA-induced allergic airway inflammation development
Wildtype (OVA: n=29), ASC$^{-/-}$ (OVA: n=15) and NLRP3$^{-/-}$ (OVA: n=20) mice were sensitized with OVA to induce allergic airway inflammation according to the alum-free OVA-inducing allergic airway inflammation model (Figure 2.1). After 31 days, mice were sacrificed and BAL and LLN cells were prepared. LLN cells ($2x10^5$) were then stimulated with or without 20µg/ml OVA for 72h. (A) IL-5, IL-13 and IFN-γ responses within the BAL or (B) IFN-γ, IL-5 and IL-10 responses within the supernatants from stimulated LLN cells were measured by ELISA technique. Results show the combined data accumulated from three independent experimental allergic airway inflammation experiments per mouse strain (A) Symbols and (B) bars show mean ± SD and asterisks show significant differences between brackets *** $p<0.001$, ** $p<0.01$ and * $p<0.05$.

As shown in Figure 3.20 A, OVA-sensitized ASC- and NLRP3-deficient mice showed significantly less IL-5 and IL-13 within the BAL compared to wildtype mice. Moreover, BAL IFN-γ levels were also slightly reduced in mice lacking NLRP3 inflammasome components (Figure 3.20). In addition, OVA stimulation of LLN cells from OVA-induced ASC- and NLRP3-deficient mice revealed significantly reduced proinflammatory IFN-γ and slightly decreased IL-5 responses (Figure 3.20 B), confirming the above mentioned observations in reduced inflammatory responses within the lungs of mice lacking the NLRP3 inflammasome (Figure 3.19). In contrast, IL-10 responses were slightly increased, suggesting an immunomodulating mechanism in ASC$^{-/-}$ and NLRP3$^{-/-}$ mice. Additionally, measurements of OVA-specific immunoglobulins IgE and IgG1 within sera showed no differences.

3.4.4 NLRP3 inflammasome-mediated IL-1β production contributes to the inflammation within the lung

Since NLRP3 inflammasome activation is crucial for inflammatory processes during OVA-induced allergic airway inflammation, it was suggested that IL-1β is the mediator for such inflammation within the lung. To analyse IL-1β levels, weighed lung pieces from OVA-sensitized wildtype, ASC- and NLRP3-deficient mice were homogenized as described in section 2.6.3 and IL-1β levels were evaluated using ELISA technique. Results are shown in Figure 3.21.

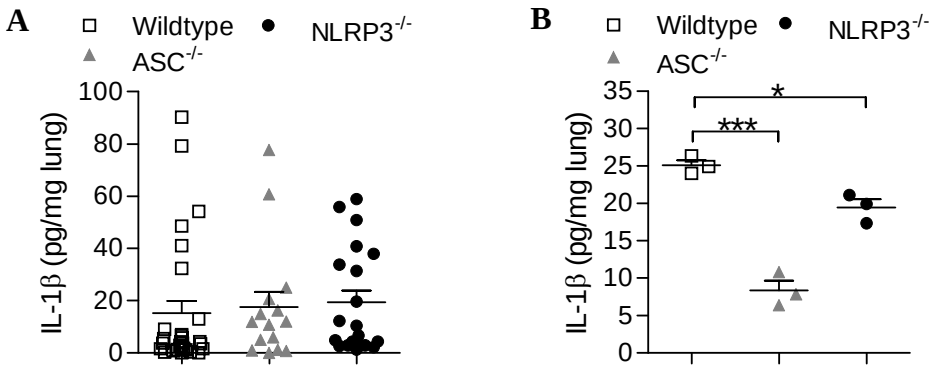

Figure 3.21: NLRP3$^{-/-}$ and ASC$^{-/-}$ mice showed decreased *in situ* IL-1β levels within lungs immediately after contact with the OVA antigen
Wildtype, ASC$^{-/-}$ and NLRP3$^{-/-}$ mice were sensitized with OVA to induce allergic airway inflammation according to the alum-free OVA-inducing allergic airway inflammation model (Figure 2.1). After (A) 31 days or (B) 28 days (directly after OVA-challenge), mice were sacrificed and weighed pieces of lungs from individual mice were homogenized and centrifuged. The resulting supernatant was then assessed for its *in situ* IL-1β content by ELISA. (A) Results show the combined data accumulated from three independent experimental allergic airway inflammation experiments per mouse strain (Wildtype n=29; ASC$^{-/-}$ n=15; NLRP3$^{-/-}$ n=20). (B) Results show the combined data from two experimental allergic airway inflammation experiments per mouse strain (Wildtype n=3, ASC$^{-/-}$ n=3; NLRP3$^{-/-}$ n=3). Symbols show mean ± SD and asterisks show significant differences between brackets *** $p<0.001$ and * $p<0.05$.

Surprisingly, no differences in IL-1β levels were detectable within lungs of asthmatic wildtype, ASC- and NLRP3-deficient mice on day 31 (Figure 3.21 A). In a further experiment, IL-1β levels were evaluated directly after the last OVA-challenge on day 28. Here significantly decreased IL-1β levels within the lungs of ASC- and NLRP3-deficient could be detected (Figure 3.21 B). These data suggest that both NLRP3 inflammasome activation and IL-1β induction are responsible for the first inflammatory response against the

OVA antigen, whereas secondary inflammatory immune responses are probably mediated by additional immune mechanisms.

3.4.5 Inhibition of IL-1 signalling leads to alteration of allergic airway inflammation

Anakinra (Kineret®) is an IL-1Ra, which binds to the IL-1 receptor with almost the same affinity as IL-1β and therefore blocks IL-1 signalling. Anakinra is now used to cure IL-1β mediated diseases, such as rheumatoid arthritis, Still's disease, gout, type 2 diabetes and diverse fever syndromes (section 1.4.4). Since previous results (sections 3.4.1-3.4.4) highlighted the role of NLRP3 inflammasome mediated IL-1β production during the development of OVA-induced allergic airway inflammation, it was hypothesized that blocking IL-1β could lead to a decreased airway inflammation. Therefore, to investigate the ability of Anakinra to inhibit airway inflammation, wildtype BALB/c mice were treated with 100µg Anakinra per day either during OVA sensitization or challenge in the following procedure depicted in Figure 3.22.

A

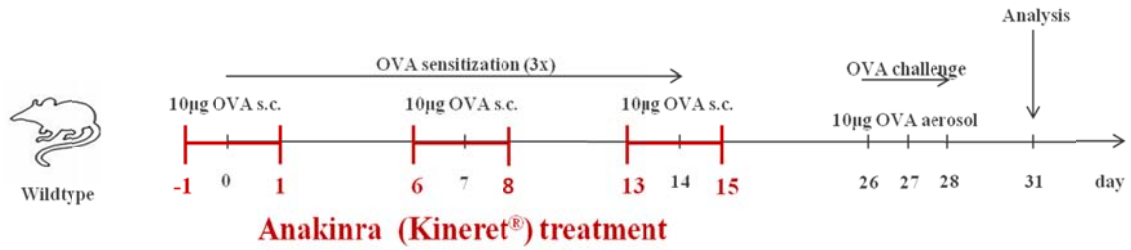

B

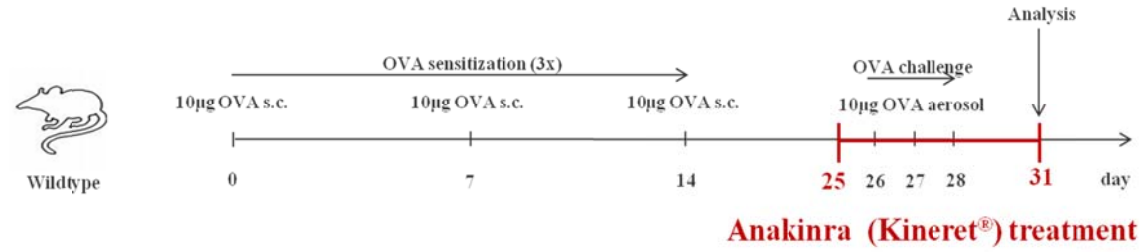

Figure 3.22: Anakinra treatment during the alum-free OVA-induced allergic airway inflammation model
Wildtype mice were treated with PBS (control groups) or OVA to induce allergic airway inflammation according to the alum-free OVA-inducing allergic airway inflammation model (Figure 2.1). Additionally, (A) wildtype mice were treated i.p. with 100µg Anakinra (Kineret®) per day during OVA sensitization (days -1-1; 6-8; 13-15). Alternatively, (B) wildtype mice were treated i.p. with 100µg Anakinra (Kineret®) per day during OVA challenge and continuing until the analysis day (days 25-31). Finally on day 31, mice were sacrificed and immunological parameters were investigated.

After treatment with Anakinra according to the description in Figure 3.22, wildtype mice were sacrificed and infiltration of eosinophils, lung inflammation and cytokine responses were evaluated. Results are summarized in Figure 3.23.

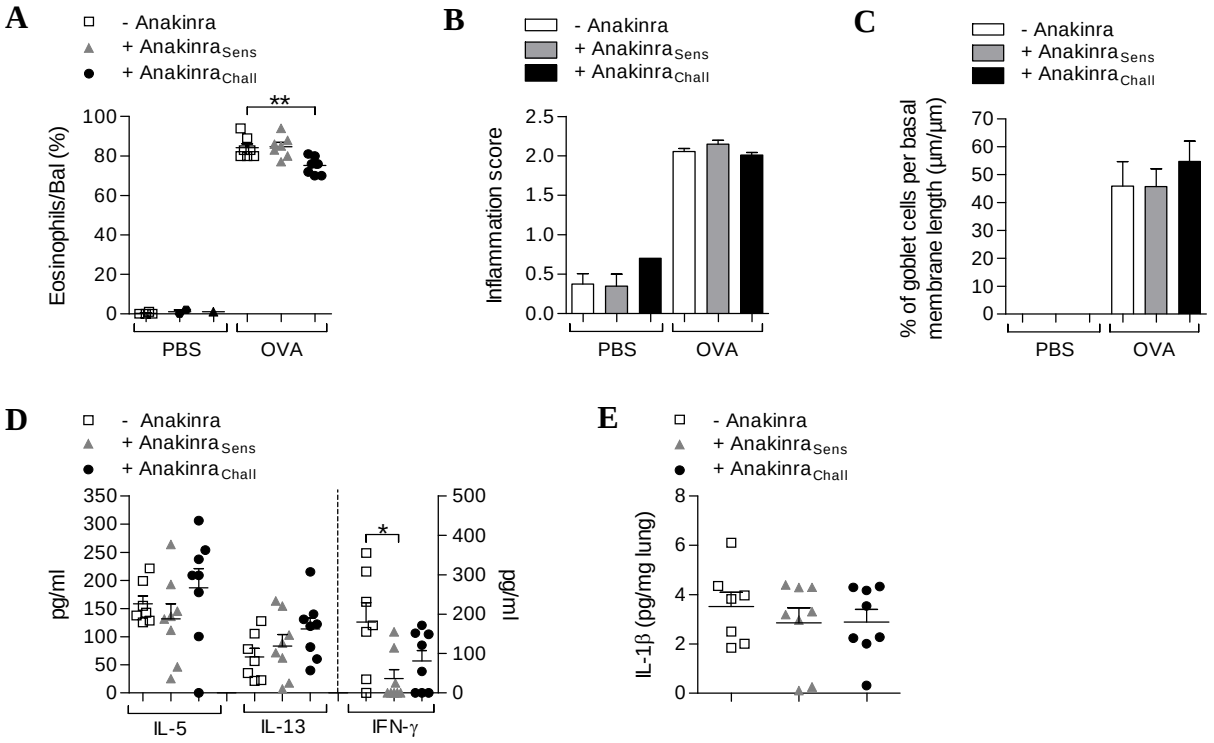

Figure 3.23: Anakinra treatment altered OVA-induced allergic airway inflammation
Wildtype mice were sensitized with PBS (control groups) or OVA to induce airway inflammation according to the alum-free OVA-inducing allergic airway inflammation model (Figure 2.1). Moreover, wildtype mice were treated with Anakinra (Kineret®) either during OVA sensitization (+ $Anakinra_{Sens}$) or OVA challenge (+ $Anakinra_{Chall}$) according to the model depicted in Figure 3.22. After 31 days, wildtype mice were sacrificed and assessed for (A) eosinophil infiltration, (B) inflammation within the lungs (inflammation score), (C) goblet cell infiltration within the lungs, (D) cytokine responses within the BAL and (E) *in situ* IL-1β levels within the lungs. Results show the combined data accumulated from two independent anakinra experiment with PBS control groups of n=4 (- Anakinra), n=2 (+ $Anakinra_{Sens}$) and n=2 (+ $Anakinra_{Chall}$) and OVA groups of n=7 (- Anakinra), n=8 (+ $Anakinra_{Sens}$) and n=8 (+ $Anakinra_{Chall}$). (A, D-E) Symbols and (B-C) bars show mean ± SD and asterisks show significant differences between brackets ** $p<0.01$ and * $p<0.05$.

As illustrated in Figure 3.23 A, eosinophil infiltration was only significantly decreased when mice were treated with Anakinra during OVA challenge, confirming recent results (Figure 3.21 B), which showed that IL-1β is crucial for the first immune response against the OVA antigen. Interestingly, inflammation (Figure 3.23 B) and goblet cell infiltration (Figure 3.23 C) within the lungs were not altered by either Anakinra treatment. However, IFN-γ responses within the BAL were decreased by Anakinra treatment during OVA sensitization and

challenge (Figure 3.23 D), confirming that IL-1β is crucial for the initiation of proinflammatory immune responses. Surprisingly, *in situ* IL-1β levels within lung homogenates were only slightly decreased in all Anakinra treated mice (Figure 3.23 E), suggesting that the IL-1β production was not completely blocked by Anakinra. In addition, cytokine responses, such as IL-5, IL-10 and IFN-γ of OVA restimulated LLN cells from Anakinra treated mice showed no alterations compared to untreated BALB/c mice (data not shown). Summarizing, these results revealed a pivotal role of IL-1β during the first proinflammatory responses against the OVA antigen, showing that OVA-induced allergic airway inflammtion depends on NLRP3 inflammasome mediated IL-1β induction.

4 Discussion

4.1 Immunomodulating abilities of *Schistosoma mansoni*

The helminth *Schistosoma mansoni* (*S. mansoni*) can cause a chronic disease in humans called Schistosomiasis which, next to malaria, is the second most socioeconomically devastating parasitic disease. According to the World Health Organization, over 207 million people are infected worldwide with an estimated risk of 700 million people [56-58]. The coevolutionary development of schistosomes and humans has driven the helminth to create evasion tactics by manipulating and modulating immune mechanisms and responses. *S. mansoni*-mediated immunopathology and immune responses are only marginally different between mice and humans [244, 245], therefore murine infection models provide an excellent experimental platform. In addition, several studies have revealed that C57BL/6 mice are more resistant to *S. mansoni* infection compared to BALB/c or C3H/HeN mice [246, 247], but nevertheless develop the *Schistosoma*-specific T_H2 based immune responses and granulomas [87, 90, 248, 249]. For the experiments performed in this thesis C57BL/6 mice were employed, since at that time there was a border range of available inflammasome deficient mice.

4.1.1 SEA-mediated immunosuppression of innate activated cells is directed by (glyco-)lipids

The ability of *S. mansoni* to evade and exploit the host`s immune system is an essential strategy by the helminth to ensure survival. An indispensable part of *schistosome*-mediated immunomodulation is the development of a dominant T_H2 immune response which is purported to be initiated through egg production and the consequent release of soluble egg antigen (SEA) [87-91]. SEA is a complex mixture consisting of highly glycosylated proteins and lipids [108, 109] and has been demonstrated to promote both T_{reg} generation and T_H2 polarization [110-120]. Over the last decade, much research has focused on the protective effects of helminth infections on Western illnesses, such as diabetes [120, 250] and asthma [251]. These effects have been attributed to the instigation of such T cell populations [252]. Indeed several studies have observed a protective effect against allergic airway inflammation and asthma development within *S. mansoni* infected mice [252, 253] and humans [254], respectively. These data confirm that a murine infection model is sufficient to explain phenomena observed in humans and can be used to decipher the responsible immune

mechanisms or helminth-mediating components that may contribute to the development of new strategies to prevent allergic diseases.

Despite these intriguing findings in allergy, the majority of research has focused on the ability of SEA to specifically inhibit TLR-mediated immune responses of DCs. Interestingly, this augments IL-10 production [122-127], which is in turn important for the above mentioned T_H2 immune responses, mentioned above [61, 87, 129]. In confirmation with such studies, the results presented within this thesis demonstrated that SEA can indeed suppress TNF-α and IL-6 secretion from TLR2 (P_3Cys) and TLR4 (LPS) triggered BMDCs. In addition, TLR9 (CpG) initiated TNF-α and IL-6 responses were also inhibited (section 3.1.1), demonstrating the capacity of SEA to down-regulate TLR-initiated responses in the extra- and intracellular compartments. In addition, even though SEA strongly manipulates TLR-triggered responses, DCs remain silent when cultured with SEA alone since there was neither secretion of pro-inflammatory cytokines nor up-regulation of co-stimulatory surface molecules such as CD80 and CD86. Although these data confirm findings from other studies [123, 125] they do not exclude the possibility of yet undetected TLR ligands within the SEA, but rather suggest that their concentrations are too low to induce expression and maturation signals. Indeed, highly purified and concentrated components within SEA, such as lysophosphatidylserine [110] and Lewis X [114], have been shown to trigger TLR2 and TLR4 respectively and *in vivo* studies highlighted that TLR3 is triggered by egg-derived dsRNA [121].

Further experiments within this thesis demonstrated that the inhibition of phagocytotic processes with cytochalasin D (CytD), which blocks actin polymerization, particle internalization and the binding stage of phagocytosis, did not alter the ability of SEA to mediate TNF-α suppression (section 3.2.4), suggesting that the responsible component within SEA triggers a specific receptor. To ascertain the biochemical compound within SEA that facilitates TNF-α and IL-6 suppression, SEA was either heat inactivated or digested with proteinase K. Interestingly, inactivated SEA could still suppress TNF-α responses (section 3.1.4), revealing that it is likely a non-protein component within SEA, such as a (glyco-)lipid, that is responsible for the observed suppressive effects. To date, the suppressive lipid component(s) have not been identified or isolated. Nevertheless, some phospholipids from different SEA preparations, such as *L*-α-phosphatidylethanolamine, *L*-α-phosphatidylinositol, *L*-α-phosphatidyl-*L*-serine and *L*-α-phosphatidylcholine-β-linoleoyle-γ-palmitoyle, could be identified via thin layer chromatography (TLC) within this thesis (data not shown). However, the functionality of those phospholipids remains unclear and therefore further investigations

are required to clarify the potential immunomodulating role of lipids within SEA. Moreover, investigations into the receptors that recognize glycosylated lipids could lead to a better understanding of SEA-mediated immunomodulating mechanisms. Indeed, as described in section 1.3.5, different C-type lectin receptors (CLRs), which are triggered by glycosylated molecules, are known to recognize components within SEA and lead to the suppression of TLR-mediated immune responses [122, 123, 130-132]. Furthermore, some studies already demonstrated that (glyco-)lipids within SEA induce signalling via TLR2 [110] and the CLR L-SIGN [255].

4.1.2 Concurrent immunomodulation mechanism by schistosomal components: IL-1β induction

Currently, no direct stimulatory effects of SEA have been observed on innate responses, especially those that induce strong pro-inflammatory or T_H1 immune responses. Unexpectedly, this study deciphered that co-culturing SEA with TLR-primed BMDCs lead to the production of IL-1β (section 3.1.2), which is a potent proinflammatory cytokine for the initiation of inflammation and T_H1 as well as T_H2 immune responses [152, 200]. IL-1β has been shown to induce fever [142, 143] and IL-1β signalling mechanisms *in vivo* are considered to play a crucial role during various autoinflammatory diseases, such as gout [152], diabetes [153], rheumatoid arthritis [154] and bronchial asthma [155-157]. In addition, SEA-mediated IL-1β production was dose dependent and independent of the employed TLR stimuli, since all three tested stimuli (P_3Cys, LPS or CpG) elicited the same response (Figure 3.2). Moreover, stimulation of TLR-pulsed BMDCs with worm antigen, frozen whole eggs or egg shells was not sufficient to induce IL-1β production, confirming that only SEA preparations from viable eggs release the specific SEA component(s) that induce IL-1β production. In contrast to the observed suppressive effects of SEA, inactivation of helminth-derived antigen lead to impaired IL-1β production (section 3.1.4), revealing that a different component was responsible and that the component might be a (glyco-)protein. These findings highlight the complexity of the immunomodulating mechanisms that occur during *S. mansoni* infection and show that different components within SEA can act in tandem to balance ongoing immune responses. In general, IL-1β is secreted when DAMPs or PAMPs trigger various cell types, such as DCs or macrophages. Interestingly, products of dying or necrotic cells that might act as danger signals also initiate IL-1β secretion [200, 226], confirming the important role of IL-1β secretion during the response against danger signals.

In this study it was demonstrated that SEA did not induce cell death (section 3.1.3) which in turn confirmed that it is an active component within SEA that specifically induces IL-1β production from TLR-primed BMDCs. In addition, the TLR stimuli P_3Cys, LPS and CpG did not enhance secretion of lactate dehydrogenase (LDH) that is released from dying and necrotic cells, proving that the BMDCs stimulation conditions did not disrupt cell viability. In addition, to decipher the IL-1β inducing component, SEA was fractionated using liquid size exclusion chromatography which allows high-resolution separation of proteins, peptides and other molecules. The SEA fractions were then tested for their ability to induce IL-1β but unfortunately, none of the tested fractions induced the cytokine. Reasons surrounding this lack of induction could be the fractionation procedure itself since such techniques cause disruption of protein structures and lead to the loss of glycosylated residues that may have been important for recognition and initiation of immune responses [115-119, 122, 123].

4.2 SEA-mediated inflammasome activation

In general, secretion of IL-1β depends on the activation of intricate pathways which are mediated by a cytoplasmic multiprotein complex called the inflammasome. This consists of a protein from the NALP family, ASC and caspase-1 [150-152, 158-161, 172]. Casp1 cleaves the precursor cytokine pro-IL-1β into the bioactive IL-1β form and is therefore a pivotal member of the inflammasome complex [150, 151]. Currently, five different inflammasome complexes, NLRP1 [163], AIM2 [164-167], NLRP3 [168], NRLC4 [169] and NLRP6 [170, 171] have been described which are functionally active towards certain PAMPs and DAMPs. The discovery of the inflammasome and its activation mechanisms has provided the basis for a deeper understanding into various inflammatory diseases associated with IL-1β activity and has lead to the development of several successful therapies including arthritic diseases [152, 210], refractory adult Still's disease [211], gout [212], type 2 diabetes [213] and diverse fever syndromes [200]. Since SEA-mediated cell death was excluded, it was predicted that a (glyco-)protein within the SEA promotes inflammasome activity leading to IL-1β secretion. To test this hypothesis, several *in vitro* stimulation assays with different inflammasome-deficient BMDCs were performed.

4.2.1 *Schistosoma mansoni*: a new member of NLRP3 inflammasome activators

Over the last few years the activation mechanisms of the various inflammasome complexes have been intensively investigated and have revealed that the NLRP3 inflammasome is the most widely employed family member since it responds to an array of pathogens, such as viruses [179, 180], fungi [134, 135] and bacteria [181-184], and a wide range of structurally unrelated stimuli including elevated levels of ATP [181], ultraviolet B irradiation [185], crystalline forms of monosodium urate (MSU) [186], asbestos and silica [187-189] and amyloid-β aggregates [190]. In addition, NLRP3 inflammasome-mediated responses towards hemozoin crystals, which are generated by Plasmodium parasites during malaria disease have also been observed [223-225]. In contrast to the NLRP3 inflammasome, which serves as a platform for responses against various antigens, the other four inflammasome complexes are more specific and directed against exclusive pathogenic molecules. Examples include the cell wall component MDP (NLRP1) [174], anthrax lethal toxin (murine NLRP1) [163], type III or type IV secretion systems of *Salmonella, Shigella, Legionella* and *Pseudomonas* species (NLRC4) [175-178], cytosolic DNA (AIM2) [164-167] and bacterial components within the colon (NLRP6) [170, 171]. However, until the findings reported in this thesis, the importance of the inflammasome and a direct recognition of helminth antigens by inflammasome complexes had not been deciphered.

This study demonstrated for the first time that schistosome-derived products directly trigger inflammasome activation and moreover influence the immunopathological outcome during infection. In essence, SEA stimulation of TLR-primed BMDCs lacking Casp1, NLRP3 and ASC molecules did not produce the normally observed secretion of IL-1β (sections 3.2.1 and 3.2.2). The essentialness of the inflammasome in SEA-mediated IL-1β production was further confirmed via Western blot detection of cysteine protease Casp1, since in the absence of either NLRP3 and ASC, pro-Casp1 was not cleaved into Casp1. Collectively, these findings demonstrated that SEA triggers the NLRP3 inflammasome to activate the central regulatory component Casp1, which cleaves pro-IL-1β into functional IL-1β. Interestingly, the accumulation of pro-IL-1β was independent of the assembling of NLRP3 inflammasome components NLRP3, ASC and Casp1, confirming that precursor accumulation of pro-IL-1β is based on the activation of the NF-κB pathway activation. However, stimulation with SEA alone did not lead to cleavage of Casp1 and IL-1β, underlining the necessity of cell priming (signal 1), which is achieved *in vitro* via stimulation of TLR which elicits the synthesis and accumulation of pro-IL-1β [186-190]. Unexpectedly, slight cleavage of IL-1β and Casp1 was

observed without TLR-priming in the Western blot studies using the strong NLRP3 inflammasome stimulus ATP (Figure 3.5). This was probably a result of the long stimulation period of 1h and the high ATP concentration of 5mM used in the experimental setup. Indeed, stimulations with ATP alone for 30min produced only minimal cleavage of IL-1β and Casp1. Moreover, it was also shown that ATP activates reactive oxygen species (ROS) and oxidative stress responses leading to Casp1 activation and IL-1β cleavage [256]. However, ATP-mediated IL-1β and Casp1 secretion of TLR-primed BMDCs was accelerated compared to unprimed BMDCs. In general, these findings implied the helminth *S. mansoni* as a novel pathogen that induces NLRP3 inflammasome activation, confirming that the NLRP3 inflammasome complex is a central sensor of numerous pathogens and danger signals. However, further experiments have to be performed to decipher the specific SEA component(s) that triggers NLRP3 inflammasome assembling. Currently, it is known that NLRP3 inflammasome activation can be initiated by phagocytosis of crystalline structures, such as monosodium urate, asbestos, silica and amyloid-β aggregates [186-190], and via specific receptors, such as P2X7 that is triggered by ATP [191-193] or the CLR Dectin-1 that is triggered by *C. albicans* [134, 135]. Since, both SEA and the cell wall of *C. albicans* consist of highly glycosylated proteins, we suggested that SEA is probably also recognized by a CLR (see section 4.2.3). Interestingly, SEA-mediated TNF-α suppression was independent of Casp1, NLRP3 and ASC, confirming that different components within the SEA modulate immune responses through different signalling mechanism and pathways.

4.2.2 SEA-mediated NLRP3 inflammasome activity depends on several intracellular molecules

Several studies have demonstrated that NLRP3 inflammasome-mediated IL-1β production depends on the induction of intracellular molecules, such as potassium efflux and reactive oxygen species (ROS) production [135, 187-193, 257]. The activation of such molecules leads to the assembly and activation of the NLRP3 inflammasome complex and is initiated by all known NLRP3 stimulating antigens and pathogens. Nevertheless, the specific mechanisms and signalling processes of potassium efflux and ROS production are poorly understood and need further investigation. Indeed, increasing extracellular potassium to cytoplasmic levels or blocking potassium channels reduced SEA-mediated reduced IL-1β production (section 3.2.3). This is in contrast to the bacterial toxin nigericin, which creates potassium efflux by forming pores in the cell membrane [193, 258]. Thus, at the moment it remains less obvious

what mechanisms SEA employs to increase potassium efflux. Several studies have demonstrated that ATP triggers the P2X7 receptor leading to pannexin-1 mediated pore formation, potassium efflux and IL-1β production [191-193]. To exclude the possibility that SEA contained ATP or indirectly triggers the NLRP3 inflammasome by inducing the release of ATP, BMDCs lacking the ATP-receptor P2X7 were tested. Indeed, ATP stimulated $P2X7^{-/-}$ BMDCs could not produce sufficient amounts of IL-1β, whereas SEA-mediated IL-1β induction was not altered (section 3.2.5). Furthermore, no ATP could be detected within SEA preparations, confirming that intracellular ATP, and moreover, no presence of ATP within SEA is required for IL-1β production.

As mentioned above, ROS production is another crucial intracellular signal leading to NLRP3 inflammasome activation. ROS are chemically reactive molecules that are released from the metabolism of oxygen. These highly reactive molecules are important for cell signalling and homeostasis and are tightly regulated by a variety of proteins involved in reduction and oxidation mechanism [259]. For example, enzymes like superoxide dismutase or peroxidases and antioxidants, such as ascorbic acid (vitamin C) or uric acid are able to neutralize ROS and thus defend the cell from damage [260]. However, to decipher the role of ROS during SEA-mediated NLRP3 inflammasome activation, TLR-primed BMDCs were treated with the antioxidant and free radical scavenger *N*-acetyl-*L*-cysteine (Nac) or the NADPH-oxidase inhibitor (2R,4R)-4-aminopyrrolidine-2,4-dicarboxylic acid (APDC) to neutralize ROS within the cells (section 3.2.3). Interestingly, neutralization of ROS leads to impaired IL-1β production of TLR-primed BMDCs upon SEA or ATP stimulation. Recently, Bauernfeind *et al.* claimed that ROS production is important for the priming process to induce NLRP3 [261], implying that ROS is upstream of NLRP3 inflammasome assembly and not necessary for the activation. These findings are in contrast to the data obtained in the present study, as well as several other studies that have deciphered and confirmed the crucial role of ROS during NLRP3 inflammasome activation and not for priming processes, such as NLRP3 and pro-IL-1β accumulation [135, 187, 189, 241, 257]. Nevertheless, these controversial data illustrate the complexity of the different signalling processes and moreover how different molecules employ various mechanisms to instigate NLRP3 inflammasome activation. Additional, studies have shown how the phagocytosis of crystalline structures elicits lysosomal acidification, lysosomal damage and the release of cathepsin B into the cytosol resulting in NLRP3 inflammasome activation [187, 188]. Such phagocytosis processes have been further shown to induce ROS generated by NADPH oxidase [187, 188] which leads to oxidization of

thioredoxin (TRX) and the release of the TRX-interacting protein (TXNIP) that binds and activates the NLRP3 inflammasome [262, 263]. Therefore, to test whether SEA induces ROS via phagocytosis mechanisms, BMDCs were treated with cytochalasin D (CytD), which blocks actin polymerization, particle internalization and the binding stage of phagocytosis (section 3.2.4). Interestingly, blocking phagocytosis did not alter IL-1β release, suggesting that SEA-mediated IL-1β secretion is independent of phagocytosis processes and therefore induces NLRP3 inflammasome activation via triggering of a receptor. Recently, using the fungus *Candida albicans* another ROS-inducing mechanism was suggested since NLRP3 inflammasome activation could be initiated by ROS derived from mitochondria [195]. Thus, to investigate the role of mitochondrial ROS production, BMDCs were treated with 2,4-dinitrophenole (DNP) and carbonyl cyanide p-(tri-fluromethoxy)phenyl-hydrazone) (FCCP). These reagents uncouple the oxidative phosphorylation within the mitochondrial electron transport chain by carrying protons across the mitochondrial membrane, leading to impaired ROS production and ATP generation. Surprisingly, SEA-mediated IL-1β secretion was impaired when mitochondrial ROS production was blocked by the addition of the two uncouplers (section 3.2.3), suggesting that SEA-initiated ROS production depends on mitochondrion activation. Interestingly, high concentrations of DNP (100µM-1mM) and FCCP (100µM) lead to enhanced IL-1β production. With these high concentrations, the mitochondrial electron transport chain is uncoupled leading to the loss of ATP and consequently to dying or necrotic cells that act as danger signal to induce IL-1β [200, 226].

Thus, the presented *in vitro* findings establish that a (glyco-)protein within SEA triggers a receptor to activate the NLRP3 inflammasome via potassium efflux and mitochondrial ROS production. The observed effects by SEA were verified using the specific NLRC4 inflammasome activator *Salmonella typhimurium* (*S.typh.*), since IL-1β production here was not abolished by the inhibition of potassium efflux or ROS (Figure 3.7), demonstrating again that these intracellular signals are specific for NLRP3 inflammasome [135, 187, 189, 257], but not for NLRC4 inflammasome activation [135, 172]. Nevertheless, the specific SEA-mediated mechanisms leading to potassium efflux and ROS production remain unclear and need further investigation. Interestingly, SEA-mediated TNF-α suppression was not altered by blocking potassium efflux or ROS (Figure 3.7), confirming that several components within SEA mediate different immunomodulating processes and perhaps act in tandem during *S. mansoni* infection to balance the immune responses.

4.2.3 SEA triggers the Dectin-2/FcRγ/Syk receptor axis to induce NLRP3 inflammasome activation

As mentioned above, SEA is a mixture of highly glycosylated proteins and lipids. Since the work described within this thesis demonstrated that a (glyco-)protein within the SEA mediates IL-1β secretion, the next logical step was to investigate whether CLR were involved in the induction of the NLRP3 inflammasome. This important receptor family sense glycosylated molecules and indeed, several studies have shown that CLRs are triggered by SEA [122, 123, 130-132]. In addition, CLRs have been demonstrated to partially mediate the internalization of glycosylated SEA components leading to the modulation of TLR-mediated immune responses [115-119, 122, 123] (section 1.3.5). This study illustrated that SEA-mediated IL-1β production was specifically achieved through the signalling of the CLR Dectin-2 (section 3.2.5). This receptor is mainly expressed on antigen presenting cells, such as macrophages and DCs [264, 265] and is triggered by highly mannosed structures [230, 231].

Interestingly, experiments with *C. albicans* revealed that the CLR Dectin-1 plays a critical role in the activation of NLRP3 inflammasome [133-135]. Furthermore, it was shown that triggering the Dectin-2 receptor by *C. albicans* lead to coupling of the Fc receptor γ (FcRγ) chain. This contains the ITAM signalling molecule which is phosphorylated through the spleen tyrosine kinase (Syk) to transduce the signal into the cytosol [232, 236, 237]. These data can be now expanded to the schistosomal component within SEA. Here it was found that SEA triggers the Dectin-2 receptor but additionally required a functional FcRγ chain aswell to transduce Syk activation and consequently the induction of IL-1β secretion (sections 3.2.5 and 3.2.6). With regards to the effects on adaptive immunity, studies with *C. albicans* also revealed that the Dectin-2/FcRγ/Syk axis preferentially elicits IL-23 mediated T_H17 cell differentiation and IL-17 cytokine secretion [231, 233, 237, 266] but also initiates IL-2, IL-10, TNF and IL-6 responses [232, 266]. Interestingly, IL-1β has also been shown to induce IL-17A production and T_H17 cell differentiation [205-207] and moreover, these T_H17 immune responses influence immunopathology during *S. mansoni* infection [92, 267, 268]. Collectively, this study reveals a novel signalling mechanism that modulates immune responses during Schistosomiasis through a previously unidentified pathway. Moreover, the data strongly imply that SEA-mediated activation of Dectin-2/FcRγ/Syk axis could induce adaptive immune responses *in vivo* (see section 4.3 for details). Finally, analysis of SEA has revealed that different components within SEA, such as lipids [110] or glycans [111-114] are responsible for immunomodulating mechanisms (section 1.3.5). Thus, the elucidation of the

specific (glyco-)protein within the SEA that triggers the Dectin-2 receptor could benefit our understanding of *S. mansoni*-derived immunomodulation. Interestingly, molecules, especially *C. albicans* glycans that bind specifically to Dectin-1 and Dectin-2 could be detected and characterized using soluble Dectin-1 [269] and Dectin-2 receptors [230], respectively. For further investigations, this method could be used to detect and characterize the specific (glyco-)protein within the SEA that triggers the Dectin-2 receptor and initiate IL-1β secretion.

In contrast to the IL-1β induction, SEA-mediated TNF-α suppression was independent of Dectin-2, FcRγ chain and Syk activation (sections 3.2.5 and 3.2.6), showing again that SEA-mediated suppression and IL-1β induction mechanisms are distinct. However, IL-1β secretion was only reduced and not totally abolished in BMDCs lacking Dectin-2 or treated with Dectin-2 antibody. This suggested that either another component within SEA induced a partial signal via another receptor or two molecules of the Dectin-2 stimulating component simultaneously bound and activated two receptors. Since identifying the responsible components was not feasible at this time the research primarily focused on elucidating other possible receptors. Several different receptors, such as CD36, CD206, Dectin-1 and the adaptor molecule DAP12 were tested using the *in vitro* assay and none were responsible for SEA triggering and initiation of IL-1β secretion (section 3.2.5). However, these findings did confirm that SEA-mediated IL-1β production is due to an (glyco-)protein and independent of phagocytosis mechanisms, since the coreceptor CD36 senses lipid structures [227] and the mannose receptor CD206 initiates phagocytosis [228]. Moreover, CD206 was shown to specifically detect antigens that are released during transformation of cercariae into schistosomulae leading to the modulation of IFN-γ production [270]. In addition, the specificity of the Dectin-2/FcRγ/Syk axis for SEA triggering is also highlighted by the fact that the ITAM containing transducer molecule DAP12 [229] and the Dectin-1 receptor, seem to be dispensable for SEA-mediated IL-1β production. Surprisingly, preliminary experiments with BMDCs lacking the macrophage-inducible C-type lectin (Mincle) receptor revealed a reduced IL-1β secretion upon SEA stimulation. Mincle is closely related to Dectin-2 [271] and has been shown to play a significant role in the immune response against the fungus *C. albicans* [272, 273]. Similar to the Dectin-2 receptor, the Mincle receptor binds glycosylated compounds, especially trehalose containing molecules [274, 275] and selectively couples to the FcRγ chain to induce Syk signalling leading to the production of inflammatory cytokines and chemokines [276]. To date however, no association with inflammasome activity has been observed. Nevertheless, these experiments do imply that the Mincle receptor could be

important for SEA triggering and NLRP3 inflammasome activity. The association of Mincle could explain why the lack of Dectin-2 within BMDCs did not lead to a completely abolished IL-1β responses. However, further experiments have to be performed to clarify the role of the Mincle receptor within SEA-mediated NLRP3 inflammasome activation mechanisms.

4.2.4 The Card9 complex is important for NLRP3 inflammasome activation

Syk is crucial for downstream signalling in CLR family members, such as Dectin-1, Dectin-2 and Mincle [234]. Moreover, Syk together with the related protein ζ-chain-associated protein kinase 70kDa (ZAP70) promote early T and B cell development [133, 277]. In addition, several intermediary molecules that are directly associated with Syk and/or ZAP70 also become activated. These include phospholipase Cγ isoforms, regulatory subunits of the phosphoinositide 3-kinase and the SH2 (sarcoma homology 2) domain-containing leukocyte protein (SIP) family members SIP76 and SIP65 [133]. These activated molecules trigger further downstream processes, such as Ca^{2+} and protein kinase C signalling, cytoskeletal rearrangement, ROS production, phagocytosis and transcriptional regulation [133]. Interestingly, hemozoin-induced IL-1β production depends on Syk association with the inflammasome component ASC and modulation of cathepsin B [224]. Since, hemozoin-mediated NLRP3 inflammasome activation depends on phagocytosis [223-225], we assumed that another mechanism was employed for SEA-mediated IL-1β production. Several studies have demonstrated that Syk activation leads to aggregation of the Card9 complex which consists of the caspase recruitment domain 9 (Card9), the adapter protein B cell lymphoma 10 (Bcl10) and the mucosa-associated lymphoid tissue lymphoma translocation protein 1 (Malt1) [233, 234, 239, 240]. Further research with *C. albicans* has also deciphered that Syk/Card9 signalling induces the nuclear factor-κB (NF-κB) leading to the production of cytokines, such as TNF-α, IL-2 and IL-10 [239, 240, 278]. Card9 has been shown to be important for effective anti-fungal responses, since $Card9^{-/-}$ mice are more susceptible to *C. albicans* infection [239, 240] and humans carrying Card9 mutations have increased susceptibility to the fungus [279]. In addition, Card9 signalling was shown to be essential for pro-IL-1β accumulation but not inflammasome activation directly [133, 135]. Nevertheless, these discoveries are mainly based on experiments with the fungus *C. albicans* and whether Card9 plays a role in SEA-mediated NLRP3 inflammasome activation remained unknown. Therefore, Card9-deficient BMDCs were stimulated with SEA to decipher the role of the Card9/Bcl10/Malt1 complex during SEA-mediated NLRP3 inflammasome activation. Indeed,

BMDCs lacking Card9 showed reduced IL-1β secretion upon SEA stimulation (section 3.2.7) but this could have been due to impaired pro-IL-1β accumulation. Surprisingly, pro-IL-1β levels of stimulated Card9$^{-/-}$ BMDCs were even augmented, suggesting that the Card9 molecule is important for SEA-mediated NLRP3 inflammasome activation, but not for accumulation of the precursor pro-IL-1β. These findings implied a necessary role of Card9 signalling for the initiation of IL-1β production during *S. mansoni* infection and revealed an unknown signalling mechanism within NLRP3 inflammasome activation processes. Indeed, *in vivo S. mansoni* infection studies have revealed reduced immunopathology and deviated immune responses (unpublished data). However, to confirm these preliminary data experiments with BMDCs lacking Bcl10 and Malt1 have to be performed. Furthermore, the possibility that Syk associates with ASC to induce NLRP3 inflammasome activation could be also a possibility that has to be investigated.

4.2.5 SEA-mediated NLRP3 inflammasome activation: a novel signalling pathway

In summary, this study revealed for the first time that alongside the well described immune suppressive effects, components within SEA can also induce a strong proinflammatory IL-1β response via NLRP3 inflammasome activation. Figure 4.1 depicts the specific NLRP3 inflammasome activation mechanism involving the Dectin-2/FcRγ/Syk axis, Card9 signalling, potassium efflux, as well as mitochondrial ROS production. The SEA-mediated signalling platform highlights the complexity of *S. mansoni*-mediated immunomodulation and represents an evolutionary evolved example of host-parasite interaction. The ability of SEA to induce the NLRP3 inflammasome activation could be a crucial immunomodulating mechanism during Schistosomiasis. Different studies have substantiated this hypothesis, for example, IL-1β is known to induce T_H17 immune responses [205-207] and deviations into this direction elicit severe *S. mansoni*-derived immunpathology [92, 267, 268]. Further investigations into these helminth-mediated immunomodulation mechanisms could lead to new therapeutic strategies against helminth infections.

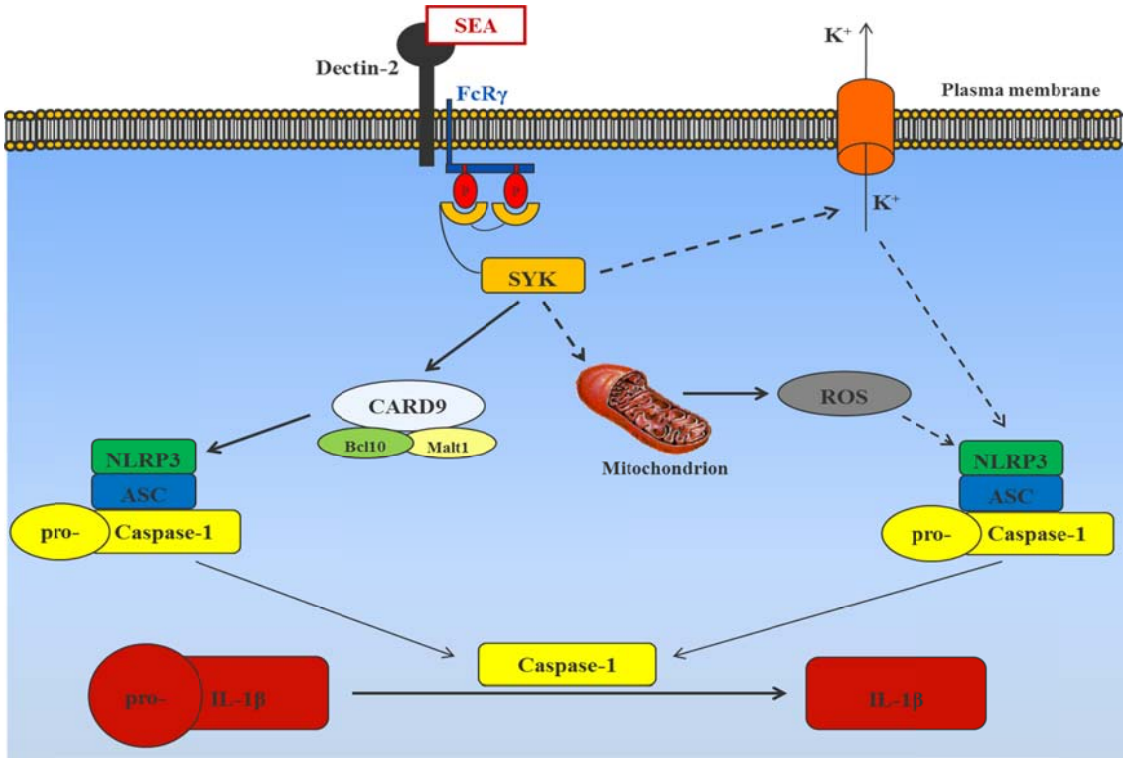

Figure 4.1: Model of SEA-mediated IL-1β induction
In brief, SEA triggers the Dectin-2 receptor that couples with the FcRγ chain to activate Syk. This leads to mitochondrial ROS production and potassium efflux. In addition, Syk also appears to activate Card9 that is associated with Bcl10 and Malt1 pathway. Afterwards, ROS production, potassium efflux and probably Card9 activate the NLRP3 inflammasome containing NLRP3, ASC and pro-Casp1, which cleaves that latter into active Casp1. Finally, the activated Casp1 cleaves pro-IL-1β into the bioactive IL-1β, which is secreted out of the cell.

4.3 Lack of inflammasome components skews both parasitological and immunological responses during *S. mansoni* infection

The *in vitro* BMDC stimulation assays demonstrate that SEA triggers the Dectin-2/FcRγ/Syk axis to initiate NLRP3 inflammsome activation and IL-1β induction. Hence, we proceeded to investigate functional aspects of this signalling pathway during an ongoing *S. mansoni* infection. Interestingly, earlier studies showed that the IL-1 receptor antagonist (IL-1Ra), which binds to the IL-1 receptor (IL-1R) with almost the same affinity as IL-1β and therefore blocks IL-1 signalling, was upregulated during *S. mansoni* infection [243]. In addition, treatment with an anti-IL-1Ra antibody enlarged granuloma development and enhanced T_H immune responses, such as IL-10 and IFN-γ [242]. Although these studies demonstrated a role for IL-1β *in vivo*, they did not address the mechanisms behind the cytokine's induction. The model described for SEA-mediated IL-1β induction in Figure 4.1 demonstrates the

signalling mechanism *in vitro* and potentially addressed IL-1β induction mechanisms during *S. mansoni* infection. To observe immunopathology, parasitology and pathological changes in the absence of inflammasome components, wildtype, NLRP3-, ASC-, Dectin-2-, IL-1R- and Dectin-1-deficient mice were infected with *S. mansoni* and analyzed after 8 weeks of infection. The analysis of parasitological and immunological parameters was performed after 8 weeks, since at this time point both T_H1 and T_H2 *S. mansoni-specific* immune responses are present within the host [61] (Figure 1.6).

4.3.1 NLRP3 inflammasome activation and IL-1β secretion influence schistosome-derived immunopathology

In general, the different knockout mice showed no significant differences to infected wildtype mice in terms of parasitology, such as the degree of infection (DOI) or worm and egg burden (section 3.3.1). This outcome did not even alter when mice were analysed during the chronic phase (12 weeks) of *S. mansoni* infection (data not shown). As with any infectious system, slight differences in DOI and parasite burden do occur between the mice but this is due to the complexity of schistosome biology within the host which includes several life stages (Figure 1.4). Thus, these data implied that NLRP3 inflammasome activation and IL-1β secretion did not influence worm development and maturation, as well as egg production. Indeed, this was not surprising, since *S. mansoni* infection of various knockout mice (IL-$4^{-/-}$, IL-$5^{-/-}$, IL-$6^{-/-}$, IL-$10^{-/-}$, IL-$13^{-/-}$ or IFN-$\gamma^{-/-}$) did not alter worm development and fecundity [280]. Even in severe combined immunodeficiency (SCID) mice, which lack functional B and T cells, egg laying was delayed but worm fecundity was equivalent to that in wildtype mice [281]. As mentioned above, the main feature of *S. mansoni* infection is the development of granuloma formation within the liver and intestine. Granulomas are initiated when schistosome eggs are trapped within the liver and intestinal tissue and secrete SEA, which is a powerful promoter of T_H2 responses [86-91]. For example, IL-13 is the main T_H2 cytokine promoting fibrosis development [100-103]. The essential role of T_H2 immune responses is highlighted by the fact that the conversion from a T_H2-dominant to a T_H1-dominant reaction leads to a reduced granuloma formation and fibrosis development within infected mice [104-107]. Interestingly, granuloma formation is further characterized by the alteration of infiltrating T_H and T_{reg} cell populations. As granulomas become older the makeup of immune cell composition alters from high numbers of $CD4^+$ T cells, macrophages and eosinophils to enhanced levels of $Foxp3^+$ T_{reg} cells that accumulated in the circumference of granulomas to control the

infiltration of immune cells and their responses [98, 99]. Moreover, depletion of T_{reg} cells leads to enhanced granuloma formation and skewed T_H1/T_H2 responses [98], underlining the essential role of this population. Interestingly, Layland *et al.* further observed that the IL-1R gene is upregulated within T_{reg} cells from infected *S. mansoni* mice but not in T_{regs} from naive mice [99]. As mentioned in the previous section, IL-1Ra was shown to be upregulated within infected mice [243] and blocking IL-1Ra lead to increased granuloma formation and enhanced T_H immune responses [242]. In summary, these data suggest that IL-1 signalling is important for granuloma formation and immune responses during Schistosomiasis. Indeed, infected MyD88 deficient mice, which have no functional IL-1R [10], developed smaller granulomas and reduced antigen-specific T_H1 responses [96]. Within the studies presented here, infected NLRP3-, ASC-, Dectin-2- and IL-1R-deficient mice had significantly smaller granulomas compared to wildtype mice (section 3.3.2). Furthermore, Dectin-$1^{-/-}$ mice developed normal sized granulomas, confirming the specificity of SEA-mediated Dectin-2 receptor triggering for the initiation of NLRP3 inflammasome activation. Additionally, infected Card9-deficient mice revealed also smaller granulomas (Layland *et al*. unpublished data). This finding confirms the *in vitro* Card9 experiments (section 3.2.7) and implicates a critical role of Card9 for NLRP3 inflammasome activation *in vivo*. Nevertheless, IL-1β *in situ* levels within liver and intestine tissue were only reduced in NLRP3- and ASC-deficient mice (section 3.3.3), showing that the specific NLRP3 inflammasome components are central for the initiation of IL-1β. Interestingly, *in situ* IL-1β levels were not impaired in Dectin-$2^{-/-}$ mice, indicating that probably another receptor could be also important for NLRP3 inflammasome activation *in vivo*. Indeed, preliminary *in vitro* experiments demonstrated that Mincle-deficient BMDCs showed reduced IL-1β production upon SEA stimulation (see section 4.2.3 for details). Thus, Mincle could be an additional receptor for SEA-mediated NLRP3 inflammasome activation *in vivo* and *in vitro*. Furthermore, mice lacking the IL-1R showed an enhanced IL-1β production, demonstrating that impaired IL-1 signalling can lead to unregulated IL-1β secretion within the tissue. However, granuloma formation was impaired in the Dectin-2- as well as in the IL-1R-deficient mice, suggesting that the granuloma formation does not strictly depend on IL-1β levels within infected organs.

4.3.2 NLRP3 inflammasome activation skews adaptive immune responses

Since granuloma formation depends on T_H [94-96], T_{reg} [98, 99] and T_H17 cell populations [92, 267, 268] and IL-1β can initiate such T_H cells and immune responses [200, 202-207] (see sections 1.4.3, 4.2.4 and 4.3.1 for details), we hypothesized that SEA-mediated NLRP3 inflammasome activation influences adaptive immune responses. Indeed, antigen-specific T_H1 (IFN-γ), T_H2 (IL-5, IL-10) and T_H17 (IL-17A) responses of restimulated spleen and mesenteric lymph node (MLN) cells were strongly suppressed within infected NLRP3-, ASC-, IL-1R- and Dectin-2-deficient mice compared to wildtype mice (section 3.3.4). With regards to *S. mansoni*-derived immunopathology, elevated IFN-γ and IL-17 responses have been associated with enlarged granuloma development [282, 283]. Moreover, *S. mansoni* infected IL-5-deficient mice showed reduced liver granuloma size with decreased numbers of eosinophils [284], which are a prominent cell type in granulomas provoking inflammatory responses [72, 245]. Also, IL-10 has been shown to regulate and control the polarized egg-specific T_H cell responses [129, 285]. Interestingly, several studies from Fallon *et al.* demonstrated that diminished T_H2 immune responses, especially in the absence of IL-4 and $CD4^+$ T cells, lead to enhanced T_H1 immune responses, hepatocyte damage and intestinal pathology, which are detrimental to the host [80, 100, 286]. Furthermore, in the absence of T cells egg excretion within the host is impaired [286-289]. These data highlight the importance of $CD4^+$ T cells and T_H2 immune responses during Schistosomiasis for the survival of host and helminth. Alongside the reduced T_H immune responses, IL-13 levels of restimulated spleen and MLN cells of infected $NLRP3^{-/-}$ and $ASC^{-/-}$ mice were significantly enhanced, indicating that not all schistosome-specific immune responses were suppressed. Moreover, $Dectin\text{-}2^{-/-}$ mice also revealed increased IL-13 responses. As mentioned in section 4.3.1, the functional role of IL-13 is distinct compared to the other T_H2 cytokines. IL-13 is the key mediator of fibrosis and granuloma formation and in the absence of IL-13 signalling infected mice fail to develop fibrotic granuloma, which is beneficial for host survival [100-103]. In contrast, increased hepatocyte damage, intestinal pathology and mortality could be observed in IL-4 deficient mice [100]. In addition, besides T cell populations, IL-4/IL-13 signalling in alternative-activated macrophages was also shown to be critical for host survival during Schistosomiasis [290]. Since, granuloma formation was reduced in infected NLRP3 inflammasome-, Dectin-2- and IL-1R-deficient mice, the enhanced IL-13 could be due to the reduced T_H2 responses. For further investigations, IL-4 levels and hepatocyte damage have to be quantified. In general, these findings demonstrate that the NLRP3 inflammasome-mediated

IL-1β signalling balances T_H1 (IFN-γ), T_H2 (IL-5, IL-10, IL-13) and T_H17 (IL-17A) immune responses to drive T_H2-polarized pathogenesis and parasite survival. Again, the specificity of the Dectin-2/NLRP3 inflammasome signalling was confirmed, since SEA-specific responses of MLN and spleen cells from infected Dectin-$1^{-/-}$ mice were not altered upon restimulation with SEA.

Collectively, the *in vivo* infection experiments using various knockout mice demonstrated that components released during *S. mansoni* infection trigger the Dectin-2 receptor to initiate NLRP3 inflammasome activation leading to IL-1β secretion. Interestingly, in the absence of these signalling components both granuloma formation and T_H immune responses were deviated. Besides IL-1β induction, NLRP3 inflammasome activation also leads to IL-18 production [150-152]. Interestingly, IL-18 mRNA is strongly produced upon percutaneous infection of *S. mansoni* [291], indicating that IL-18 plays a role during the penetration of cercariae into the host. Again, these data highlight the important role of NLRP3 inflammasome activation during Schistosomiasis. However, further studies have to decipher the role of IL-18 in comparison with IL-1β to elucidate the connection of NLRP3 inflammasome and T_H2 immune responses. Summarizing, the discovery of this SEA-mediated NLRP3 inflammasome signalling platform contributes towards a better understanding of *S. mansoni* modulation mechanisms and may unravel further information that can be used for new vaccination strategies against autoimmune diseases or allergy (section 4.4).

4.4 NLRP3 inflammasome activation drives allergic asthma development

Throughout this thesis, components within SEA were shown to trigger the NLRP3 inflammasome signalling platform which in turns initiated inflammatory immune responses to modulate and balance T_H immune responses and granuloma formation during the T_H2-polarized *S.mansoni* infection. Interestingly, several autoimmune diseases have been associated with inflammasome activation and IL-1β secretion (section 1.4), such as chronic allergic asthma [202, 203, 214]. According to the WHO, over 235 million people currently suffer from allergic asthma disease, a potentially life-threating illness that causes breathing difficulties, dyspnea, tight chest, cough or bronchospasm [215]. Interestingly, asthma disease is characterized by dominant T_H2 immune responses including enhanced IL-4, IL-5 and IL-13 responses, allergen-specific immunoglobulin production, eosinophilic inflammation, goblet cell infiltration and increased mucus production within the lung leading to airway

hyperresponisveness (AHR) [216, 217]. Typically, the long-term unresolved airway inflammation leads to airway remodeling and to continuous inflammed and swollen respiratory airways [218, 219] (see section 1.4.5 for details). To date, general causes of the disease are unknown. However, it is known that risk factors are the combination of genetic predisposition with environmental substances, such as indoor allergens (house dust mites or pet dander); outdoor allergens (pollens or moulds); tobacco smoke and air pollution; certain medications (aspirin or other non-steroid anti-inflammatory drugs) [215]. Treatment of asthma is divided into two classes: 1. Treatment of acute symptoms with quick-relief medications, such as anticholinergics, SABAs (short acting beta agonists) or systemic corticosteroids; 2. Prevention of further exacerbation with long-term control medications, such as corticosteroids, cromolyn sodium and nedocromil, immunomodulators, leukotriene modifiers, methylxanthines or LABAs (long acting beta agonists) [292, 293]. Although, asthma symptoms can be controlled in a large proportion of patients with these therapeutic agents, a small percentage of individuals with severe asthma remain symptomatic and inadequately controlled leading to a high risk of serious morbidity and mortality [294, 295]. Interestingly, several studies have demonstrated that ongoing parasitic helminth infection in humans lower the prevalence of allergic disorders [253, 254 296, 297]. The relationship between helminth-derived modulating mechanisms and allergy are not well understood. For example, infection studies using the murine *S. mansoni* model have shown that infections modulate T_H and T_{reg} cell differentiation to promote T_H2 immune responses and immunoglobulins, especially IgE production, that leads to the protective effect against allergic diseases, such as asthma [251, 252, 298-300]. This modulatory effect also seems to be dependent on the intensity and chronicity of infection [301].

In this study, we hypothesized that NLRP3 inflammasome activation lead to IL-1β production and consequently T_H2 polarization during an ongoing *S. mansoni* infection. Several studies have demonstrated that IL-1β is an important cytokine for bronchial asthma development by promoting the infiltration of eosinophils and inflammation within the lung [155-157, 202, 203] (section 1.4.5). Thus, we studied allergic airway inflammation in female BALB/c inflammasome-deficient mice that were sensitized with albumin from chicken egg white (OVA) in an alum-free manner (see section 2.6.1 for details). Interestingly, male mice did not develop allergic airway inflammation, indicating an essential role for gender within asthma development. The murine OVA-inducing allergic airway inflammation model is widely used and well characterized and displays features similar to those seen in human allergic asthma, including dominant OVA-specific T_H2-type immune responses (IL-4 or IL-5), eosinophilia,

increased mucus production within the lung, airway hyperresponsiveness (AHR) and allergen-specific IgE production [220]. Additionally, aluminium hydroxide (alum) is frequently administered with OVA during the sensitization phase as an adjuvant. However, within this study an alum-free OVA-inducing allergic airway inflammation model was performed because, as mentioned and shown previously, alum is a strong inducer of the NLRP3 inflammasome and IL-1β secretion (section 3.2.4) [188, 302-304]. In contrast to the BMDC or *S. mansoni* infection experiments, BALB/c mice were used for the allergic airway inflammation experiments. BALB/c mice induce strong T_H2 immune responses, elevated OVA-specific IgE levels and pulmonary eosinophilia, as well as an elevated response to metacholine that is a marker for AHR sensitivity compared to mice on C57BL/6 background [220, 305-307]. Therefore, wildtype, NLRP3- and ASC-deficient mice on BALB/c background were sensitized with OVA to analyse allergic airway inflammation.

4.4.1 NLRP3 inflammasome activation influences allergic airway inflammation

To evaluate the degree of allergic airway inflammation, several parameters have to be analysed, such as infiltration of immune cells and cytokine levels within the bronchoalveolar lavage (BAL), lung inflammation and specific immunoglobulin production. As expected, the OVA exposed wildtype mice presented an enhanced infiltration of eosinophils within the BAL compared to PBS treated control mice (section 3.4.1). Eosinophils are known to be one of the key effector cells driving lung pathogenesis, since they release proinflammatory cytokines and cytotoxic proteins from their granules to induce lung epithelial damage, edema and AHR [308-310]. Therefore, eosinophil infiltration within the BAL is a marker for asthma development. Interestingly, in NLRP3- and ASC-deficient mice significantly less eosinophil infiltration could be observed, suggesting that the NLRP3 inflammasome plays a crucial role in the recruitment process of eosinophils within the lung. Furthermore, evaluation of OVA-sensitized wildtype mice revealed thick basal membranes and enhanced mucus-secreting goblet cell infiltration within the lungs (section 3.4.2), confirming on a pathology level that wildtype mice developed chronic allergic airway inflammation. In contrast, pathological aspects were significantly reduced in $ASC^{-/-}$ mice, whereas $NLRP3^{-/-}$ showed significantly less inflammation but goblet cell infiltration was comparable to wildtype controls. These data illustrate that NLRP3 inflammasome activation is important for the initiation of inflammation within the lung but other factors and perhaps signalling mechanisms induce immune cells, such as goblet cells, to drive secondary inflammatory responses. In addition, these findings

implicated that probably another inflammasome complex consisting of ASC could be involved. Another important feature of allergic asthma is the initiation T_H2 immune cells that secrete cytokines, such as IL-5 and IL-13 to augment inflammatory responses and airway remodeling [311, 312] (section 1.4.5). Indeed, OVA-sensitized wildtype mice secreted significantly higher amounts of IL-5 and IL-13 within the BAL compared to NLRP3$^{-/-}$ and ASC$^{-/-}$ mice (section 3.4.3). Interestingly, the ability of lung lymph node (LLN) cells to respond to OVA antigen upon *in vitro* restimulation was only impaired in IFN-γ secretion, suggesting that NLRP3 inflammasome activation and IL-1β secretion initiate proinflammatory cytokines to modulate T_H2 immune responses. In addition, IL-10 levels were slightly increased in the culture supernatants of OVA-restimulated LLN cells from NLRP3- and ASC-deficient mice, confirming that the NLRP3 inflammasome signalling pathway balances T_H immune responses and that in the absence of NLRP3 inflammasome components a more regulatory phenotype is induced. However, OVA-specific IgE and IgG1 levels within sera showed no alterations within NLRP3 inflammasome-deficient mice.

In general, these data demonstrate that NLRP3 inflammasome activation is essential for the initiation of inflammatory responses within the lung (eosinophil and partially goblet cell infiltration) and modulation of T_H2 immune responses (BAL IL-5 and IL-13 levels), but is dispensable for secondary mechanisms, such as OVA-specific immunoglobulin production. In contrast to the findings observed within this study, Besnard *et al.* demonstrated that goblet cell infiltration and OVA-specific IgE as well as eosinophil infiltration within the lung, BAL cytokine responses and lung inflammation were abolished in mice lacking the NLRP3 inflammasome [214]. These data claimed that allergic airway inflammation depends strictly on NLRP3 inflammasome activation including secondary mechansims, such as OVA-specific immunoglobulin production and goblet cell infiltration. However, this study was performed with C57BL/6 mice, which were shown to develop reduced allergic airway inflammation and dominant T_H1 based immune responses [220, 305-307]. Indeed, Allen *et al.* claimed that allergic airway inflammation within NLRP3$^{-/-}$ mice on C57BL/6 background is similar to wildtype control mice [313], indicating that C57BL/6 mice are not the optimal model to investigate allergic airway inflammation. These contrary findings demonstrate the complexity of allergic asthma development and highlight the necessity of using a BALB/c mouse model within this study. In addition, an alternative explanation for the diverse phenotypic outcome could be the composition of the host microbiome that depends on the individual mouse facility. Indeed, studies have demonstrated that oral treatment of *Bifidobacterium* and *Lactobacillus* lead to reduced allergic airway inflammation [314, 315]. However, this study

implied an essential role of the NLRP3 inflammasome signalling platform for the induction and modulation of T_H2-polarized immune responses. The understanding of complex T_H2 polarized immune responses which arise during *S. mansoni* infection or allergic asthma could contribute to the development of novel vaccination strategies against autoimmune diseases.

4.4.2 Blocking IL-1 signalling reduces allergic airway inflammation

Since NLRP3 inflammasome activation appeared to play a role in allergic asthma development, it was conjectured that IL-1β could initiate and drive lung inflammation. Interestingly, *in situ* IL-1β levels within the lungs were not altered in OVA-sensitized NLRP3- and ASC-deficient mice when compared to wildtype mice (section 3.4.4). These evaluations were performed on day 31, three days after the OVA-challenge (see section 2.6.1 for details), because this time point shows strong lung inflammation and T_H2 immune responses. Such results suggested that NLRP3 inflammasome activation and IL-1β production is important for the initiation of inflammation and T_H2 polarization, whereas the other immune responses are driven by different mechanisms (section 4.4.1). To confirm this hypothesis, IL-1β levels were measured immediately after the last sensitization to OVA (day 28). Indeed, $NLRP3^{-/-}$ and $ASC^{-/-}$ mice had significantly less IL-1β within the lung compared to wildtype mice, demonstrating that NLRP3 inflammasome activation is initiated immediately after antigen contact and could therefore actively participate in the events leading to proinflammatory responses and recruitment of immune cells (eosinophils).

Over the last few years, the understanding of inflammasome activation pathways has provided the basis for the treatment of several autoinflammatory diseases, such as juvenile idiopathic arthritis [210], refractory adult Still's disease [211], gout [212], type 2 diabetes [213], rheumatoid arthritis [152] and diverse fever syndromes [200]. A standard therapeutic agent for such autoinflammatory diseases is Anakinra (Kineret®), an IL-1 receptor antagonist (IL-1Ra) that blocks IL-1 signalling and thus prevents continuous IL-1β-mediated inflammation. The initial allergic airway experiments described here demonstrated an association of IL-1β-mediated inflammation and allergic asthma disease. Therefore, it was considered that Anakinra treatment could probably reduce inflammatory responses within the lung and thus dampen asthma development. To verify this hypothesis, mice were treated with Anakinra during OVA sensitization or challenge (section 3.4.5). Interestingly, eosinophil infiltration was only significantly reduced in mice treated with Anakinra during the challenge phase. However, inflammation and goblet cell infiltration within the lung were not abolished.

Additionally, IFN-γ responses within the BAL were decreased when mice were treated with Anakinra during OVA challenge or sensitization, but IL-5 and IL-13 responses remained unchanged, as well as OVA-specific IgE and IgG1 levels. The Anakinra data imply that functional IL-1β is critical for eosinophil infiltration, but not for secondary effects, such as OVA-specific immunglobulins, confirming previous results in ASC and NLRP3-deficient mice (section 4.4.1). In contrast, data obtained from NLRP3 inflammasome-deficient mice demonstrated that infiltration of eosinophils as well as inflammation and cytokine responses within lungs depends on NLRP3 inflammasome activation. Eosinophil infiltration is an essential process within asthma development. To evaluate the role of eosinophil activation, measurements of eosinophil activation marker, such as peroxidase (EPO), eosinophil cationic protein (ECP) and myeloperoxidase (MPO) have to be performed. However, this study demonstrated that Anakinra treatment reduces eosinophil infiltration within the lungs. Thus, Anakinra could be included into the long-term control medications and moreover may contribute to a novel therapy for patients with severe uncontrolled asthma disease.

Interestingly, IL-1β levels within the lungs were not altered when mice were treated with Anakinra (section 3.4.5), suggesting that Anakinra treatment was not sufficient to significantly reduce IL-1β production. This effect could be explained by the short half-life of 4-6h. Therefore, for further investigations a higher dose of Anakinra should be applied. Moreover, alternative reagents, such as rilonacept (IL-1 trap) and canakinumab (specific anti-IL-1β antibody) should be employed since they have a longer half-life of approximately 7 and 26 days, respectively. These drugs have also been developed and approved for treatment against diverse autoinflammatory diseases [200]. In addition, IL-1R$^{-/-}$ mice should be evaluated, since preliminary data demonstrate that these mice also show reduced allergic airway inflammation (unpublished data). Similar results have been obtained in IL-18$^{-/-}$ mice [316], confirming that IL-1 family members influencing asthma development. However, the specific IL-1 signalling mechanisms that contribute to this disease remain unclear. Interestingly, a novel research avenue includes the T_H17 cell population, since several studies have shown that IL-1β can induce IL-17A and T_H17 cell differentiation [205-207]. Furthermore, T_H17 immune responses have been shown to influence allergic asthma development [317, 318]. Thus, T_H17 immune responses could be the link between NLRP3 inflammasome-mediated IL-1β and allergic asthma development. Collectively, these data reveal that impaired IL-1 signalling lead to reduced inflammatory responses against OVA, implicating new treatment strategies against allergic asthma.

4.5 NLRP3 inflammasome is a central signalling platform that drives T_H2-polarized immune responses

Within this study, NLRP3 inflammasome activation mechanisms were investigated during T_H2-dominated immune responses of *S. mansoni* infection and allergic airway inflammation. This research concludes that the outcome of pathology and deviation in immune responses during Schistosomiasis and allergic airway inflammation is dependent on NLRP3 inflammasome activation.

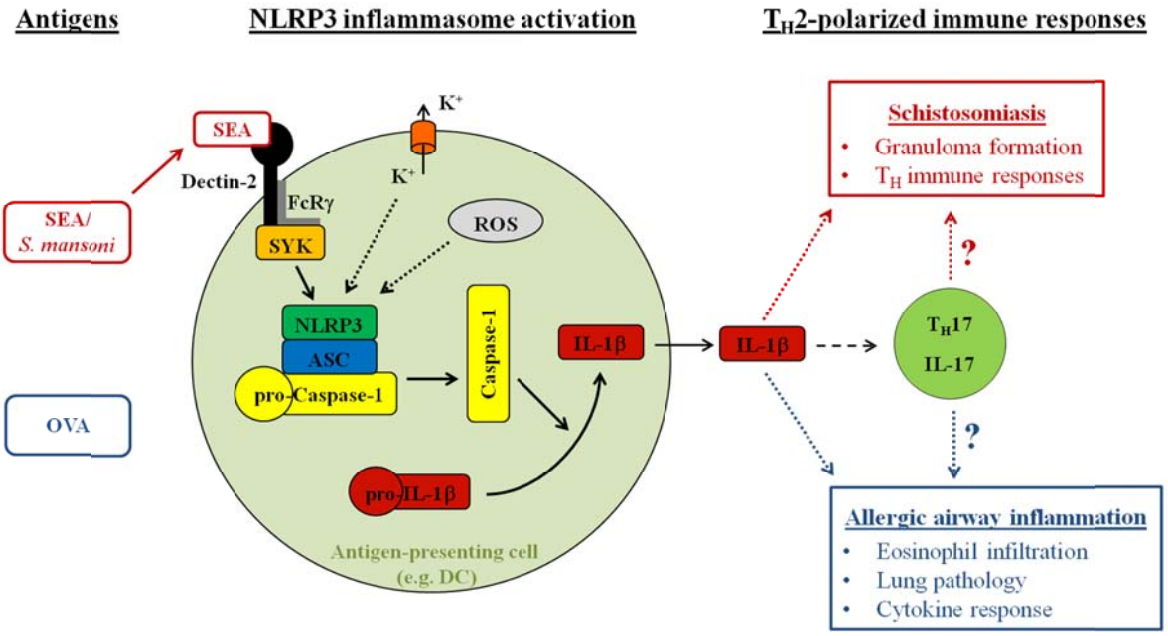

Figure 4.2: NLRP3 inflammasome is a central signalling complex that drives T_H2-polarized immune responses
In brief, the NLRP3 inflammasome is triggered through different antigens, such as SEA/*S. mansoni* in a Dectin-2/FcRγ/Syk/ROS/potassium efflux-dependent manner or OVA through an unknown mechanism. Thus, NLRP3 inflammasome activation leads to IL-1β production that influences granuloma formation and T_H immune responses during Schistosomiasis or eosinophil infiltration, lung pathology and cytokine responses during allergic airway inflammation. In addition, IL-1β can also induce T_H17 immune responses that have been shown to drive T_H2 polarized immune responses.

As depicted in Figure 4.1, the NLRP3 inflammasome is a central signalling complex driving T_H2-polarized immune responses during Schistosomiasis and allergic airway inflammation. The understanding of NLRP3 inflammasome signalling mechansims could lead to novel treatment strategies against T_H2-dominated diseases, such as helminth infections (section 4.3) or asthma disease (section 4.4). Nevertheless, further investigations have to be performed to elucidate the antigen-specific NLRP3 inflammasome signalling mechansims and the potential role of IL-1β-mediated T_H17 immune responses that both could influence T_H2 immune responses.

References

[1] Murphy, K.P., Travers, P. and Walport, M. (2008). Janeway`s Immunobiology, 7th edition. *Garland science publishing*

[2] Riedel, S. (2005). Edward Jenner and the history of smallpox and vaccination. *Proc (Bayl Univ Med Cent)* 18:21–25

[3] Koch, R. (1876). Die Aetiologie der Milzbrand-Krankheit, begründet auf die Entwicklungsgeschichte des *Bacillus Anthracis*. *Grohns Beitrage zur Biologie der Pflanzen* 2:277–310

[4] Ullmann, A. (2007). Pasteur-Koch: Distinctive ways of thinking about infectious diseases. *Microbe (American Society for Microbiology)* 2:383–387

[5] Tan, S.Y. and Grimes, S. (2010). Paul Ehrlich (1854-1915): man with the magic bullet. *Singapore Med J* 51:842-843

[6] Tan, S.Y. and Dee, M.K. (2009). Elie Metchnikoff (1845-1916): discoverer of phagocytosis. *Singapore Med J* 50:456-457

[7] Beck, G. and Habicht, G.S. (1996). Immunity and the invertebrates. *Scientific American* 60–66

[8] Bruce, A., Johnson, A., Lewis, J., Raff, M., Roberts, K. and Walters, P. (2002). Molecular Biology of the Cell, 4th Edition. *Garland science publishing*

[9] Medzhitov, R. and Janeway, C.A. (1997). Innate immunity: the virtues of a nonclonal system of recognition. *Cell* 91:295-298

[10] Medzhitov, R. (2001). Toll-like receptors and innate immunity. *Nature Reviews Immunology* 1:135-145

[11] Akira, S., Takeda, K. and Kaisho, T. (2001). Toll-like receptors: critical proteins linking innate and acquired immunity. *Nature Immunol* 2:675-680

[12] Aliprantis, A.O., Yang, R.B., Mark, M.R., Suggett, S., Devaux, B., Radolf, J.D., Kimpel, G.R., Godowski, P. and Zychlinsky, A. (1999). Cell activation and apoptosis by bacterial lipoproteins through Toll-like receptor-2. *Science* 285:736-739

[13] Poltorak, A., He, X., Smirnova, I., Liu, M.Y., Van Huffel, C., Du, X., Birdwell, D., Alejos, E., Silva, M., Galanos, C., Freudenberg, M., Ricciardi-Castagnoli, P., Layton, B. and Beutler, B. (1998). Defective LPS signaling in C3H/HeJ and C57BL/10ScCr mice mutations in TLR4 gene. *Science* 282:2085-2088

[14] Hemmi, H., Takeuchi, O., Kawai, T., Kaisho, T., Sato, S., Sanjo, H., Matsumoto, M., Hoshino, K., Wagner, H., Takeda, K., Akira, S. (2000). A Toll-like receptor recognizes bacterial DNA. *Nature* 408:740-745

[15] Liew, F.Y., Xu, D., Brint, E.K. and O'Neill, L.A. (2005). Negative regulation of Toll-like receptor-mediated immune responses. *Nature Reviews Immunology* 5:446-458

[16] Medzhitov, R., Preston-Hurlburt, P. and Janeway, C.A.Jr. (1997). A human homologue of the drosophila toll protein signals activation of adaptive immunity. *Nature* 388:394-397

[17] Fitzgerald, K.A., Palsson-McDermott, E.M., Bowie, A.G., Jefferies, C.A., Mansell, A.S., Brady, G., Brint, E., Dunne, A., Gray, P., Harte, M.T., McMurray, D., Smith, D.E., Sims, J.E., Bird, T.A. and O'Neill, L.A. (2001). Mal (MyD88-adapter-like) is required for Toll-like receptor-4 signal transduction. *Nature* 413:78-83

[18] Yamamoto, M., Sato, S., Hemmi, H., Sanjo, H., Uematsu, S., Kaisho, T., Hoshino, K., Takeuchi, O., Kobayashi, M., Fujita, T., Takeda, K. and Akira S. (2002). Essential role for TIRAP in activation of the signalling cascade shared by TLR2 and TLR4. *Nature* 420:324-329

[19] Yamamoto, M., Sato, S., Hemmi, H., Hoshino, K., Kaisho, T., Sanjo, H., Takeuchi, O., Sugiyama, M., Okabe, M., Takeda, K. and Akira, S. (2003). Role of adaptor TRIF in the MyD88-independent toll-like receptor signaling pathway. *Science* 301:640-643

[20] Oshiumi, H., Matsumoto, M., Funami, K., Akazawa, T., Seya, T. (2003). TICAM-1, an adaptor molecule that participates in Toll-like receptor 3-mediated interferon-beta induction. *Nat Immunol* 4:161-167

[21] Yamamoto, M., Sato, S., Hemmi, H., Uematsu, S., Hoshino, K., Kaisho, T., Takeuchi, O., Takeda, K. and Akira, S. (2003). TRAM is specifically involved in the Toll-like receptor 4-mediated MyD88-independent signaling pathway. *Nat Immunol* 4:1144-1150

[22] Medzhitov, R., Preston-Hurlburt, P., Kopp, E., Stadlen, A., Chen, C., Ghosh, S. and Janeway, C.A.Jr. (1998). MyD88 is an adaptor protein in the hToll/IL-1 receptor family signaling pathways. *Mol Cell* 2:253-258

[23] Takeda, K. and Akira, S. (2004). TLR signaling pathways. *Semin Immunol* 16:3-9

[24] Dumitru, C.D., Ceci, J.D., Tsatsanis, C., Kontoyiannis, D., Stamatakis, K., Lin, J.H., Patriotis, C., Jenkins, N.A., Copeland, N.G., Kollias, G. and Tsichlis, P.N. (2000). TNF-alpha induction by LPS is regulated posttranscriptionally via a Tpl2/ERK-dependent pathway. *Cell* 103:1071-1083

[25] Huang, Q., Yang, J., Lin, Y., Walker, C., Cheng, J., Liu, Z.G. and Su, B. (2004). Differential regulation of interleukin 1 receptor and Toll-like receptor signaling by MEKK3. *Nat Immunol* 5:98-103

[26] Langerhans, P. (1868). Ueber die Nerven der Menschlichen Haut. *Virchows Arch* 44:325-337

[27] Steinman, R.M. and Cohn, Z.A. (1973). Identification of a novel cell type in peripheral lymphoid organs of mice. I. Morphology, quantitation, tissue distribution. *J Exp Med* 137:1142-1162

[28] Banchereau, J. and Steinman, R.M. (1998). Dendritic cells and the control of immunity. *Nature* 392:245-252

[29] Cella, M., Scheidegger, D., Palmer-Lehmann, K., Lane, P., Lanzavecchia, A. and Alber, G. (1996). Ligation of CD40 on dendritic cells triggers production of high levels of interleukin-12 and enhances T cell stimulatory capacity: T-T help via APC activation. *J Exp Med* 184:747-752

[30] Koch, F., Stanzl, U., Jennewein, P., Janke, K., Heufler, C., Kämpgen, E., Romani, N. and Schuler, G. (1996). High level IL-12 production by murine dendritic cells: upregulation via MHC class II and CD40 molecules and downregulation by IL-4 and IL-10. *J Exp Med* 184:741-746

[31] Dodge, I.L., Carr, M.W., Cernadas, M. and Brenner, M.B. (2003). IL-6 production by pulmonary dendritic cells impedes Th1 immune responses. *J Immunol* 170:4457-4464

[32] Dubois, B., Vanbervliet, B., Fayette, J., Massacrier, C., Van Kooten, C., Brière, F., Banchereau, J. and Caux C. (1997). Dendritic cells enhance growth and differentiation of CD40-activated B lymphocytes. *J Exp Med* 185:941-951

[33] Fayette, J., Dubois, B., Vandenabeele, S., Bridon, J.M., Vanbervliet, B., Durand, I., Banchereau, J., Caux, C. and Brière F. (1997). Human dendritic cells skew isotype switching of CD40-activated naive B cells towards IgA1 and IgA2. *J Exp Med* 185:1909-1918

[34] McKinstry, K.K., Strutt, T.M. and Swain, S.L. (2010). The potential of CD4 T-cell memory. *Immunology* 130:1-9

[35] Elgueta, R., de Vries, V.C. and Noelle, R.J. (2010). The immortality of humoral immunity. *Immunol Rev* 236:139-150

[36] Calame, K.L. (2001). Plasma cells: finding new light at the end of B cell development. *Nat Immunol* 2:1103-1108

[37] Titus, J.A., Perez, P., Kaubisch, A., Garrido, M.A. and Segal, D.M. (1987). Human K/natural killer cells targeted with hetero-cross-linked antibodies specifically lyse tumor cells in vitro and prevent tumor growth in vivo. *J Immunol* 139:3153-3158

[38] Stone, K.D., Prussin, C. and Metcalfe, D.D. (2010). IgE, mast cells, basophils, and eosinophils. *J Allergy Clin Immunol* 125:73-80

[39] Anderson, C.L., Shen, L., Eicher, D.M., Wewers, M.D. and Gill, J.K. (1990). Phagocytosis mediated by three distinct Fc gamma receptor classes on human leukocytes. *J Exp Med* 171:1333-1345

[40] Henkart, P.A. (1985). Mechanism of lymphocyte-mediated cytotoxicity. *Annu Rev Immunol* 3:31-58

[41] Berke, G. (1994). The binding and lysis of target cells by cytotoxic lymphocytes: molecular and cellular aspects. *Annu Rev Immunol* 12:735-73

[42] Germain, R.N. (1994). MHC-dependent antigen processing and peptide presentation: providing ligands for T lymphocyte activation. *Cell* 76:287-299

[43] Mosmann, T.R, Cherwinski, H., Bond, M.W., Giedlin, M.A. and Coffman, R.L. (1986). Two types of murine helper T cell clone. I. Definition according to profiles of lymphokine activities and secreted proteins. *J Immunol* 136:2348-2357

[44] Mosmann, T.R. and Coffman, R.L. (1989). TH1 and TH2 cells: different patterns of lymphokine secretion lead to different functional properties. *Annu Rev Immunol* 7:145-173

[45] Sher, A. and Coffman, R.L. (1992). Regulation of immunity to parasites by T cells and T cell-derived cytokines. *Annu Rev Immunol* 10:385-409

[46] O'Garra, A. (1998). Cytokines induce the development of functionally heterogeneous T helper cell subsets. *Immunity* 8:275-283

[47] Jenkins, M.K., Khoruts, A., Ingulli, E., Mueller, D.L., McSorley, S.J., Reinhardt, R.L., Itano, A. and Pape, K.A. (2001). *In vivo* activation of antigen-specific CD4 T cells. *Annu Rev Immunol* 19:23-45

[48] Fontenot, J.D., Gavin, M.A. and Rudensky, A.Y. (2003). Foxp3 programs the development and function of $CD4^+CD25^+$ regulatory T cells. *Nat Immunol* 4:330-336

[49] Mills, K.H. and McGuirk, P. (2004). Antigen-specific regulatory T cells-their induction and role in infection. *Semin Immunol* 16:107-117

[50] Sakaguchi, S., Ono, M., Setoguchi, R., Yagi, H., Hori, S., Fehervari, Z., Shimizu, J., Takahashi, T. and Nomura, T. (2006). $Foxp3^+$ $CD25^+$ $CD4^+$ natural regulatory T cells in dominant self-tolerance and autoimmune disease. *Immunol Rev* 212:8-27

[51] Roncarolo, M.G., Gregori, S., Battaglia, M., Bacchetta, R., Fleischhauer, K. and Levings, M.K. (2006). Interleukin-10-secreting type 1 regulatory T cells in rodents and humans. *Immunol Rev* 212:28-50

[52] Harrington, L.E., Hatton, R.D., Mangan, P.R., Turner, H., Murphy, T.L., Murphy, K.M. and Weaver, C.T. (2005). Interleukin 17-producing CD4+ effector T cells develop via a lineage distinct from the T helper type 1 and 2 lineages. *Nat Immunol* 6:1123-1132

[53] Bettelli, E., Korn, T., Oukka, M. and Kuchroo, V.K. (2008). Induction and effector functions of T_H17 cells. *Nature* 453:1051-1057

[54] Veldhoen, M., Uyttenhove, C., van Snick, J., Helmby, H., Westendorf, A., Buer, J., Martin, B., Wilhelm, C. and Stockinger, B. (2008). Transforming growth factor-beta 'reprograms' the differentiation of T helper 2 cells and promotes an interleukin 9-producing subset. *Nat Immunol* 9:1341-1346

[55] Soroosh, P. and Doherty, T.A. (2009). Th9 and allergic disease. *Immunology* 127:450-458

[56] Boros, D.L. (1989). Immunopathology of *Schistosoma manoni* infection. *Clin Mircobiol Rev* 2:250-269

[57] World Health Organization (2010). Schistosomiasis Fact Sheet. *http://www.who.int/mediacentre/factsheets/fs115/en/index.html*

[58] King, C. H. (2010). Parasites and poverty: The case of Schistosomiasis. *Acta Trop* 113: 95–104

[59] Center of Disease Control and Prevention (2010). Parasites - Neglected Tropical Diseases - Schistosomiasis. *http://www.cdc.gov/parasites/schistosomiasis/*

[60] Allison, A.C., Andrade, Z.A., Santos, E., Brunner, T., Butterworth, A.E., Capron, A. Cohen, S., Colley, D.G., Coombs, R.A.A., David, J.R., Davis, A., Hoffman, D.B., Hopwood, B.E.C., Houba, V. and Jordan, P. (1974). Immunology of Schistosomiasis. *Bull World Health Organization* 51:553-595

[61] Dunne, D.W. and Cooke, A. (2005). A worm's eye view of the immune system: consequences for evolution of human autoimmune disease. *Nat Rev Immunol* 5:420-425

[62] Weinstock, J.V. and Boros, D.L. (1981). Heterogeneity of the granulomatous response in the liver, colon, ileum, and ileal Peyer`s patches to schistosome eggs in murine Schistosomiasis mansoni. *J Immunol* 127:1906-1909

[63] Andrade, Z.A. and Andrade, S.G. (1970). Pathogenesis of schistosomal pulmonary arteritis. *Am J Trop Med Hyg* 19:305-310

[64] Fukuyama, K., Tzeng, S., McKerrow, J. and Epstein, W.L. (1983). The epidermal barrier to *Schistosoma mansoni* infection. *Curr Prob Dermatol* 11:185-193

[65] Hansell, E., Braschi, S., Medzihradszky, K.F., Sajid, M., Debnath, M., Ingram, J., Lim, K. C. and McKerrow, J. H. (2008). Proteomic Analysis of Skin Invasion by Blood Fluke Larvae. *PLoS Negl Trop Dis* 2:e262

[66] Fölster-Holst, R., Disko, R., Röwert, J., Böckeler, W., Kreiselmaier, I. and Christophers, E. (2001). Cercarial dermatitis contracted via contact with an aquarium: case report and review. *Brit J Derm* 145:638-640

[67] Ross, A.G., Vickers, D., Olds, G.R., Shah, S.M. and McManus, D.P. (2007). Katayama syndrome. *Lancet Infect Dis* 7:218-224

[68] Gray, D.J., Ross, A.G., Li, Y.S. and McManus, D.P. (2011). Diagnosis and management of schistosomiasis. *BMJ* 17:342:d2651. doi: 10.1136/bmj.d2651

[69] Rocha, M.O., Rocha, R.L., Pedroso, E.R., Greco, D.B., Ferreira, C.S., Lambertucci, J.R., Katz, N., Rocha, R.S., Rezende, D.F. and Neves, J. (1995). Pulmonary manifestations in the initial phase of schistosomiasis mansoni. *Rev Inst Med Trop Sao Paulo* 37:311-318

[70] McManus, D.P., Gray, D.J., Li, Y., Feng, Z., Williams, G.M., Stewart, D., Rey-Ladino, J. and Ross, A.G. (2010). Schistosomiasis in the people's Republic of China: the era of the three Gorges Dam. *Clin Microbiol Rev* 23:442-466

[71] Ross, A.G., Bartley, P.B., Sleigh, A.C., Olds, G.R., Li, Y., Williams, G.M. and McManus D.P. (2002). Schistosomiasis. *N Engl J Med* 346:1212-1220

[72] Gryseels, B., Polman, K., Clerinx, J. and Kestens, L. (2006). Human schistosomiasis. *Lancet* 368:1106-1018

[73] Lambertucci, J.R. (2010). Acute schistosomiasis *mansoni*: revisited and reconsidered *Mem Inst Oswaldo Cruz* 105:422-435

[74] Chabasse, D. Bertrand, G., Leroux, J.P., Gauthey, N. and Hocquet, P. (1985). Developmental bilharziasis caused by *Schistosoma mansoni* discovered 37 years after infestation. *Bull Soc Pathol Exot Filiales* 78:643–647

[75] Pearce, E.J. and Sher, A. (1987). Mechanisms of immune evasion in schistosomiasis *Contrib Microbiol Immunol* 8:219-232

[76] Maizels, R.M., Bundy, D.A., Selkirk, M.E., Smith, D.F. and Anderson R.M (1993). Immunological modulation and evasion by helminth parasites in human populations. *Nature* 365:797-805

[77] Carvalho-Queiroz, C., Cook, R., Wang, C.C., Correa-Oliveira, R., Bailey, N.A., Egilmez, N.K., Mathiowitz, E. and LoVerde, P.T. (2004). Cross-reactivity of *Schistosoma mansoni* cytosolic superoxide dismutase, a protective vaccine candidate, with host superoxide dismutase and identification of parasite-specific B epitopes. *Infect Immun* 72:2635–2647

[78] Duvaux-Miret, D., Stefano, G.B., Smith, E.M., Mallozzi, L.A. and Capron, A. (1992). Proopiomelanocortin-derived peptides as tools of immune evasion for the human trematode *Schistosoma mansoni*. *Acta Biol Hung* 43:281-286

[79] Karanja, D.M., Colley, D.G., Nahlen, B.L., Ouma, J.H. and Secor, W.E. (1997). Studies on schistosomiasis in western Kenya: I. Evidence for immune-facilitated excretion of schistosome eggs from patients with *Schistosoma mansoni* and human immunodeficiency virus coinfections. *Am J Trop Med Hyg* 56:515-521

[80] Fallon, P.G. and Dunne, D.W. (1999). Tolerization of mice to *Schistosoma mansoni* egg antigens causes elevated type 1 and diminished type 2 cytokine responses and increased mortality in acute infection. *J Immunol* 162:4122-4132

[81] Amiri, P., Locksley, R.M., Parslow, T.G., Sadick, M., Rector, E., Ritter, D. and McKerrow, J.H. (1992). Tumour necrosis factor α restores granulomas and induces parasite egg-laying in schistosome-infected SCID mice. *Nature* 356:604-607

[82] Beall, M.J. and Pearce, E.J. (2001). Human transforming growth factor-beta activates a receptor serine/threonine kinase from the intravascular parasite *Schistosoma mansoni*. *J Biol Chem* 276:31613-31619

[83] Freitas, T.C., Jung, E. and Pearce, E.J. (2007). TGF-beta signaling controls embryo development in the parasitic flatworm *Schistosoma mansoni*. *PLoS Pathog* 3:e52

[84] Angeli, V., Faveeuw, C., Roye, O., Fontaine, J., Teissier, E., Capron, A., Wolowczuk, I., Capron, M. and Trottein, F. (2001). Role of the parasite-derived prostaglandin D2 in the inhibition of epidermal Langerhans cell migration during schistosomiasis infection. *J Exp Med* 193:1135-1147

[85] Hervé, M., Angeli, V., Pinzar, E., Wintjens, R., Faveeuw, C., Narumiya, S., Capron, A., Urade, Y., Capron, M., Riveau, G. and Trottein F. (2003). Pivotal roles of the parasite PGD2 synthase and of the host D prostanoid receptor 1 in schistosome immune evasion. *Eur J Immunol* 33:2764-2772

[86] Grzych, J.M., Pearce, E., Cheever, A., Caulada, Z.A., Caspar, P., Heiny, S., Lewis, F. and Sher, A. (1991). Egg deposition is the major stimulus for the production of Th2 cytokines in murine schistosomiasis *mansoni*. *J Immunol* 146:1322-1327

[87] Pearce, E.J., Caspar, P., Grzych, J.M., Lewis, F.A. and Sher, A. (1991). Downregulation of Th1 cytokine production accompanies induction of Th2 responses by a parasitic helminth, *Schistosoma mansoni*. *J Exp Med* 173:159–166

[88] Wynn, T.A., Eltoum, I., Cheever, A.W., Lewis, F.A., Gause, W.C. and Sher, A. (1993). Analysis of cytokine mRNA expression during primary granuloma formation induced by eggs of *Schistosoma mansoni*. *J Immunol* 151:1430–1440

[89] Chensue, S.W., Warmington, K., Ruth, J.H., Lukacs, N., Kunkel, S.L. (1997). Mycobacterial and schistosomal antigen-elicited granuloma formation in IFN-gamma and IL-4 knockout mice: analysis of local and regional cytokine and chemokine networks. *J Immunol* 159:3565-3573

[90] Wynn, T.A., Eltoum, I., Oswald, I.P., Cheever, A.W. and Sher, A. (1994). Endogenous interleukin 12 (IL-12) regulates granuloma formation induced by eggs of *Schistosoma mansoni* and exogenous IL-12 both inhibits and prophylactically immunizes against egg pathology. *J Exp Med* 179:1551–1561

[91] Kullberg, M.C., Pearce, E.J., Hieny, S.E., Sher, A. and Berzofsky, J.A (1992). Infection with *Schistosoma mansoni* alters Th1/Th2 cytokine responses to a non-parasite antigen. *J Immunol* 148:3264-3270

[92] Shainheit, M.G., Smith, P.M., Bazzone, L.E., Wang, A.C., Rutitzky, L.I. and Stadecker, M.J. (2008). Dendritic cell IL-23 and IL-1 production in response to schistosome eggs induces Th17 cells in a mouse strain prone to severe immunopathology. *J Immunol* 181:8559-8567

[93] Fallon, P.G., Smith, P., Richardson, E.J., Jones, F.J., Faulkner, H.C., Van Snick, J., Renauld, J.C., Grencis, R.K. and Dunne, D.W. (2000). Expression of interleukin-9 leads to Th2 cytokine-dominated responses and fatal enteropathy in mice with chronic *Schistosoma mansoni* infections. *Infect Immun* 68:6005-6011

[94] Pearce, E.J. and MacDonald, A.S. (2002). The immunobiology of schistosomiasis. *Nat Rev Immunol* 2:499-511

[95] Pearce, E.J (2005). Priming of the immune response by schistosome eggs. *Parasite Immunol* 27:265-270

[96] Layland, L.E., Wagner, H. and da Costa, C.U. (2005). Lack of antigen-specific Th1 response alters granuloma formation and composition in *Schistosoma mansoni*-infected MyD88$^{-/-}$ mice. *Eur J Immunol* 35:3248-3257

[97] Silva, L.M., Fernandes, A.L., Barbosa, A. Jr., Oliveira, I.R. and Andrade, Z.A. (2000). Significance of schistosomal granuloma modulation. *Mem Inst Oswaldo Cruz* 95:353-361

[98] Layland, L.E., Rad, R., Wagner, H. and da Costa, C.U (2007). Immunopathology in schistosomiasis is controlled by antigen-specific regulatory T cells primed in the presence of TLR2. *Eur J Immunol* 37:2174-2184

[99] Layland, L.E., Mages, J., Loddenkemper, C., Hoerauf, A., Wagner, H., Lang, R. and da Costa, C.U (2010). Pronounced phenotype in activated regulatory T cells during a chronic helminth infection. *J Immunol* 184:713-724

[100] Fallon, P.G., Richardson, E.J., McKenzie, G.J. and McKenzie, A.N. (2000). Schistosome infection of transgenic mice defines distinct and contrasting pathogenic roles for IL-4 and IL-13: IL-13 is a profibrotic agent. *J Immunol* 164:2585-2591

[101] Chiaramonte, M.G., Donaldson, D.D., Cheever, A.W. and Wynn, T.A. (1999). An IL-13 inhibitor blocks the development of hepatic fibrosis during a T-helper type 2-dominated inflammatory response. *J Clin Invest* 104:777-785

[102] Jankovic, D., Kullberg, M.C., Noben-Trauth, N., Caspar, P., Ward, J.M., Cheever, A.W., Paul, W.E. and Sher, A. (1999). Schistosome-infected IL-4 receptor knockout (KO) mice, in contrast to IL-4 KO mice, fail to develop granulomatous pathology while maintaining the same lymphokine expression profile. *J Immunol* 163:337-342

[103] Mentink-Kane, M.M., Cheever, A.W., Thompson, R.W., Hari, D.M., Kabatereine, N.B., Vennervald, B.J., Ouma, J.H., Mwatha, J.K., Jones, F.M., Donaldson, D.D., Grusby, M.J., Dunne, D.W. and Wynn, T.A. (2004). IL-13 receptor alpha 2 down-modulates granulomatous inflammation and prolongs host survival in schistosomiasis. *Proc Natl Acad Sci U S A* 101:586-590

[104] Wynn, T., Cheever, A.W., Jankovic, D., Poindexter, R.W., Caspar, P., Lewis, F.A. and Sher, A. (1995). An IL-12-based vaccination method for preventing fibrosis induced by schistosome infection. *Nature* 376:594-596

[105] Hoffmann, K.F., Caspar, P., Cheever, A.W. and Wynn, T.A. (1998). IFN-gamma, IL-12, and TNF-alpha are required to maintain reduced liver pathology in mice vaccinated with *Schistosoma mansoni* eggs and IL-12. *J Immunol* 161:4201-4210

[106] Hesse, M., Cheever, A.W., Jankovic, D. and Wynn, T.A. (2000). NOS-2 mediates the protective anti-inflammatory and antifibrotic effects of the Th1-inducing adjuvant, IL-12, in a Th2 model of granulomatous disease. *Am J Pathol* 157:945-955

[107] Hesse, M., Modolell, M., La Flamme, A.C., Schito, M., Fuentes, J.M., Cheever, A.W., Pearce, E.J. and Wynn, T.A. (2001). Differential regulation of nitric oxide synthase-2 and arginase-1 by type 1/type 2 cytokines *in vivo*: granulomatous pathology is shaped by the pattern of L-arginine metabolism. *J Immunol* 167:6533-6544

[108] Hokke, C.H., Deelder, A.M. (2001). Schistosome glycoconjugates in host-parasite interplay. *Glycoconj J* 18:573-587

[109] Hokke, C.H. and Yazdanbakhsh, M. (2005). Schistosome glycans and innate immunity. *Parasite Immunol* 27:257-264

[110] Van der Kleij, D., Latz, E., Brouwers, J.F., Kruize, Y.C., Schmitz, M., Kurt-Jones, E.A., Espevik, T., de Jong, E.C., Kapsenberg, M.L., Golenbock, D.T., Tielens, A.G. and Yazdanbakhsh, M. (2002). A novel host-parasite lipid cross-talk. Schistosomal lyso-phosphatidylserine activates toll-like receptor 2 and affects immune polarization. *J Biol Chem* 277:48122-48129

[111] Faveeuw, C., Mallevaey, T., Paschinger, K., Wilson, I.B., Fontaine, J., Mollicone, R., Oriol, R., Altmann, F., Lerouge, P., Capron, M. and Trottein, F. (2003). Schistosome N-glycans containing core alpha 3-fucose and core beta 2-xylose epitopes are strong inducers of Th2 responses in mice. *Eur J Immunol* 33:1271-1281

[112] Okano, M., Satoskar, A.R., Nishizaki, K., Abe, M. and Harn, D.A. Jr. (1999). Induction of Th2 responses and IgE is largely due to carbohydrates functioning as adjuvants on *Schistosoma mansoni* egg antigens. *J Immunol* 163:6712-6717

[113] Okano, M., Satoskar, A.R., Nishizaki, K. and Harn, D.A. Jr. (2001). Lacto-N-fucopentaose III found on *Schistosoma mansoni* egg antigens functions as adjuvant for proteins by inducing Th2-type response. *J Immunol* 167:442-450

[114] Thomas, P.G., Carter, M.R., Atochina, O., Da'Dara, A.A., Piskorska, D., McGuire, E. and Harn, D.A. (2003). Maturation of dendritic cell 2 phenotype by a helminth glycan uses a Toll-like receptor 4-dependent mechanism. *J Immunol* 171:5837-5841

[115] Steinfelder, S., Andersen, J.F., Cannons, J.L., Feng, C.G., Joshi, M., Dwyer, D., Caspar, P., Schwartzberg, P.L., Sher, A. and Jankovic, D. (2009). The major component in schistosome eggs responsible for conditioning dendritic cells for Th2 polarization is a T2 ribonuclease (omega-1). *J Exp Med* 206:1681-1690

[116] Everts, B., Perona-Wright, G., Smits, H.H., Hokke, C.H., van der Ham, A.J., Fitzsimmons, C.M., Doenhoff, M.J., van der Bosch, J., Mohrs, K., Haas, H., Mohrs, M., Yazdanbakhsh, M. and Schramm G. (2009). Omega-1, a glycoprotein secreted by *Schistosoma mansoni* eggs, drives Th2 responses. *J Exp Med* 206:1673-1680

[117] Schramm, G., Falcone, F.H., Gronow, A., Haisch, K., Mamat, U., Doenhoff, M.J., Oliveira, G., Galle, J., Dahinden, C.A. and Haas, H. (2003). Molecular characterization of an interleukin-4-inducing factor from *Schistosoma mansoni* eggs. *J Biol Chem* 278:18384-18392

[118] Schramm, G., Mohrs, K., Wodrich, M., Doenhoff, M.J., Pearce, E.J., Haas, H. and Mohrs, M. (2007). Cutting edge: IPSE/alpha-1, a glycoprotein from *Schistosoma mansoni* eggs, induces IgE-dependent, antigen-independent IL-4 production by murine basophils *in vivo*. *J Immunol* 178:6023-6027

[119] Donnelly, S., Stack, C.M., O'Neill, S.M., Sayed, A.A., Williams, D.L. and Dalton, J.P. (2008). Helminth 2-Cys peroxiredoxin drives Th2 responses through a mechanism involving alternatively activated macrophages. *FASEB J* 22:4022-4032

[120] Zaccone, P., Burton, O., Miller, N., Jones, F.M., Dunne, D.W. and Cooke, A. (2009). *Schistosoma mansoni* egg antigens induce Treg that participate in diabetes prevention in NOD mice. *Eur J Immunol* 39:1098-1107

[121] Aksoy, E., Zouain, C.S., Vanhoutte, F., Fontaine, J., Pavelka, N., Thieblemont, N., Willems, F., Ricciardi-Castagnoli, P., Goldman, M., Capron, M., Ryffel, B. and Trottein, F. (2005). Double-stranded RNAs from the helminth parasite *Schistosoma* activate TLR3 in dendritic cells. *J Biol Chem* 280:277-283

[122] Cervi, L., MacDonald, A.S., Kane, C., Dzierszinski, F. and Pearce, E.J. (2004). Cutting edge: dendritic cells copulsed with microbial and helminth antigens undergo modified maturation, segregate the antigens to distinct intracellular compartments, and concurrently induce microbe-specific Th1 and helminth-specific Th2 responses. *J Immunol* 172:2016-2020

[123] Van Liempt, E. van Vliet, S.J., Engering, A., Vallejo, J.J.G., Bank, C.M.C., Sanchez-Hernandez, M., van Kooyk, Y. and van Die, I. (2007). *Schistosoma mansoni* soluble egg antigens are internalized by human dendritic cells through multiple C-type lectins and suppress TLR-induced dendritic cell activation. *Mol Immunol* 44:2605–2615

[124] Zaccone, P., Fehérvári, Z., Jones, F.M., Sidobre, S., Kronenberg, M., Dunne, D.W. and Cooke, A. (2003). *Schistosoma mansoni* antigens modulate the activity of the innate immune response and prevent onset of type 1 diabetes. *Eur J Immunol* 33:1439-1449

[125] Kane, C.M., Cervi, L., Sun, J., McKee, A.S., Masek, K.S., Shapira, S., Hunter, C.A. and Pearce, E.J. (2004). Helminth antigens modulate TLR-initiated dendritic cell activation. *J Immunol* 173:7454-7461

[126] Pearce, E.J. (2005). Priming of the immune response by schistosome eggs. *Parasite Immunol* 27:265-270

[127] Correale, J. and Farez, M. (2009). Helminth antigens modulate immune responses in cells from multiple sclerosis patients through TLR2-dependent mechanisms. *J Immunol* 183:5999-6012

[128] Moore, K.W., de Waal Malefyt, R., Coffman, R.L. and O'Garra, A. (2001). Interleukin-10 and the interleukin-10 receptor. *Annu Rev Immunol* 19:683-765

[129] Hoffmann, K.F., Cheever, A.W. and Wynn, T.A. (2000). IL-10 and the dangers of immune polarization: excessive type 1 and type 2 cytokine responses induce distinct forms of lethal immunopathology in murine schistosomiasis. *J Immunol* 164:6406-6416

[130] Van Die, I., van Vliet, S.J., Nyame, A.K., Cummings, R.D., Bank, C.M., Appelmelk, B., Geijtenbeek, T.B. and van Kooyk, Y. (2003). The dendritic cell-specific C-type lectin DC-SIGN is a receptor for *Schistosoma mansoni* egg antigens and recognizes the glycan antigen Lewis x. *Glycobiology* 13:471-478

[131] Van Vliet, S.J., van Liempt, E., Saeland, E., Aarnoudse, C.A., Appelmelk, B., Irimura, T., Geijtenbeek, T.B., Blixt, O., Alvarez, R., van Die, I. and van Kooyk, Y. (2005). Carbohydrate profiling reveals a distinctive role for the C-type lectin MGL in the recognition of helminth parasites and tumor antigens by dendritic cells. *Int Immunol* 17:661-669

[132] Saunders, S.P., Walsh, C.M., Barlow, J.L., Mangan, N.E., Taylor, P.R., McKenzie, A.N., Smith, P. and Fallon, P.G. (2009). The C-type lectin SIGNR1 binds *Schistosoma mansoni* antigens *in vitro*, but SIGNR1-deficient mice have normal responses during schistosome infection. *Infect Immun* 77:399-404

[133] Mócsai, A., Ruland, J. and Tybulewicz, V.L. (2010). The SYK tyrosine kinase: a crucial player in diverse biological functions. *Nat Rev Immunol* 10:387-402

[134] Hise, A.G., Tomalka, J., Ganesan, S., Patel, K., Hall, B.A., Brown, G.D. and Fitzgerald, K.A. (2009). An essential role for the NLRP3 inflammasome in host defense against the human fungal pathogen *Candida albicans*. *Cell Host Microbe* 5:487-497

[135] Gross, O., Poeck, H., Bscheider, M., Dostert, C., Hannesschläger, N., Endres, S., Hartmann, G., Tardivel, A., Schweighoffer, E., Tybulewicz, V., Mocsai, A., Tschopp, J. and Ruland, J. (2009). Syk kinase signalling couples to the Nlrp3 inflammasome for anti-fungal host defence. *Nature* 459:433-436

[136] Dinarello, C.A. (2010). IL-1: discoveries, controversies and future directions. *Eur J Immunol* 40:599-606

[137] Beeson, P.B. (1948). Temperature-elevating effect of a substance obtained from polymorphonuclear leucocytes. *J Clin Invest* 27:524

[138] Dinarello, C.A., Renfer, L. and Wolff, S.M. (1977). Human leukocytic pyrogen: purification and development of a radioimmunoassay. *Proc Natl Acad Sci U S A* 74:4624-4627

[139] Auron, P.E., Webb, A.C., Rosenwasser, L.J., Mucci, S.F., Rich, A., Wolff, S.M. and Dinarello, C.A. (1984). Nucleotide sequence of human monocyte interleukin 1 precursor cDNA. *Proc Natl Acad Sci U S A* 81:7907-7911

[140] March, C.J., Mosley, B., Larsen, A., Cerretti, D.P., Braedt, G., Price, V., Gillis, S., Henney, C.S., Kronheim, S.R., Grabstein, K., Conlon, P.J., Hopp, T.P. and Cosman, D. (1985). Cloning, sequence and expression of two distinct human interleukin-1 complementary DNAs. *Nature* 315:641-647

[141] Clark, B.D., Collins, K.L., Gandy, M.S., Webb, A.C. and Auron, P.E. (1986). Genomic sequence for human prointerleukin 1 beta: possible evolution from a reverse transcribed prointerleukin 1 alpha gene. *Nucleic Acids Res* 14:7897-7914

[142] Tewari, A., Buhles, W.C. Jr. and Starnes, H.F. Jr. (1990). Preliminary report: effects of interleukin-1 on platelet counts. *Lancet* 336:712-714

[143] Ogilvie, A.C., Hack, C.E., Wagstaff, J., van Mierlo, G.J., Erenberg, A.J., Thomsen, L.L., Hoekman, K. and Rankin, E.M. (1996). IL-1 beta does not cause neutrophil degranulation but does lead to IL-6, IL-8, and nitrite/nitrate release when used in patients with cancer. *J Immunol* 156:389-394

[144] Dinarello, C.A. The interleukin-1 family: 10 years of discovery (1994). *ASEB J* 8:1314-1325

[145] Eisenberg, S.P., Evans, R.J., Arend, W.P., Verderber, E., Brewer, M.T., Hannum, C.H. and Thompson, R.C. (1990). Primary structure and functional expression from complementary DNA of a human interleukin-1 receptor antagonist. *Nature* 343:341-346

[146] Carter, D.B., Deibel, M.R. Jr., Dunn, C.J., Tomich, C.S., Laborde, A.L., Slightom, J.L., Berger, A.E., Bienkowski, M.J., Sun, F.F., McEwan, R.N., Harris, P.K.W., Yem, A.W., Waszak, G.A., Chosay, J.G., Sieu, L.C., Hardee, M.M., Zurcher-Neely, H.A., Reardon, I.M., Heinrikson, R.L., Truesdell, S.E., Shelly, J.A., Eessalu, T.E., Taylor, B.M. and Tracey, D.E. (1990). Purification, cloning, expression and biological characterization of an interleukin-1 receptor antagonist protein. *Nature* 344:633-638

[147] Sims, J.E., Nicklin, M.J., Bazan, J.F., Barton, J.L., Busfield, S.J., Ford, J.E., Kastelein, R.A., Kumar, S., Lin, H., Mulero, J.J., Pan, J., Pan, Y., Smith, D.E. and Young, P.R. (2001). A new nomenclature for IL-1-family genes. *Trends Immunol* 22:536-537

[148] Okamura, H., Tsutsi, H., Komatsu, T., Yutsudo, M., Hakura, A., Tanimoto, T., Torigoe, K., Okura, T., Nukada, Y., Hattori, K., Akita, K., Namba, M., Tanabe, F., Konishi, K., Fukuda, S. and Kurimoto, M. (1995). Cloning of a new cytokine that induces IFN-gamma production by T cells. *Nature* 378:88-91

[149] Schmitz, J., Owyang, A., Oldham, E., Song, Y., Murphy E, McClanahan, T.K., Zurawski, G., Moshrefi, M., Qin, J., Li, X., Gorman, D.M., Bazan, J.F. and Kastelein, R.A. (2005). IL-33, an interleukin-1-like cytokine that signals via the IL-1 receptor-related protein ST2 and induces T helper type 2-associated cytokines. *Immunity* 23:479-490

[150] Martinon, F., Burns, K. and Tschopp, J. (2002). The inflammasome: a molecular platform triggering activation of inflammatory caspases and processing of proIL-beta. *Mol Cell* 10:417-426

[151] Martinon, F. and Tschopp, J. (2004). Inflammatory caspases: linking an intracellular innate immune system to autoinflammatory diseases. *Cell* 117:561-574

[152] Dinarello, C.A. (2009). Immunological and inflammatory functions of the interleukin-1 family. *Annu Rev Immunol* 27:519-550

[153] Bendtzen, K., Mandrup-Poulsen, T., Nerup, J., Nielsen, J.H., Dinarello, C.A. and Svenson, M. (1986). Cytotoxicity of human pI 7 interleukin-1 for pancreatic islets of Langerhans. *Science* 232:1545-1547

[154] Mizel, S.B., Dayer, J.M., Krane, S.M. and Mergenhagen, S.E. (1981). Stimulation of rheumatoid synovial cell collagenase and prostaglandin production by partially purified lymphocyte-activating factor (interleukin 1). *Proc Natl Acad Sci U S A* 78:2474-2477

[155] Broide, D.H., Lotz, M., Cuomo, A.J., Coburn, D.A., Federman, E.C. and Wasserman, S.I. (1992). Cytokines in symptomatic asthma airways. *J Allergy Clin Immunol* 89:958-967

[156] Sousa, A.R., Lane, S.J., Nakhosteen, J.A., Lee, T.H. and Poston, R.N. (1996). Expression of interleukin-1 beta (IL-1beta) and interleukin-1 receptor antagonist (IL-1ra) on asthmatic bronchial epithelium. *Am J Respir Crit Care Med* 154:1061-1066

[157] Chung, K.F. and Barnes, P.J. (1999). Cytokines in asthma. *Thorax* 54:825-857

[158] Tschopp, J., Martinon, F. and Burns, K. (2003). NALPs: a novel protein family involved in inflammation. *Nat Rev Mol Cell Biol* 4:95-104

[159] Pedra, J.H., Cassel, S.L. and Sutterwala, F.S. (2009). Sensing pathogens and danger signals by the inflammasome. *Curr Opin Immunol* 21:10-16

[160] McIntire, C.R., Yeretssian, G. and Saleh, M. (2009). Inflammasomes in infection and inflammation. *Apoptosis* 14:522-535

[161] Fitzgerald, K.A. (2010). NLR-containing inflammasomes: central mediators of host defense and inflammation. *Eur J Immunol* 40:595-598

[162] Martinon, F., Hofmann, K. and Tschopp, J. (2001). The pyrin domain: a possible member of the death domain-fold family implicated in apoptosis and inflammation. *Curr Biol* 11:R118-120

[163] Boyden, E.D. and Dietrich, W.F. (2006). Nalp1b controls mouse macrophage susceptibility to anthrax lethal toxin. *Nat Genet* 38:240-244

[164] Roberts, T.L., Idris, A., Dunn, J.A., Kelly, G.M., Burnton, C.M., Hodgson, S., Hardy, L.L., Garceau, V., Sweet, M.J., Ross, I.L., Hume, D.A. and Stacey, K.J. (2009). HIN-200 proteins regulate caspase activation in response to foreign cytoplasmic DNA. *Science* 323:1057-1060

[165] Bürckstümmer, T., Baumann, C., Blüml, S., Dixit, E., Dürnberger, G., Jahn, H., Planyavsky, M., Bilban, M., Colinge, J., Bennett, K.L. and Superti-Furga, G. (2009). An orthogonal proteomic-genomic screen identifies AIM2 as a cytoplasmic DNA sensor for the inflammasome. *Nat Immunol* 10:266-272

[166] Fernandes-Alnemri, T., Yu, J.W., Datta, P., Wu, J. and Alnemri, E.S. (2009). AIM2 activates the inflammasome and cell death in response to cytoplasmic DNA. *Nature* 458:509-513

[167] Hornung, V., Ablasser, A., Charrel-Dennis, M., Bauernfeind, F., Horvath, G., Caffrey, D.R., Latz, E. and Fitzgerald, K.A. (2009). AIM2 recognizes cytosolic dsDNA and forms a caspase-1-activating inflammasome with ASC. *Nature* 458:514-518

[168] Agostini, L., Martinon, F., Burns, K., McDermott, M.F., Hawkins, P.N. and Tschopp, J. (2004). NALP3 forms an IL-1beta-processing inflammasome with increased activity in Muckle-Wells autoinflammatory disorder. *Immunity* 20:319-325

[169] Poyet, J.L., Srinivasula, S.M., Tnani, M., Razmara, M., Fernandes-Alnemri, T. and Alnemri, E.S. (2001). Identification of Ipaf, a human caspase-1-activating protein related to Apaf-1. *J Biol Chem* 276:28309-283013

[170] Elinav, E., Strowig, T., Kau, A.L., Henao-Mejia, J., Thaiss, C.A., Booth, C.J., Peaper, D.R., Bertin, J., Eisenbarth, S.C., Gordon, J.I. and Flavell, R.A. (2011). NLRP6 inflammasome regulates colonic microbial ecology and risk for colitis. *Cell* 145:745-757

[171] Chen, G.Y., Liu, M., Wang, F., Bertin, J. and Núñez, G. (2011). A functional role for Nlrp6 in intestinal inflammation and tumorigenesis. *J Immunol* 186:7187-7194

[172] Broz, P. and Monack, D.M. (2011). Molecular mechanisms of inflammasome activation during microbial infections. *Immunol Rev* 243:174-190

[173] Dinarello, C.A., Ikejima, T., Warner, S.J., Orencole, S.F., Lonnemann, G., Cannon, J.G. and Libby, P. (1987). Interleukin 1 induces interleukin 1. I. Induction of circulating interleukin 1 in rabbits in vivo and in human mononuclear cells in vitro. *J Immunol* 139:1902-1910

[174] Faustin, B., Lartigue, L., Bruey, J.M., Luciano, F., Sergienko, E., Bailly-Maitre, B., Volkmann, N., Hanein, D., Rouiller, I. and Reed, J.C. (2007). Reconstituted NALP1 inflammasome reveals two-step mechanism of caspase-1 activation. *Mol Cell* 5:713-724

[175] Mariathasan, S., Newton, K., Monack, D.M., Vucic, D., French, D.M., Lee, W.P., Roose-Girma, M., Erickson, S. and Dixit, V.M. (2004). Differential activation of the inflammasome by caspase-1 adaptors ASC and Ipaf. *Nature* 430:213-218

[176] Zamboni, D.S., Kobayashi, K.S., Kohlsdorf, T., Ogura, Y., Long, E.M., Vance, R.E., Kuida, K., Mariathasan, S., Dixit, V.M., Flavell, R.A., Dietrich, W.F. and Roy, C.R. (2006). The Birc1e cytosolic pattern-recognition receptor contributes to the detection and control of *Legionella pneumophila* infection. *Nat Immunol* 7:318-325

[177] Suzuki, T., Franchi, L., Toma, C., Ashida, H., Ogawa, M., Yoshikawa, Y., Mimuro, H., Inohara, N., Sasakawa, C. and Nuñez, G. (2007). Differential regulation of caspase-1 activation, pyroptosis, and autophagy via Ipaf and ASC in *Shigella*-infected macrophages. *PLoS Pathog* 3:e111

[178] Sutterwala, F.S., Mijares, L.A., Li, L., Ogura, Y., Kazmierczak, B.I. and Flavell, R.A. (2007). Immune recognition of *Pseudomonas aeruginosa* mediated by the IPAF/NLRC4 inflammasome. *J Exp Med* 204:3235-3245

[179] Kanneganti, T.D., Body-Malapel, M., Amer, A., Park, J.H., Whitfield, J., Franchi, L., Taraporewala, Z.F., Miller, D., Patton, J.T., Inohara, N. and Núñez, G. (2006) Critical role for Cryopyrin/Nalp3 in activation of caspase-1 in response to viral infection and double-stranded RNA. *J Biol Chem* 281:36560-36568

[180] Muruve, D.A., Pétrilli, V., Zaiss, A.K., White, L.R., Clark, S.A., Ross, P.J., Parks, R.J. and Tschopp, J. (2008). The inflammasome recognizes cytosolic microbial and host DNA and triggers an innate immune response. *Nature* 452:103-107

[181] Mariathasan, S., Weiss, D.S., Newton, K., McBride, J., O'Rourke, K., Roose-Girma, M., Lee, W.P., Weinrauch, Y., Monack, D.M. and Dixit, V.M. (2006). Cryopyrin activates the inflammasome in response to toxins and ATP. *Nature* 440:228-232

[182] Warren, S.E., Mao, D.P., Rodriguez, A.E., Miao, E.A. and Aderem, A. (2008). Multiple Nod-like receptors activate caspase 1 during *Listeria monocytogenes* infection. *J Immunol* 180:7558-7564

[183] Duncan, J.A., Gao, X., Huang, M.T., O'Connor, B.P., Thomas, C.E., Willingham, S.B., Bergstralh, D.T., Jarvis, G.A., Sparling, P.F. and Ting, J.P. (2009). *Neisseria gonorrhoeae* activates the proteinase cathepsin B to mediate the signaling activities of the NLRP3 and ASC-containing inflammasome. *J Immunol* 182:6460-6469

[184] Broz, P., Newton, K., Lamkanfi, M., Mariathasan, S., Dixit, V.M. and Monack, D.M. (2010). Redundant roles for inflammasome receptors NLRP3 and NLRC4 in host defense against *Salmonella.* *J Exp Med* 207:1745-1755

[185] Feldmeyer, L., Keller, M., Niklaus, G., Hohl, D., Werner, S. and Beer, H.D. (2007). The inflammasome mediates UVB-induced activation and secretion of interleukin-1beta by keratinocytes. *Curr Biol* 17:1140-1145

[186] Martinon, F., Pétrilli, V., Mayor, A., Tardivel, A. and Tschopp, J. (2006). Gout-associated uric acid crystals activate the NALP3 inflammasome. *Nature* 440:237-241

[187] Dostert, C., Pétrilli, V., Van Bruggen, R., Steele, C., Mossman, B.T. and Tschopp, J. (2008). Innate immune activation through Nalp3 inflammasome sensing of asbestos and silica. *Science* 320:674-677

[188] Hornung, V., Bauernfeind, F., Halle, A., Samstad, E.O., Kono, H., Rock, K.L., Fitzgerald, K.A. and Latz, E. (2008). Silica crystals and aluminum salts activate the NALP3 inflammasome through phagosomal destabilization. *Nat Immunol* 9:847-856

[189] Cassel, S.L., Eisenbarth, S.C., Iyer, S.S., Sadler, J.J., Colegio, O.R., Tephly, L.A., Carter, A.B., Rothman, P.B., Flavell, R.A. and Sutterwala, F.S. (2008). The Nalp3 inflammasome is essential for the development of silicosis. *Proc Natl Acad Sci U S A* 105:9035-9040

[190] Halle, A., Hornung, V., Petzold, G.C., Stewart, C.R., Monks, B.G., Reinheckel, T., Fitzgerald, K.A., Latz, E., Moore, K.J. and Golenbock, D.T. (2008). The NALP3 inflammasome is involved in the innate immune response to amyloid-beta. *Nat Immunol* 9:857-865

[191] Surprenant, A., Rassendren, F., Kawashima, E., North, R.A. and Buell, G. (1996). The cytolytic P2Z receptor for extracellular ATP identified as a P2X receptor (P2X7). *Science* 272:735-738

[192] Solle, M., Labasi, J., Perregaux, D.G., Stam, E., Petrushova, N., Koller, B.H., Griffiths, R.J. and Gabel, C.A. (2001). Altered cytokine production in mice lacking P2X(7) receptors. *J Biol Chem* 276:125-132

[193] Pelegrin, P. and Surprenant, A. (2006). Pannexin-1 mediates large pore formation and interleukin-1beta release by the ATP-gated P2X7 receptor. *EMBO J* 25:5071-5082

[194] Brown, G.D. (2006). Dectin-1: a signalling non-TLR pattern-recognition receptor. *Nat Rev Immunol* 6:33-43

[195] Zhou, R., Yazdi, A.S., Menu, P. and Tschopp, J. (2011). A role for mitochondria in NLRP3 inflammasome activation. *Nature* 469:221-225

[196] Thornberry, N.A., Bull, H.G., Calaycay, J.R., Chapman, K.T., Howard, A.D., Kostura, M.J., Miller, D.K., Molineaux, S.M., Weidner, J.R., Aunins, J., Elliston, K.O., Ayala, J.M., Casano, F.J., Chin, J., Ding, G.J.-F., Egger, L.A., Gaffney, E.P., Limjuco, G., Palyha, O.C., Raju, S.M., Rolando, A.M., Salley, J.P., Yamin, T.-T., Lee, T.D., Shively, J.E., MacCross, M., Mumford, R.A., Schmidt, J.A. and Tocci, M.J. (1992). A novel heterodimeric cysteine protease is required for interleukin-1 beta processing in monocytes. *Nature* 356:768-774

[197] Andrei, C., Dazzi, C., Lotti, L., Torrisi, M.R., Chimini, G. and Rubartelli, A. (1999). The secretory route of the leaderless protein interleukin 1beta involves exocytosis of endolysosome-related vesicles. *Mol Biol Cell* 10:1463-1475

[198] Andrei, C., Margiocco, P., Poggi, A., Lotti, L.V., Torrisi, M.R. and Rubartelli, A. (2004). Phospholipases C and A2 control lysosome-mediated IL-1 beta secretion: Implications for inflammatory processes. *Proc Natl Acad Sci U S A* 101:9745-9750

[199] Qu, Y., Franchi, L., Nunez, G. and Dubyak, G.R. (2007). Nonclassical IL-1 beta secretion stimulated by P2X7 receptors is dependent on inflammasome activation and correlated with exosome release in murine macrophages. *J Immunol* 179:1913-1925

[200] Sims, J.E. and Smith, D.E. (2010). The IL-1 family: regulators of immunity. *Nat Rev Immunol* 10:89-102

[201] Voronov, E., Shouval, D.S., Krelin, Y., Cagnano, E., Benharroch, D., Iwakura, Y., Dinarello, C.A. and Apte, R.N. (2003). IL-1 is required for tumor invasiveness and angiogenesis. *Proc Natl Acad Sci U S A* 100:2645-2650

[202] Lappalainen, U., Whitsett, J.A., Wert, S.E., Tichelaar, J.W. and Bry, K. (2005). Interleukin-1beta causes pulmonary inflammation, emphysema, and airway remodeling in the adult murine lung. *Am J Respir Cell Mol Biol* 32:311-318

[203] Johnson, V.J., Yucesoy, B. and Luster, M.I. (2005). Prevention of IL-1 signaling attenuates airway hyperresponsiveness and inflammation in a murine model of toluene diisocyanate-induced asthma. *J Allergy Clin Immunol* 116:851-858

[204] Nakae, S., Asano, M., Horai, R. and Iwakura, Y. (2001). Interleukin-1 beta, but not interleukin-1 alpha, is required for T-cell-dependent antibody production. *Immunology* 104:402-409

[205] Sutton, C., Brereton, C., Keogh, B., Mills, K.H. and Lavelle, E.C. (2006). A crucial role for interleukin (IL)-1 in the induction of IL-17-producing T cells that mediate autoimmune encephalomyelitis. *J Exp Med* 203:1685-1691

[206] Acosta-Rodriguez, E.V., Napolitani, G., Lanzavecchia, A. and Sallusto, F. (2007). Interleukins 1beta and 6 but not transforming growth factor-beta are essential for the differentiation of interleukin 17-producing human T helper cells. *Nat Immunol* 8:942-949

[207] Guo, L., Wei, G., Zhu, J., Liao, W., Leonard, W.J., Zhao, K. and Paul, W. (2009). IL-1 family members and STAT activators induce cytokine production by Th2, Th17, and Th1 cells. *Proc Natl Acad Sci U S A* 106:13463-13468

[208] Hoffman, H.M., Mueller, J.L., Broide, D.H., Wanderer, A.A. and Kolodner, R.D. (2001). Mutation of a new gene encoding a putative pyrin-like protein causes familial cold autoinflammatory syndrome and Muckle-Wells syndrome. *Nat Genet* 29:301-305

[209] Aksentijevich, I., Nowak, M., Mallah, M., Chae, J.J., Watford, W.T., Hofmann, S.R., Stein, L., Russo, R., Goldsmith, D., Dent, P., Rosenberg, H.F., Austin, F., Remmers, E.F., Balow, J.E. Jr., Rosenzweig, S., Komarow, H., Shoham, N.G., Wood, G., Jones, J., Mangra, N., Carrero, H., Adams, B.S., Moore, T.L., Schikler, K., Hoffman, H., Lovell, D.J., Lipnick, R., Barron, K., O'Shea, J.J., Kastner, D.L. and Goldbach-Mansky, R. (2002). *De novo* CIAS1 mutations, cytokine activation, and evidence for genetic heterogeneity in patients with neonatal-onset multisystem inflammatory disease (NOMID): a new member of the expanding family of pyrin-associated autoinflammatory diseases. *Arthritis Rheum* 46:3340-3348

[210] Pascual, V., Allantaz, F., Arce, E., Punaro, M. and Banchereau, J. (2005). Role of interleukin-1 (IL-1) in the pathogenesis of systemic onset juvenile idiopathic arthritis and clinical response to IL-1 blockade. *J Exp Med* 201:1479-1486

[211] Fitzgerald, A.A., Leclercq, S.A., Yan, A., Homik, J.E. and Dinarello, C.A. (2005). Rapid responses to anakinra in patients with refractory adult-onset Still's disease. *Arthritis Rheum* 52:1794-1803

[212] So, A., De Smedt, T., Revaz, S. and Tschopp, J. (2007). A pilot study of IL-1 inhibition by anakinra in acute gout. *Arthritis Res Ther* 9:R28

[213] Larsen, C.M., Faulenbach, M., Vaag, A., Vølund, A., Ehses, J.A., Seifert, B., Mandrup-Poulsen, T. and Donath, M.Y. (2007). Interleukin-1-receptor antagonist in type 2 diabetes mellitus. *N Engl J Med* 356:1517-1526

[214] Besnard, A.G., Guillou, N., Tschopp, J., Erard, F., Couillin, I., Iwakura, Y., Quesniaux, V., Ryffel, B. and Togbe, D. (2011). NLRP3 inflammasome is required in murine asthma in the absence of aluminum adjuvant. *Allergy* 66:1047-1057

[215] World Health Organization (2011). Asthma Fact Sheet. *http://www.who.int/mediacentre/factsheets/fs307/en/index.html*

[216] Umetsu, D.T., McIntire, J.J., Akbari, O., Macaubas, C. and DeKruyff, R.H. (2002). Asthma: an epidemic of dysregulated immunity. *Nat Immunol* 3:715-720

[217] Bousquet, J., Jeffery, P.K., Busse, W.W., Johnson, M. and Vignola, A.M. (2000). Asthma. From bronchoconstriction to airways inflammation and remodeling. *Am J Respir Crit Care Med* 161:1720-1745

[218] Bergeron, C. and Boulet, L.P. (2006). Structural changes in airway diseases: characteristics, mechanisms, consequences, and pharmacologic modulation. *Chest* 129:1068-1087

[219] Boulet, L.P. and Sterk, P.J. (2007). Airway remodelling: the future. *Eur Respir J* 30:831-834

[220] Kumar, R.K., Herbert, C. and Foster, P.S. (2008). The "classical" ovalbumin challenge model of asthma in mice. *Curr Drug Targets* 9:485-494

[221] Tournoy, K.G., Kips, J.C., Schou, C. and Pauwels, R.A. (2000). Airway eosinophilia is not a requirement for allergen-induced airway hyperresponsiveness. *Clin Exp Allergy* 30:79-85

[222] Kwak, Y.G., Song, C.H., Yi, H.K., Hwang, P.H., Kim, J.S., Lee, K.S. and Lee, Y.C. (2003). Involvement of PTEN in airway hyperresponsiveness and inflammation in bronchial asthma. *J Clin Invest* 111:1083-1092

[223] Dostert, C., Guarda, G., Romero, J.F., Menu, P., Gross, O., Tardivel, A., Suva, M.L., Stehle, J.C., Kopf, M., Stamenkovic, I., Corradin, G. and Tschopp, J. (2009). Malarial hemozoin is a Nalp3 inflammasome activating danger signal. *PLoS One* 4:e6510

[224] Shio, M.T., Eisenbarth, S.C., Savaria, M., Vinet, A.F., Bellemare, M.J., Harder, K.W., Sutterwala, F.S., Bohle, D.S., Descoteaux, A., Flavell, R.A. and Olivier, M. (2009). Malarial hemozoin activates the NLRP3 inflammasome through Lyn and Syk kinases. *PLoS Pathog* 5:e1000559

[225] Griffith, J.W., Sun, T., McIntosh, M.T. and Bucala, R. (2009). Pure Hemozoin is inflammatory *in vivo* and activates the NALP3 inflammasome via release of uric acid. *J Immunol* 183:5208-5220

[226] Acosta-Pérez, G., Maximina Bertha Moreno-Altamirano, M., Rodríguez-Luna, G. and Javier Sánchez-Garcia, F. Differential dependence of the ingestion of necrotic cells and TNF-alpha / IL-1beta production by murine macrophages on lipid rafts. *Scand J Immunol* 68:423-429

[227] Hoebe, K., Georgel, P., Rutschmann, S., Du, X., Mudd, S., Crozat, K., Sovath, S., Shamel, L., Hartung, T., Zähringer, U. and Beutler, B. (2005). CD36 is a sensor of diacylglycerides. *Nature* 433:523-527

[228] Kleinnijenhuis, J., Oosting, M., Joosten, L.A., Netea, M.G. and Van Crevel, R. (2011). Innate immune recognition of Mycobacterium tuberculosis. *Clin Dev Immunol* 2011:405310

[229] Lanier, L.L. (2009). DAP10- and DAP12-associated receptors in innate immunity. *Immunol Rev* 227:150-160

[230] McGreal, E.P., Rosas, M., Brown, G.D., Zamze, S., Wong, S.Y., Gordon, S., Martinez-Pomares, L. and Taylor, P.R. (2006). The carbohydrate-recognition domain of Dectin-2 is a C-type lectin with specificity for high mannose. *Glycobiology* 16:422-430

[231] Saijo, S., Ikeda, S., Yamabe, K., Kakuta, S., Ishigame, H., Akitsu, A., Fujikado, N., Kusaka, T., Kubo, S., Chung, S.H., Komatsu, R., Miura, N., Adachi, Y., Ohno, N., Shibuya, K., Yamamoto, N., Kawakami, K., Yamasaki, S., Saito, T., Akira, S. and Iwakura, Y. (2010). Dectin-2 recognition of alpha-mannans and induction of Th17 cell differentiation is essential for host defense against *Candida albicans*. *Immunity* 32:681-691

[232] Sato, K., Yang, X.L., Yudate, T., Chung, J.S., Wu, J., Luby-Phelps, K., Kimberly, R.P., Underhill, D., Cruz, P.D. Jr. and Ariizumi, K. (2006). Dectin-2 is a pattern recognition receptor for fungi that couples with the Fc receptor gamma chain to induce innate immune responses. *J Biol Chem* 281:38854-38866

[233] Drummond, R.A., Saijo, S., Iwakura, Y. and Brown, G.D. (2011). The role of Syk/CARD9 coupled C-type lectins in antifungal immunity. *Eur J Immunol* 41:276-281

[234] Ruland, J. (2008). CARD9 signaling in the innate immune response. *Ann N Y Acad Sci* 1143:35-44

[235] Mócsai, A., Ruland, J. and Tybulewicz, V.L. (2010). The SYK tyrosine kinase: a crucial player in diverse biological functions. *Nat Rev Immunol* 10:387-402

[236] Bi, L., Gojestani, S., Wu, W., Hsu, Y.M., Zhu, J., Ariizumi, K. and Lin, X. (2010). CARD9 mediates dectin-2-induced IkappaBalpha kinase ubiquitination leading to activation of NF-kappaB in response to stimulation by the hyphal form of *Candida albicans*. *J Biol Chem* 285:25969-25977

[237] Saijo, S. and Iwakura, Y. (2011). Dectin-1 and Dectin-2 in innate immunity against fungi. *Int Immunol* 23:467-472

[238] Braselmann, S., Taylor, V., Zhao, H., Wang, S., Sylvain, C., Baluom, M., Qu, K., Herlaar, E., Lau, A., Young, C., Wong, B.R., Lovell, S., Sun, T., Park, G., Argade, A., Jurcevic, S., Pine, P., Singh, R., Grossbard, E.B., Payan, D.G. and Masuda, E.S.(2006). R406, an orally available spleen tyrosine kinase inhibitor blocks fc receptor signaling and reduces immune complex-mediated inflammation. *J Pharmacol Exp Ther* 319:998-1008

[239] Gross, O., Gewies, A., Finger, K., Schäfer, M., Sparwasser, T., Peschel, C., Förster, I. and Ruland, J. (2006). Card9 controls a non-TLR signalling pathway for innate anti-fungal immunity. *Nature* 442:651-656

[240] Hara, H., Ishihara, C., Takeuchi, A., Imanishi, T., Xue, L., Morris, S.W., Inui, M., Takai, T., Shibuya, A., Saijo, S., Iwakura, Y., Ohno, N., Koseki, H., Yoshida, H., Penninger, J.M. and Saito, T. (2007). The adaptor protein CARD9 is essential for the activation of myeloid cells through ITAM-associated and Toll-like receptors. *Nat Immunol* 8:619-629

[241] Ritter, M., Gross, O., Kays, S., Ruland, J., Nimmerjahn, F., Saijo, S., Tschopp, J., Layland, L.E. and Prazeres da Costa, C. (2010). *Schistosoma mansoni* triggers Dectin-2, which activates the Nlrp3 inflammasome and alters adaptive immune responses. *Proc Natl Acad Sci U S A* 107:20459-20464

[242] Chensue, S.W., Bienkowski, M., Eessalu, T.E., Warmington, K.S., Hershey, S.D., Lukacs, N.W., Kunkel, S.L. (1993). Endogenous IL-1 receptor antagonist protein (IRAP) regulates schistosome egg granuloma formation and the regional lymphoid response. *J Immunol* 151:3654-3662

[243] Ruth, J.H., Bienkowski, M., Warmington, K.S., Lincoln, P.M., Kunkel, S.L. and Chensue, S.W. (1996). IL-1 receptor antagonist (IL-1ra) expression, function, and cytokine-mediated regulation during mycobacterial and schistosomal antigen-elicited granuloma formation. *J Immunol* 156:2503-2509

[244] Fallon, P.G. (2000). Immunopathology of schistosomiasis: a cautionary tale of mice and men. *Immunol Today* 21:29-35

[245] Cheever, A.W., Hoffmann, K.F. and Wynn, T.A. (2000). Immunopathology of *schistosomiasis mansoni* in mice and men. *Immunol Today* 21:465-466

[246] Fanning, M.M., Peters, P.A., Davis, R.S., Kazura, J.W. and Mahmoud, A.A. (1981). Immunopathology of murine infection with *Schistosoma mansoni*: relationship of genetic background to hepatosplenic disease and modulation. *J Infect Dis* 144:148-153

[247] Cheever, A.W., Duvall, R.H., Hallack, T.A. Jr., Minker, R.G., Malley, J.D. and Malley, K.G. (1987). Variation of hepatic fibrosis and granuloma size among mouse strains infected with *Schistosoma mansoni*. *Am J Trop Med Hyg* 37:85-97

[248] Asahi, H., Hernandez, H.J. and Stadecker, M.J (1999). A novel 62-kilodalton egg antigen from *Schistosoma mansoni* induces a potent CD4(+) T helper cell response in the C57BL/6 mouse. *Infect Immun* 67:1729-1735

[249] Williams, D.L., Asahi, H., Botkin, D.J. and Stadecker, M.J. (2001). Schistosome infection stimulates host CD4(+) T helper cell and B-cell responses against a novel egg antigen, thioredoxin peroxidase. Infect Immun 69:1134-1141

[250] Cooke, A., Tonks, P., Jones, F.M., O'Shea, H., Hutchings, P., Fulford, A.J. and Dunne, D.W. (1999). Infection with *Schistosoma mansoni* prevents insulin dependent diabetes mellitus in non-obese diabetic mice. *Parasite Immunol* 21:169-176

[251] Araujo, M.I., Hoppe, B., Medeiros, M. Jr., Alcântara, L., Almeida, M.C., Schriefer, A., Oliveira, R.R., Kruschewsky, R., Figueiredo, J.P., Cruz, A.A. and Carvalho. E.M. (2004). Impaired T helper 2 response to aeroallergen in helminth-infected patients with asthma. *J Infect Dis* 190:1797-1803

[252] Pacífico, L.G., Marinho, F.A., Fonseca, C.T., Barsante, M.M., Pinho, V., Sales-Junior, P.A., Cardoso, L.S., Araújo, M.I., Carvalho, E.M., Cassali, G.D., Teixeira, M.M. and Oliveira, S.C. (2009). *Schistosoma mansoni* antigens modulate experimental allergic asthma in a murine model: a major role for CD4+ CD25+ Foxp3+ T cells independent of interleukin-10. *Infect Immun* 77:98-107

[253] Cardoso, L.S., Oliveira, S.C., Góes, A.M., Oliveira, R.R., Pacífico, L.G., Marinho, F.V., Fonseca, C.T., Cardoso, F.C., Carvalho, E.M. and Araujo, M.I. (2010). *Schistosoma mansoni* antigens modulate the allergic response in a murine model of ovalbumin-induced airway inflammation. *Clin Exp Immunol* 160:266-274

[254] Medeiros, M. Jr., Figueiredo, J.P., Almeida, M.C., Matos, M.A., Araújo, M.I., Cruz, A.A., Atta, A.M., Rego, M.A., de Jesus, A.R., Taketomi, E.A. and Carvalho, E.M. (2003). *Schistosoma mansoni* infection is associated with a reduced course of asthma. *J Allergy Clin Immunol* 111:947-951

[255] Meyer, S., Tefsen, B., Imberty, A., Geyer, R. and van Die, I. (2007). The C-type lectin L-SIGN differentially recognizes glycan antigens on egg glycosphingolipids and soluble egg glycoproteins from *Schistosoma mansoni*. *Glycobiology* 17:1104-1119

[256] Cruz, C.M., Rinna, A., Forman, H.J., Ventura, A.L., Persechini, P.M. and Ojcius, D.M. (2007). ATP activates a reactive oxygen species-dependent oxidative stress response and secretion of proinflammatory cytokines in macrophages. *J Biol Chem* 282:2871-2879

[257] Pétrilli, V., Papin, S., Dostert, C., Mayor, A., Martinon, F. and Tschopp, J. (2007). Activation of the NALP3 inflammasome is triggered by low intracellular potassium concentration. *Cell Death Differ* 14:1583-1589

[258] Perregaux, D. and Gabel, C.A. (1994). Interleukin-1 beta maturation and release in response to ATP and nigericin. Evidence that potassium depletion mediated by these agents is a necessary and common feature of their activity. *J Biol Chem* 269:15195-15203

[259] Ray, P.D., Huang, B.W., Tsuji, Y. (2012). Reactive oxygen species (ROS) homeostasis and redox regulation in cellular signaling. *Cell Signal* 24:981-990

[260] Novo, E. and Parola, M. (2008). Redox mechanisms in hepatic chronic wound healing and fibrogenesis. *Fibrogenesis Tissue Repair* 1:5

[261] Bauernfeind, F., Bartok, E., Rieger, A., Franchi, L., Núñez, G. and Hornung, V. (2011). Cutting edge: reactive oxygen species inhibitors block priming, but not activation, of the NLRP3 inflammasome. *J Immunol* 187:613-617

[262] Zhou, R., Tardivel, A., Thorens, B., Choi, I. and Tschopp J. (2010). Thioredoxin-interacting protein links oxidative stress to inflammasome activation. *Nat Immunol* 11:136-140

[263] Schroder, K., Zhou, R. and Tschopp, J. (2010). The NLRP3 inflammasome: a sensor for metabolic danger? *Science* 327:296-300

[264] Ariizumi, K., Shen, G.L., Shikano, S., Ritter, R. 3rd, Zukas, P., Edelbaum, D., Morita, A. and Takashima, A. (2000). Cloning of a second dendritic cell-associated C-type lectin (dectin-2) and its alternatively spliced isoforms. *J Biol Chem* 275:11957-11963

[265] Taylor, P.R., Reid, D.M., Heinsbroek, S.E., Brown, G.D., Gordon, S. and Wong, S.Y. (2005). Dectin-2 is predominantly myeloid restricted and exhibits unique activation-dependent expression on maturing inflammatory monocytes elicited *in vivo*. *Eur J Immunol* 35:2163-2174

[266] Robinson, M.J., Osorio, F., Rosas, M., Freitas, R.P., Schweighoffer, E., Gross, O., Verbeek, J.S., Ruland, J., Tybulewicz, V., Brown, G.D., Moita, L.F., Taylor, P.R., Reis e Sousa. C. (2009). Dectin-2 is a Syk-coupled pattern recognition receptor crucial for Th17 responses to fungal infection. *J Exp Med* 206:2037-2051

[267] Shainheit, M.G., Lasocki, K.W., Finger, E., Larkin, B.M., Smith, P.M., Sharpe, A.H., Dinarello, C.A., Rutitzky, L.I. and Stadecker, M.J. (2011). The pathogenic Th17 cell response to major schistosome egg antigen is sequentially dependent on IL-23 and IL-1β. *J Immunol* 187:5328-5335

[268] Smith, P.M., Jacque, B., Conner, J.R., Poltorak, A. and Stadecker, M.J. (2011). IRAK-2 regulates IL-1-mediated pathogenic Th17 cell development in helminthic infection. *PLoS Pathog* 7:e1002272

[269] Graham, L.M., Tsoni, S.V., Willment, J.A., Williams, D.L., Taylor, P.R., Gordon, S., Dennehy, K. and Brown, G.D. (2006). Soluble Dectin-1 as a tool to detect beta-glucans. *J Immunol Methods* 314:164-169

[270] Paveley, R.A., Aynsley, S.A., Turner, J.D., Bourke, C.D., Jenkins, S.J., Cook, P.C., Martinez-Pomares, L. and Mountford, A.P. (2011). The Mannose Receptor (CD206) is an important pattern recognition receptor (PRR) in the detection of the infective stage of the helminth Schistosoma mansoni and modulates IFNγ production. *Int J Parasitol* 41:1335-1345

[271] Balch, S.G., Greaves, D.R., Gordon, S. and McKnight, A.J. (2002). Organization of the mouse macrophage C-type lectin (Mcl) gene and identification of a subgroup of related lectin molecules. *Eur J Immunogenet* 29:61-64

[272] Wells, C.A., Salvage-Jones, J.A., Li, X., Hitchens, K., Butcher, S., Murray, R.Z., Beckhouse, A.G., Lo, Y.L., Manzanero, S., Cobbold, C., Schroder, K., Ma, B., Orr, S., Stewart, L., Lebus, D., Sobieszczuk, P., Hume, D.A., Stow, J., Blanchard, H. and Ashman, R.B. (2008). The macrophage-inducible C-type lectin, mincle, is an essential component of the innate immune response to *Candida albicans*. *J Immunol* 180:7404-7413

[273] Bugarcic, A., Hitchens, K., Beckhouse, A.G., Wells, C.A., Ashman, R.B. and Blanchard, H. (2008). Human and mouse macrophage-inducible C-type lectin (Mincle) bind *Candida albicans*. *Glycobiology* 18:679-685

[274] Matsunaga, I. and Moody, D.B. (2009). Mincle is a long sought receptor for mycobacterial cord factor. *J Exp Med* 206:2865-2868

[275] Ishikawa, E., Ishikawa, T., Morita, Y.S., Toyonaga, K., Yamada, H., Takeuchi, O., Kinoshita, T., Akira, S., Yoshikai, Y. and Yamasaki, S. (2009). Direct recognition of the mycobacterial glycolipid, trehalose dimycolate, by C-type lectin Mincle. *J Exp Med* 206:2879-2888

[276] Yamasaki, S., Ishikawa, E., Sakuma, M., Hara, H., Ogata, K. and Saito, T. (2008). Mincle is an ITAM-coupled activating receptor that senses damaged cells. *Nat Immunol* 9:1179-1188

[277] Wang, H., Kadlecek, T.A., Au-Yeung, B.B., Goodfellow, H.E., Hsu, L.Y., Freedman, T.S. and Weiss, A. (2010). ZAP-70: an essential kinase in T-cell signaling. *Cold Spring Harb Perspect Biol* 2:a002279

[278] Rogers, N.C., Slack, E.C., Edwards, A.D., Nolte, M.A., Schulz, O., Schweighoffer, E., Williams, D.L., Gordon, S., Tybulewicz, V.L., Brown, G.D. and Reis e Sousa, C. (2005). Syk-dependent cytokine induction by Dectin-1 reveals a novel pattern recognition pathway for C type lectins. *Immunity* 22:507-517

[279] Glocker, E.O., Hennigs, A., Nabavi, M., Schäffer, A.A., Woellner, C., Salzer, U., Pfeifer, D., Veelken, H., Warnatz, K., Tahami, F., Jamal, S., Manguiat, A., Rezaei, N., Amirzargar, A.A., Plebani, A., Hannesschläger, N., Gross, O., Ruland, J. and Grimbacher, B. (2009). A homozygous CARD9 mutation in a family with susceptibility to fungal infections. *N Engl J Med* 361:1727-1735

[280] Cheever, A.W., Lenzi, J.A., Lenzi, H.L. and Andrade, Z.A. (2002). Experimental models of *Schistosoma mansoni* infection. *Mem Inst Oswaldo Cruz* 97:917-940

[281] Cheever, A.W., Poindexter, R.W. and Wynn, T.A. (1999). Egg laying is delayed but worm fecundity is normal in SCID mice infected with *Schistosoma japonicum* and *S. mansoni* with or without recombinant tumor necrosis factor alpha treatment. *Infect Immun* 67:2201-2208

[282] Rutitzky, L.I., Hernandez, H.J., Yim, Y.S., Ricklan, D.E., Finger, E., Mohan, C., Peter, I., Wakeland, E.K. and Stadecker, M.J. (2005). Enhanced egg-induced immunopathology correlates with high IFN-gamma in murine schistosomiasis: identification of two epistatic genetic intervals. *J Immunol* 174:435-440

[283] Smith, P.M., Shainheit, M.G., Bazzone, L.E., Rutitzky, L.I., Poltorak, A. and Stadecker, M.J. (2009). Genetic control of severe egg-induced immunopathology and IL-17 production in murine schistosomiasis. *J Immunol* 183:3317-3323

[284] Reiman, R.M., Thompson, R.W., Feng, C.G., Hari, D., Knight, R., Cheever, A.W., Rosenberg, H.F. and Wynn, T.A. (2006). Interleukin-5 (IL-5) augments the progression of liver fibrosis by regulating IL-13 activity. *Infect Immun* 74:1471-1479

[285] Wynn, T.A., Cheever, A.W., Williams, M.E., Hieny, S., Caspar, P., Kühn, R., Müller, W. and Sher, A. (1998). IL-10 regulates liver pathology in acute murine Schistosomiasis *mansoni* but is not required for immune down-modulation of chronic disease. *J Immunol* 160:4473-4480

[286] Fallon, P.G., Richardson, E.J., Smith, P. and Dunne, D.W. (2000). Elevated type 1, diminished type 2 cytokines and impaired antibody response are associated with hepatotoxicity and mortalities during *Schistosoma mansoni* infection of CD4-depleted mice. *Eur J Immunol* 30:470-480

[287] Doenhoff, M., Musallam, R., Bain, J. and McGregor, A. (1978). Studies on the host-parasite relationship in *Schistosoma mansoni*-infected mice: the immunological dependence of parasite egg excretion. *Immunology* 35:771-778

[288] Cheever, A.W., Eltoum, I.A., Andrade, Z.A. and Cox, T.M. (1993). Biology and pathology of *Schistosoma mansoni* and *Schistosoma japonicum* infections in several strains of nude mice. *Am J Trop Med Hyg* 48:496-503

[289] Karanja, D.M., Colley, D.G., Nahlen, B.L., Ouma, J.H. and Secor, W.E. (1997). Studies on schistosomiasis in western Kenya: I. Evidence for immune-facilitated excretion of schistosome eggs from patients with *Schistosoma mansoni* and human immunodeficiency virus coinfections. *Am J Trop Med Hyg* 56:515-521

[290] Herbert, D.R., Hölscher, C., Mohrs, M., Arendse, B., Schwegmann, A., Radwanska, M., Leeto, M., Kirsch, R., Hall, P., Mossmann, H., Claussen, B., Förster, I. and Brombacher, F. (2004). Alternative macrophage activation is essential for survival during schistosomiasis and downmodulates T helper 1 responses and immunopathology. *Immunity* 20:623-635

[291] Dupré, L., Kremer, L., Wolowczuk, I., Riveau, G., Capron, A. and Locht, C. (2001). Immunostimulatory effect of IL-18-encoding plasmid in DNA vaccination against murine *Schistosoma mansoni* infection. *Vaccine* 19:1373-1380

[292] Global Initiative for Asthma (2010). Global strategy for asthma management and prevention. *http://www.ginasthma.org/pdf/GINA_Report_2010.pdf*

[293] National Heart Lung and Blood Institute (2007). Expert panel report 3: Guidelines for the diagnosis and management of asthma. *http://www.nhlbi.nih.gov/guidelines/asthma/asthgdln.pdf*

[294] Pelaia, G., Gallelli, L., Renda, T., Romeo, P., Busceti, M.T., Grembiale, R.D., Maselli, R., Marsico, S.A. and Vatrella, A. (2011). Update on optimal use of omalizumab in management of asthma. *J Asthma Allergy* 4:49-59

[295] Dolan, C.M., Fraher, K.E., Bleecker, E.R., Borish, L., Chipps, B., Hayden, M.L., Weiss, S., Zheng, B., Johnson, C., Wenzel, S.; TENOR Study Group (2004). Design and baseline characteristics of the epidemiology and natural history of asthma: Outcomes and Treatment Regimens (TENOR) study: a large cohort of patients with severe or difficult-to-treat asthma. *Ann Allergy Asthma Immunol* 92:32-39

[296] Araujo, M.I., Lopes, A.A., Medeiros, M., Cruz, A.A., Sousa-Atta, L., Solé, D. and Carvalho, E.M. (2000). Inverse association between skin response to aeroallergens and *Schistosoma mansoni* infection. *Int Arch Allergy Immunol* 123:145-148

[297] Cooper, P.J., Chico, M.E., Rodrigues, L.C., Ordonez, M., Strachan, D., Griffin, G.E. and Nutman, T.B. (2003). Reduced risk of atopy among school-age children infected with geohelminth parasites in a rural area of the tropics. *J Allergy Clin Immunol* 111:995-1000

[298] Mangan, N.E., van Rooijen, N., McKenzie, A.N. and Fallon, P.G. (2006). Helminth-modified pulmonary immune response protects mice from allergen-induced airway hyperresponsiveness. *J Immunol* 176:138-147

[299] Pearce, E.J., Kane, C., Sun, J., Taylor, J., McKee, A.S. and Cervi, L. (2004). Th2 response polarization during infection with the helminth parasite *Schistosoma mansoni. Immunol Rev* 201:117-126

[300] Kitagaki, K., Businga, T.R., Racila, D., Elliott, D.E., Weinstock, J.V. and Kline, J.N. (2006). Intestinal helminths protect in a murine model of asthma. *J Immunol* 177:1628-1635

[301] Smits, H.H., Hammad, H., van Nimwegen, M., Soullie, T., Willart, M.A., Lievers, E., Kadouch, J., Kool, M., Kos-van Oosterhoud, J., Deelder, A.M., Lambrecht, B.N. and Yazdanbakhsh, M. (2007). Protective effect of *Schistosoma mansoni* infection on allergic airway inflammation depends on the intensity and chronicity of infection. *J Allergy Clin Immunol* 120:932-940

[302] Li, H., Nookala, S. and Re, F. (2007). Aluminum hydroxide adjuvants activate caspase-1 and induce IL-1beta and IL-18 release. *J Immunol* 178:5271-5276

[303] Kool, M., Pétrilli, V., De Smedt, T., Rolaz, A., Hammad, H., van Nimwegen, M., Bergen, I.M., Castillo, R., Lambrecht, B.N. and Tschopp, J. (2008). Cutting edge: alum adjuvant stimulates inflammatory dendritic cells through activation of the NALP3 inflammasome. *J Immunol* 181:3755-3759

[304] Franchi, L. and Núñez, G. (2008). The Nlrp3 inflammasome is critical for aluminium hydroxide-mediated IL-1beta secretion but dispensable for adjuvant activity. *Eur J Immunol* 38:2085-2089

[305] Takeda, K., Haczku, A., Lee, J.J., Irvin, C.G. and Gelfand, E.W. (2001). Strain dependence of airway hyperresponsiveness reflects differences in eosinophil localization in the lung. *Am J Physiol Lung Cell Mol Physiol* 281:L394-402

[306] Whitehead, G.S., Walker, J.K., Berman, K.G., Foster, W.M. and Schwartz, D.A. (2003). Allergen-induced airway disease is mouse strain dependent. *Am J Physiol Lung Cell Mol Physiol* 285:L32-42

[307] Zhu, W. and Gilmour, M.I. (2009). Comparison of allergic lung disease in three mouse strains after systemic or mucosal sensitization with ovalbumin antigen. *Immunogenetics* 61:199-207

[308] Clark, K., Simson, L., Newcombe, N., Koskinen, A.M., Mattes, J., Lee, N.A., Lee, J.J., Dent, L.A., Matthaei, K.I. and Foster, P.S. (2004). Eosinophil degranulation in the allergic lung of mice primarily occurs in the airway lumen. *J Leukoc Biol* 75:1001-1009

[309] Cohn, L., Elias, J.A. and Chupp, G.L. (2004). Asthma: mechanisms of disease persistence and progression. *Annu Rev Immunol* 22:789-815

[310] Broide, D.H. (2008). Immunologic and inflammatory mechanisms that drive asthma progression to remodeling. *J Allergy Clin Immunol* 121:560-570

[311] Cho, J.Y., Miller, M., Baek, K.J., Han, J.W., Nayar, J., Lee, S.Y., McElwain, K., McElwain, S., Friedman, S. and Broide, D.H. (2004). Inhibition of airway remodeling in IL-5-deficient mice. *J Clin Invest* 113:551-560

[312] Zhu, Z., Homer, R.J., Wang, Z., Chen, Q., Geba, G.P., Wang, J., Zhang, Y. and Elias, J.A. (1999). Pulmonary expression of interleukin-13 causes inflammation, mucus hypersecretion, subepithelial fibrosis, physiologic abnormalities, and eotaxin production. *J Clin Invest* 103:779-788

[313] Allen, I.C., Jania, C.M., Wilson, J.E., Tekeppe, E.M., Hua, X., Brickey, W.J., Kwan, M., Koller, B.H., Tilley, S.L. and Ting, J.P. (2012). Analysis of NLRP3 in the development of allergic airway disease in mice. *J Immunol* 188:2884-2893

[314] Feleszko, W., Jaworska, J., Rha, R.D., Steinhausen, S., Avagyan, A., Jaudszus, A., Ahrens, B., Groneberg, D.A., Wahn, U. and Hamelmann, E. (2007). Probiotic-induced suppression of allergic sensitization and airway inflammation is associated with an increase of T regulatory-dependent mechanisms in a murine model of asthma. *Clin Exp Allergy* 37:498-505

[315] Hougee, S., Vriesema, A.J., Wijering, S.C., Knippels, L.M., Folkerts, G., Nijkamp, F.P., Knol, J. and Garssen, J. (2010). Oral treatment with probiotics reduces allergic symptoms in ovalbumin-sensitized mice: a bacterial strain comparative study. *Int Arch Allergy Immunol* 151:107-117

[316] Yamagata, S., Tomita, K., Sato, R., Niwa, A., Higashino, H. and Tohda, Y. (2008). Interleukin-18-deficient mice exhibit diminished chronic inflammation and airway remodelling in ovalbumin-induced asthma model. *Clin Exp Immunol* 154:295-304

[317] Besnard, A.G., Togbe, D., Couillin, I., Tan, Z., Zheng, S.G., Erard, F., Le Bert, M., Quesniaux, V. and Ryffel, B. (2012). Inflammasome-IL-1-Th17 response in allergic lung inflammation. *J Mol Cell Biol* 4:3-10

[318] Kudo, M., Melton, A.C., Chen, C., Engler, M.B., Huang, K.E., Ren, X., Wang, Y., Bernstein, X., Li, J.T., Atabai, K., Huang, X. and Sheppard, D. (2012). IL-17A produced by αβ T cells drives airway hyper-responsiveness in mice and enhances mouse and human airway smooth muscle contraction. *Nat Med* 18:547-554

Acknowledgements

First and foremost I would like to state my appreciation to Prof. Dr. Dirk Busch for giving me the opportunity to work in the institute and for their helpful guidance and suggestions. Special thanks also to Prof Dr. Martin Klingenspor for his supervision and for offering me the opportunity to present and discuss my data in his institute. Additionally, I want to thank Prof. Dr. Hermann Wagner for is support especially during the very first part of my thesis.

I would also like to express my thanks to Dr. Clarissa Prazeres da Costa and Dr. Laura Layland for the opportunity to carry out this work in their lab, for their mentoring during my laboratory time and for guidance and critically reading this thesis.

A special thank you also to Stephanie Schmidt, Sabine Paul, Kathrin Straubinger, Stephanie Fetzer and Ulla Henn for the help during the laboratory work and for the nice working atmosphere.

Many other people have offered me invaluable help during my experiments particularly aspects of laboratory procedures. First I must mention Dr. Olaf Groß, who introduced me into the research field of inflammasomes and gave me valuable advice on Western blotting. I also have to thank Dr. Fromme for the help with the mitochondrial reactive oxygen species blocking experiments. They, together with many other colleagues in the institute (Dr. Stefan Dreher and Dr. Stefan Paschen) have made a nice working atmosphere for me, and I am grateful for that. In addition, I have to thank many other people (Prof. Dr. Jürgen Ruland, Prof. Dr. Falk Nimmerjahn, Prof. Dr. Gordon Brown, Dr. Philip Taylor, Prof. Dr. Yoichiro Iwakura, Dr. Shinobu Saijo and Dr. Laura Helming) and especially in memorial Prof. Dr. Juerg Tschopp for the support of this thesis

Time spent outside the lab is also an essential part of life and in this regard I must thank all my friends with whom I have shared so many unforgettable moments: Trietsch, Friedl, Bummi and Emilio. And regarding important things in life I am in debt to Steffi, who has been there to share good and bad moments besides the lab work. Special thanks go to Juergen, Helmut, Klaus, Doris, Isarspringer and Hannes for the refreshing time we spent together. Finally I want to thank my family, especially my parents, for their unconditional support and encouragement in any of the objectives and projects I have undertaken, no matter how difficult or unattainable they may have appeared. My success will always be yours.